THE DESIGN, SYNTHESIS AND BIOLOGICAL ASSAY OF CYSTEINE PROTEASE SPECIFIC INHIBITORS

A thesis
submitted in partial fulfilment
of the requirements for the degree of
Doctor of Philosophy in Chemistry
at the
University of Canterbury
by
Janna M. Mehrtens

University of Canterbury
2007

WORK IN THIS THESIS HAS APPEARED IN THE FOLLOWING PUBLICATIONS

Compounds and Compositions. Abell, A. D.; Coxon, J. M.; Miyamoto, S.; Jones, M. A.; Neffe, A. T.; Aitken, S. G.; Stuart, B. G.; Nikkel, J. M.; Morton, J. D.; Bickerstaffe, R.; Robertson, L. J.; Lee, H. Y. and Muir, M. S. *Provisional Patent Appl*., **2006**, 534303.

Compounds and Compositions. Abell, A. D.; Coxon, J. M.; Jones, M. A.; Aitken, S. G.; Stuart, B. G.; Neffe, A. T.; Nikkel, J. M.; M^{c}Nabb, S. B.; Klanchantra, M.; Duncan, J. K.; Morton, J. D.; Bickerstaffe, R.; Robertson, L. J.; Lee, H. Y. and Muir, M. S. *Provisional Patent Appl*., **2006**, 550631.

TABLE OF CONTENTS

ABSTRACT

This thesis investigates the design, synthesis and biological assay of cysteine protease inhibitors within the papain superfamily of cysteine proteases. This is achieved by examining the effect of inhibitor design, especially warheads, on IC_{50} values and structure-activity relationships between cysteine protease inhibitors of the papain superfamily. The representative proteases used are m-calpain, μ-calpain, cathepsin B and papain. **Chapter One** is an introductory chapter; **Chapters Two-Four** describe the design and synthesis of cysteine protease inhibitors; **Chapter Five** discusses assay protocol; and **Chapter Six** contains the assay results and structure-activity relationships of the synthesised inhibitors.

Chapter One introduces cysteine proteases of the papain family and examines the structure, physiology and role in disease of papain, cathepsin B, m-calpain and μ-calpain. The close structural homology that exists between these members of the papain superfamily is identified, as well characteristics unique to each protease. Covalent reversible, covalent irreversible and non-covalent warheads are defined. The generic inhibitor scaffold of address region, recognition and warhead, upon which the inhibitors synthesised in this thesis are based, is also introduced.

Chapter Two introduces reversible cysteine protease inhibitors found in the literature and that little is known about the effect of inhibitor warhead on selectivity within the papain superfamily. Oxidation of the dipeptidyl alcohols **2.6**, **2.26**, **2.29**, **2.30**, **2.35** and **2.36** utilising the sulfur trioxide-pyridine complex gave the aldehydes **2.3**, **2.27**, **2.19**, **2.2**, **2.21** and **2.22**. Semicarbazones **2.37-2.40** were synthesised by a condensation reaction between the alcohol **2.3** and four available semicarbazides. The amidoximes **2.48** and **2.49** separately underwent thermal intramolecular cyclodehydration to give the 3-methyl-1,2,4-oxadiazoles **2.41** and **2.50**. The aldehydes **2.3** and **2.27** were reacted with potassium cyanide to give the cyanohydrins **2.51** and **2.52**. The cyanohydrins **2.51** and **2.52** were separately reacted to give 1) the α-ketotetrazoles **2.43** and **2.55**; 2) the α-ketooxazolines **2.42** and **2.58**; 3) the esterified cyanohydrins **2.60** and **2.61**. A two step S_N2 displacement reaction of the alcohol **2.6** to give the azide **2.62**, an example of a non-covalent cysteine protease inhibitor.

Chapter Three introduces inhibitors with irreversible warheads. The well-known examples of epoxysuccinic acids **3.1** and **3.5** are discussed in detail, highlighting the lack of irreversible cysteine protease specific inhibitors. The aldehydes **2.3** and **2.27** were reacted under *Wittig* conditions to give the α,β-unsaturated carbonyls **3.14**-**3.18**. *Horner-Emmons-Wadsworth* methodology was utilised for the synthesis of the vinyl sulfones **3.20**-**3.23**. The dipeptidyl acids **2.24** and **2.28** were separately reacted with diazomethane to give the diazoketones **3.25** and **3.26**. The diazoketones **3.25** and **3.26** were separately reacted with hydrogen bromide in acetic acid (33%) to give the α-bromomethyl ketones **3.27** and **3.28**, which were subsequently reduced to give the α-bromomethyl alcohols **3.29**-**3.32**. Under basic conditions the α-bromomethyl alcohols **3.29**-**3.32** ring-closed to form the peptidyl epoxides **3.33**-**3.36**.

Chapter Four introduces the disadvantages of peptide-based inhibitors. A discussion is given on the benefits of constraining inhibitors into the extended bioactive conformation known as a β-strand. Ring closing metathesis is utilised in the synthesis of the macrocyclic aldehyde **4.4**, macrocyclic semicarbazone **4.15**, the macrocyclic cyanohydrin **4.16**, the macrocyclic α-ketotetrazole **4.18** and the macrocyclic azide **4.19**.

Chapter Five introduces enzyme inhibition studies. The BODIPY-casein fluorogenic assay used for establishing inhibitor potency against m-calpain and μ-calpain is validated. Assay protocols are also established and validated for cathepsin B, papain, pepsin and α-chymotrypsin. A discussion of the effect of solvent on enzyme activity is also included as part of this study.

Chapter Six presents the assay results for all the inhibitors synthesised throughout this thesis and an extensive structure-activity relationship study between inhibitors is included. The alcohols **2.26** and **2.30** are unprecedented examples of non-covalent, potent, cathepsin B inhibitors (IC_{50} = 0.075 μM selectivity 80-fold and 1.1 μM, selectivity 18-fold). The macrocyclic semicarbazone **4.15** is an unprecedented example of a potent macrocyclic cysteine protease inhibitor (m-calpain: IC_{50} = 0.16 μM, selectivity 8-fold). The cyanohydrin **2.51** contains an unprecedented cysteine protease warhead and is a potent and selective inhibitor of papain (IC_{50} = 0.030 μM, selectivity 3-fold). The *O*-protected cyanohydrin **2.61** is a potent and selective inhibitor of pepsin (IC_{50} = 1.6 μM, selectivity 1.5-fold). The top ten warheads for potent, selective cathepsin B inhibition are: carboxylic

acid, methyl ester, diazoketone, esterified cyanohydrin, α-bromomethyl ketone, α,β-unsaturated aldehyde, vinyl sulfones, α-bromomethyl-C_3-***S,R***-alcohol, alcohol and α,β-unsaturated ethyl ester. The selectivity of these warheads was between 5- and 130-fold for cathepsin B. The best inhibitors for cathepsin B were the α-bromomethyl ketone **3.26** (IC_{50} = 0.075 μM, selectivity 16-fold), the α,β-unsaturated aldehyde **3.18** (IC_{50} = 0.13 μM, selectivity 13-fold) and the esterified cyanohydrin **3.59** (IC_{50} = 0.35 μM, selectivity 22-fold).

Chapter Seven outlines the experimental details and synthesis of the compounds prepared in this thesis.

ABBREVIATIONS

1,1,2-TCE	1,1,2-trichloroethane
δ	chemical shift (in NMR)
Boc	*tert*-butoxycarbonyl
BODIPY	4,4-difluoro-5,7-dimethyl-4-bora-3a,4-diaza-*s*-indacene-3-propionic acid (in assay)
bs	broad singlet (in NMR)
Cbz	benzyloxycarbonyl
COSY	correlation spectroscopy
d	doublet (in NMR)
DCM	dichloromethane
dd	doublet of doublets (in NMR)
DIPEA	*N*,*N*-diisopropylethylamine
DMF	*N*,*N*-dimethylformamide
EtOAc	ethyl acetate
EDCI	1-[3-(dimethlamino)propyl]-3-carbodiimide hydrochloride
EDTA	ethylenediaminetetraacetic acid (in assay)
EGTA	ethylene glycol tetraacetic acid (in assay)
DMSO	dimethyl sulfoxide
EI	electron impact ionization (in mass spectrometry)
equiv	equivalent(s)
ES	electrospray ionization (in mass spectrometry)
Et_2O	diethyl ether
GB/SA	generalised Born/surface area (in modeling)
Grubbs 2nd generation catalyst	benzylidene[1,3-bis(2,4,6-trimethylphenyl)-2-imidazolidinylidene]dichloro(tricyclohexylphosphine)ruthenium.
HATU	*N*,*N*,*N'*,*N'*-tetramethyl-O-(7-azabenzotriazol-1-yl)uronium hexafluorophosphate
HCl	hydrochloric acid
HOBt	1-hydroxybenzotriazole
HRMS	high resolution mass spectroscopy

hr	hour(s)
Hz	hertz (in NMR)
IR	infrared
J	coupling constant (in NMR)
KOH	potassium hydroxide
K_2CO_3	potassium carbonate
$LiAlH(O^tBu)_3$	lithium tri-*tert*-butoxy aluminium hydride
$LiAlH_4$	lithium aluminium hydride
LRMS	low resolution mass spectrometry
m	multiplet (in NMR)
MCMM	Monte Carlo multiple minimum
MeOH	methanol
min(s)	minute(s)
$MgSO_4$	magnesium sulphate
MOPS	3-(N-morpholino)propanesulfonic acid (in assay)
mp	melting point
NaOH	sodium hydroxide
NH_4Cl	ammonium chloride
NMR	nuclear magnetic resonance
Pet ether	petroleum ether (50-70^o C)
Pd/C	palladium on carbon catalyst
ppm	parts per million
RCM	ring closing metathesis
RMSD	root mean square deviation (in modelling)
rt	room temperature
SAR	structure activity relationship
s	singlet (in NMR)
SO_2Cl	thionyl chloride
SO_3.Pyr	sulfur trioxide-pyridine complex
t	triplet (in NMR)
TFA	trifluoroacetic acid
THF	tetrahydrofuran
TLC	thin layer chromatography

ACKNOWLEDGMENTS

Firstly I would like to thank my supervisor Professor Andrew Abell for his guidance throughout my PhD and especially for his tireless reading and advice during the process of writing.

Thank you to the many people who provided invaluable assistance throughout my PhD especially: Bruce Clark, Robert Stainthorpe and Marie Squire (mass spectrometry); Rewi Thompson and John Blunt (NMR); the Lincoln crew (Jim Morton, Matt Muir, Hannah Lee and Karl Gately); members of the Abell Group: Nathan and Matt for managing to read through the many drafts of my thesis without falling asleep; Steve and Wanting Jiao for modelling many of my compounds; and Kelly, Anna, Andrea and Shazia who helped keep things in perspective and were always ready for a coffee break!

To my many friends, who thought I was going to be an eternal student…. I'm finally done; and especially for Jess, Tamati, Connie and Suzy, who were always willing to put up with me complaining that I'd never finish, thanks so much for your encouragement and distractions – I'll finally be able to spend some time with you again.

I would like to thank my parents, Chris and Jean, for their never-ending encouragement and love; also Trevor and Virgina, the 'dreaded' in-laws, for making me one of the family and looking after me so well.

And finally, for Antony, thank you, thank you, thank you for your patience, love, support and encouragement. Love you forever babe xx.

CHAPTER ONE

Introduction to Cysteine Proteases

1.1 OVERVIEW OF PROTEASES

Proteases account for approximately 2% of the genes in most organisms, second in number only to transcription factors.[1] Because of this, proteases have long been the subject of intensive research.[2] Proteases are involved in numerous physiological processes that include food digestion, cell maintenance, cell signalling, wound healing, cell differentiation and cell growth.[3] Breakdown in the control of protease activity leads to undesired and unregulated proteolysis. This is the cause of many diseases, such as Alzheimer's disease, stroke, cancer, viral infections and cataracts,[4] thus inhibitors of proteases have the potential to provide successful therapeutics for a wide range of diseases.

The purpose of this chapter is to provide an overview of proteases (in particular the cysteine proteases); discussing roles in normal physiology and disease, the structure of active sites, and requirements for effective inhibition. Attention is focused on the family of cysteine proteases, particularly the calpains, cathepsin B and papain (representative cysteine proteases, see **Table 1.1**). This chapter will conclude with a section on the design of cysteine protease inhibitors.

Clan	Family	Proteases	Occurrence
CA	C1A (CL-like)	Papain	Plant
		Cathepsin L	Mammals
		Falcipains	*Plasmodium flaciparum*
		Rhodesian	*Trypanosoma brucei rhodesiense*
		Cruzain	*Trypanosoma cruzi*
	C1B (CB-like)	Cathepsin B	Mammals
	C2	Calpains	Mammals
CD	C14	Caspases	Mammals
CL	C60	Sortases	*Staphlococcus aureus*
PA	C3A-C3G	Picornaviral proteases	HRV, HAV
	C30	Coronaviral main proteases	TGEV, SARS-CoV

Table 1.1 Classification of cysteine proteases. HRV human rhinovirus, HAV hepatitis A virus, TGEV transmissible gastroenteritis virus, SARS-CoV sever acute respiratory syndrome coronavirus[5]

1.2 CLASSIFICATION OF PROTEASES

There are currently six known classes of proteases: serine, threonine, cysteine, aspartic acid, glutamic acid and metallo- proteases (S, T, C, G, M, A). The most widely recognised system of enzyme classification defines proteases by 1) catalytic mechanism, 2) structure (clans and families) and 3) individual protease.[6,7]

Catalytic mechanism

Proteases are primarily categorised according to catalytic centre composition, as the make-up of the active site residues determines the mechanism of peptide bond hydrolysis.[8] There are two fundamentally different catalytic mechanisms for hydrolysis. For serine, threonine and cysteine proteases, the key catalytic nucleophile is an intrinsic component of the active site (the residue being Ser, Thr or Cys respectively), while aspartic acid, glutamic acid and metallo proteases use an activated water molecule as the nucleophile.[9,10]

Structure

Clans are defined as groups of proteases that have arisen from a single origin and are based on the similarity of tertiary structures, with each clan representing an homologous set of proteases.[11] Clans may be composed of more than one class of protease as illustrated by the clan PA which contains examples of both serine and cysteine proteases. Within each clan, families are identified by a letter that represents the type of hydrolysis it catalyses followed by a unique number (1, 2, 3…).[12,13] **Table 1.1** above outlines the classification of cysteine proteases, the main topic of this thesis.

Individual Protease

Finally, proteases are defined to be individual and distinct if specificity and sensitivity to inhibitors is different, they are of different catalytic types or are encoded by different genes within the same organism.[14]

These three guidelines provide a unique code for all known proteases that allows inter-relationships to be studied.

1.3 CYSTEINE PROTEASES

Cysteine proteases are widely distributed throughout nature, having been found in viruses, bacteria, protozoa, plants, mammals and fungi.[8] There are three structurally distinct clans of cysteine proteases: the papain family, the caspases and the picornaviridae family. The majority of cysteine proteases known to date are members of the papain family.[15]

One of the biggest challenges faced in the design of specific cysteine protease inhibitors is the similarity in structure that exists within clans (for example clan CA, containing papain-like proteases). Effort towards identifying inhibitors that are specific for individual cysteine proteases is essential for the design of effective therapeutic drugs.

1.3.1 Cysteine Protease Active Sites

The active site of cysteine proteases consists of a) a catalytic triad (Cys, His and Asn) that is responsible for hydrolysis of the peptide bond (**Figure 1.1**) and b) subsite binding pockets where orientation of the substrate for catalysis occurs via interaction between subsites of the enzyme and amino acid residues of the substrate (**Figure 1.2**).

Mechanism of Proteolysis

The cysteine and the histidine of the catalytic triad form a thiolate-imidazolium ion pair which confers high nucleophilicity upon the cysteine thiol. Under these conditions the cysteine thiol acts as a nucleophile to hydrolyse the scissile bond of the substrate. The overall mechanism of substrate hydrolysis shown in **Figure 1.1** occurs in four steps. The initial tetrahedral intermediate (b) is stabilised by hydrogen bonding to Cys_{25} and Gly_{19} which make up the oxyanion hole (a) followed by acylation of the enzyme and release of the *C*-terminal substrate fragment. Hydrolysis of the acyl-enzyme forms a second tetrahedral intermediate (c). Collapse of this intermediate regenerates the free enzyme and releases the *N*-terminal substrate fragment (d).[15]

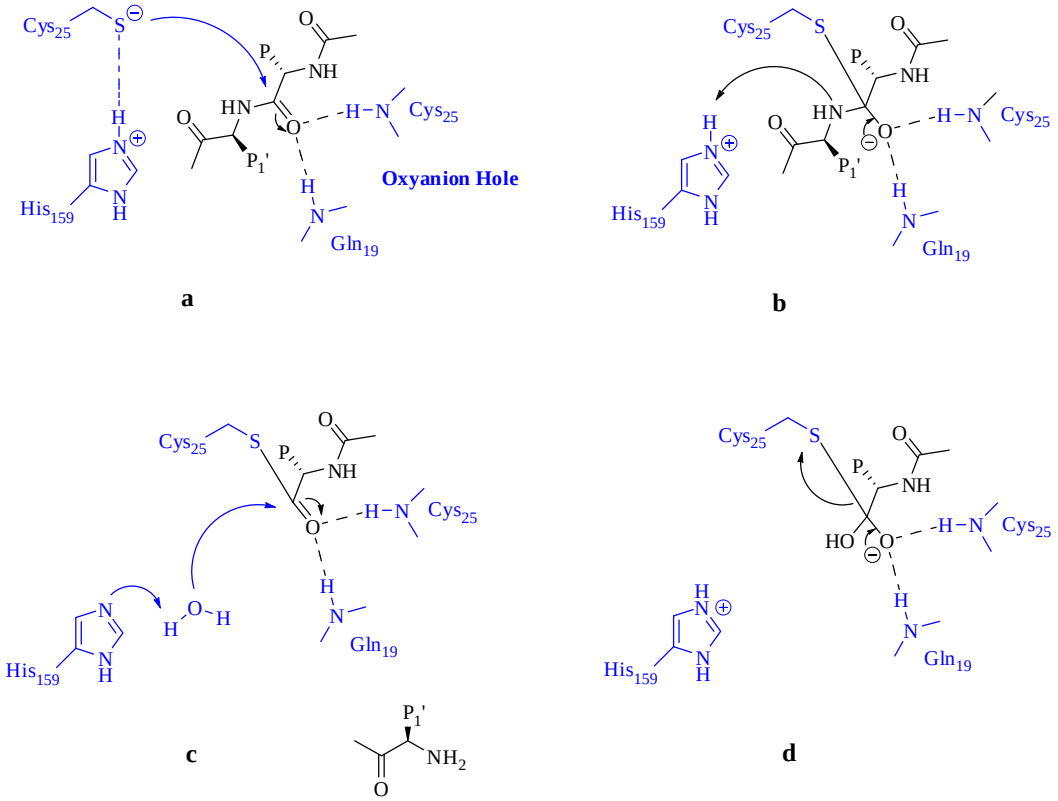

Figure 1.1 Proposed mechanism of hydrolysis by cysteine proteases (enzyme residues in blue)

Binding pockets

The nomenclature used for defining the binding pockets and selectivity of proteases is based on the notations of Schechter and Berger[16] (**Figure 1.2**) and is relative to the site of cleavage (scissile bond). S_n represents the enzyme subsites (pockets) and P_n the amino acid side chains bound in these positions. The properties of S_n and $S_{n'}$ for a given protease govern the binding of P_n and $P_{n'}$ residues, thus the choice of amino acid residues is dependent upon the target protease.

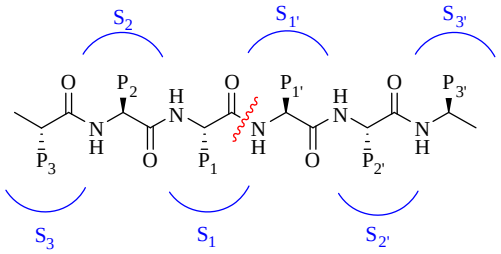

Figure 1.2 Standard Schechter and Berger nomenclature for substrate residues and corresponding binding sites.[16] Red line denotes the scissile bond.

Peptidase Activity

Proteases can show exopeptidase or endopeptidase activity towards substrates. Exopeptidases are proteases that hydrolyse an amino acid from the end of a polypeptide chain while endopeptidases hydrolyse a peptide bond within a polypeptide chain (see **Figure 1.3**).[17] Some proteases (such as cathepsin B) exhibit both modes of cleavage.

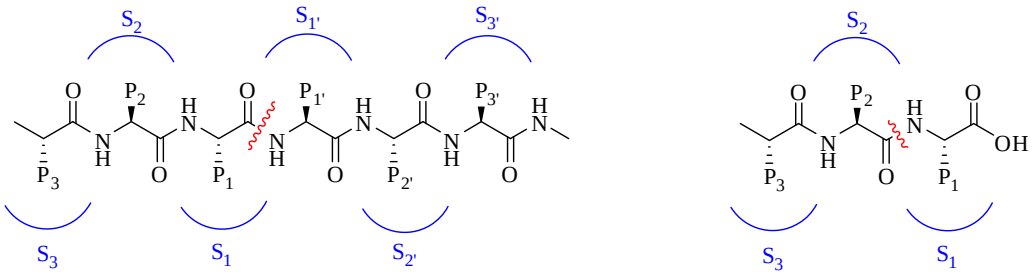

a **b**

Figure 1.3 a) endopeptidases cleave within a peptide chain and b) exopeptidases at the end of a peptide chain

1.4 THE PAPAIN SUPERFAMILY

Papain-like cysteine proteases (henceforth referred to as the papain superfamily)[18] belong to clan CA and include cathepsin B and calpains (refer to **Table 1.1**).[19] Cysteine proteases of the papain superfamily have been implicated in numerous diseases and cellular processes and are thus attractive targets for therapeutic drugs.[11] The high degree of conservation of structure within proteases of the papain superfamily (clan CA) means that the design of selective inhibitors has long proven a challenge for the synthetic chemist.[11] Better understanding of the differences between active site specificities of cysteine proteases will aid the development of therapeutic drugs for the diseases associated with specific cysteine proteases, thus cathepsin B (CA.C1B) and calpains (CA.C2) were chosen as representatives of each family within the clan CA for investigation. Papain, as the archetypal protease of the papain superfamily, was important for this investigation as all other members of the clan CA are closely related to it. Cathepsin B and the calpains are involved in many diseases (specified in following sections) that currently have few therapeutic treatments, thus an increased understanding of selectivity within the papain superfamily will aid the treatment of diseases associated with these proteases. Papain, cathepsin B and calpain will be discussed in turn in the following **Sections 1.4.1-1.4.3** with regard to structure, function and role in disease (see **Table 1.2**).

Chapter	Section	Focus of discussion
1	**1.4.1**	Papain: structure, specificity, function and role in disease
1	**1.4.2**	Cathepsin B: structure, specificity, function and role in disease
1	**1.4.3**	Calpain (m- and μ-): structure, specificity, function and role in disease
1	**1.4.4**	Structural homology between papain, cathepsin B and the calpains (m- and μ-)
1	**1.5**	Design of cysteine protease inhibitors
1	**1.6**	Contents of this thesis

Table 1.2 Structure for the remainder of Chapter One.

1.4.1 Papain

Papain is a plant protease isolated from *Carica papaya* (papaya latex).[8] It has a monomeric polypeptide structure[6] with a molecular weight of around 23 kDa and consists of 212 amino acid residues with three disulfide bridges (Cys_{22}-Cys_{63}, Cys_{56}-Cys_{95} and Cys_{153}-Cys_{200}). The polypeptide chain is folded into two domains, the L-domain consisting of residues 10-11 and 207-212 while the R-domain is made up of the remaining residues.[20] The two domains (L and R) are separated by a cleft which contains the active site thiol (Cys_{25}) positioned at the entrance of the α-helix (residues 24-42) on the L-domain. On the opposite side of the cleft (R-domain) but still in close proximity is a His_{159} residue. The His_{159} residue is positioned to act as the base catalyst for activation of the thiol group during peptide hydrolysis. The last member of the catalytic triad (Asn_{175}) is thought to orientate His_{159} for interaction with Cys_{25},[15] resulting in the activation of both the His_{159} and Cys_{25}. The backbone NH group of Cys_{25} and the side chain NH_2 group of Gln_{19} (both hydrogen bond donors) form the oxyanion hole (see **Figure 1.4**) for binding substrate and promoting reactivity for nucleophilic attack.[21] The *N*-terminal domain (L) consists of a

bundle of α-helices while the *C*-terminal (R) domain contains a β-barrel. A long helix runs through the middle of the molecule. The catalytic cysteine is at the start of this helix (see **Figure 1.5**).

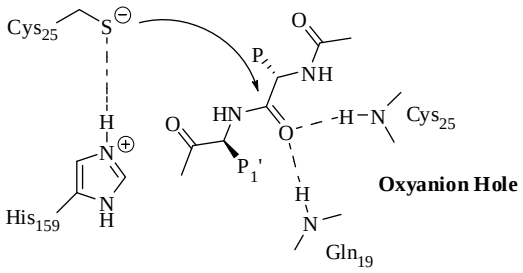

Figure 1.4 The oxyanion hole of papain

Typically, papain is isolated in an inactive form (known as a zymogen or pro-enzyme)[17] in which the active site is blocked by a disulfide bond between the active site Cys_{25} and Cys_{22} (in the active form, this disulfide bond links the Cys_{22} and Cys_{63} residues). This inactive form of papain is essential for forming the correct quaternary structure of the enzyme before it is activated. [8] Activation of papain occurs via either disulfide exchange with thiol reagents or reducing agents.[8]

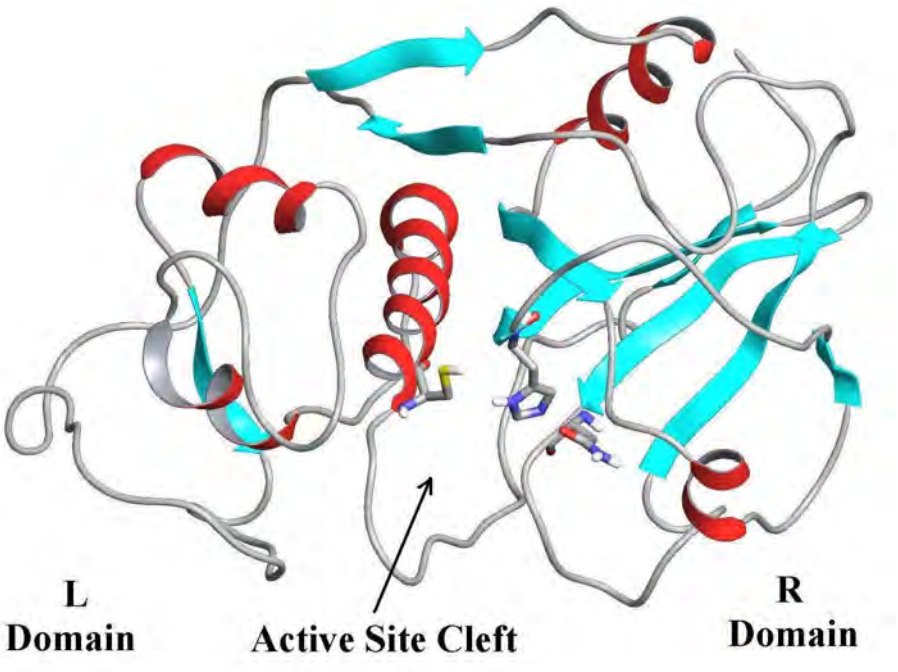

Figure 1.5 Crystal structure of papain showing secondary structure (α-helices in red and β-sheets in aqua). Catalytic residues are shown in ball-and-stick representation, Cys_{25} His_{159} and Asn_{175}. (PDB 1PPP)

Specificity

Papain exhibits endopeptidase, amidase and esterase activities. The active site of papain consists of the subsites S_1-S_4 and $S_{1'}$-$S_{3'}$ (seven in total).[8] The S_2 subsite of papain is the most important primary substrate recognition site of the protease and is defined by the residues Tyr_{69}, Tyr_{67}, Phe_{207}, Pro_{68}, Ala_{160} Val_{133} and Val_{157}. The other subsites of papain are not as well defined or as strict in amino acid preferences.[22]

The preferred amino acids at the S_2 subsite are those with bulky nonpolar side chains, such as Phe. This was utilised by Menard[23] who, with a fluorogenic peptide fixed at the P_2 position (with a Phe residue), varied the amino acid at the $P_{1'}$ position and identified the specificity of $S_{1'}$ subsite of papain. The results of Menard's study[23] have been graphed according to amino acid properties, namely hydrophobicity (non-polarity), polarity, acidity and basicity (see **Figure 1.6**). It is apparent that amino acids with large nonpolar side chains are the most readily hydrolysed (Leu, Ala and Phe).

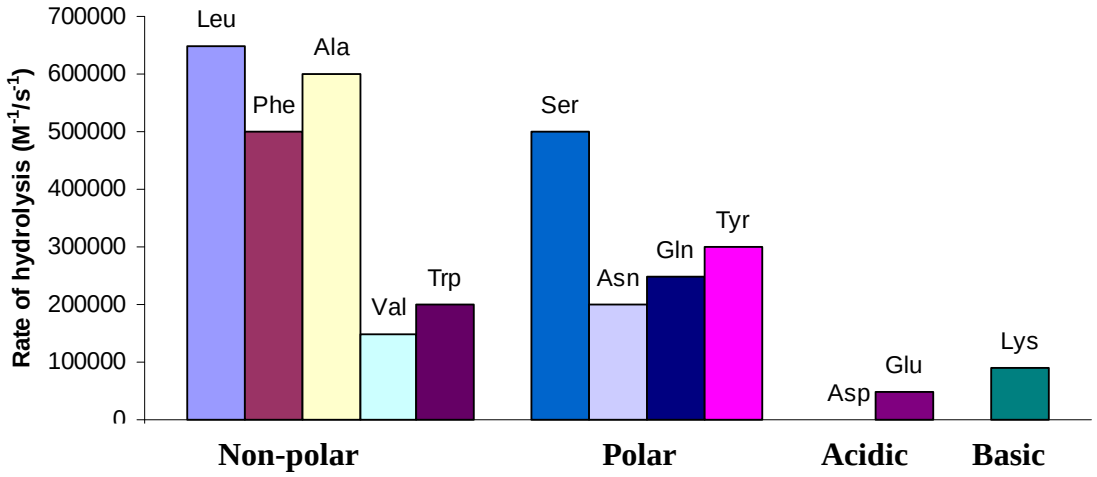

Figure 1.6 Specificity of $S_{1'}$ subsite of papain

Hydrogen bonding of substrates to the active site cleft

The active site cleft of papain runs along the interface of the two domains in a V-shaped valley (see **Figure 1.7**). This cleft is broad but narrows around the active site. A crystal structure of papain with leupeptin bound[24] shows the critical hydrogen bonds that are formed. The Gly_{66} residue on the L-domain forms two critical hydrogen bonds (A and B as shown in **Figure 1.8**) while the backbone carbonyl of Asp_{158} residue also participates by forming hydrogen bond C to the substrate.

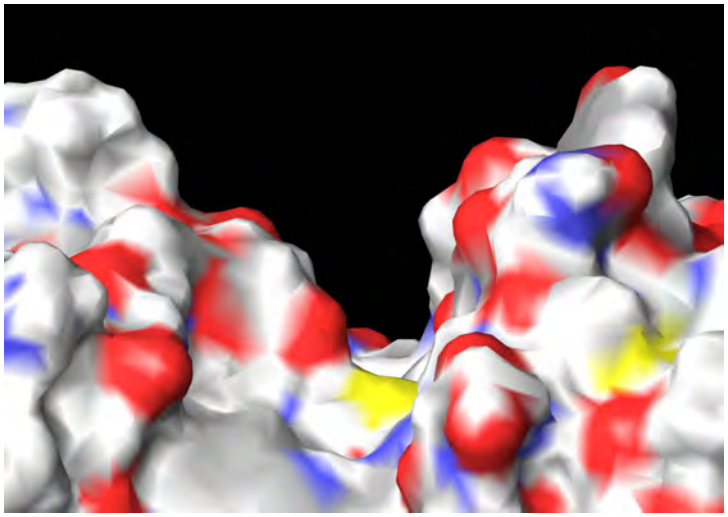

Figure 1.7 Surface diagram of the active site cleft of papain. The active site is a V-shaped valley where the L and R domains meet. The active site cysteine is shown in yellow at the base of the cleft (PDB 1PPP)

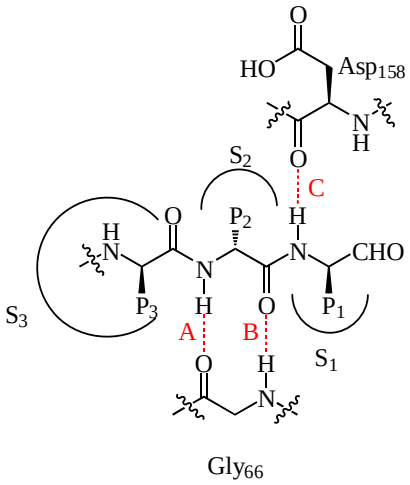

Figure 1.8 Hydrogen bonding to the active site cleft of papain

Function and disease states of papain

The large quantities of papain found within *Carica papaya* and its general specificity toward substrates suggest it has a protective role, guarding the plant against pests.[6] Papain is not thought to be involved in any human diseases as it is only expressed in plants.

1.4.2 Cathepsin B

Cathepsin B is initially synthesised in an inactive form comprising 314 amino acid residues. Amino acids 1-62 at the *C*-terminal end are essential for correct folding and stabilisation of the protease. These 62 residues are subsequently cleaved to liberate the active enzyme.[25] The mature, active cathepsin B enzyme is a polypeptide chain of 252 residues[26] (two chains consisting of 47 and 205 amino acid residues respectively[27]) showing close structural homology to papain. About 166 amino acid residues of cathepsin B are equivalent to those in papain.

Active cathepsin B is a 30 kDa bilobal protease that is disc shaped (diameter 50 Å, thickness 30 Å) with access to the active site via a large cleft on the top of the molecule.[27] The quaternary structure of cathepsin B is reminiscent of papain, being folded into two distinct domains. The active site cleft is located at the interface of the two lobes (domains). The left-hand (L) domain comprises the *N*-terminal half of the polypeptide chain (residues 11-148) while the R domain is made up of residues 1-10 and the *C*-terminal part (residues 149-252) of the chain (see **Figure 1.9**).

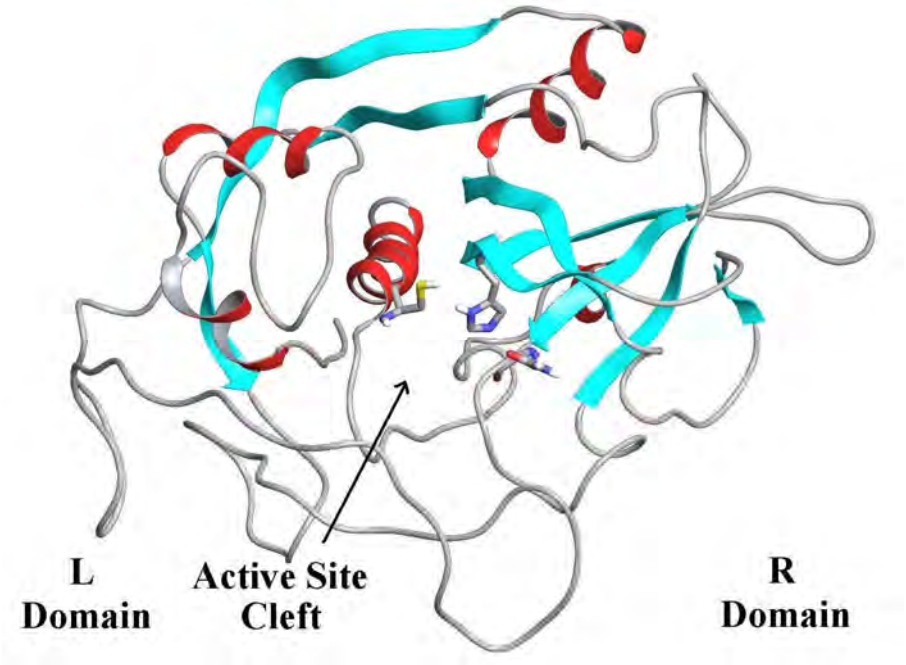

Figure 1.9 Crystal structure of Cathepsin B showing secondary structure (α-helices in red and β-sheets in aqua). Active site in ball-and-stick representation: Cys_{29}, His_{199} and Asn_{219}. Occluding loop indicated by red box (PDB 1ITO)

The structure of the L-domain of cathepsin B is predominantly defined by three central α-helices equivalent to those found in papain and other plant proteases. The section of polypeptide chain from Ile_{105} to Pro_{126} represents a novel structural feature known as the occluding loop (see **Figure 1.10**). This occluding loop is a covalently closed section of the polypeptide chain that partially blocks access to the active site; the boundary of the occluding loop is defined by a disulfide bridge between Cys_{108} and Cys_{119}.

It is this occluding loop that confers exopeptidase activity upon cathepsin B due to the presence of the positively charged histidine residues (His_{110} and His_{111}) that can accept a negative charge at the *C*-terminus of the substrate. The flexibility of the occluding loop allows it to adopt another conformation, in which it no longer blocks the binding cleft; in this conformation cathepsin B acts as an endopeptidase.[25,28,29] The *C*-terminal half of the chain (R-domain) has a barrel-like structure formed by six extended strands aligned in a β-sheet. The residues Asn_{219} to Gly_{229} form the support for the occluding loop.

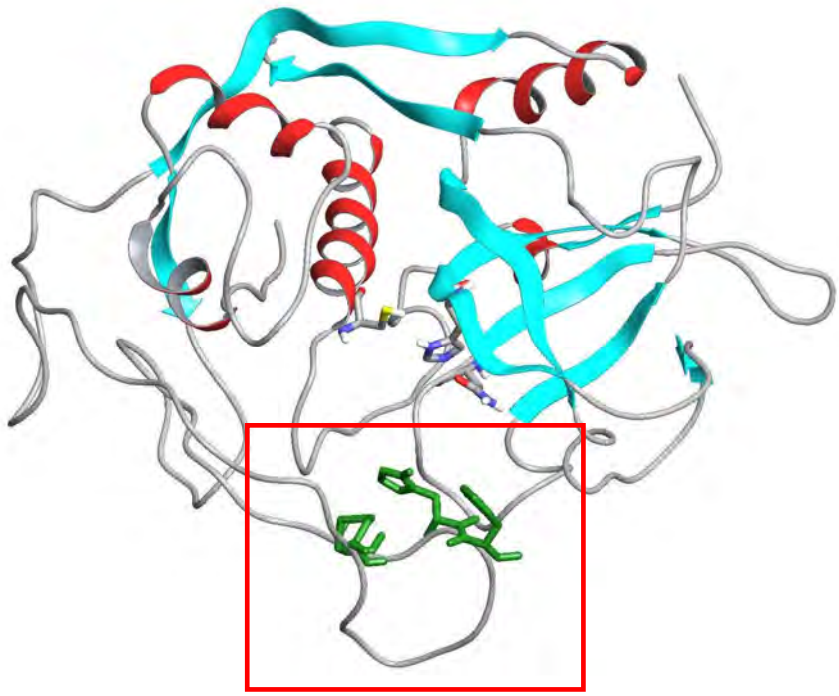

Figure 1.10 Crystal structure of Cathepsin B showing the occluding loop (in red box). The His_{110} and His_{110} (green, left side of loop) and the disulfide bridge (green, right side of loop) of the occluding loop are also shown. (PDB 1ITO)

The active site of cathepsin B is much like that of papain, with the S_2 subsite comprised of the residues Trp_{221}, Gln_{23}, His_{199}, Ala_{200} and Ala_{173}. The active site residues Cys_{29} (Cys_{25}

in papain) and His_{199} (His_{159}) are on opposite sides of the cleft[7] (as in papain) but close enough to interact, forming an ion-pair at a pH range of 4.0-8.5. The pH within a biological system also has a determining role in whether cathepsin B displays endopeptidase or exopeptidase activity. The stability of the occluding loop is pH dependent, giving rise to endopeptidase activity at neutral pH (membrane) and exopeptidase activity at acidic pH (lysosomes), thus the location of cathepsin B determines the substrate specificity.[28]

Specificity

Cathepsin B has broad substrate specificity, showing only a slight preference for basic residues and Phe at the P_2 position, while bulky side chains are disfavoured at P_1.[30] Menard's study[23] of the preferred residues for $P_{1'}$ of papain (as previously described) also included a study of cathepsin B preferences. These results (see **Figure 1.11**), graphed according to amino acid properties (hydrophobicity, polarity, acidity and basicity), indicate that cathepsin B prefers amino acids with large hydrophobic side chains, such as Trp, Tyr, Phe, Val and Leu, at the $P_{1'}$ position. The $S_{1'}$ pocket of cathepsin B has a broader specificity than that of papain which preferentially accepts only Phe, Leu and Ala (refer to **Figure 1.6**). This suggests that inhibitors with good binding affinity for papain will also bind well in the active site of cathepsin B, making the design of specific inhibitors a challenge.

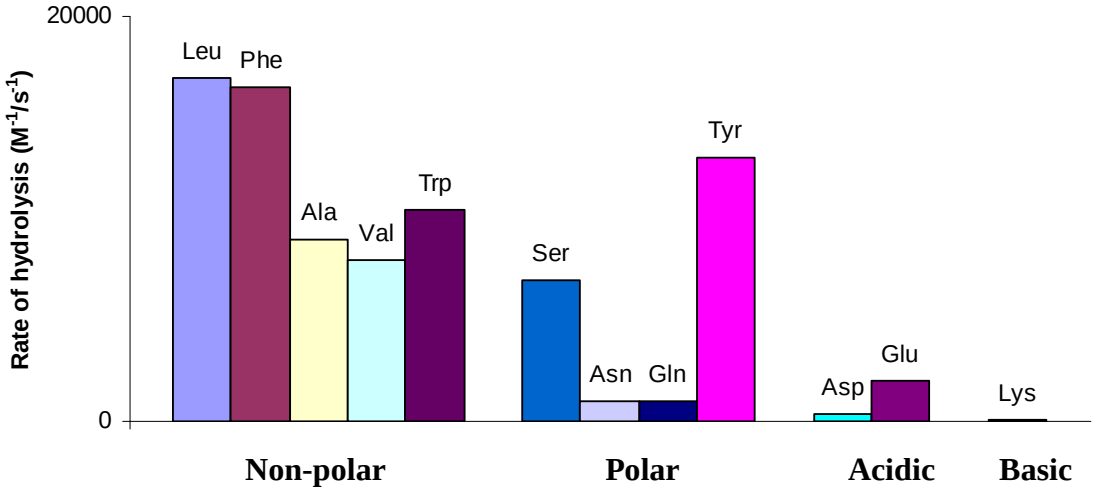

Figure 1.11 Specificity of $S_{1'}$ subsite of cathepsin B

Hydrogen bonding of substrates to the active site cleft

The active site cleft of cathepsin B is slightly narrower than that of papain (see **Figure 1.12**). Jia *et al*[31] published a crystal structure of cathepsin B* with a chloromethyl ketone inhibitor bound. This crystal structure suggested that only the hydrogen bonds B and C (as denoted in **Figure 1.13**) were formed.[31] Gly_{74} (topologically identical to Gly_{66} in papain) forms the hydrogen bond B and Gly_{198} the hydrogen bond C. It is assumed that if a crystal structure of cathepsin B with leupeptin bound was available, hydrogen bond A would also be formed.

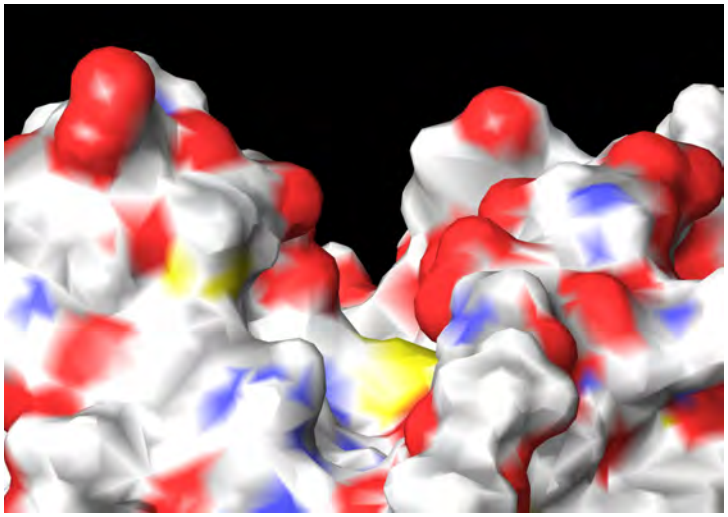

Figure 1.12 Surface diagram of the active site cleft of cathepsin B. The active site is a cleft between the L- and R-domains of cathepsin B. The active site cysteine is shown in yellow at the base of the cleft (PDB 1POP)

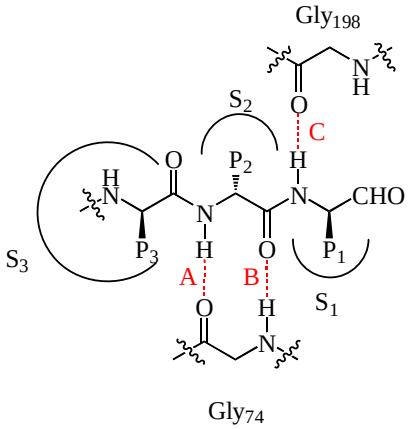

Figure 1.13 Hydrogen bonding to the active site cleft of cathepsin B

* 22 crystal structures of cathepsin B, with and without inhibitors bound can be found on the protein data base: www.rcsb.org/pdb/home/home.do

Role in Physiology and Disease

Cathepsin B is found ubiquitously throughout tissues, suggesting it has an essential function. Its presence in the lysosomes implies a role in protein degradation as the lysosomes are the organelles responsible for digesting waste and recycling products.[26] Other roles of cathepsin B are proposed to include remodelling of the extracellular matrix, wound healing, bone remodelling and apoptosis.[28,32]

Cathepsin B is implicated in a number of pathological states, some of which include: inflammatory airways diseases, bone and joint disorders, acute pancreatitis, tumour metastasis, Alzheimer's disease and ischemic neuronal death.[11,25,33,34] The role cathepsin B plays in these diseases is summarised in **Table 1.3**. The design of specific inhibitors for cathepsin B is considered important for chemotherapy and other cancer treatments.

Disease	**Proposed Cathepsin B Disruption**	**Ref**
Inflammatory Airways Disease	Secretion of cathepsin B by bronchial epithelial cells and activated by Neutrophil Elastase	25
Bone and Joint Disorders	Breakdown of the cartilage extracellular matrix occurs via cathepsin B activated metalloproteinases	25
Acute Pancreatitis	Cathepsin B rapidly activates trypsin which can activate pancreatic enzymes that damage the pancreas	25
Tumour Metastasis	Increased expression and secretion of cathepsin B in tumours	11,28,33,34
Alzheimer's Disease	Cathepsin B is associated with amyloid plaques in Alzheimer's Disease brains. Insufficient activity proposed to promote Alzheimer's	28,35

Table 1.3 Role of cathepsin B in some disease states

1.4.3 Calpains (m- and μ-)

Calpains are calcium-activated neutral cysteine proteases that are ubiquitous and intracellular in distribution within biological systems. Two major isoforms have been identified (m- and μ-) that differ in the requirements of calcium concentration for activation (mM and μM amounts respectively). m-Calpain and μ-calpain are of interest in this thesis due to an important role in the development of cataract (this topic is discussed in detail below).

The calpains (m- and μ-) are heterodimers comprising two distinct subunits: the large highly homologous 80 kDa subunit and the common small 30 kDa subunit. The large subunit of μ-calpain is usually slightly heavier than the corresponding m-calpain large subunit (81.9 kDa compared with 79.9 kDa respectively),[3] but in both calpains it consists of four domains (I-IV); domains V and VI make up the small subunit of m-calpain and μ-calpain (see **Figure 1.14**). Domain I is a single α-helix that plays a role in stabilising and activating the enzyme. The amino acid sequence has no homology with any known polypeptide.[3] Domain II contains the active site and is generally divided into two subdomains IIa and IIb. The active site Cys_{105} resides on IIa, while the His_{262} and Asn_{286} which complete the catalytic triad are on IIb (see **Figure 1.15**).

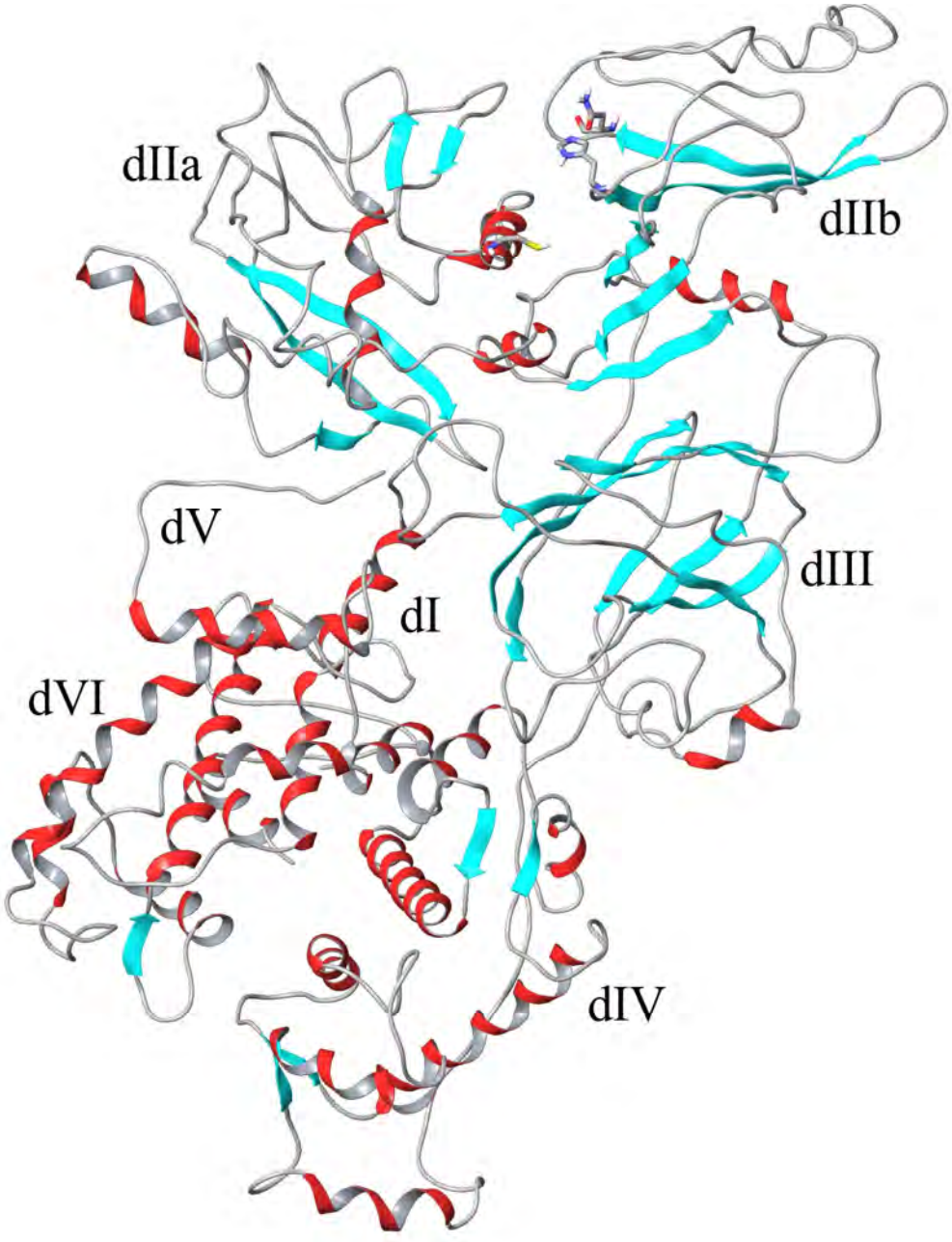

Figure 1.14 The structure of m-calpain. Secondary structure is depicted: α-helices in red, β-sheets in aqua. The domains are annotated (PDB 1KFU)

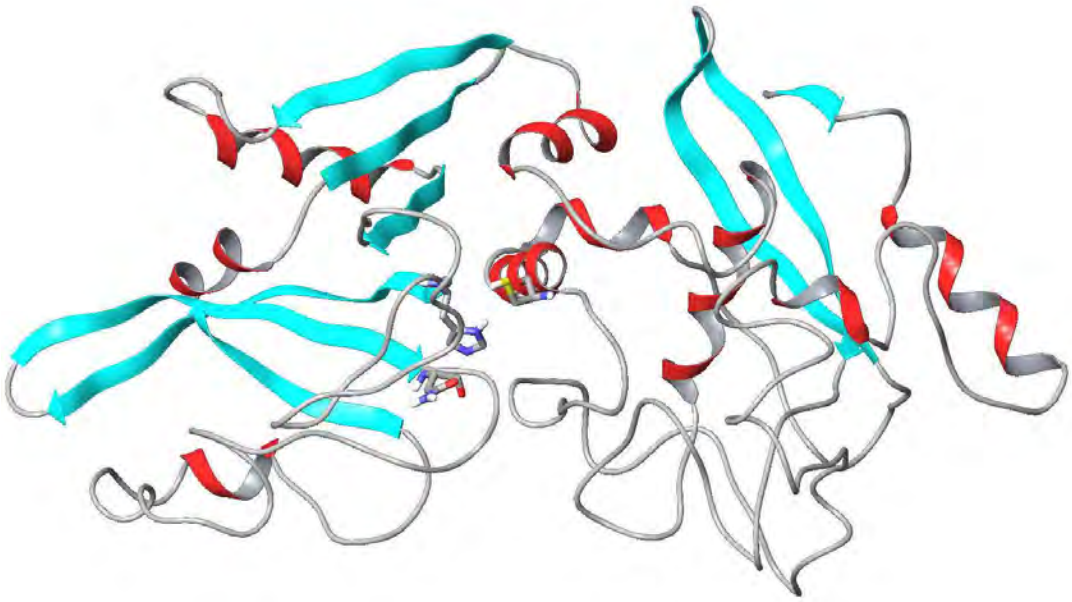

Figure 1.15 Crystal structure of the domain IIa and IIb of μ-calpain (calcium bound).[36] Active site in ball-and-stick representation: Cys_{115}, His_{272} and Asn_{296}. (PDB 1TLO)

The calpains are unique among cysteine proteases in having an absolute requirement of calcium for activation.[37] The importance of calcium binding for activation was highlighted by Moldoveanu *et al*,[38,39] who established that the binding of calcium ions to calpain results in a conformational change to the active site of the enzyme. The catalytic Cys_{105} is 8.5 Å removed from His_{262} in the absence of calcium, too great a distance for formation of the active catalytic triad. Binding of calcium to calpain induces a conformational change that reduces the distance between the Cys_{105} and His_{262} to 3.7 Å, a distance at which interactions are possible (see **Figure 1.16**).

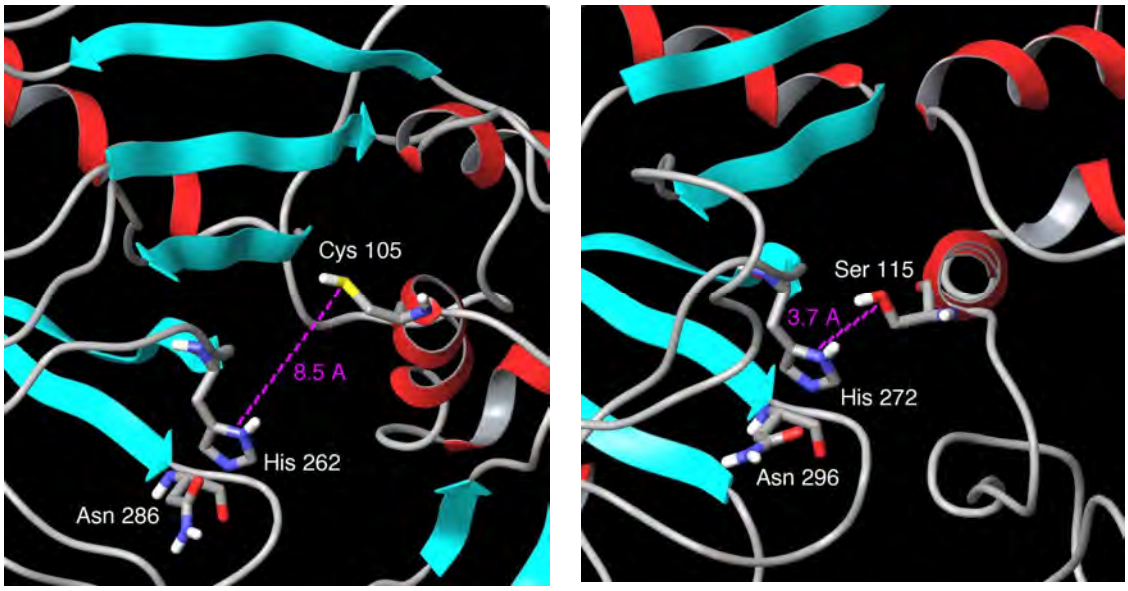

Figure 1.16 Arrangement of the active site without calcium bound (left) and with calcium bound (right)

The calcium binding sites are located on domains IV and VI in the form of EF-hand structures (see **Figure 1.17**). EF-hand motifs are defined by a helix-loop-helix structure. A calcium ion binds in the loop region of the EF-hand as shown in the **Figure 1.17**. Domains IV and VI each have five EF-hand motifs, of which eight bind calcium. One EF-hand motif from each of domains IV and V interact, forming a link between the large and small subunits respectively. Domain III comprises 8 β-strands that are shaped into a β-sandwich structure. This domain is most likely responsible for the translocation of calpain to the membrane (a process which is calcium dependent). Domain V comprises one half of the S subunit and contains clusters of Gly residues which contributes to the overall hydrophobic nature of calpain.[40]

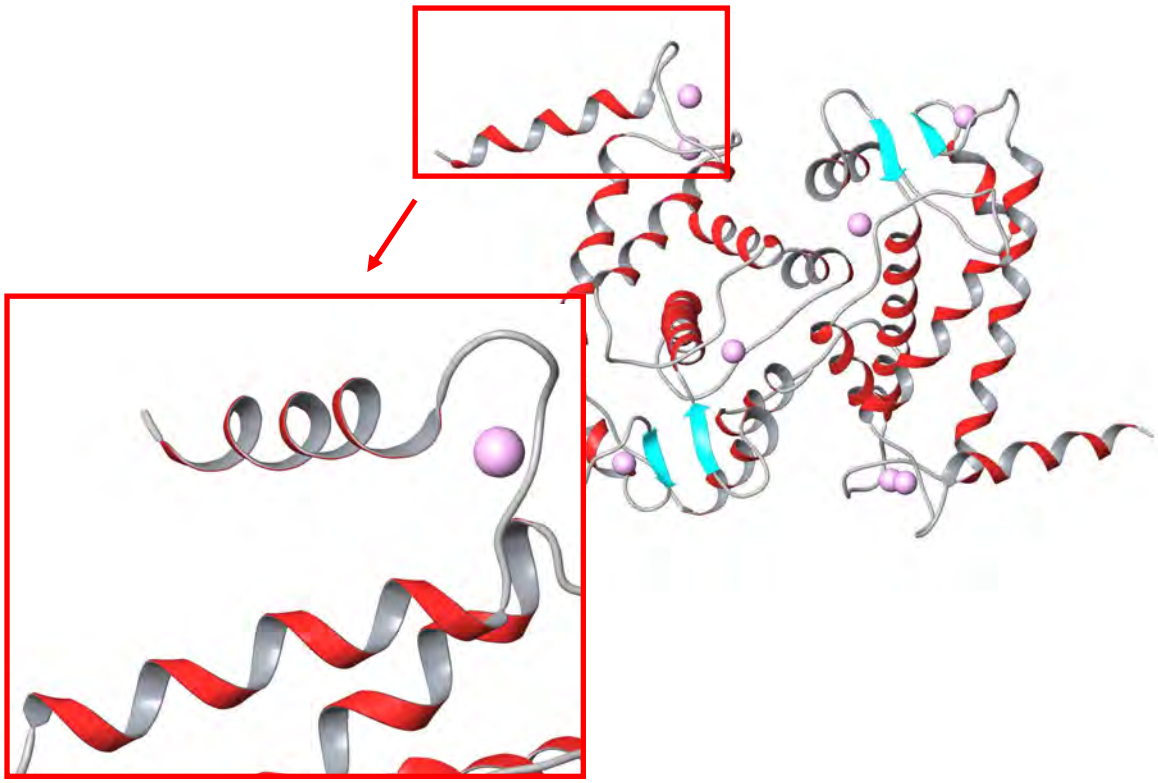

Figure 1.17 Domain IV of calpain with calcium ions bound (pink). A single EF-hand is inset. (PDB 1DVI)

The overall topology of calpain is highly conserved relative to that of papain (and thus cathepsin B). A loop containing four Tyr residues (Tyr_{297}, Tyr_{304}, Tyr_{325} and Tyr_{356}), unique to calpains, is thought to be important for the formation and conformation of the calpain catalytic domain. The *N*- and *C*- terminal portions of this loop are highly conserved among calpains and contain acidic residues. The calcium requirement of calpain activation has been ascribed to this region.[40]

Specificity

Calpains m- and μ- have limited and specific subsite specificity. This is supported by the finding that cleavage of proteins by calpain results in large polypeptide fragments rather than small peptides or amino acids thus suggesting that calpains only cleave at limited sites.[3] The specificities of m- and μ-calpain are very similar if not identical.

Several reviews[41-43] on calpain inhibitors have shown 1) that bulky aromatic groups are most favoured at P_3; 2) the P_1 position favours Leu over other amino acids and 3) the P_2

position requires an amino acid with a side chain able to form a hydrogen-bond. [36] A Leu or Val residue in the P_2 position is favourable, but as a variety of amino acids are accepted, this is not a strict requirement. Thus the S_2 subsite of calpain has only a marginal effect on specificity.[3] Cuerrier *et al*[44] performed a subsite preference study using recombinant μ-calpain (similar to Menard's[23] study of papain and cathepsin B). This study indicated that μ-calpain has a preference for Ala and Met in the $P_{1'}$ position (these results are assumed to hold true for both natural μ-calpain and m-calpain). The results obtained are depicted in **Figure 1.18** where it is apparent that calpain has a preference for large non-polar side chains, furthermore, the basic amino acids Lys and Arg are favoured, which is significantly different from papain and cathepsin B.

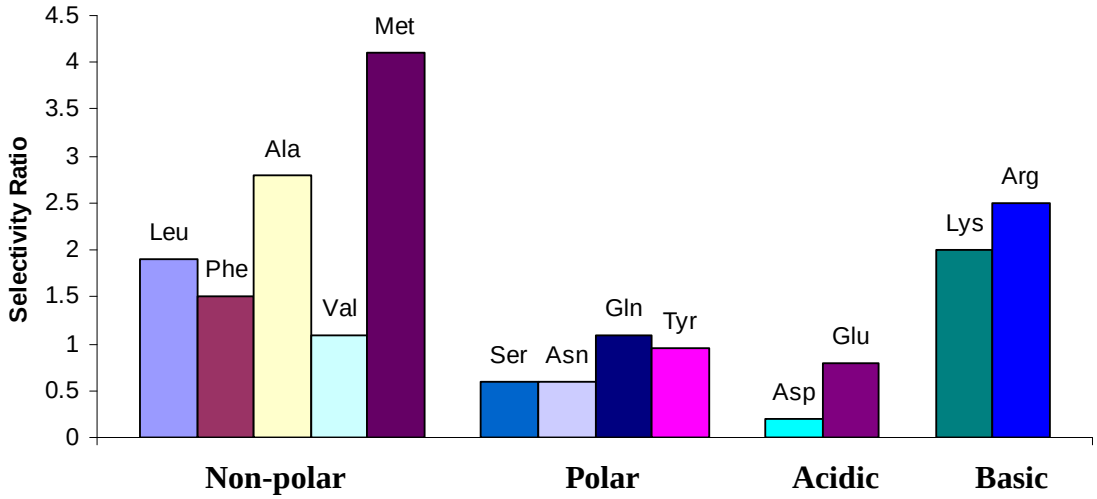

Figure 1.18 $S_{1'}$ specificity of μ-calpain

Hydrogen bonding of substrates to the active site cleft

In the case of calpain, having the polypeptide substrate in a bioactive conformation that extends along the active site and forms hydrogen bonds with adjacent residues, appears to be more important than the exact amino acid sequence of the substrate. It has been suggested that calpain has a much narrower active site cleft than papain and cathepsin B (see **Figure 1.19**), thus the three defined hydrogen bonds (A, B and C in **Figure 1.20**) are more important for the binding affinity of a substrate.[45]

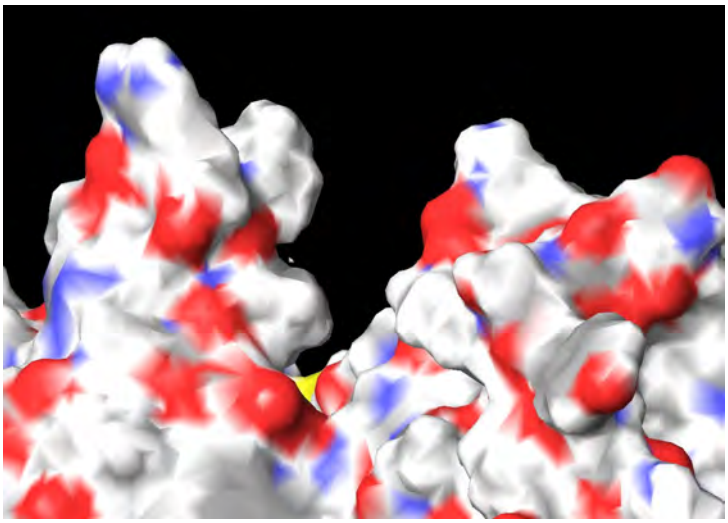

Figure 1.19 Surface diagram of serine mutated μ-calpain active site cleft (1KXR PDB).

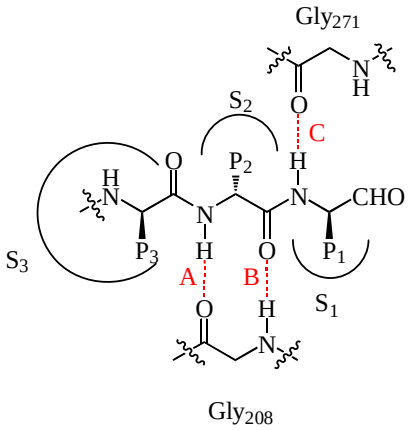

Figure 1.20 Critical sites involved in hydrogen-bonding at the calpain active site.

Physiological Functions

The ubiquitous nature of calpains is highly indicative of a fundamental role in nature. The limited manner in which calpains degrade enzymes suggests that the normal function of calpains m- and μ- is a regulatory or signalling one rather than a digestive role.[46] Calpains are involved in many other cellular functions including cell motility, proteolytic modification of molecules in signal transduction pathways, apoptosis and regulation of gene expression.

The ratios of m- and μ -calpain within different cell types varies greatly. The fact that m- and μ-calpain have similar subsite specificities and virtually identical structures suggests that the two isoforms can perform identical functions. This assumption is strengthened by

the finding that human platelets contain exclusively μ-calpain while bovine platelets contain exclusively m-calpain; the function of the platelets is identical in both species.[3]

Diseases associated with calpains

Disruption to the calpain system is linked to number of degenerative conditions, which include cataract, myocardial infarction, neuronal ischemia, Alzheimer's disease and gastric cancer.[47-51] The role of calpain in these disease states is summarised in **Table 1.4**. The range of diseases with which calpain is associated make it a desirable therapeutic target.

Disease	**Proposed Calpain Disruption**	**Ref**
Cataracts	Calcium influx activates m-calpain, cleaves crystallins into fragments that aggregate	47,52
Myocardial Infarction	Calcium homeostasis is lost in ischemic area which triggers calpain over-activation	48,53,54
Neuronal Ischemia (Stroke)	Calpains participate in apoptosis and necrosis which results in tissue damage in ischemic areas	36,48
Alzheimer's Disease	Increased amount of m-calpain in the cytosolic part of brain	48,49
Obsessive Compulsive Disorder	Patients with obsessive compulsive disorder have significantly elevated calpain activity levels	50
Gastric Cancer	Associated with down regulation of μ-calpain	51,55

Table 1.4 Some of the diseases associated with disruptions to the calpain system.

One disease that has merited much attention over the past 10 years is that of cataract formation.[56] The design of specific calpain inhibitors for the purpose of treating cataract is of special interest as there is currently no pharmaceutical treatment for cataract on the market; surgery is the only intervention available. Research at the University of Canterbury, in collaboration with Lincoln University and Douglas Pharmaceuticals, is currently underway to develop a drug to slow the progression of cataracts to benefit the millions afflicted.

Cataract formation is a well defined example of protease over-activation leading to a pathological state.[57] Defined by Webster as "a clouding of the lens of the eye…that obstructs the passage of light", cataract is the leading cause of blindness in the world.[58] The World Health Organization estimates that of the 37 million people who are blind worldwide, about half are affected by cataract.[59] Cataract surgery is the most frequent operation performed in the United States of America (20 million Americans over 40 years of age are affected; over 1.5 million cataract surgeries)[60] and Australasia.[61] Cataract surgery is successful, with over 80% of patients regaining at least 80% normal sight. There are two disadvantages of cataract surgery: the occurrence of a secondary cataract and the length of time that lapses before surgery. Secondary cataracts arise from the outside layer of the lens, left in place to hold the artificial lens, becoming cloudy. Patients that must wait for surgery often experience significant eyesight deterioration that affects everyday activities, thus a topical or oral treatment for cataract that can be applied while patients await surgery will greatly benefit their quality of life.

There are three main types of cataract, all age-related: cortical, post sub-capsular and nuclear. [61] Cortical cataracts form in the periphery of the lens and account for 24% of all cataracts. Post sub-capsular cataracts are the least common and develop at the back of the lens, affecting vision at a fast rate. Nuclear cataracts, the most common type, develop from the centre of the lens and characteristically cause the lens to become brown in appearance.[61] An inhibitor targeted for calpain should, in theory slow the progression of all three types of cataract. The University of Canterbury, in collaboration with Lincoln University is currently involved in the elucidation of cortical cataract formation, a condition that has been observed naturally within a flock of Romney sheep.

The lens of the human eye is located behind the cornea (**Figure 1.21**) and focuses light on to the retina, adjusting the focus to allow for depth perception.[62] The main structural components of the lens are soluble crystallin proteins (three types: α, β and γ) that are arranged in a highly ordered matrix. The ordered arrangement of crystallins in the lens is fundamental to transparency; fragmentation of the crystallins by calpain and subsequent aggregation and precipitation of insoluble protein fragments results in a change in the refractive properties of the lens. Under these conditions, light can no longer be transmitted through to the retina, but is scattered away from the eye, resulting in impaired vision (see

Figure 1.22). The clouding of the lens (cataract) is the physical result of the proteolysis of the α, β and γ crystallins.[52,63]

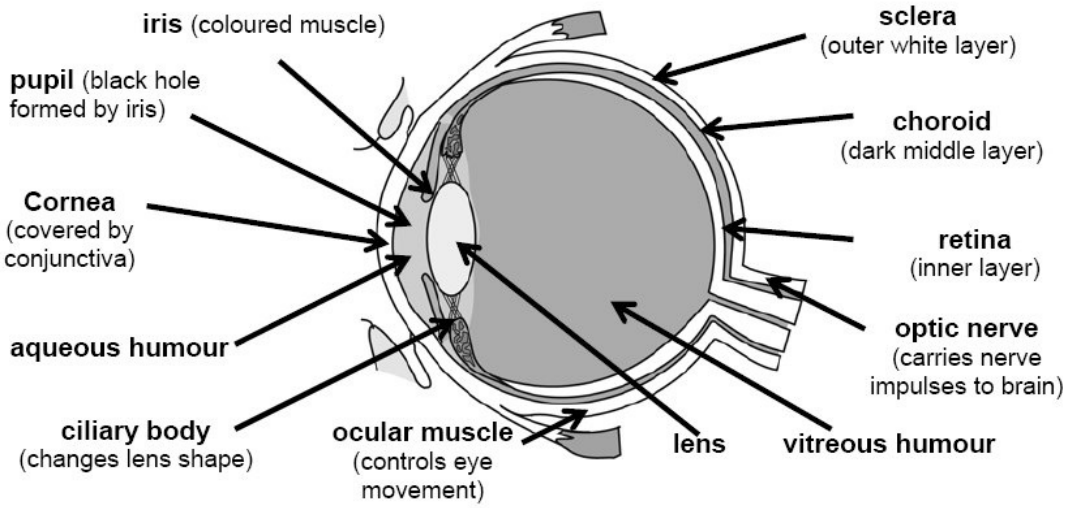

Figure 1.21 Structure of the eye showing the position of the lens within the eyeball[58]

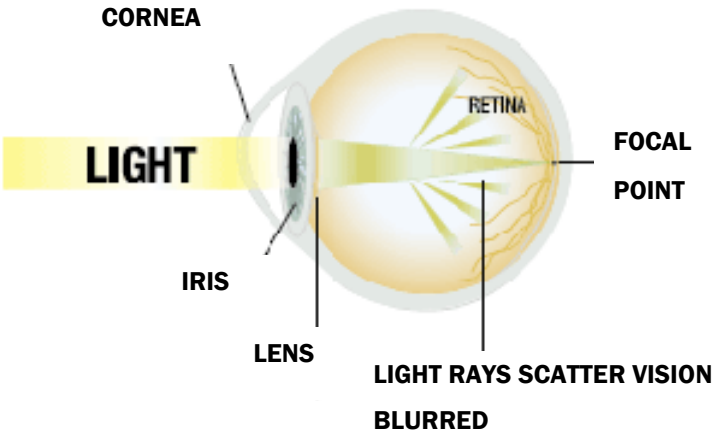

Figure 1.22 The difference in focusing of light between a normal and cataractous lens.

The mechanism of cataract formation is thought to be triggered by injury to the lens, genetics or ageing. Over the human lifetime eyes are exposed to UV light, toxins and free radicals, all of which damage the lens and compromise membrane integrity. Any damage, whether environmental or genetic, allows increased passage of ions, such as calcium, into the lens.[64] The resulting increase in calcium ion concentration leads to the over activation of calpain, which cause excess proteolysis of the crystallins within the lens.[52]

This thesis, through inhibitor design and biological assays, will investigate specificities between proteases of the papain superfamily. The results obtained will aid the design of specific calpain inhibitors that could potentially be used for the treatment of cataract.

1.4.4 Structural Homology of Clan CA Cysteine Proteases

The Clan CA cysteine proteases papain, cathepsin B and calpain (m- and μ-) have some structural similarity, especially in and around the active sites. Crystal structures of μ-calpain, cathepsin B and papain available from the Protein Database were downloaded, the structures overlaid and the active sites isolated. **Figure 1.23** shows the resulting superposition of the active sites of papain, cathepsin B and calpain, clearly emphasising that the alignment of the catalytic triad Cys, His and Asn is almost identical in each protease. The α-helix, to which the active site cysteine is attached, is also similarly positioned in both papain and cathepsin B (blue and red respectively); the corresponding α-helix in calpain is tilted slightly as a result of overall enzyme structure. This is a structure-based difference that provides an opportunity for the design of specific cysteine protease inhibitors.

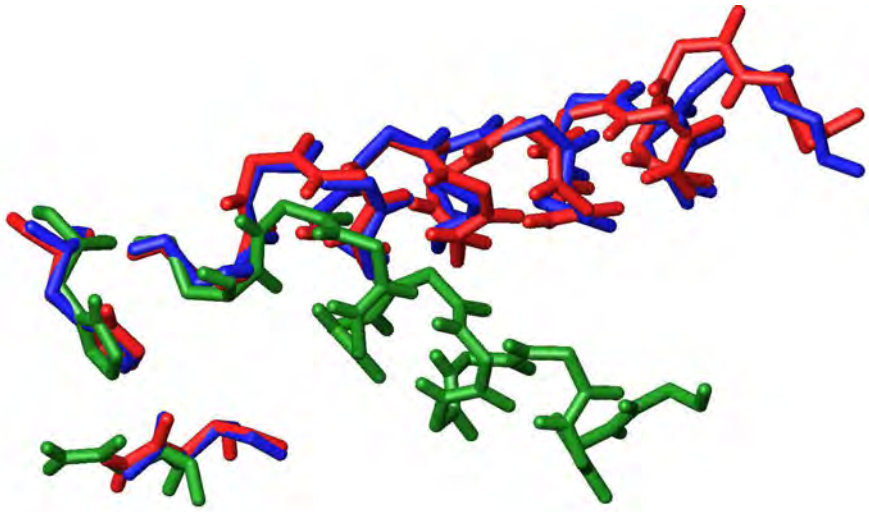

Figure 1.23 Active site superposition of calpain (green) and papain (blue) and cathepsin B (red) show the structural conservation between these cysteine proteases.[65] The active site cysteine in each case is situated at the end of the α-helix. (PDB codes 1PPP, 1ITO and 1TLO)

Comparison of the amino acid sequences surrounding the active site residues also illustrates the structural similarities between papain, cathepsin B and μ-calpain (see **Figure 1.24**). The sequence alignments were created by downloading the amino acid sequences of papain, cathepsin B and μ-calpain from the Protein Data Base. The amino acid sequences 6-7 residues either side of each of the catalytic triad residues (Cys, His and Asn) were identified and selected for each protease (Cys_{25}, His_{159}, Asn_{175} in papain; $Cys_{29,}$ His_{199}, Asn_{219} in cathepsin B; Cys_{105}, His_{262}, Asn_{286} in calpain). A sequence alignment was prepared in the CLC workbench for each of the three residues Cys, His and Asn (annotated with an asterisk) as shown in **Figure 1.24**. The consensus row (uncoloured) gives the residues most common to the three sequences and the conservation row provides a visual approximation of the similarity of the sequences between papain, cathepsin B and μ-calpain (the higher the pink bar the more alike the amino acids). This sequence comparison highlights the close structural homology that exists between cysteine proteases of the papain superfamily, as similar residues are found around each member of the catalytic triads for μ-calpain, cathepsin B and papain.

These two visual aids (**Figures 1.23** and **1.24**), showing the closeness in structure between cysteine proteases within the papain superfamily help to illustrate the difficulties faced in the design and synthesis of selective inhibitors.

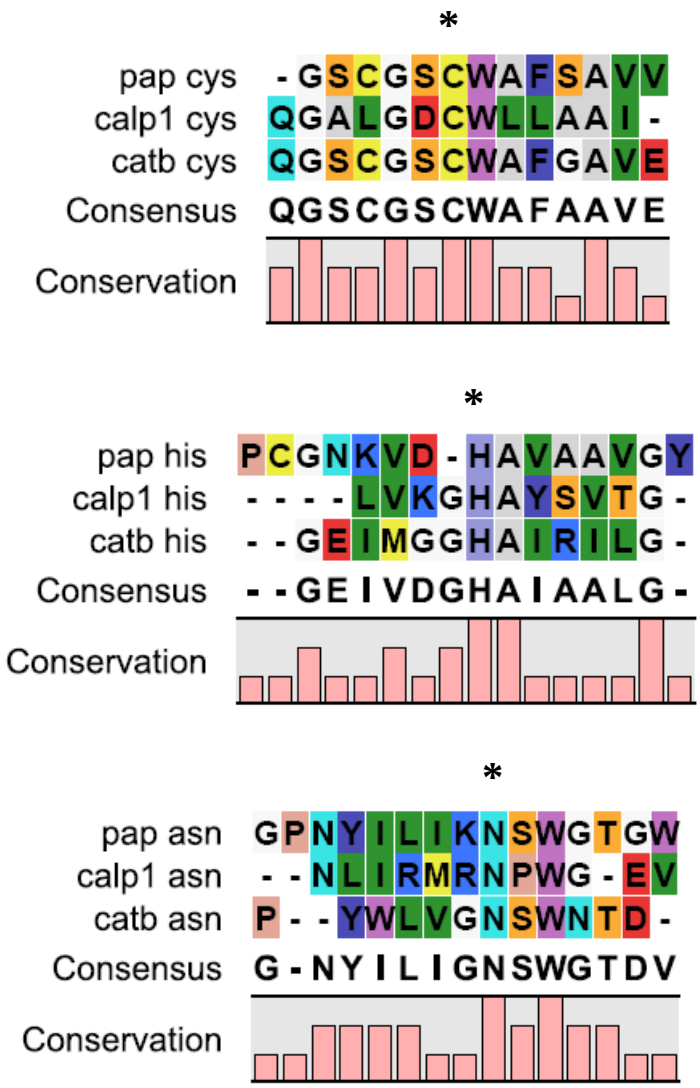

Figure 1.24 Partial sequence comparison around the active site residues of papain, cathepsin B, m-calpain and μ-calpain. The asterisks denote the catalytic triad residues Cys (top), His (middle) and Asn (bottom) respectively. The amino acids are coloured according to RasMol predefined colours, where polar amino acids are designated with bright colours and non-polar amino acids with darker colours.

1.5 DESIGN OF CYSTEINE PROTEASE INHIBITORS

Many different types of inhibitors have found application with cysteine proteases, the modes of action of which are discussed below.

Allosteric effectors

Inhibitors of this type interact with a site other than the active site of the enzyme.[17] A good example is the mercaptoacrylic acid PD15606 (**Figure 1.25** below) which competes with calcium ions for the calcium binding sites of calpain. This thesis does not consider inhibitors of this type.

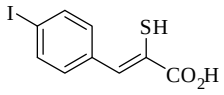

Figure 1.25 PD15606 an allosteric inhibitor of calpain

Active site directed inhibitors

These are defined as inhibitors that interact with the active site.[17] Most inhibitors are in fact, active site directed and can be further divided according to the specific type of interaction that occurs between inhibitor and active site residues. These sub-categories are listed in **Table 1.5** and include substrate analogues, product analogues, affinity labels, transition-state analogues and enzyme-activated inhibitors. The classification depends upon which catalytic step the inhibitor exhibits its inhibitory action.

Non-covalent inhibitors

The main interactions of non-covalent inhibitors with the enzyme active site are through hydrogen bonds and electrostatic interactions. Non-covalent inhibitors are further subdivided into substrate analogues and transition state analogues according to similarity to catalytic pathway intermediates.[8] Reversible inhibitors that bind to the enzyme with high affinity are called tightbinding inhibitors. Transition state analogue multidomain inhibitors are generally tightbinding.

Covalent inhibitors

Covalent inhibitors are subdivided according to whether reaction takes place via catalysis (mechanism based) or by an alternative chemical pathway (affinity labelling).[8,10] Mechanism-based inhibitors are further classified by the type of intermediate generated upon reaction with the active site. These are as follows:

- *Transition state analogues*. Reaction of the inhibitor with the active site results in a product that is analogous to the transition state of the substrate but which cannot react further
- *Enzyme activated inhibitors*. The reactive intermediate is released upon reaction with the active site and goes on to react with the enzyme along a non-catalytic pathway
- *Dead end inhibitors*. Which react with the enzyme active site to form an irreversible enzyme-inhibitor adduct that cannot react any further
- *Alternate substrate inhibitors*. These react in the same manner as dead end inhibitors but can react further with the enzyme.

Affinity label inhibitors have a warhead that reacts with the active site to form a permanent or irreversible enzyme-inhibitor complex. If the inhibitor can react with other molecules that have similar functional groups to the active site it is called a chemically reactive affinity label. On the other hand if the inhibitor is only reactive towards the enzyme's active site it is called a quiescent affinity label.[8]

Active-site Directed Inhibitor Categories

	Category	Type	Warhead example
1. Non-covalent interactions	substrate analogues		
	tightbinding analogues	transition state analogues	
2. Covalent interactions	mechanism based	transition state analogues	aldehydes
		enzyme activated inhibitors	esters, amides
		dead end inhibitors	peptidyl nitriles
	affinity labels		halomethyl ketones, epoxy derivatives

Table 1.5 Different classes of active-site directed inhibitors[8,10]

1.5.1 Inhibitors Synthesised in This Thesis

The design of the inhibitors synthesised in this thesis is based on an address region, a recognition region and a warhead as outlined in **Figure 1.26**. The recognition region is usually a di- or tripeptide with amino acids chosen to fit the target enzyme binding pockets. This may not be enough to confer specificity for a particular cysteine protease on the inhibitor, so additional recognition is often bestowed upon the inhibitor by the addition of an address region in the P3 position (often a large hydrophobic group). The warhead is generally an electrophilic moiety that can react with the active site cysteine thiol. Warheads can interact covalently or non-covalently with the active site (see above **Table 1.5**).

Figure 1.26 The three components of protease inhibitors

The covalent reversible inhibitors synthesised in **Chapter Two** are transition state analogues; the irreversible inhibitors synthesised in **Chapter Three** are dead end inhibitors or affinity labels (as described in **Table 1.5**).

There are abundant reviews on cysteine protease inhibitors[†] that focus on potency; however, there is a lack of information available about the selectivity of cysteine proteases within clans, especially within the papain superfamily. One recent review[66] highlights that target selectivity remains a major problem, even though potent inhibitors are available for most cysteine proteases.

The purpose of this thesis is to provide insight into the selectivity that can be achieved between members of the papain superfamily, especially focussing on the nature of the inhibitor warhead. This will be achieved through the design, synthesis and biological assay of cysteine protease inhibitors with a variety of warheads. The warheads utilised were chosen on the basis of: previous successful use in the literature and in-house molecular modelling results that suggested the proposed target inhibitor would bind to the substrate in the extended β-sheet conformation that is favoured by cysteine proteases.

[†] The database Scifinder Scholar identifies 229 reviews about cysteine protease inhibitors as of March 2007

1.6 OVERVIEW OF THIS THESIS

Chapter Two discusses literature examples of inhibitors that bind reversibly to cysteine proteases and then details the synthesis of a range of dipeptidyl inhibitors as cysteine protease inhibitors. Covalent reversible warhead examples synthesised include aldehydes, semicarbazones, oxadiazoles, α-ketotetrazoles, α-ketooxazolines and peptidyl nitriles. An inhibitor with an azide 'warhead' was also synthesised as an example of a non-covalent reversible warhead.

Chapter Three discusses irreversible cysteine protease inhibitors and includes the synthesis of cysteine protease inhibitors with Michael acceptor (α,β-unsaturated carbonyls and vinyl sulfones), α-bromomethyl ketones, α-bromomethyl alcohols and peptidyl epoxides as irreversible warheads for application as cysteine protease inhibitors.

Chapter Four introduces the importance of having inhibitors constrained into a bioactive conformation and highlights macrocyclic compounds as a means of achieving this goal. Warheads previously investigated in **Chapters Two** and **Three** and found to be potent and selective against cysteine proteases are applied to the macrocyclic scaffold. The warheads used include primary alcohols, aldehydes, semicarbazones, α-ketotetrazoles and azides.

Chapter Five details the design and validation of the assay protocols utilised for the *in vitro* biological testing of the inhibitors synthesised in **Chapters Two** through **Four**. The proteases the inhibitors were tested against were m-calpain, μ-calpain, cathepsin B, papain, pepsin and α-chymotrypsin.

Chapter Six presents structure-activity relationships of the inhibitors synthesised and biologically evaluated against the cysteine proteases m-calpain, μ-calpain, cathepsin B and papain. The relationships discussed are on the basis of the assay results in combination with molecular modelling and knowledge of protease active site structure. Emphasis is placed on the selectivity achieved between cysteine proteases of the papain superfamily, although some points of interest are made about the inhibitory effects of selected inhibitors against α-chymotrypsin and pepsin.

1.7 REFERENCES FOR CHAPTER ONE

(1) Hedstrom, L. *Chemical Reviews (Washington, DC, United States)* **2002**, *102*, 4429-4430.

(2) Sommerhoff, C. P.; Dunn, B. M.; Pike, R. N. *Biological Chemistry* **2006**, *387*, 825.

(3) Goll, D. E.; Thompson, V. F.; Li, H.; Wei, W.; Cong, J. *Physiological Reviews* **2003**, *83*, 731-801.

(4) Powers, J. C.; Asgian, J. L.; Ekici, O. D.; James, K. E. *Chemical Reviews (Washington, DC, United States)* **2002**, *102*, 4639-4750.

(5) Vicik, R.; Busemann, M.; Baumann, K.; Schrimeister, T. *Current Topics in Medicinal Chemistry (Sharjah, United Arab Emirates)* **2006**, *6*, 331-353.

(6) *Handbook of Proteolytic Enzymes*; 2nd ed.; Barrett, A. J.; Rawlings, N. D.; Woessner, J. F., Eds.; Elsvier Academic Press: London, 2004; Vol. 2.

(7) *Proteases: New Perspectives*; Turk, V., Ed.; Birkhauser Verlag: Boston, 1999.

(8) Otto, H.-H.; Schirmeister, T. In *Chemical Reviews (Washington, D. C.)* 1997; Vol. 97, p 133-171.

(9) Mykles, D. L. *Methods in Cell Biology* **2001**, *66*, 247-287.

(10) Demuth, H. U. *Journal of Enzyme Inhibition* **1990**, *3*, 249-278.

(11) McKerrow, J. H.; James, M. N. G.; Editors *Cysteine Proteases: Evolution, Function, and Inhibitor Design. [In: Perspect. Drug Discovery Des., 1996; 6]*, 1996.

(12) Rawlings, N. D.; Morton, F. R.; Barrett, A. J. *Nucleic Acids Research* **2006**, *34*, D270-D272.

(13) Rawlings, N. D.; Morton, F. R.; Kok, C. Y.; Barrett, A. J.; http://merops.sanger.ac.uk/: 2006.

(14) Turk, V. E. *Proteases: New Perspectives*; Birkhauser, 1999.

(15) Leung, D.; Abbenante, G.; Fairlie, D. P. *Journal of Medicinal Chemistry* **2000**, *43*, 305-341.

(16) Berger, A.; Schechter, I. *Biochemical & Biophysical Research Communications* **1967**, *27*, 157-162.

(17) Garret, R. H.; Grisham, C. M. *Biochemistry*; 2 ed.; Harcourt Brace College Publishers: New York, 1999.

(18) Berti, P. J.; Storer, A. C. *Journal of Molecular Biology* **1995**, *246*, 273-283.

(19) Gotz, M. G.; Caffrey, C. R.; Hansell, E.; McKerrow, J. H.; Powers, J. C. *Bioorganic & Medicinal Chemistry* **2004**, *12*, 5203-5211.

(20) Kim, M.-J.; Yamamoto, D.; Matsumoto, K.; Inoue, M.; Ishida, T.; Mizuno, H.; Sumiya, S.; Kitamura, K. *Biochemical Journal* **1992**, *287*, 797-803.

(21) Lin, Y.; Welsh, W. J. *Journal of Molecular Graphics* **1996**, *14*, 62-72.

(22) Kim, D. H. *Biopolymers* **1999**, *51*, 3-8.

(23) Menard, R.; Carmona, E.; Plouffe, C.; Bromme, D.; Konishi, Y.; Lefebvre, J.; Storer, A. C. *FEBS Letters* **1993**, *328*, 107-110.

(24) Schroder, E.; Phillips, C.; Garman, E.; Harlos, K.; Crawford, C. *FEBS Letters* **1993**, *315*, 38-42.

(25) Mort, J. S.; Buttle, D. J. *International Journal of Biochemistry & Cell Biology* **1997**, *29*, 715-720.

(26) Bromme, D.; Kaleta, J. *Current Pharmaceutical Design* **2002**, *8*, 1639-1658.

(27) Katunuma, N.; Suzuki, K.; Travis, J.; Fritz, H. In *The Refined X-Ray Crystal Structure of Human and Rat Liver Cathepsin B*; Japan Scientific Societies Press: Japan, 1994, p 274.

(28) Frlan, R.; Gobec, S. *Current Medicinal Chemistry* **2006**, *13*, 2309-2327.

(29) Lindvall, M. K. *Current Pharmaceutical Design* **2002**, *8*, 1673-1681.

(30) Musil, D.; Zucic, D.; Turk, D.; Engh, R. A.; Mayr, I.; Huber, R.; Popovic, T.; Turk, V.; Towatari, T.; Katunuma, N. *The EMBO journal* **1991**, *10*, 2321-2330.

(31) Jia, Z.; Hasnain, S.; Hirama, T.; Lee, X.; J.S., M.; To, R.; Huber, C. P. *The Journal of Biological Chemistry* **1995**, *270*, 5527-5533.

(32) Stern, I.; Schaschke, N.; Moroder, L.; Turk, D. *Biochemical Journal* **2004**, *381*, 511-517.

(33) Jedinak, A.; Maliar, T. *Neoplasma* **2005**, *52*, 185-192.

(34) Lim, I. T.; Meroueh, S. O.; Lee, M.; Heeg, M. J.; Mobashery, S. *Journal of the American Chemical Society* **2004**, *126*, 10271-10277.

(35) Mueller-Steiner, S.; Zhou, Y.; Arai, H.; Roberson, E. D.; Sun, B.; Chen, J.; Wang, X.; Yu, G.; Esposito, L.; Mucke, L.; Gan, L. *Neuron* **2006**, *51*, 703-714.

(36) Huang, Y.; Wang, K. K. W. *Trends in Molecular Medicine* **2001**, *7*, 355-362.

(37) Jia, Z.; Hosfield, C. M.; Davies, P. L.; Elce, J. S. *Methods in Molecular Biology (Totowa, NJ, United States)* **2002**, *172*, 51-67.

(38) Moldoveanu, T.; Campbell, R. L.; Cuerrier, D.; Davies, P. L. *Journal of Molecular Biology* **2004**, *343*, 1313-1326.

(39) Moldoveanu, T.; Hosfield, C. M.; Lim, D.; Elce, J. S.; Jia, Z.; Davies, P. L. *Cell (Cambridge, MA, United States)* **2002**, *108*, 649-660.

(40) Sorimachi, H.; Suzuki, K. *Journal of Biochemistry* **2001**, *129*, 653-664.

(41) Donkor, I. O. *Current Medicinal Chemistry* **2000**, *7*, 1171-1188.

(42) Perrin, B. J.; Huttenlocher, A. *International Journal of Biochemistry & Cell Biology* **2002**, *34*, 722-725.

(43) Iqbal, M.; Messina, P. A.; Freed, B.; Das, M.; Chatterjee, S.; Tripathy, R.; Tao, M.; Josef, K. A.; Dembofsky, B. *Bioorganic & Medicinal Chemistry Letters* **1997**, *7*, 539-544.

(44) Cuerrier, D.; Moldoveanu, T.; Davies, P. L. *The Journal of Biological Chemistry* **2005**, *280*, 40632-40641.

(45) Dolle, R. E.; Singh, J.; Whipple, D.; Osifo, I. K.; Speier, G.; Graybill, T. L.; Gregory, J. S.; Harris, A. L.; Helaszek, C. T. *Journal of Medicinal Chemistry* **1995**, *38*, 220-222.

(46) Sorimachi, H.; Ishiura, S.; Suzuki, K. *Journal of Biochemistry* **1997**, *328*, 721-732.

(47) Biswas, S.; Harris, F.; Singh, J.; Phoenix, D. *Molecular & Cellular Biochemistry* **2004**, *261*, 151-159.

(48) Wang, K. K. W.; Yuen, P.-W. *Trends in Pharmacological Sciences* **1994**, *15*, 412-419.

(49) Tsuji, T. S., S.; Kimura, J.; Shimizu, K. *Neuroscience Letters* **1998**, *248*, 109-112.

(50) Vanderklish, P. W.; Bahr, B. A. *International Journal of Experimental Pathology* **2000**, *81*, 323-339.

(51) Yoshikawa, Y.; Mukai, H.; Hino, F.; Asada, K.; Kato, I. *Japanese Journal of Cancer Research* **2000**, *91*, 459-463.

(52) Biswas, S.; Harris, F.; Dennison, S.; Singh, J.; Phoenix, D. A. *Trends in Biochemical Science* **2004**, *10*, 78-84.

(53) Papp, Z.; van der Velden, J.; Stienen, G. J. M. *Cardiovascular Research* **2000**, *45*, 981-993.

(54) Sandmann, S. Y., M. H.; Unger, T. *British Journal of Pharmacology* **2001**, *132*, 767-777.

(55) Benetti, R.; Copetti, T.; Dell'Orso, S.; Melloni, E.; Brancolini, C.; Monte, M.; Schneider, C. *Journal of Biological Chemistry* **2005**, *280*, 22070-22080.

(56) Fukiage, C.; Azuma, M.; Nakamura, Y.; Tamada, Y.; Nakamura, M.; Shearer, T. R. *Biochimica et Biophysica Acta* **1997**, *1361*, 304-312.

(57) Shearer, T. R.; Ma, H.; Shih, M. In *CALPAIN: Pharmacology and Toxicology of Calcium-Dependent Proteases*; Wang, K. K. W., Yuen, P.-W., Eds.; Taylor and Francis: 1999, p 331-347.

(58) Nakamura, M.; Yamaguchi, M.; Sakai, O.; Inoue, J. *Bioorganic & Medicinal Chemistry* **2003**, *11*, 1371-1379.

(59) www.FredHollows.org (Access Date: 12 Jan 2007).

(60) *www.eyeinfo.org/national.html* (Access Date: 14 Jan 2007).

(61) In *www.cvr.org.au* (Access Date: 23 Feb 2007).

(62) http://www.steen-hall.com/g_howeye.html (Access Date: 15 Mar 2007).

(63) Graw, J. *Biological Chemistry* **1997**, *378*, 1331-1348.

(64) Mathur, P.; Gupta, S. K.; Wegener, A. R.; Breipohl, W.; Ahrend, M. H.; Sharma, Y. D.; Gupta, Y. K.; Vajpayee, R. B. *Current Eye Research* **200**, *21*, 926-933.

(65) Strobl, S.; Fernandez-Catalan, C.; Braun, M.; Huber, R.; Masumoto, H.; Nakagawa, K.; Irie, A.; Sorimachi, H.; Bourenkow, G.; Bartunik, H.; Suzuki, K.; Bode, W. *Proceedings of the National Academy of Sciences of the United States of America* **2000**, *97*, 588-592.

(66) Leung-Toung, R.; Zhao, Y.; Li, W.; Tam, T. F.; Karimian, K.; Spino, M. *Current Medicinal Chemistry* **2006**, *13*, 547-581.

CHAPTER TWO

Design and Synthesis of Reversible Cysteine Protease Inhibitors

2.1 INTRODUCTION TO REVERSIBLE INHIBITORS

Covalent reversible inhibitors inactivate cysteine proteases by reacting with the active site cysteine thiol, resulting in the formation of a hemi-thioacetal, ketal or similar tetrahedral intermediate, the nature of which depends on the warhead.[1] The general mechanism of this is shown in **Figure 2.1** below.

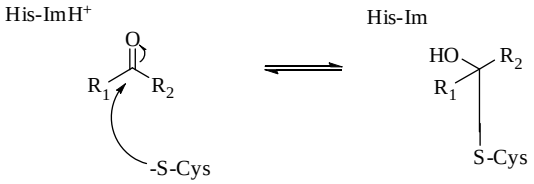

Figure 2.1 General mechanism of inactivation of cysteine proteases by reversible inhibitors

Several types of natural reversible cysteine protease inhibitors have been isolated from micro-organisms,[2] with the most common being the peptidyl aldehydes. Among those isolated from *Streptomyces* and *Actinomycete* are the leupeptins,[3,4] chymostatins,[1] antipain[1] and elastinal[1] (see **Figure 2.2)**. These naturally occurring aldehydes are non-specific, inhibiting both cysteine and serine proteases (**Table 2.1**).[1,5] Peptidyl aldehyde Leupeptin (**Figure 2.2** and **Table 2.1**) for example, inhibits papain, cathepsin B and μ-calpain (IC_{50} values of 0.50, 0.44 and 0.10 μM respectively), along with the serine proteases trypsin (IC_{50} = 5.0 μM). Further, because of structural similarities within the papain superfamily (see **Chapter One**); leupeptin shows little selectivity between papain, cathepsin B and calpain. This is typical of peptidyl aldehydes.

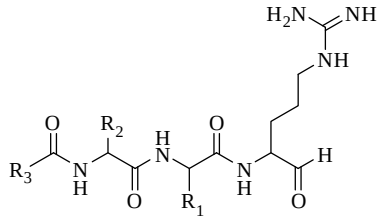

R_3 = Me, Et
R_1, R_2 = *i*-propyl, *i*-butyl, *sec*-butyl

Leupeptins

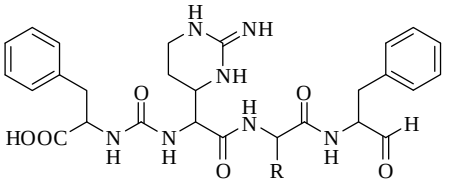

R = *i*-butyl, *i*-propyl, *sec*-butyl

Chymostatins

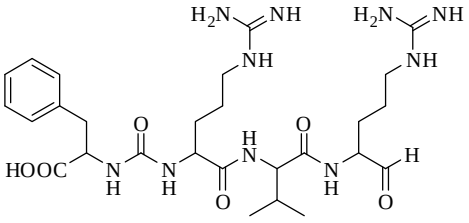

Antipain

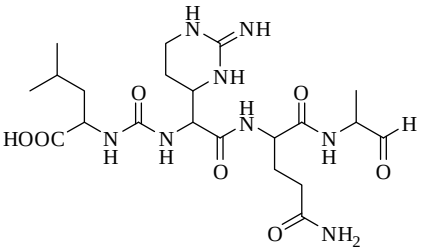

Elastinal

Figure 2.2 Peptidyl aldehydes isolated from natural sources

Enzyme	IC_{50} (μM)[1] Leupeptin*	Antipain	Chymostatin*
Papain	0.50	0.16	7.5
Cathepsin B	0.44	-	2.6
μ-Calpain	0.10	-	-
Trypsin	2.00	0.26	>250
Chymotrypsin	>500	>250	0.15

Table 2.1 Inhibitory potency of natural peptidyl aldehydes against a range of proteases.[6] * Where leupeptin is defined as R_1, R_2 = *i*-butyl, R_3 = Me; Chymostatin is defined as R = *i*-butyl

The modification of the Arg, Ala and Asn residues in the P_1 and P_2 subsites (see **Figure 2.2**) to Phe, Leu or Val residues which are favoured by cysteine proteases (refer to **Chapter One**) and the addition of an aryl protecting group on the *N*-terminus resulted in synthetic inhibitors that were selective for cysteine proteases over serine proteases (see **Table 2.2**); yet reported peptidyl aldehydes remain non-specific towards the cysteine protease family. This is highlighted for peptidyl aldehydes **2.1** to **2.5** in **Table 2.2**. Aldehyde **2.1** shows 2-fold selectivity towards the calpains (0.040-0.050 μM) over papain

(0.14 μM) and cathepsin B (0.13 μM) but does not distinguish between papain and cathepsin B. Aldehyde **2.2** has similar potency against the m- and μ-calpain and cathepsin B (0.060 μM, 0.027 μM and 0.027 μM respectively) and is at least 18-fold less active against papain (IC_{50} = 1.1 μM). The aldehyde **2.3** is highly potent against all of the papain-like cysteine proteases tested (all IC_{50} values between 0.005-0.080 μM, see **Table 2.2**). Similarly, aldehyde **2.4** shows little specificity between the cysteine proteases m-calpain, μ-calpain and cathepsin B (IC_{50} = 0.19 μM, 0.086 μM and 0.15 μM respectively); while aldehyde **2.5** shows little specificity between m-calpain and μ-calpain (K_i = 0.050 μM and 0.036 μM respectively).

	Peptidyl Aldehyde	IC_{50} (μM) m-calpain	μ-calpain	papain	cathepsin B	Ref
2.1	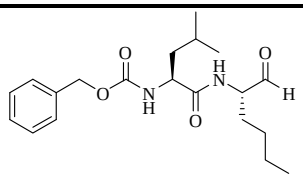	0.040	0.050	0.14	0.13	1,2,7
2.2	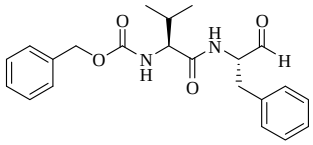	0.35	0.056	1.1	0.027	1,8,9
2.3	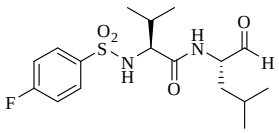	0.080	0.005	0.023	0.016	1, 10
2.4	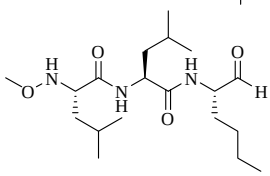	0.19	0.086	-	0.15	1,9,11
2.5	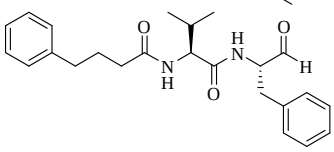	K_i = 0.050* μM	K_i = 0.036* μM	-	-	2

Table 2.2 Inhibitory potency of the synthetic peptidyl aldehydes **2.1** calpeptin; **2.2** MDL28170; **2.3** SJA6017**; 2.4** calpain inhibitor I. These are broad spectrum cysteine protease inhibitors. * no reported IC_{50} values

The dipeptidyl aldehyde **2.3** shows therapeutic potential against a rat selenite-induced cataract lens culture assay and more recently, *in vivo* in a sheep animal model.[9] However, this aldehyde has limited aqueous solubility (0.1 mg/ml), a lack of metabolic stability (97.5% of sample metabolised after incubating for 1 h in human microsomes) and binds to proteins (95%); see **Table 2.3**. These properties, along with its rapid metabolism into the alcohol **2.6** and acid **2.7** (**Figure 2.3**)[12] suggest that the aldehyde reacts with biological proteins *in vivo*, limiting its membrane permeability and bioavailability.

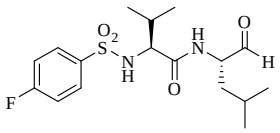

2.3

Toxicity	LD_{50}* >1000 µM
Permeability:	1.41 x 10^{-6} cm/s, 33% recovery
Protein Binding	95%
Metabolic Stability	97.5% metabolised (2.5% recovery after 1 hr)
Aqueous solubility	0.1 mg/ml

Table 2.3 Properties exhibited by aldehyde **2.3**.[9] *Toxicity tested against human neuroblastoma SY5Y cells

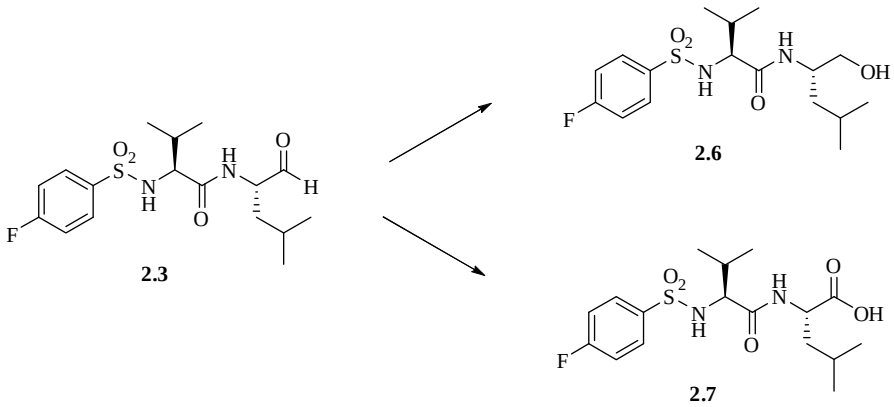

2.3 **2.6** **2.7**

Figure 2.3 The aldehyde **2.3** is readily metabolised into the corresponding alcohol **2.6** and acid **2.7**

The above examples highlight the fact that aldehydes are potent inhibitors, but the reactivity of the aldehyde moiety under biological conditions results in non-specific inhibition of cysteine proteases. As a result, a number of chemically less reactive

reversible warheads have been investigated as protease inhibitors. A summary of some reversible warheads and their contribution to the inhibition of cysteine proteases follows.

2.2 REVERSIBLE WARHEADS UTILISED IN CYSTEINE PROTEASE INHIBITORS

2.2.1 Semicarbazone Warheads

Semicarbazones have long been established in synthetic chemistry as a means of purifying aldehydes.[13] More recently, semicarbazones have been utilised as inhibitor warheads for the cysteine proteases cruzain,[14] cathepsin K[15] and calpain[16] with moderate success. While still being potent inhibitors, the semicarbazones are generally reported as being weaker than the corresponding parent aldehyde.[15] The semicarbazones **2.9** to **2.11** illustrate this point (see **Table 2.4**), being 4- to 8-fold less potent than the parent aldehyde **2.8** (IC_{50} = 0.051 μM). The loss of potency however, is offset by increased aqueous solubility and better pharmacokinetic profiles than the parent aldehyde **2.8** (data not given).[15]

Peptidyl semicarbazones inhibit cysteine proteases by reversible attack of the thiolate on the protected carbonyl carbon to form a tetrahedral adduct as depicted in **Figure 2.4**.[1,14] The incorporation of a semicarbazone moiety is thought to be advantageous as it contains both hydrogen bond acceptors and donors.

	Compound	IC_{50} (μM) against Cathepsin K
2.8	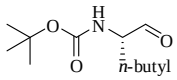	0.051
2.9	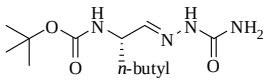	0.35
2.10	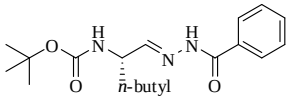	0.22
2.11	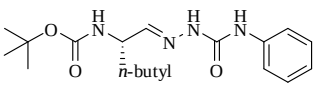	0.40

Table 2.4 Semicarbazones are weaker inhibitors than the parent aldehyde[15]

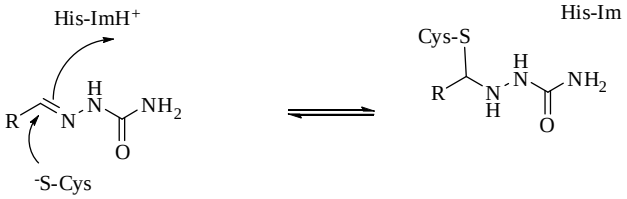

Figure 2.4 Mechanism of inactivation by semicarbazones.

2.2.2 Heterocyclic Warheads

There are many examples of inhibitors of cysteine proteases bearing heterocyclic warheads,* for example see **Figure 2.5**, which includes the heterocycles: oxazole, oxazoline, oxatriazole, thiazole, thiazoline and imidazole that have been utilised in the literature.[17-19]

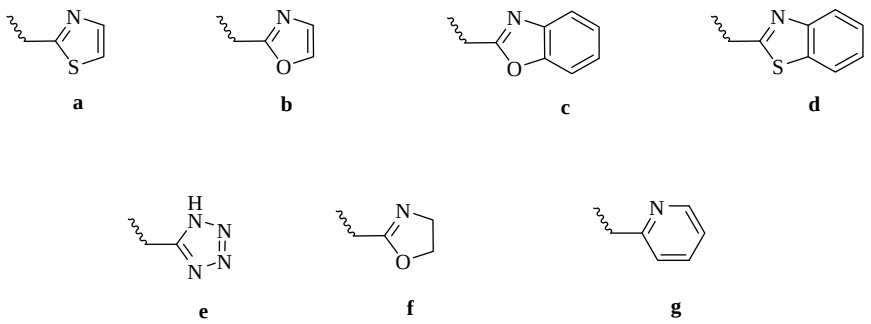

Figure 2.5 Some heterocyclic warheads used in protease inhibitors a) thiazole, b) oxazole, c) benzoxazole, d) benzothiazole e) tetrazole, f) oxazoline and g) pyridine

The mechanism of heterocyclic inhibition is analogous to that of aldehydes and ketones, either through a hemi-thioacetal or ketal intermediate (refer to **Figure 2.1**). The heterocyclic warhead can be considered a masked aldehyde or α-ketoamide as depicted in **Figure 2.6**. Masking the reactivity of electrophilic groups such as aldehydes with a heterocycle increases the metabolic stability of the inhibitor and may aid localisation of the inhibitor to the target enzyme.[2]

* There have been over 300 patents filed regarding heterocyclic protease inhibitors filed.

Figure 2.6 The heterocyclic warhead as a) a masked aldehyde and b) a masked α-ketoamide

Oxadiazoles

Examples of 3,5 disubstituted 1,2,4-oxadiazoles are provided by Hamze[20] and co-workers (see **Figure 2.7**), who synthesised a range of novel heterocyclic containing α- and β-amino acids for incorporation into peptides and protease inhibitors. Condensation reactions between a carboxylic group with a range of substituted amidoximes and subsequent cyclisation resulted in substituted 1,2,4-oxadiazoles. These oxadiazoles were substituted in the 5 position by the carboxylic acid moiety and in the 3 position by the amidoxime substituent.

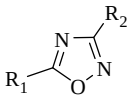

Figure 2.7 Generic structure of 1,2,4-oxadiazoles substituted in the 3 position by R_2 and in the 5 position by R_1

α-Ketoamides and α-ketoheterocycles

The α-ketoamide inhibitors **2.12** and **2.13** shown in **Figure 2.8** are potent μ-calpain inhibitors (IC_{50} values of 0.021 and 0.032 μM respectively). These examples are effective at protecting rats against ischemic brain damage.[12] The α-ketoamide moiety is an isosteric replacement of aldehydes, with potency thought to arise from formation of a stabilised tetrahedral adduct due to hydrogen bonding between the electrophilic carbonyl of the α-ketoamide and catalytic residues of the protease.[21] There are over 40 patents associated with α-ketoamide inhibitors, only a few of which are specifically for cysteine proteases. Further, α-ketoheterocycles are isosteres of α-keto acids[22,23] and can provide conformational restraint upon the inhibitor in which they are incorporated.[24,25]

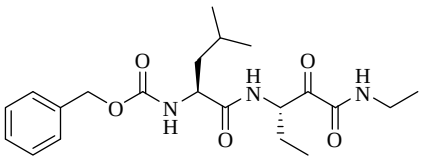

2.12

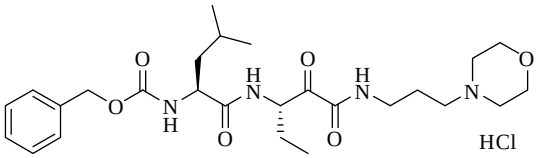

2.13

Figure 2.8 Peptidyl α-ketoamides that are potent calpain inhibitors.[16,26] **2.12** IC_{50} = 0.021 μM and **2.13** IC_{50} = 0.032 μM

Edwards *et al*[27] reported a series of peptidyl α-ketoheterocycles as potent inhibitors of Human Neutrophil Elastase (HNE) (see **Table 2.5**). Both the α-ketooxazoline **2.16** and the α-ketobenzoxazole **2.15** were more potent than the analogous peptidyl aldehyde **2.14**. The increase in activity against Human Neutrophil Elastase is thought to partly arise from the heterocyclic ring possessing high electron withdrawing potential,[28] denoted as σ_I.[†] The more electron withdrawing the heterocycle, the more it can activate the adjacent ketone group towards nucleophilic addition by active site residues. The electron withdrawing potentials for a number of heterocycles are given in **Table 2.6**. Perusal of this data indicates that α-ketotetrazoles (σ_I = 0.49)[29] are one of the most electron-withdrawing heterocycles, making this moiety a desirable warhead for cysteine protease inhibitors. The electron-withdrawing ability of α-ketooxazolines (σ_I = 0.32)[29] is less than that for α-ketotetrazoles; however, the hydrogen bond accepting ability of the α-ketooxazoline ring is excellent.[19,27] The combination of electron with-drawing ability and hydrogen bond acceptance make both α-ketotetrazoles and α-ketooxazolines desirable inhibitor warheads.

[†] The σ values are values that represent the electrical effects of the heterocycle as calculated by the Hammett Equation

	Compound	K_i (μM)
2.14	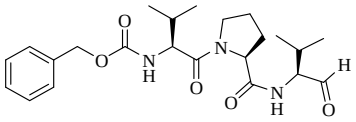	0.041
2.15	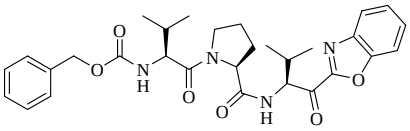	0.003
2.16	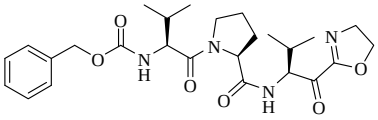	0.0006

Table 2.5 Potent α-ketoheterocyclic HNE protease inhibitors

Heterocycle	σ_I	Heterocycle	σ_I
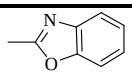	0.41	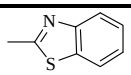	0.37
	0.38		0.34
	0.49		0.49
	0.32		0.32
	0.13		

Table 2.6 Electron withdrawing properties of heterocycles[28,29]

2.2.3 Nitrile Warheads

Peptidyl nitriles have been known as inhibitors of papain for over 30 years[1] and more recently touted as potent, selective cathepsin B inhibitors. Greenspan *et al*[30] synthesised a range of peptidyl nitriles of cathepsin B. One of these, inhibitor **2.16**, shown in **Figure 2.9**

was a potent inhibitor of cathepsin B (IC_{50} = 0.012 μM). This peptidyl nitrile displayed greater than 100-fold selectivity for cathepsin B over other cathepsins. It also has a plasma concentration of 5.27 μM, corresponding to excellent bioavailability.[30] X-ray crystal structure data (cathepsin B with a peptidyl nitrile inhibitor bound) helped to elucidate the mechanism of inhibition by peptidyl nitriles, showing the formation of a reversible thioimidate complex between the cysteine thiol of the enzyme and the nitrile moiety of the inhibitor (see **Figure 2.10**).[30,31]

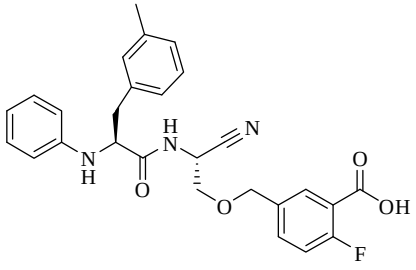

2.16

Figure 2.9 A peptidyl nitrile protease inhibitor. IC_{50} = 0.0012 μM; plasma concentration = 5.27 μM[30]

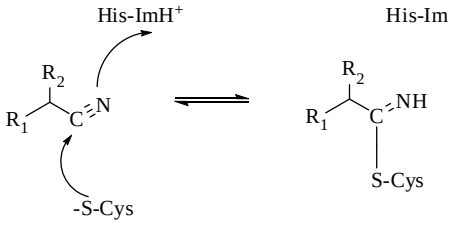

Figure 2.10 Mechanism of inhibition by peptidyl nitriles

2.2.4 The Non-Covalent Azide 'Warhead'

Fairlie[32] and co-workers recently reported the first instance of the azide moiety being utilised as part of a cysteine protease inhibitor. The inhibitors **2.19a-f** (see **Table 2.7**), with an azidomethylene moiety acting as a non-covalent 'warhead', showed excellent inhibition of cysteine protease inhibitors (IC_{50} values in the sub μM region). The azides **2.19a-f** were only tested for activity against caspases and cathepsins K, S and B; however,

it was suggested that the azide moiety would be useful for the inhibition of other cysteine proteases.

2.19

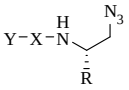

	Y	X	R	Enzyme	IC_{50} (μM)
2.19a	Biphenoyl-Val	Ala	CH_2COOH	Casp-1	0.0045
2.19b	Ac-Asp-Glu	Leu	CH_2COOH	Casp-3	0.39
2.19c	Cbz-Glu	Leu	CH_2COOH	Casp-8	0.16
2.19d	2-Naphthoyl	Leu	$(CH_2)_3CH_3$	Cat K	0.0012
2.19e	1-Naphthoyl	Leu	$(CH_2)_3CH_3$	Cat S	0.018
2.19f	Biphenoyl	Phe	$CH_2CH(CH_3)_2$	Cat B	0.058

Table 2.7 Azidomethylene inhibitors of cysteine proteases[32]

2.3 DESIGN AND SYNTHESIS OF REVERSIBLE CYSTEINE PROTEASE INHIBITORS

2.3.1 Design of Peptidyl Aldehydes

This thesis focuses on the effect the inhibitor warhead has on selectivity between cysteine proteases of the papain superfamily. Two general scaffolds were used; a Val-Leu and a Val-Phe dipeptide, all of which are preferred amino acids of cysteine proteases (see **Chapter One** for more detail). Four aryl groups (4-fluorobenzenesulfonyl, benzyloxycarbonyl, 2-pyrrole carbonyl and 2-thiophene acetyl) were briefly investigated to determine the effect of the *N*-terminal group on selectivity between members of the papain superfamily. Of the aldehydes synthesised, four were literature compounds.[9,33,34] The purpose of synthesising the literature aldehydes was two-fold: firstly, to provide a measure of reproducibility and validation for assay results; and secondly, as will be discussed in this and subsequent chapters, the reactivity of the aldehyde moiety provides an excellent starting point for chemical modification of the warhead to produce less reactive, more selective inhibitors of cysteine proteases. The synthesis of aldehydes **2.3** and **2.20** (see **Figure 2.11**) proved to be high yielding (this is discussed below); subsequent assay showed both of these aldehydes to be potent broad spectrum cysteine protease inhibitors (see **Chapter Six** for details), thus **2.3** and **2.20** were used as lead compounds for the design of specific cysteine protease inhibitors in this thesis.

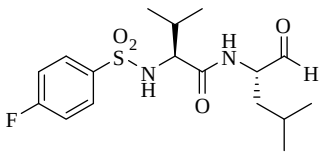

2.3

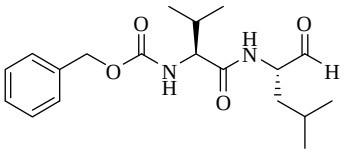

2.20

Figure 2.11 The aldehydes **2.3** and **2.20** were the lead compounds for inhibitors synthesised in this thesis

Molecular Modelling

Using the general scaffolds as described above, moieties that had previously been utilised as cysteine protease inhibitor warheads were used to design the target compounds. The

target compounds were docked into the molecular modelling program and the proposed binding modes resulting from this were used to determine the priority of synthesis. Cysteine proteases are known to bind substrates in an extended β-sheet conformation,[35] thus target compounds that exhibited an extended β-sheet conformation (as defined by three critical hydrogen bonds) were assumed to have good binding affinity to the protease and were subsequently synthesised and assayed for *in vitro* potency.

Molecular modelling[‡] was performed on target compounds using the following method: a model of the active site of calpain was developed from the crystal structure of engineered μ-calpain published by Moldoveanu *et al.*[36] The grid file was prepared from the crystal structure for these experiments by the mutation *in silico* of Ser_{115} to Cys_{115} to re-establish the natural amino acid composition of μ-calpain. A minimization of this structure, using the OPSL2001 force field and water as simulated solvent, resulted in a relaxed structure differing with an RMSD of the heavy atoms (C, N, O, S) of 0.96 Å from the reported crystal structure. Cys_{115} was deprotonated and His_{262} protonated to better mimic the amino acids in the active enzyme. A docking grid was generated, and inhibitor **2.3** was docked to the calpain model using GLIDE (Schrodinger)[37] to establish the docking of this reference compound of known inhibitory activity. **Figure 2.12** shows an overlay of the crystal structure of the Leupeptin-calpain co-crystal with the structure of each inhibitor docked to calpain.

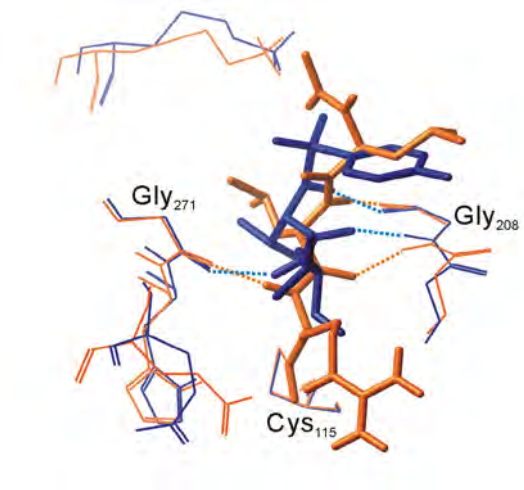

Figure 2.12 Overlay of **2.3** docked to the μ-calpain model (blue) and the leupeptin/engineered μ-calpain co-crystal (orange). Hydrogen bonds to Gly_{208} and Gly_{271} are shown by the dotted lines

[‡] Molecular modelling was performed by Wanting Jiao of the University of Canterbury

Leupeptin and aldehyde **2.3** adopt the same overall orientation on binding where the aldehyde is located close to the active site cysteine. Importantly, both leupeptin and **2.3** have their backbone conformations defined in the extended β-strand geometry with three hydrogen bonds to Gly_{208} and Gly_{271} (these will subsequently be referred to as hydrogen bonds A, B and C). Significantly, this binding motif is also apparent in published crystal structures. The β-strand motif is recognized by calpain on the carboxyl side of the scissile bond, the position in which most calpain inhibitors bind. However, while the crystal structure of the calpain-leupeptin complex suggests the existence of a covalent bond between protein and ligand, the docking experiments simply evaluate non-covalent interactions. The binding energy from the formation of a covalent bond is therefore not represented in the calculated docking scores. All molecular modelling reported in this thesis follows the aforementioned protocol as developed at the University of Canterbury[§] and will be referred to as the rigid μ-calpain model henceforth.

The in-house heterocyclic aldehyde calpain inhibitor **2.20** was docked into the rigid μ-calpain model and the best pose shown in **Figure 2.13**. This suggests that the aldehyde **2.20** forms the hydrogen bonds A, B and C (as defined above). Additional hydrogen bonds are suggested to form between the sulfur atom of the heterocycle and Asn_{253}, and the same sulfur atom and Lys_{347} (see **Figure 2.13**). Heterocycles have previously been used to induce an extended conformation in peptide sequences, leading to the preparation and testing of calpain inhibitors that incorporated pyrrole and furan heterocyclic functionality within the University of Canterbury.[38]

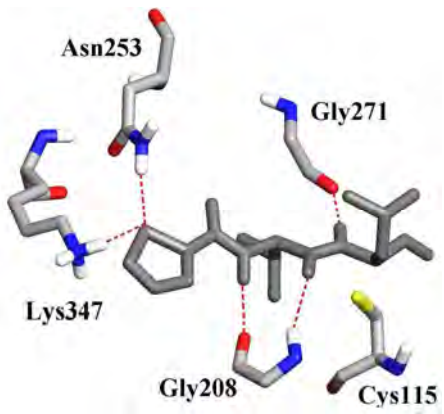

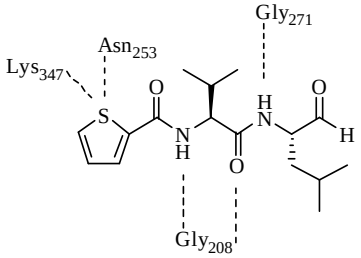

2.20

Figure 2.13 The in-house furan containing aldehyde inhibitor **2.20** and its molecular modelling results

[§] Molecular modelling protocol was established by Blair Stuart, Axel Neffe and Steven McNabb

The heterocyclic aldehydes **2.21** and **2.22** were docked into the rigid μ-calpain model and the best poses for each are shown in **Figure 2.14**. This suggested that both aldehydes **2.21** and **2.22** bind calpain in an extended bioactive conformation defined by hydrogen bonds A, B and C. No additional hydrogen bonds were suggested to form, the NH group of the 2-pyrrolecarbonyl **2.21** being a mismatch with the Asn_{253} which requires a donor atom; and the sulfur atom of the 2-thiophene acetyl **2.22** is not in close proximity to the Asn_{253} or Lys_{347} due to the methylene insertion.

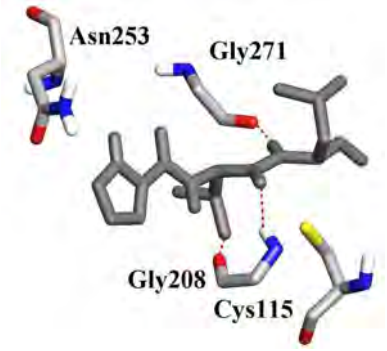

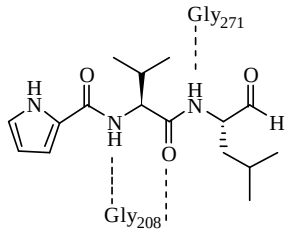

2.21

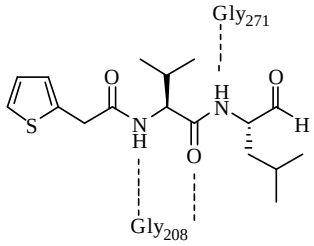

2.22

Figure 2.14 The heterocyclic aldehydes **2.21** and **2.22** synthesised for comparison to the heterocyclic aldehyde **2.20** and their molecular modelling results (low energy conformations)

2.3.2 Synthesis of Peptidyl Aldehydes

The synthesis of the aldehyde **2.3** was optimised from Inoue's methodology[10] as shown in **Scheme 2.1**. Commercially available 4-fluorobenzenesulfonyl chloride **2.23** was coupled to *L*-valine under aqueous conditions to give the acid **2.24**. Reaction of this acid **2.24** with *N*-hydroxysuccinimide in the presence of 1-(3-dimethylaminopropyl)-3-ethylcarbodiimide hydrochloride (EDCI) gave the activated ester **2.25** as a white solid in 95% yield. Samples of the ester **2.25** were separately reacted with *L*-leucinol or *L*-phenylalaninol to give the

dipeptides **2.6** or **2.26** respectively. The precursors **2.24**, **2.25**, **2.6** and **2.26** were purified by rinsing in a mixture of 5% ethyl acetate and 95% petroleum ether. Subsequent oxidation of samples of the primary alcohols **2.6** and **2.26** using sulphur trioxide-pyridine complex and dimethylsulfoxide in the presence of DIPEA (Parikh-Doering Oxidation)[39] gave the aldehydes **2.3** and **2.27** as white solids in 89% and 77% yields respectively. The oxidised products **2.3** and **2.27** were characterised by ^{1}H NMR, which showed the absence of the alcohol methylene peaks at around 2.5 ppm; a singlet peak at around 9.0 ppm was observed; this is characteristic of an aldehyde peak.

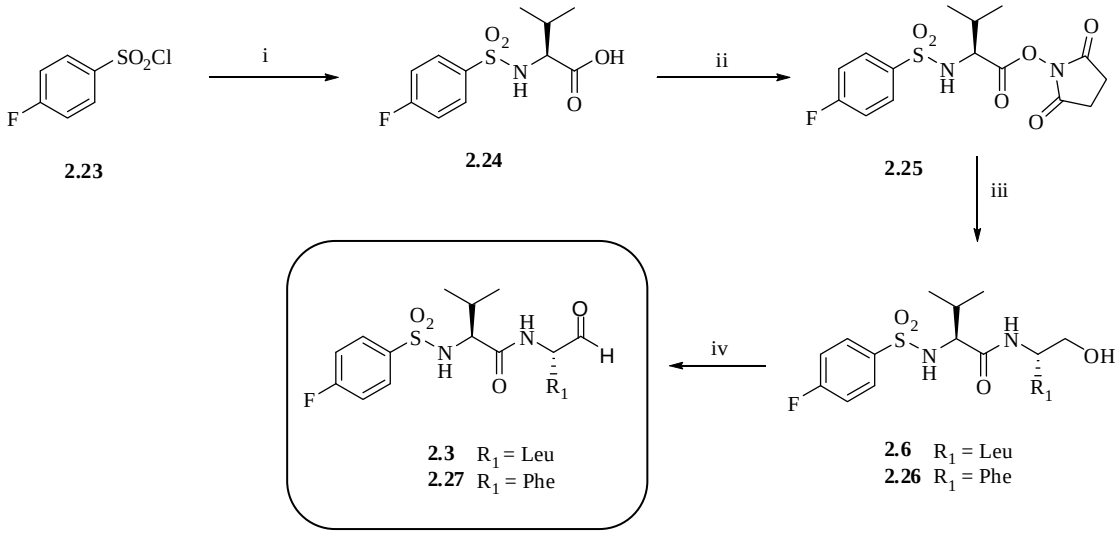

Scheme 2.1 *Reagents and Conditions:* i) THF, H_2O, *L*-valine, NaOH (75%); ii) *N*-hydroxysuccinimide, EDCI, DCM, THF (95%); iii) *L*-leucinol, DCM, DIPEA (87%); iv) SO_3-pyr, DMSO, DIPEA, DCM (77-89%)

The sulfur trioxide-pyridine complex was used to oxidise the alcohols **2.6** and **2.26** to the aldehydes **2.3** and **2.27** because the reaction conditions are mild and isolation of the desired aldehyde is free from side products.[40] This is highly beneficial as aldehydes are easily epimerised when undergoing chromatographic purification. Examination of the ^{1}H and ^{13}C NMR spectra of aldehydes **2.6** and **2.27** for epimerization of the peptide aldehydes revealed only a single isomer was present in each case (see **Figure 2.15**).

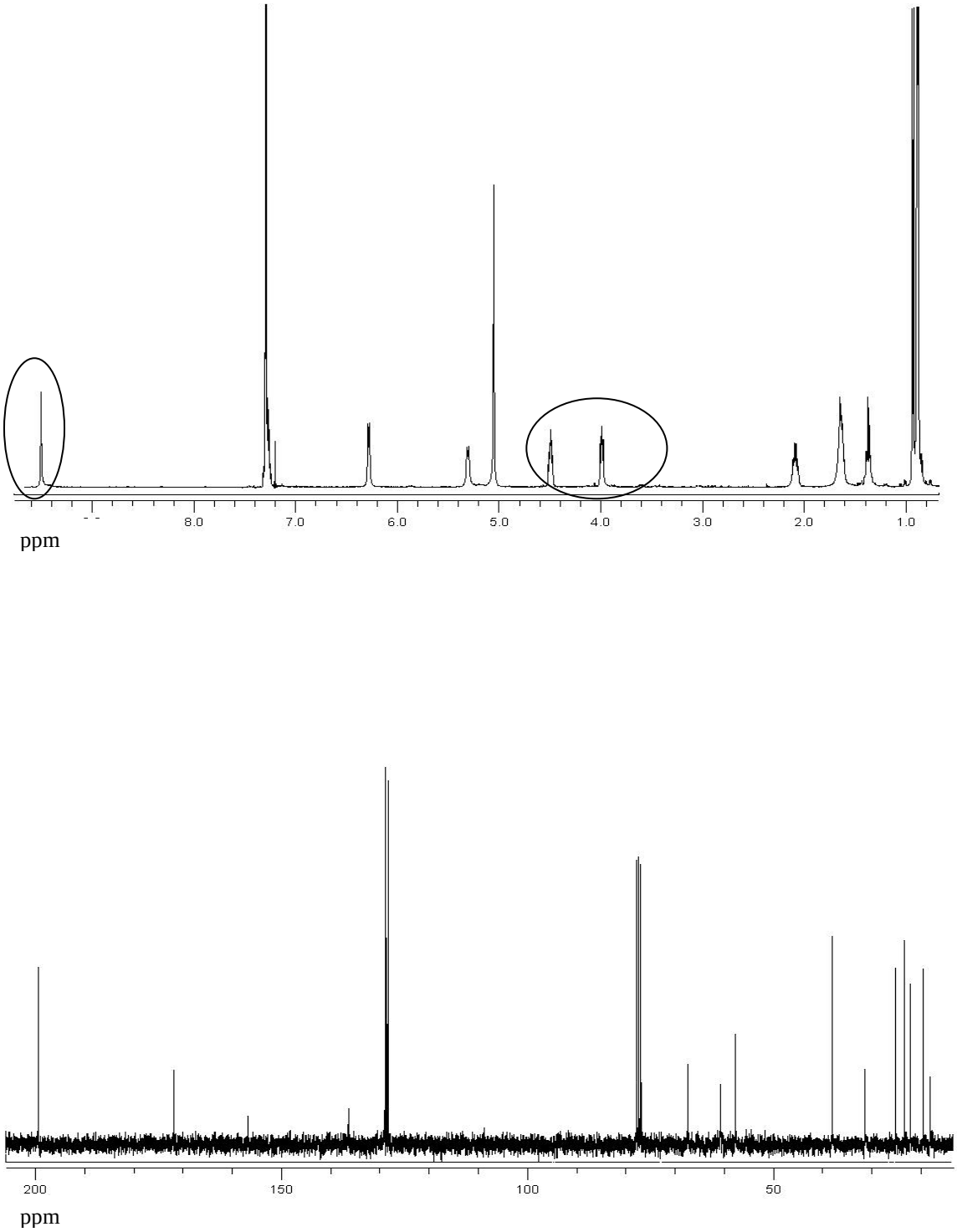

Figure 2.15 ^{1}H NMR spectra (top) of aldehyde **2.27** showing the clearly single resonances for the CHO peak and the α-protons of the Leu and Val (circled); ^{13}C NMR spectra (bottom) of aldehyde **2.27** showing the clearly single peaks of the Leu and Val sidechains (18-70 ppm) and the CHO peak (198 ppm)

In cases where epimerization has occurred, both isomers are clearly evident by ^{13}C and ^{1}H NMR. This is particularly true of the the P_1 residue** (Leu in the case of both **2.6** and **2.27**) and the aldehyde hydrogen and these signals are all clearly defined as single resonances for the aldehydes **2.6** and **2.27** (see example given in **Figure 2.15**). The Parikh-Doering oxidation removed any need for purification of the aldehyde **2.3**; however, purification of the aldehyde **2.27** was required. This was achieved by recrystallisation of the crude material from a minimal amount of ethyl acetate. The mechanism by which the sulfur trioxide-pyridine complex oxidises alcohols is shown in **Figure 2.16**. The sulfur trioxide-pyridine complex reacts with dimethylsulfoxide to give an activated sulfonium species. This reacts with the alcohol to yield the sulfonium intermediate which is deprotonated under basic conditions to generate the aldehyde and dimethylsulfide.[41]

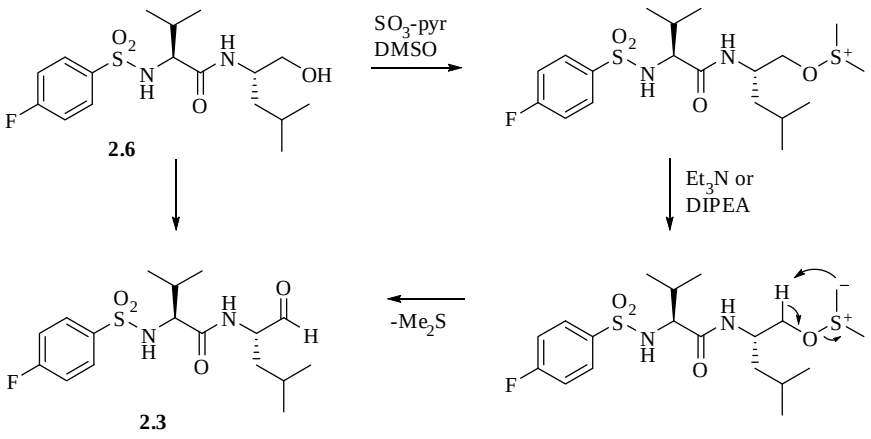

Figure 2.16 Mechanism of oxidation by sulfur trioxide-pyridine[41]

The aldehydes **2.19** and **2.2** were synthesised by the method outlined in **Scheme 2.2**. Samples of commercially available benzyloxycarbonyl-*L*-valine **2.28** were separately coupled to *L*-leucinol and *L*-phenylalaninol under standard *N,N,N',N'*-tetramethyl-*O*-(7-azabenzotriazol-1-yl)uronium hexafluorophosphate (HATU) conditions to give the dipeptidyl alcohols **2.29** and **2.30** in 87% and 76% yields respectively. Subsequent oxidation utilising the sulfur trioxide-pyridine complex gave the aldehydes **2.19** and **2.2** as white solids in 89% and 79% yields respectively.[40] NMR analysis of the aldehydes **2.19** and **2.2** showed an absence of the starting alcohol methylene peaks and there was no evidence of epimerisation (as previously described).

** The P_1 residue is more susceptible to epimerization than the P_2 residue because the P_1 residue part of the aldehyde moiety whereas the P_2 residue is a protected amino acid.

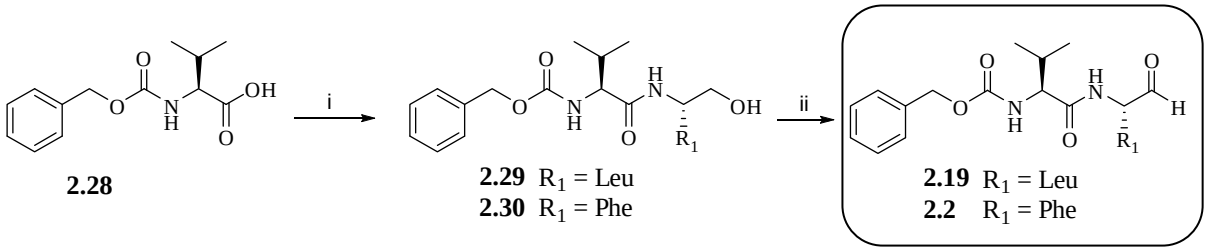

Scheme 2.2 *Reagents and Conditions*: i) HATU, DIPEA, *L*-leucinol or *L*-phenylalaninol (87%, 76%); ii) SO_3-pyr, DMSO, DIPEA, DCM (89%, 79%)

Syntheses of the aldehydes **2.21** and **2.22** are outlined in **Scheme 2.3**. The *N*-protecting groups of the aldehydes **2.21** and **2.22** were 2-pyrrole carbonyl and 2-thiophene acetyl respectively. Commercially available *tert*-butoxycarbonyl-*L*-valine **2.31** was coupled to *L*-leucinol under standard HATU conditions to give the *N*-protected dipeptidyl alcohol **2.32**. The *tert*-butoxycarbonyl protecting group of **2.32** was cleaved using trifluoroacetic acid to give the aminoalcohol **2.33** in excellent yield (>95%). Coupling of the thiophene-2-acetyl chloride to the aminoalcohol **2.33** proved problematic. The original solvent used was dichloromethane; however, analysis of the product by mass spectrometry established that both amide bond formation and esterification of the aminoalcohol **2.33** had occurred, giving the side product **2.34** as shown in **Figure 2.17**.

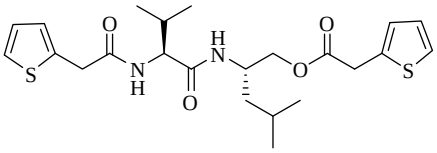

Figure 2.17 The product obtained from coupling amino-alcohol **2.34** with thiophene-2-acetyl chloride in a dichloromethane solvent system

The formation of the side product **2.34** was overcome by adjusting the solvent system used. Tetrahydrofuran, dichloromethane:*N,N*-dimethylformamide (1:1) and *N,N*-dimethylformamide were used in separate reactions of the aminoalcohol **2.33** with thiophene-2-acetyl chloride, and the isolated products analysed by ^{1}H NMR and mass spectrometry (see **Table 2.8**). *N,N*-Dimethylformamide was found to facilitate the coupling of 2-thiophene acetyl chloride to the aminoalcohol **2.33** to give the desired *N*-protected alcohol **2.35** with no

evidence of the side product **2.34** by mass spectrometry. Under these new conditions, samples of the free amine **2.33** were separately coupled to 2-pyrrole carboxylic acid and 2-thiophene acetyl chloride to give the dipeptidyl alcohols **2.35** and **2.36** in excellent yields of 78% and 83% respectively. Oxidation of the alcohols **2.35** and **2.36** using the sulfur trioxide-pyridine complex gave the aldehydes **2.21** and **2.22** in 89% and 86% yield respectively.

Solvent	**% Product 2.35**	**% Side product 2.34**
Dichloromethane	20%	80%
Tetrahydrofuran	50%	50%
N,*N*-Dimethylformamide/Dichloromethane (1:1)	80%	20%
N,*N*-Dimethylformamide	100%	0%

Table 2.8 Solvent effects on formation of side product

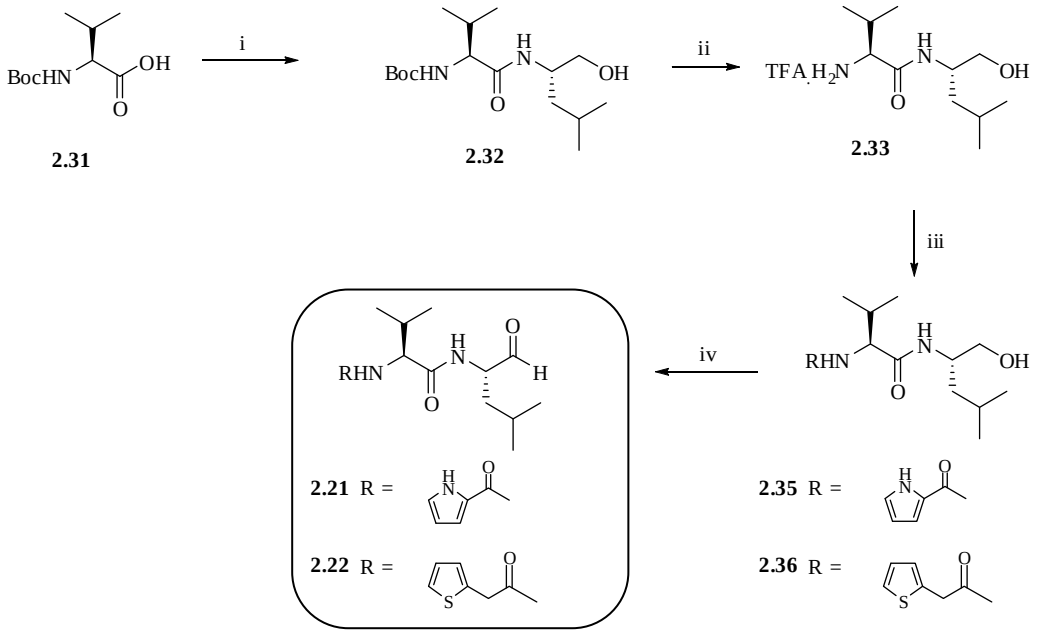

Scheme 2.3 *Reagents and Conditions:* i) HATU, DIPEA, *L*-leucinol, DMF, (68%); ii) TFA, DCM (100%); iii) 2-pyrrole carboxylic acid or 2-thiophene acetyl chloride, DIPEA, DMF (**2.35** 78%, **2.36** 83%); iv) SO_3-pyr, DMSO, DIPEA, DCM (**2.21** 89%, **2.22** 86%)

2.3.3 Design and Synthesis of Semicarbazones

The semicarbazone **2.37** was docked into the rigid μ-calpain model and the best pose is shown in **Figure 2.18**. This suggested that the semicarbazone **2.37** adopts a β-sheet conformation[††] as defined by hydrogen bonds A, B and C. Two additional hydrogen bonds were observed between the sulfonamide oxygen groups and Asn_{253} or Lys_{347} and the semicarbazone NH group and Cys_{105}. It was hoped these extra hydrogen bonds will enhance the binding affinity of the semicarbazone **2.37** (see **Chapter Six** for more detail). The semicarbazone **2.37** was originally synthesised by Nakamura[16] as a more water-soluble alternative to the aldehyde **2.3**, showing that the semicarbazone **2.37** was 16-fold more water soluble than the aldehyde **2.3**. However, no other semicarbazone moieties were tested. This provided impetus for the synthesis of novel semicarbazone containing inhibitors. The readily available semicarbazides[‡‡] 4-phenylsemicarbazone, thiosemicarbazone and the related phenylhydrazine hydrochloride were utilised to prepare semicarbazones as warheads for the exploration of P' subsites of the cysteine proteases m-calpain, μ-calpain, cathepsin B and papain.

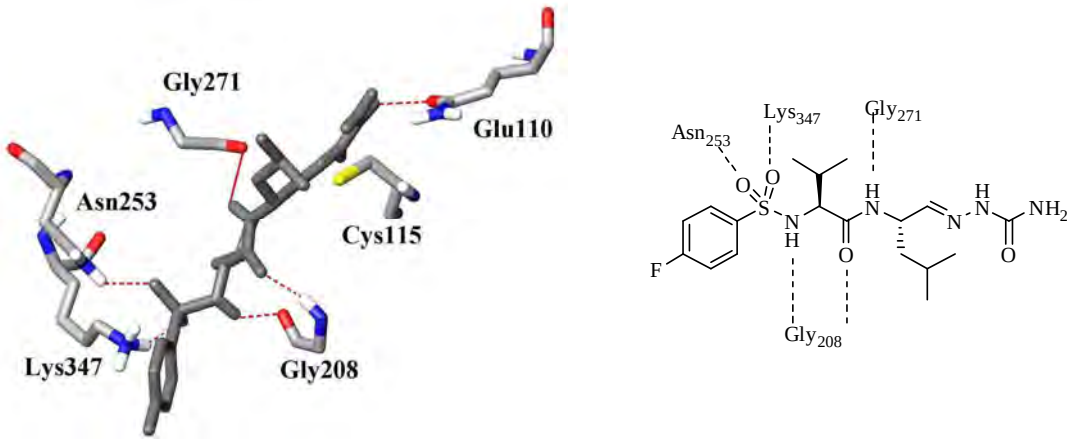

Figure 2.18 The semicarbazone **2.37** and molecular modelling results showing the hydrogen bonds formed to the enzyme

The semicarbazone analogues were prepared as shown in **Scheme 2.4** following the method described by Nakamura.[16] The aldehyde **2.3** was reacted with the chosen

[††] The parameters that define a β-sheet conformation are described in detail in **Chapter Four**
[‡‡] Note that phenylhydrazine hydrochloride is not a semicarbazide, but has been included in this section for discussion purposes

semicarbazide (semicarbazide hydrochloride, 4-phenylsemicarbazide hydrochloride, thiosemicarbazone, or the related phenylhydrazine hydrochloride) in a condensation reaction to give the desired semicarbazones **2.37**-**2.40** in high yields (90%, 83%, 85% and 70% respectively) after recrystallisation from ethyl acetate.

Neither the aldehyde **2.3** nor the four semicarbazides were sufficiently water-soluble for solely aqueous reaction conditions to be utilised, thus a suitable water miscible solvent was required. Each semicarbazide was tested for solubility in water, tetrahydrofuran and methanol. Semicarbazide hydrochloride and thiosemicarbazide hydrochloride were found to be soluble in a 1:1 mixture of tetrahydrofuran:water; aldehyde **2.3** was also soluble in this solvent system. 4-Phenylsemicarbazide hydrochloride and phenylhydrazine hydrochloride were found to be soluble in methanol; this too was a suitable solvent for the aldehyde **2.3** (see **Table 2.9** for a summary of the solvent systems used).

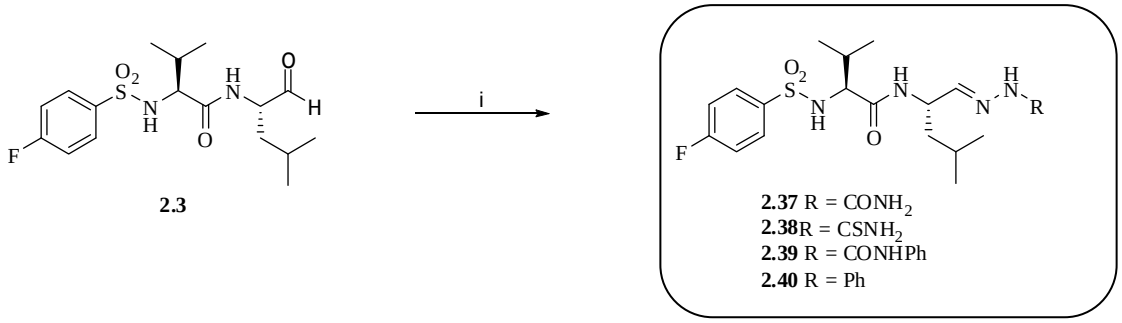

2.3

Scheme 2.4 *Reagents and Conditions*: i) NaOAc, H_2NNHR, solvent

Compound	Semicarbazone	Solvent	% Yield
2.37	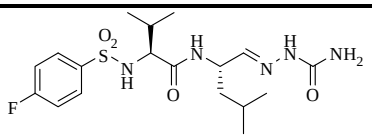	1:1 THF:H_2O	90
2.38	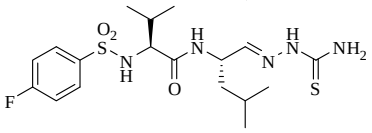	1:1 THF:H_2O	70
2.39	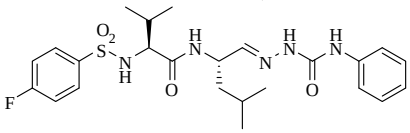	MeOH	85
2.40	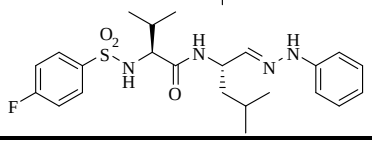	MeOH	83

Table 2.9 Solvent systems used for the semicarbazones **2.37-2.40** synthesised. The percentage yields of the products are also given

2.3.4 Design and Synthesis of Heterocycles

The oxadiazole **2.41** and the α-ketooxazoline **2.42** were docked into the rigid μ-calpain model and the best poses shown in **Figure 2.19**. This suggested that oxadiazole **2.41** formed two critical hydrogen bonds between the sulfonamide NH group and Gly_{208} and the amide NH group and Gly_{271} (A and C); with additional hydrogen bonds suggested between the sulfonamide oxygen groups and Asn_{253} or Lys_{347}. α-Ketooxazoline **2.42** was suggested to adopt a β-sheet conformation as defined by hydrogen bonds A, B and C (see **Figure 2.19**). The α-ketotetrazole **2.43** (see **Figure 2.20**) was not modelled.

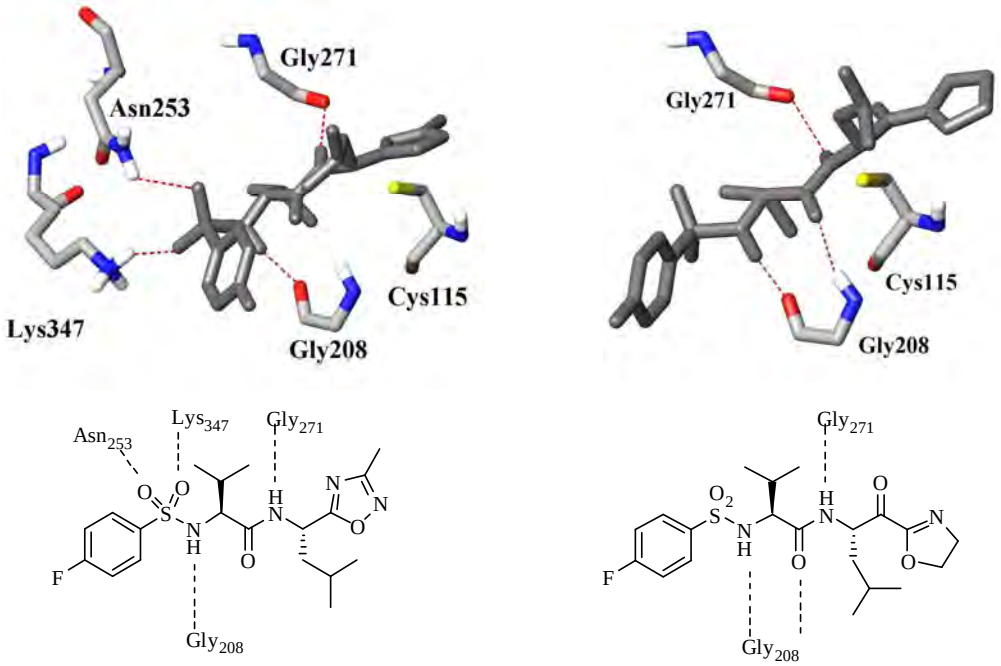

Figure 2.19 The heterocyclic warheads a) oxadiazole **2.41** and b) α-ketooxazoline **2.42** are suggested to form the hydrogen bonds as shown

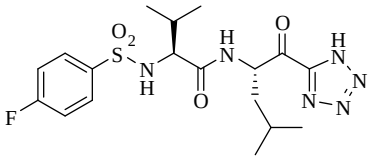

2.43

Figure 2.20 The α-ketotetrazole **2.43** was not modelled; it was assumed to be able to form similar hydrogen bonds to the α-ketooxazoline **2.42** above.

Samples of 4-fluorobenzenesulfonyl valine **2.24** and benzyloxycarbonyl valine **2.28** were separately reacted with to *L*-leucine methyl ester under standard HATU conditions to give the dipeptide methyl esters **2.44** and **2.45** in 96% and 95% yields respectively. This reaction was optimised from the BOP methodology employed previously by Payne *et al.*[42] The methyl esters **2.44** and **2.45** were separately hydrolysed in the presence of lithium hydroxide to give the free acids **2.7** and **2.46**. *N*-Hydroxyethanimidamide (**2.47**) was prepared by the addition of hydroxylamine to acetonitrile and subsequently coupled to carboxylic acids **2.7** and **2.46** to yield the amidoximes **2.48** and **2.49** as colourless glassy solids in 79% and 82% yields respectively. The 3-methyl-1,2,4-oxadiazoles **2.41** and **2.50** were formed via thermal intramolecular cyclodehydration of the amidoximes **2.48** and **2.49** in the presence of sodium acetate. The crude products were separately recrystallised from

ethyl acetate/petroleum ether to give the pure oxadiazoles **2.41** and **2.50** as colourless glassy solids in 88% and 90% yields respectively.

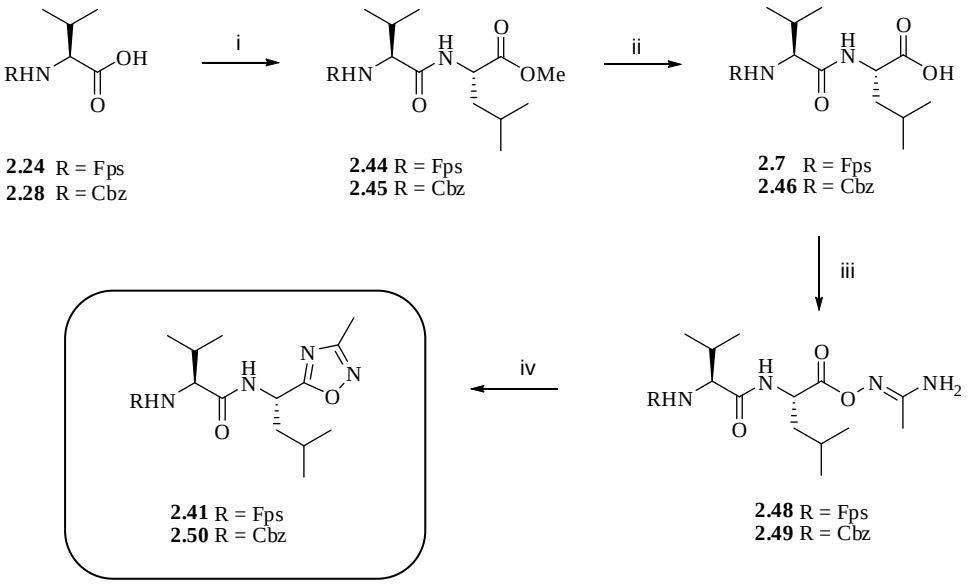

Scheme 2.5 *Reagents and Conditions*: i) *L*-leucine methyl ester, DMF, HATU (96%, 92%); ii) LiOH, THF, H_2O (94%, 98%); iii) *N*-hydroxyethanimidamide **2.47**, DCM/DMF (9:1), HOBt.H_2O, EDCI, -10°C (79%, 82%); iv) NaOAc, EtOH, reflux (88%, 90%)

The synthesis of the α-ketotetrazoles follows the method outlined in **Scheme 2.6** (left hand side of diverging synthesis). The aldehydes **2.3** or **2.19** were each reacted with sodium hydrogen sulfite and potassium cyanide to give the diastereomeric cyanohydrins **2.51** and **2.52** respectively, in good yield (82% and 86%). The cyanohydrins **2.51** and **2.52** were separately reacted with sodium azide and triethylamine hydrochloride[22] to give the α-hydroxytetrazoles **2.53** and **2.54** respectively. Separate recrystallisation of the α-hydroxytetrazoles **2.53** and **2.54** gave both of the pure products as pale yellow glassy solids (67% and 72% respectively).

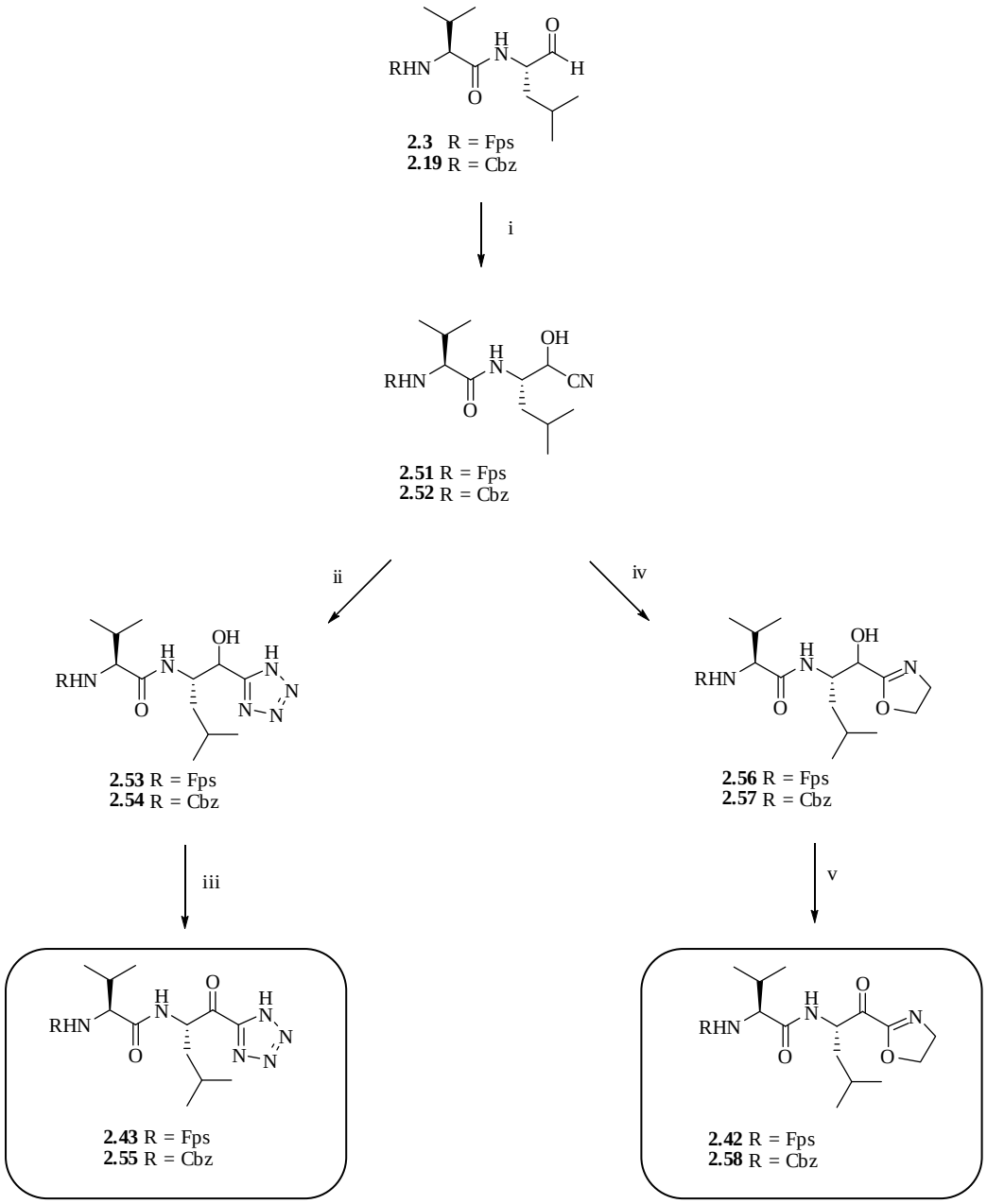

Scheme 2.6 *Reagents and Conditions*: i) $NaHSO_3$, MeOH, H_2O, KCN, EtOAc; ii) NaN_3, $Et_3N.HCl$, toluene, reflux; iii) TEMPO, NaOCl, KBr, DCM/H_2O; iv) Acetyl chloride, MeOH, $CHCl_3$, ethanolamine, DIPEA; v) SO_3-pyr, DMSO, DIPEA, DCM

The tetrazole ring was indistinguishable by ^1H NMR from the starting cyanohydrin. Thus infrared spectroscopy and mass spectrometry were utilised to determine whether formation of the α-hydroxytetrazole had occurred. Low resolution mass spectrometry was performed on separate samples of the α-hydroxytetrazoles **2.53** and **2.54**, giving the required masses of 443.1 $gmol^{-1}$ and 419.2 $gmol^{-1}$ respectively; similarly, the infrared spectra of α-hydroxytetrazoles **2.53** and **2.54** showed peaks around 1692 and 1649 cm^{-1}, characteristic

of an N-N aromatic stretch and markedly different from the nitrile peak observed at 2220 cm^{-1} for **2.52** (see **Chapter Seven, Section 7.2.3**).[43] Use of these two spectroscopic methods provided evidence that the α-hydroxytetrazole was present. Oxidation of the α-hydroxytetrazole **2.53** to the α-ketotetrazole **2.43** using sulfur trioxide-pyridine complex returned starting material only, as evident from the ^{1}H NMR of the isolated product. The nitroxide 2,2,6,6-tetramethylpiperidinyl-1-oxyl (TEMPO) has been reported as a mild oxidant[44] that maintains chiral integrity in oxidations of primary alcohols to aldehydes. TEMPO has also been used successfully in the oxidation of α-hydroxy amides to α-ketoamides without evidence of epimerisation.[45] Under these new conditions, **2.53** and **2.54** were oxidised separately utilising TEMPO-NaOCl to give the α-ketotetrazoles **2.43** and **2.55** successfully. ^{1}H NMR was used to assess the formation of the ketone by observing the absence of the proton at the β-carbon. The ^{1}H spectra of the α-hydroxytetrazoles **2.53** and **2.54** showed two distinct peaks for the hydrogen of the β-carbon at around 4.5 ppm, due to the diastereomeric nature of the β-carbon (see **Figure 2.21**, β-carbon hydrogen peaks circled). Oxidation to the α-ketotetrazoles **2.43** and **2.55** resulted in the loss of the hydrogen of the β-carbon. Further evidence for successful oxidation was observed in the ^{1}H and ^{13}C NMR spectra, as the signals associated with the P_1 residues were clearly defined as single resonances. This indicated that the diastereomeric centre of the α-hydroxytetrazole had been oxidised. Mass spectrometry and infrared analysis was again used to ensure that the tetrazole ring itself had remained intact during the oxidation and isolation of the product. Once again, mass spectrometry gave the required masses (441.1 $gmol^{-1}$ and 417.2 $gmol^{-1}$), and peaks at 1946 and 1923 cm^{-1} confirmed the conservation of the tetrazole ring.

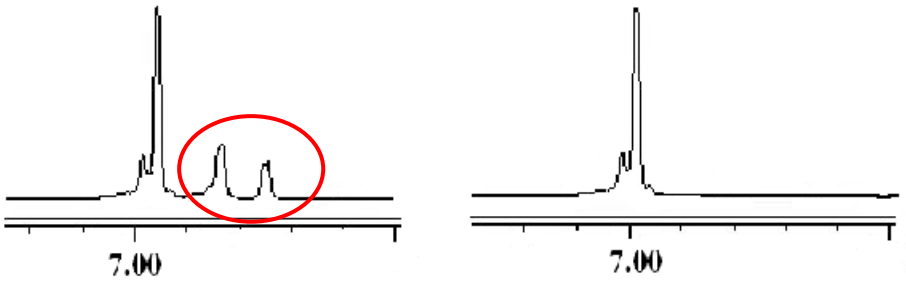

Figure 2.21 Partial ^{1}H NMR spectrum of α-hydroxytetrazole **2.53** and α-ketotetrazole **2.42**. The methine hydrogen peaks are circled.

The synthesis of the α-ketooxazolines[46] **2.42** and **2.58** on the right hand side of divergent synthesis is shown in **Scheme 2.6**. Acetyl chloride was reacted with anhydrous methanol

to generate anhydrous hydrogen chloride *in situ* which was reacted with separate samples of the cyanohydrins **2.51** and **2.52** to give imidate intermediates that were immediately reacted with DIPEA and ethanolamine to give the α-hydroxyoxazolines **2.56** and **2.57**. The mechanism of the oxazoline formation is as follows: the nitrogen of the nitrile of **2.51** or **2.52** is protonated by the acid and subsequently reacts with excess methanol, forming the imidate shown in **Figure 2.22** below (known as the Pinner reaction and the imidate a Pinner salt).[47] Attack on the imidate by the oxygen and nitrogen atoms of ethanolamine constructs the α-hydroxyoxazolines (**2.56** and **2.57**). The reaction is driven to completion by the loss of ammonia and the methoxy group. Finally, the α-hydroxyoxazolines **2.56** and **2.57** were oxidised with the sulfur trioxide-pyridine complex to give the α-ketooxazolines **2.42** and **2.58** in reasonable yield (45% and 63% respectively).

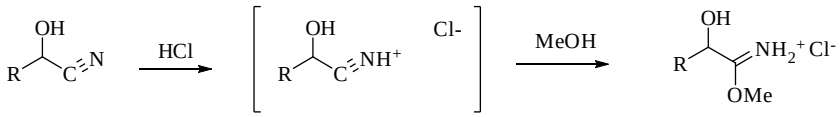

Figure 2.22 Mechanism of formation of imidates **2.55** and **2.56** (Pinner salts)[47]

2.3.4 Design and Synthesis of Peptidyl Nitriles

The cyanohydrins **2.51** and **2.52** were initially synthesised as intermediates of the heterocyclic inhibitors; however, subsequent docking of **2.51** into the rigid μ-calpain model suggested that it was a potential cysteine protease inhibitor, with the best pose shown in **Figure 2.23**.[§§] The warhead was purported to be in close contact with the active site cysteine thiol (comparable with parent aldehyde **2.3**); the backbone of the inhibitor was suggested to bind in an extended bioactive conformation defined by hydrogen bonds A, B and C; and an additional hydrogen bond between the cyanohydrin ***R***-OH group and Gly_{113} or the cyanohydrin ***S***-OH group and Cys_{115} was also suggested to occur.

[§§] The cyanohydrin could not be modeled as a diasteromeric mixture, hence the cyanohydrin was docked twice, once for each position of the secondary alcohol

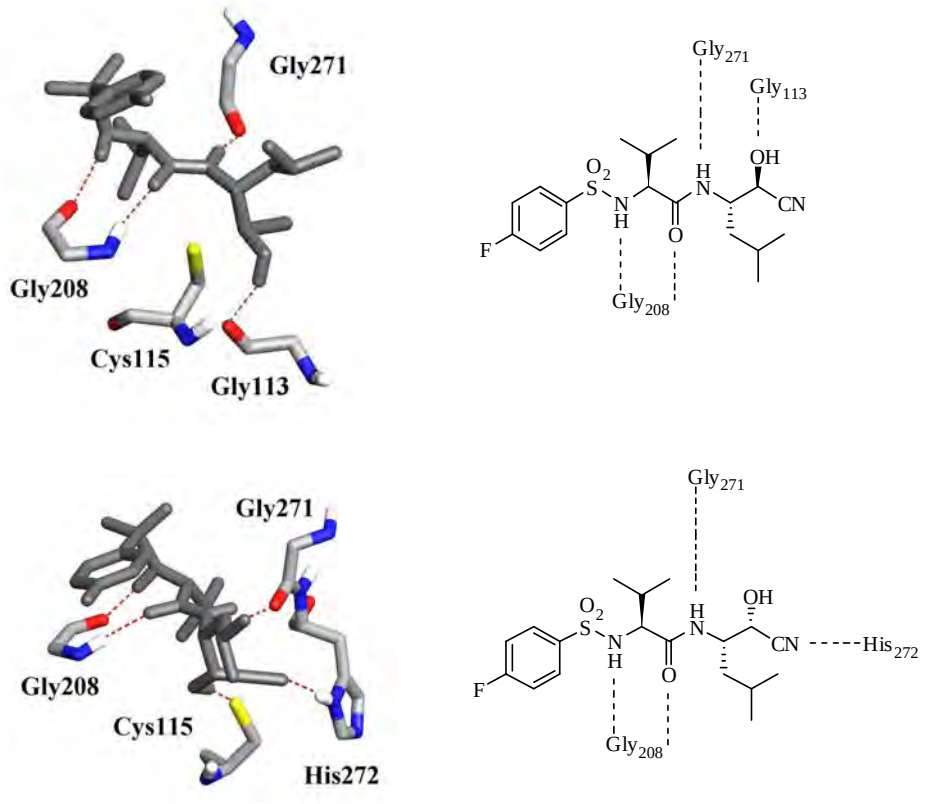

Figure 2.23 Molecular modelling results of the cyanohydrin **2.51**

Two further peptidyl nitrile analogues **2.59** and **2.60**, the protected esters of **2.51** and **2.52**, were also synthesised on the basis of the molecular modelling results for the cyanohydrin **2.51**. Further impetus was lent to this synthesis because the additional bulkiness provided by the benzyl protecting group might help identify differences in the $P_{1'}$ subsites of m-calpain, μ-calpain, cathepsin B and papain.

Samples of the cyanohydrins **2.51** and **2.52** were separately reacted with *N*-hydroxysuccinimide activated phenylacetic acid **2.59** to give the alcohol-protected nitriles **2.60** and **2.61** as 1:1 diastereoisomers (see **Scheme 2.7**).

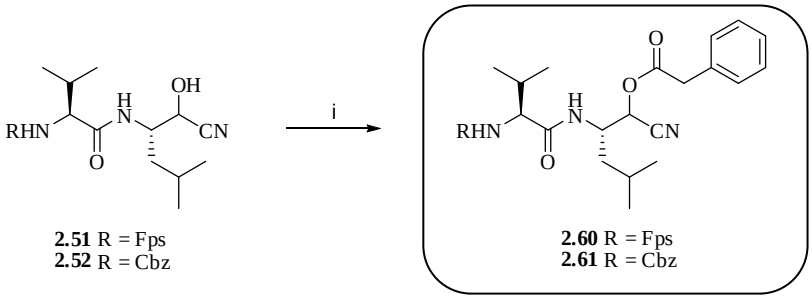

2.51 R = Fps
2.52 R = Cbz

2.60 R = Fps
2.61 R = Cbz

Scheme 2.7 *Reagents and Conditions*: i) Suc-phenylacetic acid **2.59**, DIPEA, DCM

2.3.5 Synthesis of the Azide Analogue

The azide **2.62** was docked into the rigid μ-calpain model and the best pose shown in **Figure 2.24**. This suggested that the azide **2.62** binds to calpain in an extended bioactive conformation defined by the hydrogen bonds A, B and C (see **Figure 2.24**). This model also suggested that the azide moiety was in close contact with the active site cysteine thiol. These findings made the azide **2.62** a desirable target for cysteine protease inhibition.

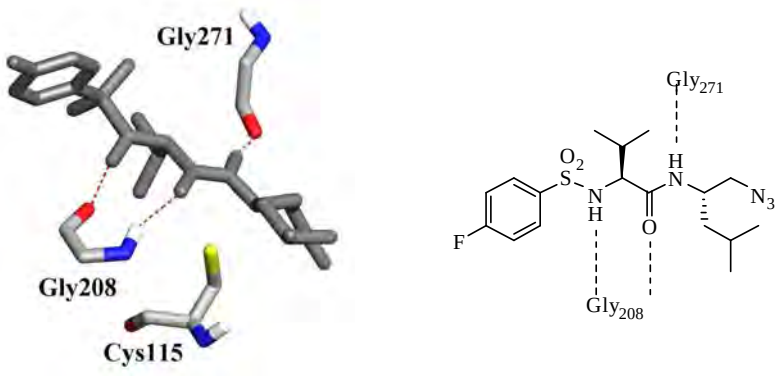

Figure 2.24 Molecular modelling of the azide **2.62** showing the three critical hydrogen bonds formed

Commercially available 4-fluorobenzenesulfonyl chloride **2.23** was reacted with *L*-valine to give the *N*-protected carboxylic acid **2.24**. Subsequent reaction of the acid **2.24** with *N*-hydroxysuccinimide gave the activated ester **2.25** in 95% yield. The ester **2.25** was reacted with *L*-leucinol to give the alcohol **2.6** as a white solid in 87% yield. No purification was needed. The azide **2.62** was formed in a two-step reaction. The alcohol **2.6** was reacted with mesyl chloride followed by sodium azide to give the azide **2.62**. S_N2 displacement of

the mesylate with sodium azide occurred without isolation of the intermediate mesylate (see **Scheme 2.8**). Column chromatography on silica gave the pure azide **2.62** as a white solid in a 53% yield.

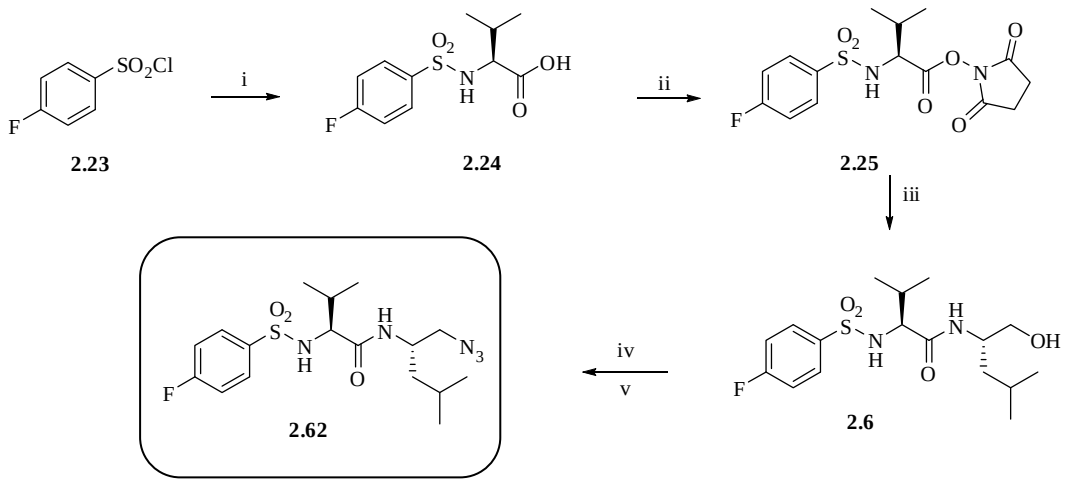

Scheme 2.8 *Reagents and Conditions*: i) THF, H_2O, *L*-valine, NaOH (75%); ii) *N*-hydroxysuccinimide, EDCI, DCM, THF (95%); iii) *L*-leucinol, DCM, DIPEA (87%); iv) Et_3N, MsCl, DCM (not isolated); v) DMF, NaN_3 (53%)

2.4 CONCLUSION AND FUTURE WORK

A series of dipeptidyl aldehydes were synthesised (**2.3**, **2.27**, **2.19**, **2.2**, **2.21** and **2.22)**. Four of these aldehydes (**2.3, 2.27, 2.19** and **2.2**) were literature compounds synthesised to validate the *in vitro* assay protocols. The aldehydes **2.21** and **2.22** were also broad spectrum cysteine protease inhibitors. The high yielding reactions and ease of synthesis of **2.3** and **2.19**, as well as their potency (see **Chapter Six**) against cysteine proteases led to these being used as lead compounds for the design of novel, selective cysteine protease inhibitors.

Subsequent replacement of the aldehyde moiety with warheads that were less chemically reactive resulted in the synthesis of novel cysteine protease inhibitors. These inhibitors included: semicarbazone warheads (**2.37-2.40**), oxadiazole warheads (**2.41** and **2.50**), α-ketotetrazole warheads (**2.43** and **2.55**), α-ketooxazoline warheads (**2.42** and **2.58**) and nitrile warheads (**2.51, 2.52, 2.60** and **2.61**). A non-covalent inhibitor with an azide moiety (**2.62**) in place of the warhead was also synthesised.

Assay results of these inhibitors against the cysteine proteases m-calpain, μ-calpain, papain and cathepsin B and a structure-activity relationship discussion can be found in **Chapter Six**.

Future work in the area of reversible cysteine protease inhibitors would involve further utilisation of non-covalent warheads. Warheads that are non-covalent and non-reactive are of increasing interest as little or no interaction should occur between the warhead and *in vivo* nucleophiles. Molecular modelling could be used to predict the hydrogen-bonding pattern of inhibitors and more importantly ensure the close proximity of the warhead to the active site cysteine.

2.5 REFERENCES FOR CHAPTER TWO

(1) Otto, H.-H.; Schirmeister, T. In *Chemical Reviews (Washington, D. C.)* 1997; Vol. 97, p 133-171.

(2) Donkor, I. O. *Current Medicinal Chemistry* **2000**, *7*, 1171-1188.

(3) Aoyagi, T.; Takeuchi, T.; Matsuzaki, A.; Kawamura, K.; Kondo, S. *Journal of Antibiotics* **1969**, *22*, 283-286.

(4) Leung-Toung, R.; Li, W.; Tam, T. F.; Karimian, K. *Current Medicinal Chemistry* **2002**, *9*, 979-1002.

(5) McKerrow, J. H.; James, M. N. G.; Editors *Cysteine Proteases: Evolution, Function, and Inhibitor Design. [In: Perspect. Drug Discovery Des., 1996; 6]*, 1996.

(6) Mykles, D. L. *Methods in Cell Biology* **2001**, *66*, 247-287.

(7) Iqbal, M.; Messina, P. A.; Freed, B.; Das, M.; Chatterjee, S.; Tripathy, R.; Tao, M.; Josef, K. A.; Dembofsky, B. *Bioorganic & Medicinal Chemistry Letters* **1997**, *7*, 539-544.

(8) Mehdi, S. *Trends in Biochemical Science* **1991**, *16*, 150-153.

(9) Inoue, J.; Nakamura, M.; Cui, Y.-S.; Sakai, Y.; Sakai, O.; Hill, J. R.; Wang, K. K. W.; Yuen, P.-W. *Journal of Medicinal Chemistry* **2003**, *46*, 868-871.

(10) Fukiage, C.; Azuma, M.; Nakamura, Y.; Tamada, Y.; Nakamura, M.; Shearer, T. R. *Biochimica et Biophysica Acta* **1997**, *1361*, 304-312.

(11) Sasaki, T.; Kishi, M.; Saito, M.; Tanaka, T.; Higuchi, N.; Kominami, N.; Katunuma, N.; Murachi, T. *Journal of Enzyme Inhibition* **1990**, *3*.

(12) Shirasaki, Y.; Miyashita, H.; Yamaguchi, M.; Inoue, J.; Nakamura, M. *Bioorganic & Medicinal Chemistry* **2005**, *13*, 4473-4484.

(13) Armarego, W. L. F.; Perrin, D. D. *Purification of Laboratory Chemicals*; 4th ed.; Butterworth-Heinemann: New York, 1996.

(14) Du, X.; Guo, C.; Hansell, E.; Doyle, P. S.; Caffrey, C. R.; Holler, T. P.; McKerrow, J. H.; Cohen, F. E. *Journal of Medicinal Chemistry* **2002**, *45*, 2695-2707.

(15) Adkison, K. K.; Barrett, D. G.; Deaton, D. N.; Gampe, R. T.; Hassell, A. M.; Long, S. T.; McFadyen, R. B.; Miller, A. B.; Miller, L. R.; Payne, J. A.; Shewchuk, L. M.; Wells-Knecht, K. J.; Willard, D. H. J.; Wright, L. L. *Bioorganic & Medicinal Chemistry Letters* **2006**, *16*, 978-983.

(16) Nakamura, M.; Inoue, J. *Bioorganic & Medicinal Chemistry Letters* **2002**, *12*, 1603-1606.

(17) Kumar, S.; Pearson, A. L.; Pratt, R. F. *Bioorganic & Medicinal Chemistry* **2001**, *9*, 2035-2044.

(18) Tsutsumi, S.; Okonogi, T.; Shibahara, S.; Ohuchi, S.; Hatsushiba, E.; Patchett, A. A.; Christensen, B. G. *Journal of Medicinal Chemistry* **1994**, *37*, 3492-3502.

(19) Edwards, P. D.; Wolanin, D. J.; Andisik, D. W.; Davis, M. W. *Journal of Medicinal Chemistry* **1995**, *38*, 76-85.

(20) Hamze, A.; Hernandez, J.-F.; Fulcrand, P.; Martinez, J. *Journal of Organic Chemistry* **2003**, *68*, 7316-7321.

(21) Angelastro, M. R.; Peet, N. P.; Bey, P. *Journal of Organic Chemistry* **1989**, *54*, 3913-3916.

(22) Johansson, A.; Poliakov, A.; Akerblom, E.; Wiklund, K.; Lindeberg, G.; Winiwarter, S.; Danielson, U. H.; Samuelsson, B.; Hallberg, A. *Bioorganic & Medicinal Chemistry* **2003**, *11*, 2551-2568.

(23) Demko, Z. P.; Sharpless, K. B. *Journal of Organic Chemistry* **2001**, *66*, 7945-7950.

(24) May, B. C. H.; Abell, A. D. *Tetrahedron Letters* **2001**, *42*, 5641-5644.

(25) Abbenante, G.; Fairlie, D. P.; Gahan, L. R.; Hanson, G. R.; Pierens, G. K.; van den Brenk, A. L. *Journal of the American Chemical Society* **1996**, *118*, 10384-10388.

(26) Nakamura, M.; Miyashita, H.; Yamaguchi, M.; Shirasaki, Y.; Nakamura, Y.; Inoue, J. *Bioorganic & Medicinal Chemistry* **2003**, *11*, 5449-5460.

(27) Edwards, P. D.; Meyer Jr., E. F.; Vijayalakshmi, J.; Tuthill, P. A.; Andisik, D. A.; Gomes, B.; Strimpler, A. *Journal of the American Chemical Society* **1992**, *114*, 1854-1863.

(28) Chan, A. W. E.; Golec, J. M. C. *Bioorganic & Medicinal Chemistry* **1996**, *4*, 1673-1677.

(29) Taylor, P. J.; Wait, A. R. *Journal of the Chemical Society, Perkins Transactions II* **1986**, 1765-1770.

(30) Greenspan, P. D.; Clark, K. L.; Cowen, S. D.; McQuire, L. W.; Tommasi, R. A.; Farley, D. L.; Quadros, E.; Coppa, D. E.; Du, Z.; Fang, Z.; Zhou, H.; Doughty, J.; Toscano, K. T.; Wigg, A. M.; Zhou, S. *Bioorganic & Medicinal Chemistry Letters* **2003**, *13*, 4121-4124.

(31) Dufour, E.; Storer, A. C.; Menard, R. *Biochemistry* **1995**, *34*, 9136-9143.

(32) Le, G. T.; Abbenante, G.; Madala, P. K.; Hoang, H. N.; Fairlie, D. P. *Journal of the American Chemical Society* **2006**, *128*, 12396-12397.

(33) Nakamura, M.; Yamaguchi, M.; Sakai, O.; Inoue, J. *Bioorganic & Medicinal Chemistry* **2003**, *11*, 1371-1379.

(34) Tao, M.; Bihovsky, R.; Wells, G. J.; Mallamo, J. P. *Journal of Medicinal Chemistry* **1998**, *41*, 3912-3916.

(35) Tyndall, J. D. A. N., T.; Fairlie, D.P. *Chemical Reviews* **2005**, *105*, 973-999.

(36) Moldoveanu, T.; Campbell, R. L.; Cuerrier, D.; Davies, P. L. *Journal of Molecular Biology* **2004**, *343*, 1313-1326.

(37) Friesner, R. A.; Banks, J. L.; Murphy, R. B.; Halgren, T. A.; Klicic, J. J.; Mainz, D. T.; Repasky, M. P.; Knoll, E. H.; Shelley, M.; Perry, J. K.; Shaw, D. E.; Francis, P.; Shenkin, P. S. *Journal of Medicinal Chemistry* **2004**, *47*, 1739-1749.

(38) Abell, A. D.; Jones, M. A.; Neffe, A.; Jones, S. A., Personal Communication.

(39) Hamada, Y.; Shioiri, T. *Chemical & Pharmaceutical Bulletin* **1982**, *30*, 1921-1924.

(40) Parikh, J. R.; Doering, W. v. E. *Journal of the American Chemical Society* **1967**, *89*, 5505-5507.

(41) Moulin, A.; Martinez, J.; Fehrentz, J.-A. *Journal of Peptide Science* **2007**, *13*, 1-15.

(42) Payne, R. J.; Brown, K. M.; Coxon, J. M.; Morton, J. D.; Lee, H. Y.-Y.; Abell, A. D. *Australian Journal of Chemistry* **2004**, *57*, 877-884.

(43) Silverstein, R. M.; Webster, F. X. *Spectrometric Identification of Organic Compounds*; 6 ed.; John Wiley and Sons: New York, 1998.

(44) Ma, Z.; Bobbitt, J. M. *Journal of Organic Chemistry* **1991**, *56*, 6110-6114.

(45) Harbeson, S. L.; Abelleira, S. M.; Akiyama, A.; Barrett, R., III; Carroll, R. M.; Straub, J. A.; Tkacz, J. N.; Wu, C.; Musso, G. F. *Journal of Medicinal Chemistry* **1994**, *37*, 2918-2929.

(46) Dunn, D.; Chatterjee, S. *Bioorganic & Medicinal Chemistry Letters* **1998**, *8*, 1273-1276.

(47) Hunter, M. J.; Ludwig, M. L. *Journal of the American Chemical Society* **1962**, *84*, 3491-3504.

CHAPTER THREE

Design and Synthesis of Irreversible Inhibitors of Cysteine Proteases

3.1 INTRODUCTION TO IRREVERSIBLE INHIBITORS

Many examples of irreversible warheads used in cysteine protease inhibitor design can be found in the literature. Some important examples include diazoketones, halomethyl ketones, alkylating agents,[1] acylating groups, phosphonylating groups and sulfonylating groups.[2,3] Members of these irreversible groups are depicted in **Figure 3.1**

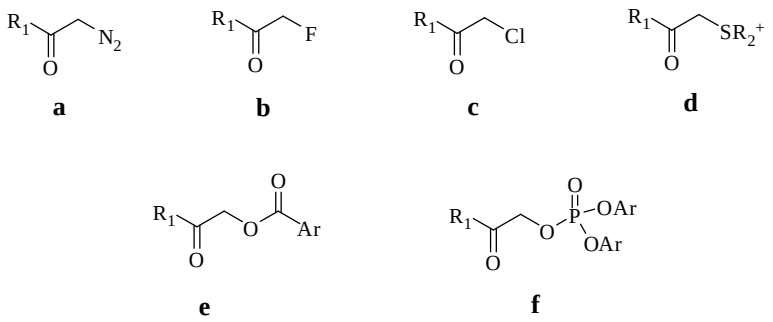

Figure 3.1 Irreversible inhibitor warheads include a) diazoketones, b) fluoromethyl ketones, c) chloromethyl ketones, d) sulfonium groups, e) acyl groups and f) phosphonium groups

A number of naturally occurring irreversible inhibitors have been isolated, for example, the epoxysuccinic acid E-64 (**3.1**) (see **Figure 3.2**) has been isolated from *Aspergillus japonicus*.[4,5] Epoxide **3.1** inhibits papain (IC_{50} = 0.29 µM), cathepsins B (IC_{50} = 0.24 µM) and L (IC_{50} = 0.11 µM), m-calpain (IC_{50} = 2.6 µM), µ-calpain (IC_{50} = 1.0 µM) and numerous other cysteine proteases, but is inactive against serine proteases.[2,4,6] The derivatives **3.2** and **3.3** are also potent cysteine proteases inhibitors (IC_{50} values in sub µM range) see **Table 3.1**. Extensive research has shown that active site thiol reacts with the C-2 carbon (as labeled in **Figure 3.2**) of the oxirane ring in a suggested S_N2 manner.[7,8] Crystal structures of **3.1** bound in the active site of papain show that it binds *N*-terminal to *C*-terminal relative to the scissile bond (see **Figure 3.3**) [9]

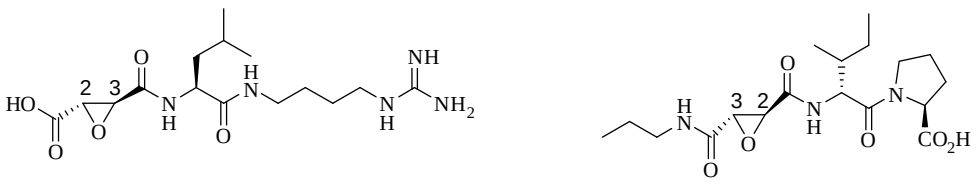

Figure 3.2 Numbering of the oxirane ring carbons relative to attack by the active site cysteine thiol.

Compound		IC_{50} (μM)				
		Papain	Cat B	Cat L	m-calpain	μ-calpain
3.1	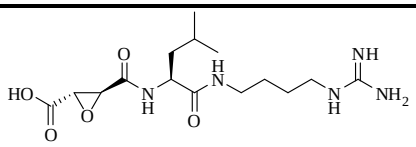	0.29	0.24	0.11	2.6	1.0
3.2	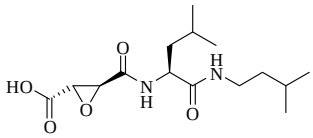	-	0.24	0.13	-	3.0
3.3	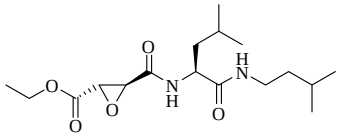	0.013	0.0034	-	-	-
3.4	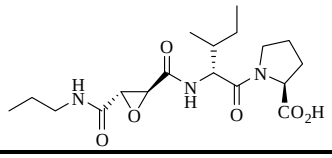	57	0.0022	17	-	200

Table 3.1 Potency of epoxysuccinyl esters against cysteine proteases[1]

Crystal structures of **3.1** bound in papain[10] have been used to predict the mode of binding of **3.1** to the active site of cathepsin B. Subsequent modifications to increase binding affinity of the inhibitor to the enzyme led to the development of the epoxide **3.4**. The synthetic peptidyl epoxysuccinate **3.4** (**Figure 3.2**), is a potent, selective irreversible inhibitor of cathepsin B (IC_{50} = 0.0022 μM, selectivity 8000-fold, see **Table 3.1**).[7,11] Yamamoto *et al*[12] proved through use of an X-ray crystal of papain with **3.4** bound, that **3.4** binds *N*-terminus to *C*-terminus in the active site (this opposite to **3.1**, which binds *C*-terminus to *N*-terminus) (see **Figure 3.3**). Thus attack of the cysteinyl thiol occurs on the C-3 carbon of the epoxide rather than the C-2 as in the case of **3.1**.

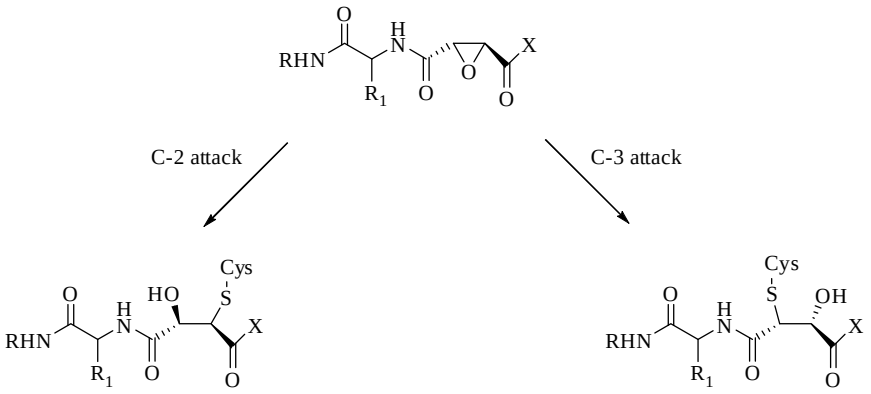

Figure 3.3 The binding modes of different epoxysuccinyl inhibitors. The cysteinyl thiol can attack the C-2 carbon of the epoxide as for **3.1** or can attack the C-3 carbon as for **3.4**.

Irreversible inhibitors have not found much therapeutic use due to problems associated with toxicity and side effects as the inhibitor accumulates within biological systems. It has been suggested that long-term usage of irreversible inhibitors for the treatment of disease may lead to immune disorders.[13] This is highlighted by the example of **3.3**, [11] (**Table 3.1**) which was considered a promising pro-drug for the treatment of muscular dystrophy. However, clinical trials revealed that **3.3** caused hepatic injury in rats and teratogenic effects on rat embryogenesis.[6,14] Irreversible inhibitors however, are still desirable for the treatment of disease as a short-term treatment, especially in the case of bacterial, viral or parasitic diseases.[13] Furthermore, an inhibitor that is specific for and forms an irreversible covalent bond to its target enzyme is an excellent candidate for obtaining crystal structures of the enzyme with inhibitor bound, which will help elucidate the active site and binding clefts of enzymes that are not fully characterised.

The inhibitors that are described in **Chapter Three** were designed to be specific, potent cysteine proteases. All of the inhibitors in the following synthetic sections belong to the 'alkylating agents' group of irreversible inhibitors.

3.2 IRREVERSIBLE WARHEADS UTILISED IN PROTEASE INHIBITORS

3.2.1 Michael Acceptor Warheads

Michael acceptor inhibitors have been reported as potent inhibitors of cysteine proteases.[15,16] Kong[17] and co-workers synthesised a series of potent Michael acceptor inhibitors for human rhinovirus (**3.5a-c**), with IC_{50} values less than 0.30 μM (see **Table 3.2**). The α,β-unsaturated acid **3.5d** was 70-fold less potent than the α,β-unsaturated esters **3.5a-c** and the single amino acid α,β-unsaturated ester **3.5e** was 50-fold less potent than the tripeptide analogue **3.5c**.

3.5

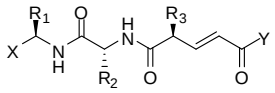

	X	R_1	R_2	R_3	Y	IC_{50} (μM)
3.5a	Boc	Val	Leu	Phe	OMe	0.25
3.5b	Boc	Val	Leu	Phe	OEt	0.13
3.5c	Cbz	Val	Leu	Phe	OMe	0.17
3.5d	Boc	Val	Leu	Phe	OH	18
3.5e	Cbz	Phe	-	-	OMe	9.5

Table 3.2 Michael acceptors showing inhibition of human rhinovirus[17]

Michael acceptors such as vinyl sulfones and α,β-unsaturated carbonyls are proposed to inhibit cysteine proteases in a similar manner. The active site cysteine undergoes a 1,4-Michael addition reaction that results in the enzyme becoming permanently alkylated. The oxygen atoms of the sulfone or the carbonyl are involved in hydrogen-bonding to the enzyme active site, thus helping to activate the β-carbon of the vinyl group for nucleophilic attack by the cysteine (**Figure 3.4**).

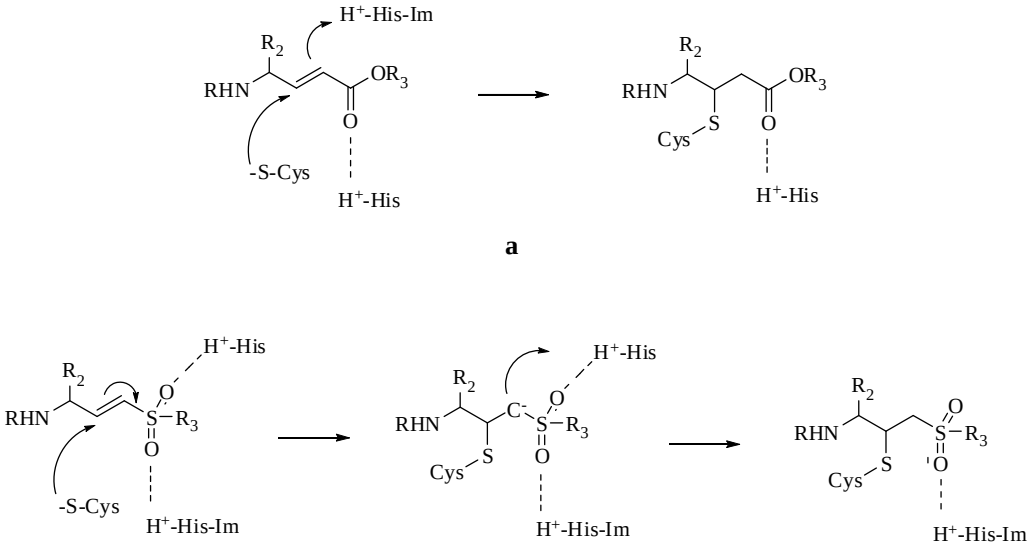

Figure 3.4 The proposed mechanism of inactivation of cysteine proteases by a) α,β-unsaturated carbonyl derivatives[5] and b) by vinyl sulfones[18]

3.2.2 Diazoketone Warheads

Peptidyl diazomethyl ketones can act as cysteine protease inhibitors. This was observed by Leary *et al*,[19] who tested the diazoketones **3.6** and **3.7** inhibitory activity against papain. These assay results (measured as rates of inactivation) are shown in **Table 3.3**. The dipeptidyl diazoketone **3.7** was found to be 200-fold more potent than diazoketone **3.6** against papain. Subsequently, Green *et al*[20] tested the analogous dipeptidyl diazoketones **3.6-3.9** against the cysteine protease cathepsin B and clostripain (a serine protease) in order to determine the selectivity of diazoketones for cysteine proteases. The diazoketones **3.7** and **3.9** were shown to be selective for cysteine proteases over the serine protease clostripain by 135- and 25000-fold respectively; however, there was no comparison within the cysteine protease family.

	Inhibitor	Rate of Inactivation (K_i/t) ($M^{-1}.s^{-1}$)		
		Papain[19]	Cathepsin B[20]	Clostripain[20]
3.6	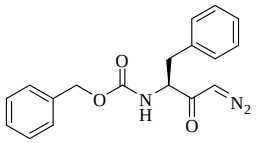	10.5	0.27	20
3.7	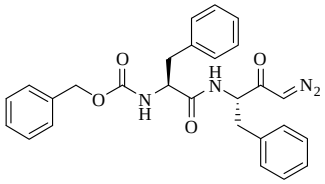	2030	-	15
3.8	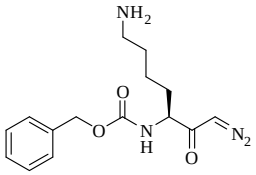	-	302	467
3.9	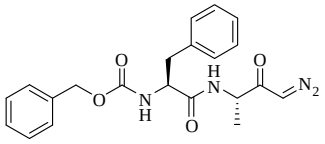	-	1250	0.05

Table 3.3 The inactivation rate of papain by diazoketone inhibitors

X-ray crystal structure analysis[19] of papain treated with the diazoketone **3.6** showed that inhibition of the enzyme occurred via alkylation of the active site cysteine thiol. The proposed mechanism of inactivation occurs via reaction of the carbonyl carbon with the active site thiolate to form a hemithioketal species. Proton transfer from the active site histidine to the methylene carbon occurs as in **Figure 3.5**. The final step to give the thioether is proposed to occur via a three-membered transition state with simultaneous cleavage of nitrogen.[1,6]

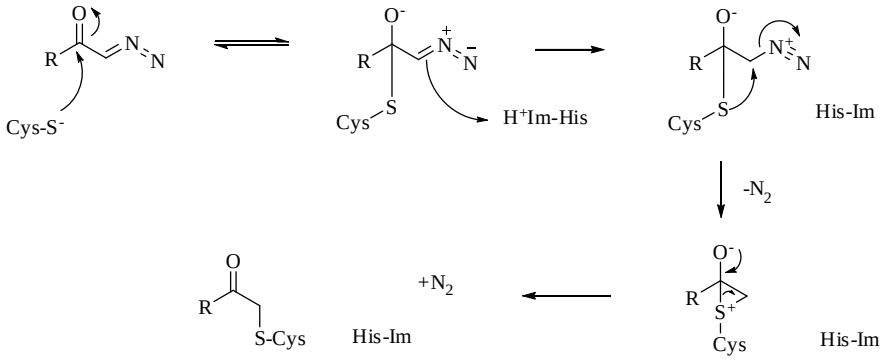

Figure 3.5 Proposed mechanism of inactivation by diazoketones

3.2.3 Halomethylketone Warheads

Chloromethyl and fluoromethyl ketones have been reported as cysteine protease inhibitors.[21-23] The fluoromethyl ketones **3.10a-e**[22] in **Table 3.4** were tested against the cysteine proteases μ-calpain, cathepsin B and cathepsin L. Inhibition was measured as a rate of inactivation (the faster the rate, the more potent the inhibitor). The inhibitors **3.10a-e** are significantly more potent against μ-calpain than cathepsin B or L. The fluoromethyl ketones **3.10a** and **3.10b** show over 20-fold selectivity for μ-calpain than the other cysteine proteases tested.

3.10

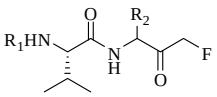

R_1	R_2	Rate of inactivation (M^{-1} s^{-1})		
		μ-calp	cath B	cath L
3.10a Cbz	benzyl	136300	300	5000
3.10b Morpholino- 4-sulfonyl	benzyl	67200	100	3200
3.10c (Benzylamino)carbonyl	benzyl	67000	275	9400
3.10d Cbz	CH_2OTHP	100000	9000	22600
3.10e Cbz-Leu	benzyl	290000	4600	256000

Table 3.4 Some potent fluoromethyl ketone calpain inhibitors.[22]

A review by Donkor[2] highlights that fluoromethyl ketones are usually more potent inhibitors than the corresponding chloromethyl ketones, as evidenced by the chloromethyl

ketone **3.11** (rate of inactivation 9500 $M^{-1}s^{-1}$) compared to the fluoromethyl ketone **3.12** (rate of inactivation 290000 $M^{-1}s^{-1}$)[2] in **Figure 3.6**. Both fluoromethyl and chloromethyl ketones are indiscriminately reactive. This property is reflected by the ability to inhibit both cysteine and serine proteases, as well as glutathione and nonproteolytic enzymes.[21]

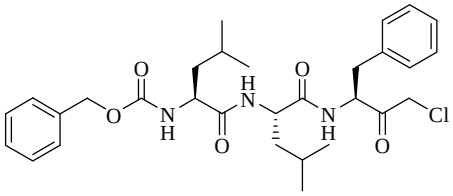

3.11
Rate of inactivation 9500 $M^{-1}s^{-1}$

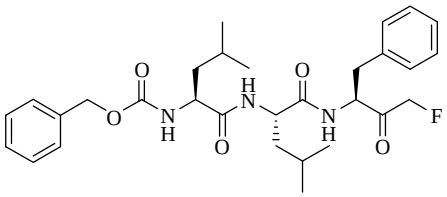

3.12
Rate of inactivation 290000 $M^{-1}s^{-1}$

Figure 3.6 Comparison of rate of inactivation of a choromethyl ketone versus a fluoromethyl ketone against μ-calpain

Two possible mechanisms have been postulated to explain the inactivation of cysteine proteases by halomethyl ketones (**Figure 3.7**).[1] In mechanism A (red), the active site thiol reacts directly with the carbon of the halomethyl in a nucleophilic substitution reaction. Alternatively, in B (blue), the active site thiol reacts with the carbonyl carbon forming a covalent bond via a three-membered ring. This second pathway is thought to be the most plausible since a tetrahedral intermediate is formed.

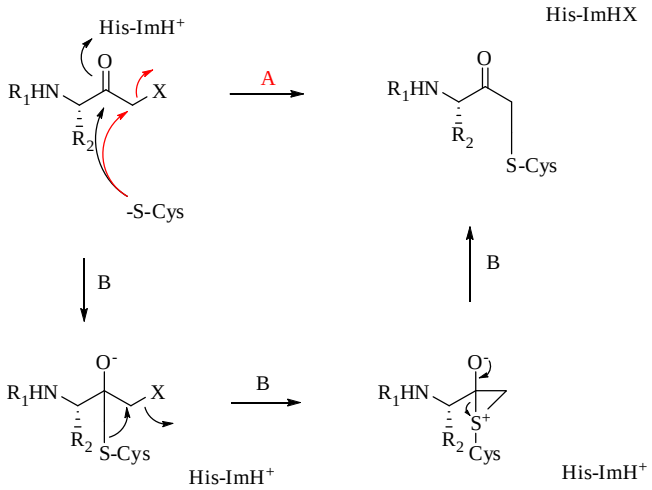

Figure 3.7 Proposed mechanisms for inactivation of cysteine proteases by halomethyl ketones. X denotes the halogen: Cl, Br, F

3.2.4 Peptidyl Epoxide Warheads

Albeck and co-workers[24] designed peptidyl epoxides **3.13a-d** as selective inactivators of cysteine proteases (see **Table 3.5**), showing the epoxide moiety to be a weak electrophile that is stable under neutral or basic conditions but highly electrophilic upon protonation, such as would occur in the active site of an enzyme. The epoxides **3.13a-d** are weak inhibitors of papain and cathepsin B (K_i values >10 µM). The epoxide **3.13d** is the most potent inhibitor with K_i values of 30 µM and 10 µM against cathepsin B and papain respectively. The selectivity observed between cathepsin B and papain ranges from between 2- and 6-fold in favour of papain, inclusive of the inhibitors **3.13a-d**.

3.13

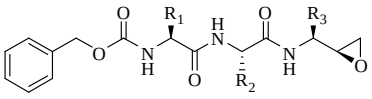

		K_i (μM)	
	R_1-R_2-R_3	**Cathepsin B**	**Papain**
3.13a	Gly-Leu-Phe	640	-
3.13b	- - Phe	570	370
3.13c	- Phe-Ala	320	60
3.13d	Phe-OBn-Thr	30	10

Table 3.5 Peptidyl epoxide inhibitors of cysteine proteases

Peptidyl or amino epoxides interact directly with the cysteine of the active site (**Figure 3.8**). Epoxides are weak electrophiles that require activation by the catalytic histidine; upon protonation, epoxides become highly electrophilic.[24] This protonation is thought to occur prior to, or simultaneously with, the nucleophilic attack of the thiolate.[25]

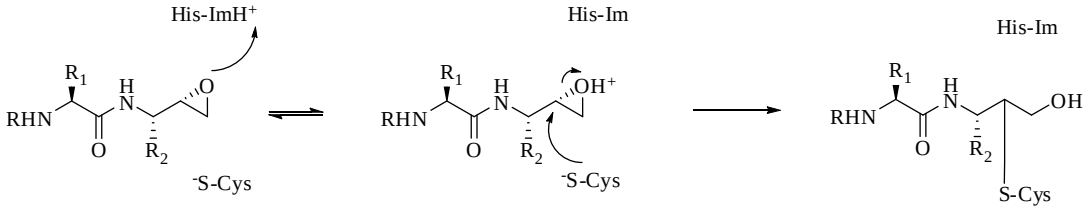

Figure 3.8 Proposed mechanism of inhibition of cysteine proteases by peptidyl epoxides.

3.3 DESIGN AND SYNTHESIS OF IRREVERSIBLE CYSTEINE PROTEASE INHIBITORS

3.3.1 Design and Synthesis of Michael Acceptor Inhibitors

Michael acceptors contain a double bond that is activated by the presence of an electrophilic group, such as an ester or sulfone (see **Figure 3.9**).[16] This class of irreversible inhibitors require the catalytic cysteine residue for activation, being unreactive towards nucleophiles (including free thiols) under physiological conditions.[26] Michael acceptor warheads are less reactive than aldehyde warheads, thus it is expected inhibitors with a Michael acceptor-type warhead will show increased selectivity between cysteine proteases of the papain superfamily.

a **b**

Figure 3.9 The general structure of a double bond activated by an adjacent a) sulfone group and b) ester group

The target Michael acceptor **3.14** was docked in the rigid μ-calpain model and the best pose shown in **Figure 3.10**. This suggests that the Michael acceptor **3.14** binds to calpain in a β-sheet, defined by hydrogen bonds A, B and C (as previously defined in **Chapter Two**). The hydrogen bonds suggested to form to the Michael acceptor **3.14** are analogous to the hydrogen bonds purported to form to the aldehyde **2.3** (see **Figure 3.9**). An additional hydrogen bond is suggested to exist between the methyl ester carbonyl oxygen group and His_{272} of **3.14**.

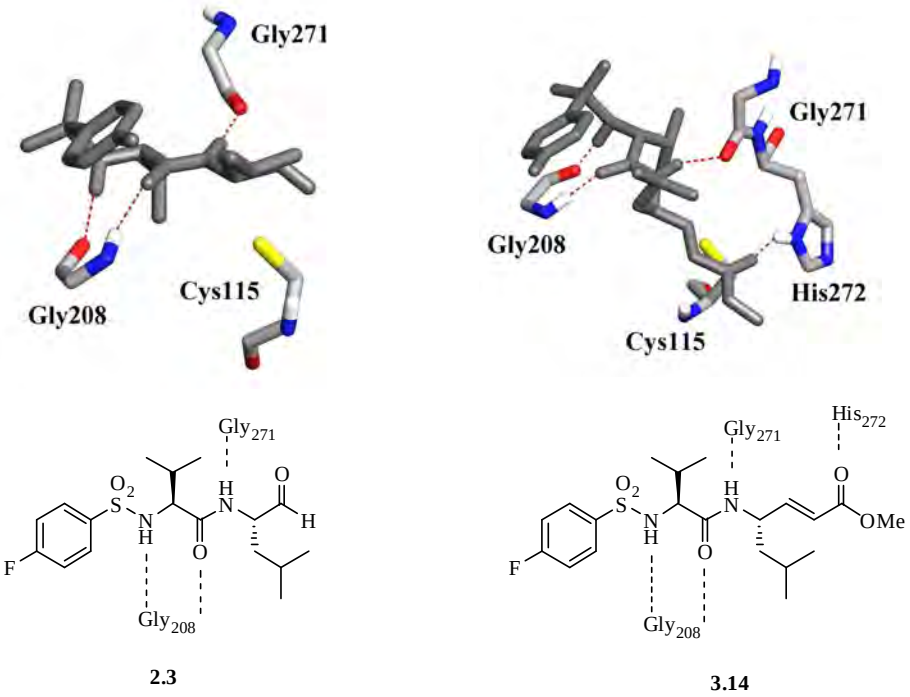

2.3 **3.14**

a) **b)**

Figure 3.10 Molecular modelling results of a) aldehyde **2.3** in comparison to b) Michael acceptor **3.14**

Synthesis of α,β-Unsaturated Carbonyls

Samples of the aldehydes **2.3** and **2.19** were separately reacted with methyl(triphenylphosphoranylidene)acetate, ethyl(triphenylphosphoranylidene)acetate, or triphenylphosphoranylidene acetaldehyde to give the α,β-unsaturated carbonyls (**3.14-3.18**). Separate purification of each of the α,β-unsaturated carbonyls **3.14-3.18** by flash chromatography gave the pure α,β-unsaturated carbonyls as white solids in good yield (**3.14**, 93%; **3.15**, 95%; **3.16**, 89% and **3.17**, 91%).

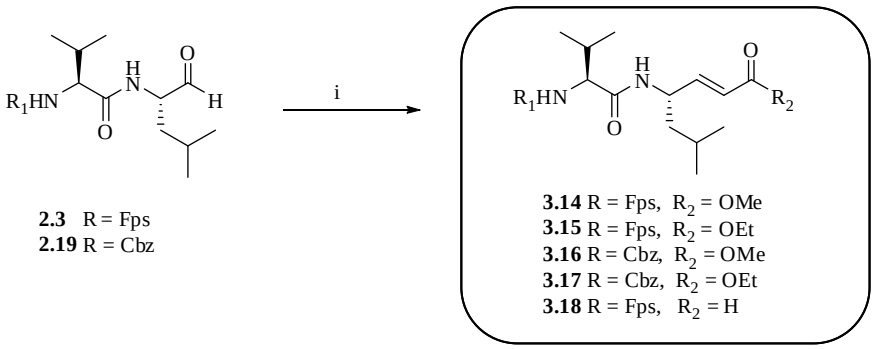

2.3 R = Fps
2.19 R = Cbz

3.14 R = Fps, R_2 = OMe
3.15 R = Fps, R_2 = OEt
3.16 R = Cbz, R_2 = OMe
3.17 R = Cbz, R_2 = OEt
3.18 R = Fps, R_2 = H

Scheme 3.1 *Reagents and Conditions*: i) PPh_3CHCO_2Me, PPh_3CHCO_2Et or PPh_3CHCHO, DCM

Utilisation of the *Wittig* reaction to yield the α,β-unsaturated aldehyde **3.18** proved problematic, as both the desired product **3.18**, the diene **3.19** and the starting aldehyde **2.3** (see **Figure 3.11**) were observed by mass spectrometry (being found as 399.1741, 425.1329 and 373.1613 $gmol^{-1}$ respectively

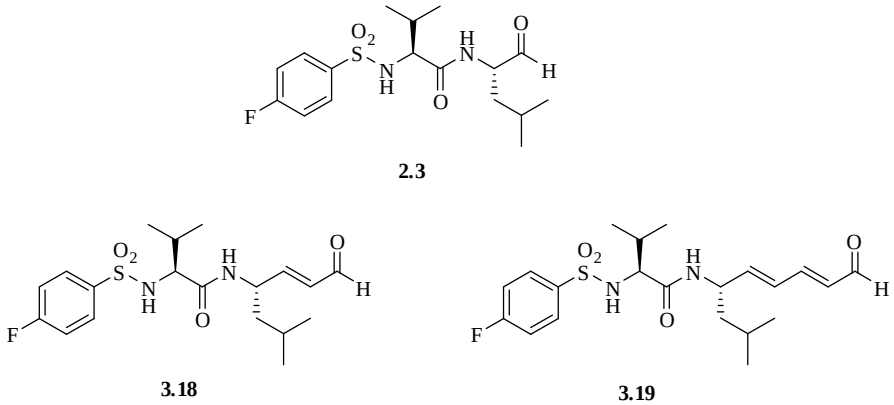

2.3 **3.18** **3.19**

Figure 3.11 The starting material **2.3** and the two products **3.18** and **3.19** observed

Each of these three products was distinguishable by its unique aldehyde peak observed as in the partial ^{1}H spectra in **Figure 3.12**. The starting material (aldehyde **2.3**) has a characteristic singlet peak at 9.40 ppm; the product **3.18** and diene **3.19** both have characteristic multiplet peaks. The use of 2D NMR techniques (COSY) allowed the unambiguous assignment of the multiplet at 9.65 ppm as the aldehyde peak of the desired α,β-unsaturated aldehyde **3.18** and the multiplet at 10.33 ppm as the aldehyde peak of the diene **3.19**.[*]

[*] Note that the diene **3.19** was not isolated.

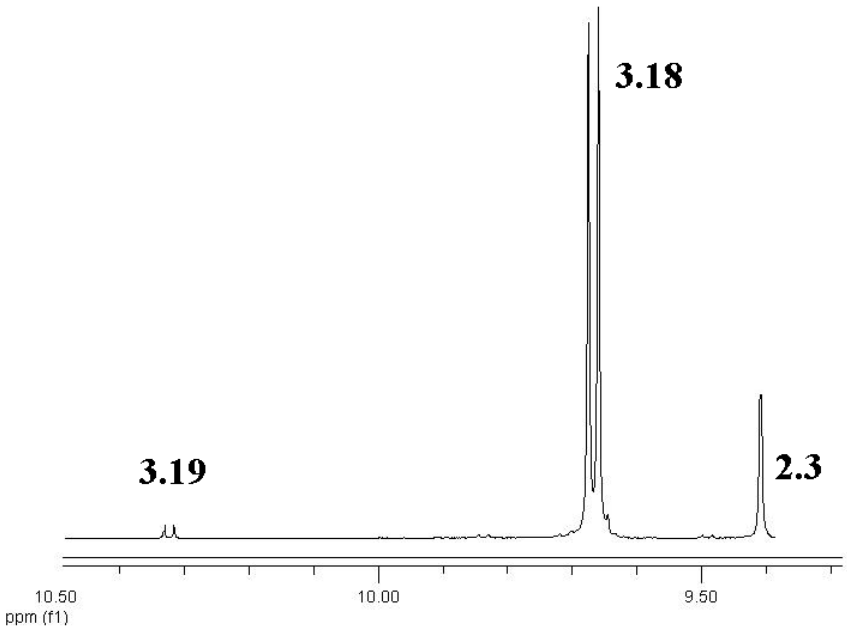

Figure 3.12 Partial ^{1}H NMR showing the aldehyde peaks in a crude sample of α,β-unsaturated aldehyde **3.18** that also contains a small amount of the side product **3.19** and starting material **2.3**

The reaction of the aldehyde **2.3** with triphenylphosphoranylidene acetaldehyde was optimised by investigating different ratios of triphenylphosphoranylidene acetaldehyde to aldehyde **2.3** and subsequent quantification of the products (see **Table 3.6**). The conditions that gave the best yield of the desired product **3.18** were one equivalent of the aldehyde **2.3** and 0.9 equivalents of triphenylphosphoranylidene acetaldehyde. The small amount of diene **3.19** formed was removed via column chromatography to give the desired α,β-unsaturated aldehyde **3.18** as a pale yellow solid in a 68% yield.

Aldehyde 2.3 (equiv)	Ylide (equiv)	% 3.18	% 3.19 diene	% Starting material
1.0	1.1	40	60	-
1.0	1.0	70	30	-
1.0	0.9	70	-	30
1.0	0.8	50	-	50

Table 3.6 Optimisation of experimental conditions for unsaturated aldehyde **3.18**.

Synthesis of Dipeptidyl Vinyl Sulfones

The vinyl sulfone moiety is more electron withdrawing than the α,β-unsaturated carbonyls of **3.14-3.18**, so extension of the Michael acceptor series of cysteine protease inhibitors to include vinylogous sulfones will provide a direct comparison between the reactivity of the warhead and the selectivity shown between proteases of the papain superfamily.

The formation of the vinyl sulfones **3.20-3.23** can be achieved in a number of ways. Olefination reactions such as *Horner-Emmons-Wadsworth* and *Peterson* can be used.[27] *Peterson* olefination occurs *via* the reaction of a trialkylsilane with an aldehyde or ketone to give a β-hydroxysilane which spontaneously eliminates water to give the desired alkene. Generally, the *Peterson* method leads to mixtures of geometric isomers.[28] The synthesis of vinyl sulfones described in this section utilises *Horner-Emmons-Wadsworth* chemistry.[29] This methodology exclusively gives the *trans* product.[27,30] Further, the phosphonate carbanions used in *Horner-Emmons-Wadsworth* reactions are more nucleophilic than the phosphonium ylides used in *Wittig* reactions, hence the phosphonate carbanions will react with a wide variety of aldehydes and ketones.[29]

The vinyl sufones **3.20-3.23** were synthesised directly from the corresponding aldehydes **2.3**, **2.27**, **2.19** and **2.2**. Commercially available diethyl(methylthiomethyl) phosphonate was oxidised in the presence of potassium permanganate to give diethyl(methylsulfonylmethyl) phosphonate **3.24** as a pale yellow glassy solid in excellent yield (89%).[31] The phosphonium ylide **3.24** was subsequently reacted with separate samples of the aldehydes **2.3**, **2.27, 2.19** and **2.2** using *Horner-Emmons-Wadsworth* methodology to give the vinyl sulfones **3.20-3.23** (see **Scheme 3.2**). The vinyl sulfones **3.20-3.23** were isolated and subsequently purified (**3.20** and **3.22** by recrystallisation; **3.21** and **3.23** by flash chromatography) to give the pure vinyl sulfones **3.20** and **3.22** as white solids (89% and 78% yields respectively) and **3.22** and **3.23** as colourless oils (84% and 66% yields respectively).

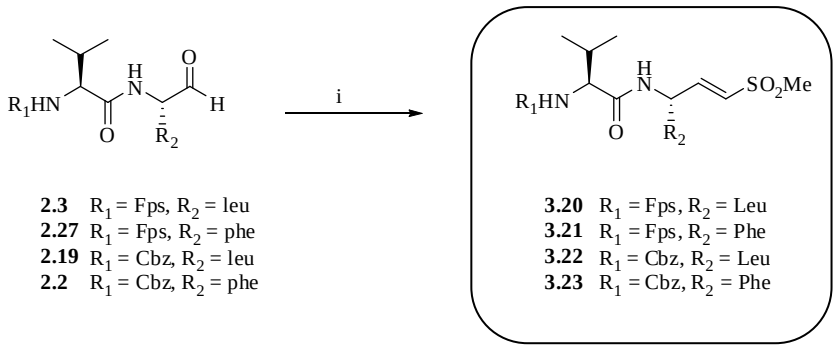

2.3 R_1 = Fps, R_2 = leu
2.27 R_1 = Fps, R_2 = phe
2.19 R_1 = Cbz, R_2 = leu
2.2 R_1 = Cbz, R_2 = phe

3.20 R_1 = Fps, R_2 = Leu
3.21 R_1 = Fps, R_2 = Phe
3.22 R_1 = Cbz, R_2 = Leu
3.23 R_1 = Cbz, R_2 = Phe

Scheme 3.2 *Reagents and Conditions*: i) $(EtO)_2P(O)CH_2SO_2CH_3$ **3.24**, n-butyllithium, -78°C, THF.

Analysis of the products **3.20-3.23** by ^1H and ^{13}C NMR showed the presence of only one isomer, as determined by the clearly single resonances for P_1 residues (for **3.20** and **3.22** this was Leu; for **3.21** and **3.23**, Phe) and the alkene. The double bond of the vinyl sulfones was determined to be the *trans* isomer on the basis that the coupling constants observed for the vinyl sulfones **3.20-3.23** were 15.1 Hz, 15.2 Hz, 15.0 Hz and 15.0 Hz respectively. The coupling of protons across a *trans* alkene (13-18 Hz) is known to be larger than that for *cis* alkenes (8-12 Hz) as shown in **Figure 3.13**.[32] The *trans* isomers formed are also consistent with the *Horner-Emmons-Wadsworth* methodology used.

cis
J = 7-12 Hz

trans
J = 13-18 Hz

Figure 3.13 The size of the coupling constants (in Hz) observed for *cis* and *trans* alkenes.[32]

3.3.2 Design and Synthesis of Diazoketones

Leary[19] and Green[20] (detailed in **Section 3.2.2** above) established diazoketones as specific cysteine proteases inhibitors, but did not effectively compare selectivity within the papain superfamily. Thus the diazoketones **3.25** and **3.26** were synthesised (see **Scheme 3.3**).

Samples of the dipeptidyl carboxylic acids **2.24** and **2.28** were separately reacted with ethyl chloroformate to form the corresponding mixed anhydrides, which were reacted immediately with diazomethane (prepared from Diazald and potassium hydroxide) to give

the diazoketones **3.25** and **3.26** as yellow oils. Purification by flash chromatography on silica (1:4 ethyl acetate:petroleum ether) gave the pure diazoketones as pale yellow solids in 83% and 61% yields respectively.

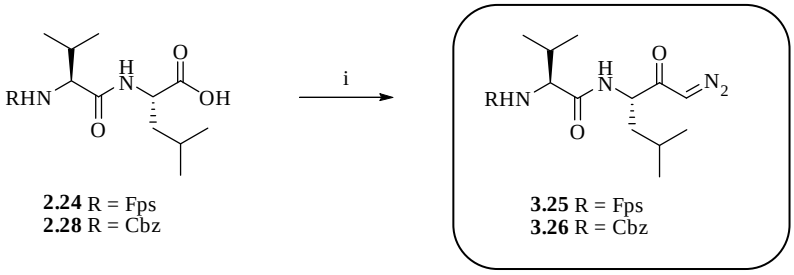

2.24 R = Fps
2.28 R = Cbz

3.25 R = Fps
3.26 R = Cbz

Scheme 3.3 *Reagents and Conditions*: i) Et_3N, $ClCO_2Et$, CH_2N_2, -15 °C to rt.

3.3.3 Design and Synthesis of Peptidyl Epoxides

An essential property of any protease inhibitor is that of stability, especially under physiological conditions.[33] Peptidyl epoxides are stable under both neutral and basic conditions.[25] Furthermore, the epoxide moiety shows little reactivity towards non-proteolytic thiols, thus peptidyl epoxides are desirable targets for *in vivo* cysteine protease inhibition.[33] The selectivity of inhibition by peptidyl epoxides within the papain superfamily of cysteine proteases has not been investigated; however, it has been shown that peptidyl epoxides do not inhibit serine proteases.[24,25]

The 3*R*-epoxide[†] **3.27** was docked into the rigid μ-calpain model and the best pose shown in **Figure 3.14**. This suggested that epoxide **3.27** would form only the hydrogen bonds A and C; however, an additional hydrogen bond was suggested between the oxirane oxygen group and His_{272}. Subsequent docking of the 3*S*-epoxide **3.27** into the rigid μ-calpain model suggested the hydrogen bonds A, B and C would all be formed. These results would seem to indicate that the 3*S*-epoxide would have better binding affinity and thus be a more potent inhibitor if the three hydrogen bonds are important for good binding affinity to cysteine proteases (see **Chapter Six** for assay results and further discussion).

[†] Where 3*R* refers to the stereochemistry at the third stereocentre of the compound from left to right

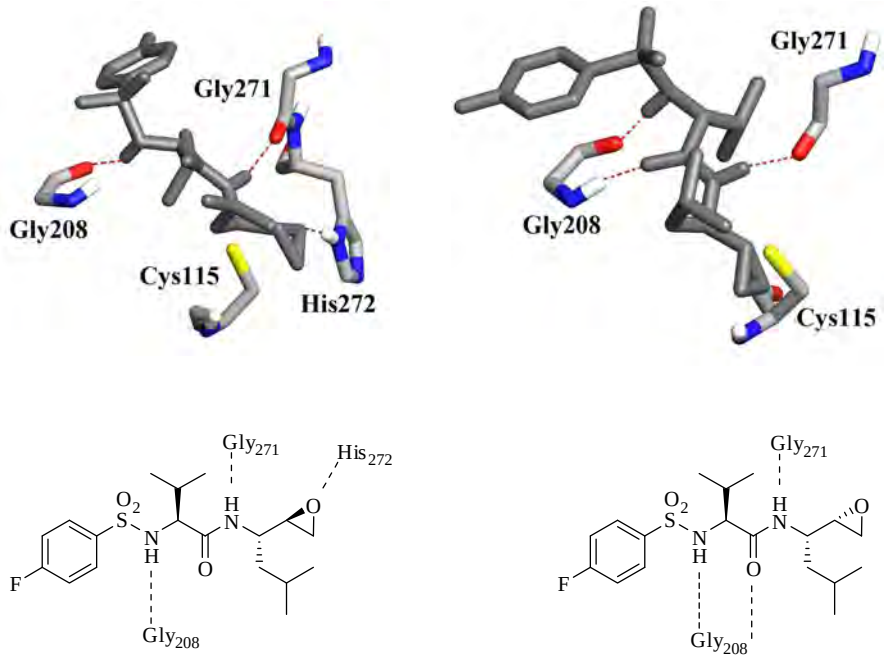

3.27 3*R*- epoxide **3.27 3*S*-epoxide**

Figure 3.14 Molecular modelling results of the 3*R*- and 3*S*- epoxide **3.27**

Synthesis of α-Bromomethyl Intermediates

The diazoketones **3.25** and **3.26** were reacted with 33% hydrogen bromide in glacial acetic acid to give the α-bromomethyl ketones **3.28** and **3.29**. Care was needed in the formation of **3.29** as the benzyloxycarbonyl group is acid sensitive. Thus, the hydrogen bromide solution was added dropwise until the yellow colour of the diazoketone disappeared then the solvent immediately removed from the reaction. The residue was dissolved in dichloromethane and dried two or three more times to ensure excess acid was removed.

Two methods of reduction were employed to give the α-bromomethyl alcohols **3.30-3.31** (see **Scheme 3.4**). Samples of the α-bromomethyl ketones **3.28** and **3.29** were stereospecifically reduced in the presence of lithium tri-*t*-butoxyaluminium hydride to give the α-bromomethyl alcohols **3.30** and **3.31** with the absolute configuration 1*S*, 2*S*, 3*R* (the alcohol moiety being *anti* with respect to the P_1 sidechain).[34] Further purification of the α-bromomethyl alcohols **3.30** and **3.31** was not required. Analysis of the α-bromomethyl alcohols **3.30** and **3.31** by ^{1}H NMR showed the presence of only one diastereoisomer as determined by the clearly single resonances for the Leu (P_1) residue. The isolated products **3.30** and **3.31** were assumed to be the *anti* isomers. This assumption was based on the results of Hoffman[34] and coworkers, who used lithium tri-*tert*-butoxyaluminium hydride for the reduction of α-bromomethyl ketones to α-bromomethyl alcohols; subsequent

reaction with base gave the corresponding epoxides, which were literature compounds of known stereochemistry. Comparison of the ^{1}H protons determined that the synthesised epoxides were of the same stereochemistry as the literature epoxides; both had *anti* orientation. Lithium tri-*tert*-butoxyaluminium hydride was prepared from a solution of lithium aluminium hydride in diethyl ether, the product being precipitated by the addition of *tert*-butyl alcohol.[35] The lithium tri-*tert*-butoxyaluminium hydride conferred stereospecifity upon the reduced products **3.30** and **3.31** by acting as a chelation-controlled reduction.[34] Alternatively, samples of the bromomethyl ketones **3.28** and **3.29** were separately reduced in the presence of sodium borohydride to give the α-bromomethyl alcohols **3.32** and **3.33** as 1:1 racemic mixtures at the 3C position.

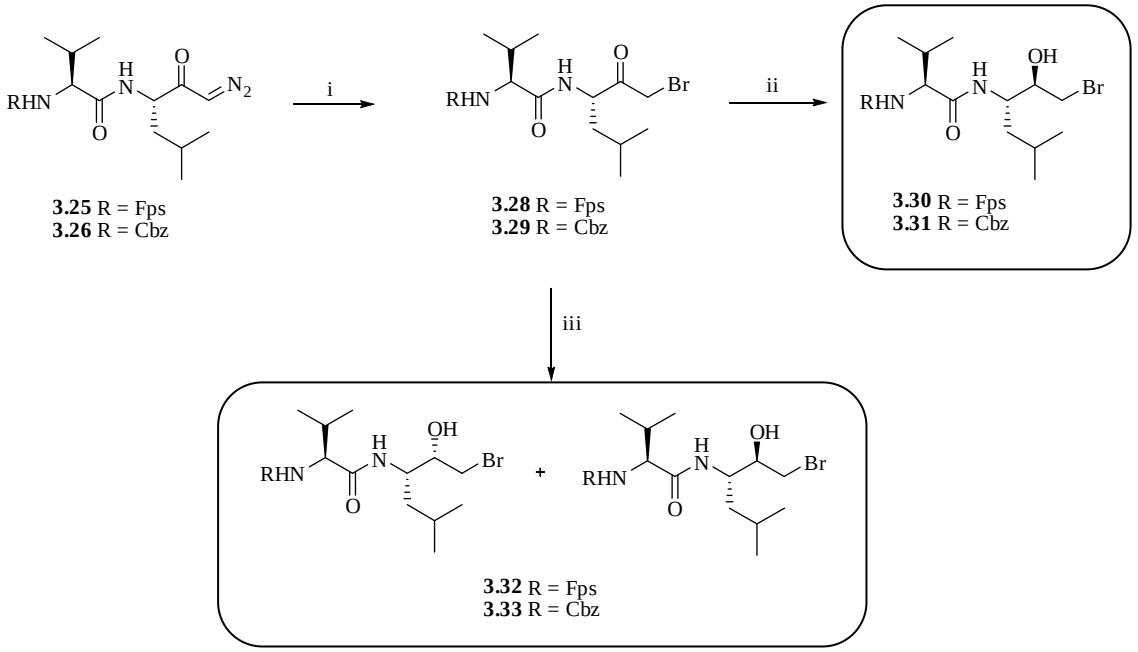

Scheme 3.4 *Reagents and Conditions*: i) 33% HBr in glacial acetic acid, DCM; ii) $LiAlH(O^tBu)_3$, EtOH, -78°C; iii) $NaBH_4$, EtOH, rt.

The amino epoxides **3.27**, **3.34-3.36** were synthesised from the α-bromomethyl alcohols **3.30-3.33**. Samples of the 3*R*-alcohols **3.30** and **3.31** were separately reacted with potassium carbonate to give the 3*R*-epoxides **3.27** and **3.34** in yields of 82% and 89% respectively (see **Scheme 3.5**).

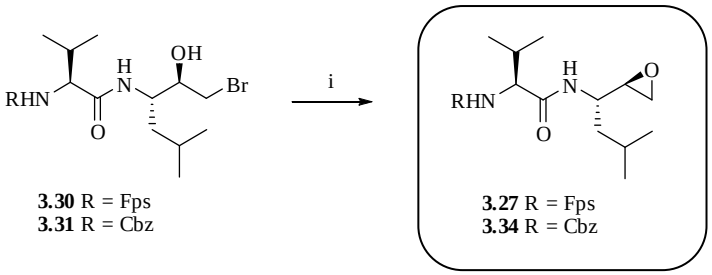

3.30 R = Fps
3.31 R = Cbz

3.27 R = Fps
3.34 R = Cbz

Scheme 3.5 *Reagents and Conditions*: i) K_2CO_3, MeOH

In a similar manner, samples of the diastereomeric 3-*S*/*R*-alcohols **3.32** and **3.33** were separately reacted with potassium carbonate to give the 3-*S*/*R*-epoxides **3.35** and **3.36** as white solids in 74% and 83% respectively (see **Scheme 3.6**).

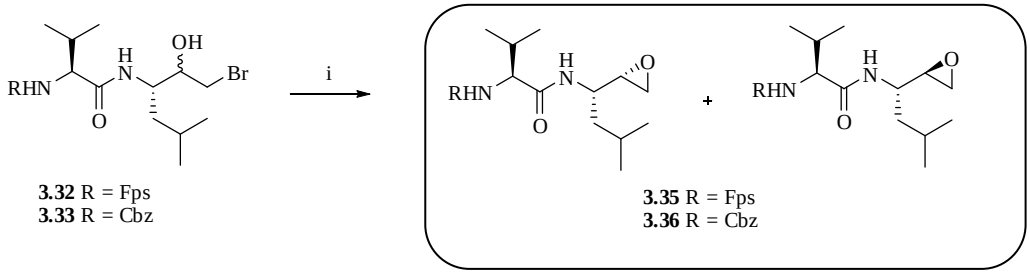

3.32 R = Fps
3.33 R = Cbz

3.35 R = Fps
3.36 R = Cbz

Scheme 3.6 *Reagents and Conditions*: i) K_2CO_3, MeOH

3.4 CONCLUSION AND FUTURE WORK

The irreversible cysteine protease inhibitors synthesised included α,β-unsaturated carbonyls **3.14-3.18** and vinyl sulfones **3.20-3.23**. These were synthesised from the corresponding aldehydes (**2.3, 2.27, 2.19** or **2.2** respectively) via *Wittig* or *Horner-Emmons-Wadsworth* (modified *Wittig*) reactions. Other irreversible inhibitors synthesised were based on the common diazoketone intermediates **3.25** and **3.26**. These were α-bromomethyl ketones **3.28** and **3.29**, α-bromomethyl alcohols **3.30-3.33** and amino epoxides **3.27**, **3.34-3.36**.

It is envisaged that future work could include P' extended vinyl sulfones of the nature shown in **Figure 3.15**, where R is an aryl *N*-protecting group and the X group includes large aryl groups, electron withdrawing groups and alkyl chains for exploration of the P' subsites of cysteine proteases. Such irreversible inhibitors could be used to aid structural elucidation of the active site and active cleft residues of cysteine proteases of the papain superfamily.

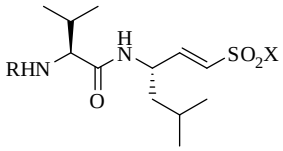

Figure 3.15 Generic structure of vinyl sulfones that extend into the P_1, subsites.

3.5 REFERENCES FOR CHAPTER THREE

(1) Otto, H.-H.; Schirmeister, T. In *Chemical Reviews (Washington, D. C.)* 1997; Vol. 97, p 133-171.

(2) Donkor, I. O. *Current Medicinal Chemistry* **2000**, *7*, 1171-1188.

(3) Demuth, H. U. *Journal of Enzyme Inhibition* **1990**, *3*, 249-278.

(4) Hanada, K.; Tamai, M.; Yamagishi, M.; Ohmura, S.; Sawada, J.; Tanaka, I. *Agricultural and Biological Chemistry* **1978**, *42*, 523-528.

(5) Vicik, R.; Busemann, M.; Baumann, K.; Schrimeister, T. *Current Topics in Medicinal Chemistry (Sharjah, United Arab Emirates)* **2006**, *6*, 331-353.

(6) Powers, J. C.; Asgian, J. L.; Ekici, O. D.; James, K. E. *Chemical Reviews (Washington, DC, United States)* **2002**, *102*, 4639-4750.

(7) Matsumoto, K.; Mizoue, K.; Kitamura, K.; Tse, W.-C.; Huber, C. P.; Ishida, T. *Biopolymers* **1999**, *51*, 99-107.

(8) Yabe, Y.; Guillaume, D.; Rich, D. H. *Journal of the American Chemical Society* **1988**, *110*, 4043-4044.

(9) Varughese, K. I.; Ahmed, F. R.; Carey, P. R.; Hasnain, S.; Huber, C. P.; Storer, A. C. *Biochemistry* **1989**, *28*, 1330-1332.

(10) Yamamoto, D.; Matsumoto, K.; Ohishi, H.; Ishida, T.; Inoue, M.; Kitamura, K.; Mizuno, H. *Journal of Biological Chemistry* **1991**, *266*, 14771-14777.

(11) Inoue, J.; Yoshida, Y.; Nakamura, M.; Cui, Y.-S.; Nagao, Y. *Drug Design & Discovery* **1999**, *16*, 165-169.

(12) Yamamoto, A.; Tomoo, K.; Matsugi, K.-i.; Hara, T.; In, Y.; Murata, M.; Kitamura, K.; Ishida, T. *Biochimica et Biophysica Acta, Protein Structure and Molecular Enzymology* **2002**, *1597*, 244-251.

(13) Leung-Toung, R.; Zhao, Y.; Li, W.; Tam, T. F.; Karimian, K.; Spino, M. *Current Medicinal Chemistry* **2006**, *13*, 547-581.

(14) Fukiage, C.; Azuma, M.; Nakamura, Y.; Tamada, Y.; Nakamura, M.; Shearer, T. R. *Biochimica et Biophysica Acta* **1997**, *1361*, 304-312.

(15) Liu, S.; Hanzlik, R. P. *Journal of Medicinal Chemistry* **1992**, *35*, 1067-1075.

(16) Palmer, J. T.; Rasnick, D.; Klaus, J. L.; Bromme, D. *Journal of Medicinal Chemistry* **1995**, *38*, 3193-3196.

(17) Kong, J.-S.; Venkatraman, S.; Furness, K.; Nimkar, S.; Shepherd, T. A.; Wang, Q. M.; Aube, J.; Hanzlik, R. P. *Journal of Medicinal Chemistry* **1998**, *41*, 2579-2587.

(18) Gotz, M. G.; Caffrey, C. R.; Hansell, E.; McKerrow, J. H.; Powers, J. C. *Bioorganic & Medicinal Chemistry* **2004**, *12*, 5203-5211.

(19) Leary, R.; Larsen, D.; Watanabe, H.; Shaw, E. *Biochemistry* **1977**, *16*, 5857-5861.

(20) Green, G. D. J.; Shaw, E. *The Journal of Biological Chemistry* **1981**, *256*, 1923-1928.

(21) Drenth, J.; Kalk, K. H.; Swen, H. M. *Biochemistry* **1976**, *15*, 3731-3738.

(22) Chatterjee, S.; Ator, M. A.; Bozyczko-Coyne, D.; Josef, K.; Wells, G.; Tripathy, R.; Iqbal, M.; Bihovsky, R.; Senadhi, S. E.; Mallya, S.; O'Kane, T. M.; McKenna, B. A.; Siman, R.; Mallamo, J. P. *Journal of Medicinal Chemistry* **1997**, *40*, 3820-3828.

(23) Powers, J. C.; Tuhy, P. M. *Journal of the American Chemical Society* **1972**, *94*, 6544-6544.

(24) Albeck, A.; Fluss, S.; Persky, R. *Journal of the American Chemical Society* **1996**, *118*, 3591-3596.

(25) Albeck, A.; Kliper, S. *Biochemical Journal* **1997**, *322*, 879-884.

(26) Bogyo, M.; McMaster, J. S.; Gaczynska, M.; Tortorella, D.; Goldberg, A. L.; Ploegh, H. *Proceedings of the National Academy of Sciences of the United States of America* **1997**, *94*, 6629-6634.

(27) Meadows, D. C.; Gervay-Hague, J. *Medicinal Research Reviews* **2006**, 1-22.

(28) Smith, M. B.; March, J. *March's Advanced Organic Chemistry*; John Wiley and Sons, Inc: New York, 2001.

(29) Boutagy, J.; Thomas, R. *Chemical Reviews (Washington, DC, United States)* **1974**, *74*, 87-99.

(30) Blasdel, L. K.; Myers, A. G. *Organic Letters* **2005**, *7*, 4281-4283.

(31) Gokel, G. W.; Gerdes, H. M.; Dishong, D. M. *Journal of Organic Chemistry* **1980**, *45*, 3634-3639.

(32) Williams, D. H.; Fleming, I. *Spectroscopic Methods in Organic Chemistry*; 4th ed.; McGraw-Hill Book Company: United Kingdom, 1989.

(33) Albeck, A. *Drug Development Research* **2000**, *50*, 425-434.

(34) Hoffman, R. V.; Weiner, W. S.; Maslouh, N. *Journal of Organic Chemistry* **2001**, *66*, 5790-5795.

(35) Brown, H. C.; Subba Rao, B. C. *Journal of Organic Chemistry* **1958**, *80*, 5377-5380.

CHAPTER FOUR

Design and Synthesis of Macrocyclic Cysteine Protease Inhibitors

4.1 INTRODUCTION TO PEPTIDOMIMETICS

The inhibitors synthesised in **Chapters Two** and **Three** are peptide based; however, peptidic nature can be detrimental in terms of good drug character. This observation has made the field of peptidomimetics* increasingly popular. Effective drugs generally have the following characteristics: minimal peptide character, high metabolic stability, good membrane permeability, high selectivity for the target protease and good bioavailability. Qualitative analysis of inhibitors in terms of these criteria is described by Lipinski's Rule of 5 (**Table 4.1)**.[1] Lipinski's guidelines predict that better absorption or permeation of an orally administered compound are more likely if the compound meets two or more of these rules.

Lipinski's Rule of 5	
The compound should	- not contain more than 5 hydrogen bond donors (OH, NH) - not contain more than 10 hydrogen bond acceptors (N, O) - have a molecular weight under 500 g mol^{-1} - have a partition coefficient logP < 5

Table 4.1 Requirements for drug-like properties

Chemical modifications to make peptide-like structures can enhance the stability or biological activity of a peptide structure. One important means by which the peptidic nature of a compound can be reduced is by incorporating a conformational restriction into the backbone. Such macrocycles are increasingly being used as protease inhibitors.[2] Macrocyclic inhibitors are beneficial in two ways: 1) constraining the structure of an inhibitor into a bioactive conformation and 2) protecting the inhibitor against proteolytic cleavage, thus assisting stability of the inhibitor *in vivo*.

* For the purposes of this thesis peptidomimetics are defined as peptide-like structures derived from peptide chains by means of chemical modification.

Benefits of a bioactive conformation

It is widely acknowledged that proteases (including serine, cysteine, aspartic and metalloproteases) bind inhibitors in an extended β-strand conformation.[3] This was well illustrated in a recent review by Tyndall,[4] in which the binding conformation of substrates, products and inhibitors bound in the active sites of serine, cysteine, aspartic, threonine and metalloproteases were analysed. Out of the 1500 structures studied, 99.6% bound ligands in an extended β-strand conformation. Thus compounds constrained in a β-strand conformation should exhibit improved binding affinity for the target protease relative to their conformationally flexible analogues. A β-strand is a linear "saw-tooth" structure of amino acids as shown in **Figure 4.1**, where the side chains alternate above and below the plane of the peptide backbone.[5] The bond angles that define a β-strand are Φ, ψ, and ω, (with optimum angles of -120°, 120° and 180° respectively).

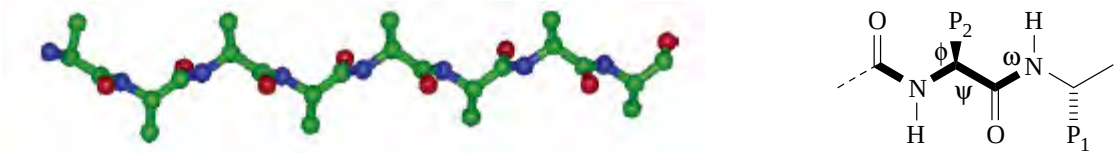

Figure 4.1 "saw-tooth" nature of the β-strand and the angles denoted above (nomenclature according to Schechter and Berger)[6]

The purpose of this chapter is to apply several warheads that have proven to be active against cysteine proteases to a β-sheet constrained backbone. This will allow for comparison between the acyclic inhibitors (from **Chapters Two** and **Three**) and the constrained inhibitors (described below in **Sections 4.2** and **4.3**) to determine whether constraining the inhibitor into an extended β-sheet conformation does improve binding affinity. The IC_{50} values for these inhibitors will be used as the basis for determining increased binding activity; assuming that an increased binding affinity will be reflected in an increase in potency against the cysteine proteases tested (results are presented and discussed in **Chapter Six**).

Proteolytic protection via macrocycles

The ease with which peptide inhibitors are metabolised in biological systems has resulted in the design of non-peptidic and peptidomimetic inhibitors. Macrocyclic compounds have

been demonstrated to possess both higher resistance to proteolytic cleavage and improved cell permeability relative to their acyclic analogues. Chen[7] and co-workers compared the acyclic HIV protease inhibitor **4.1** with its cyclic analogue **4.2** (see **Figure 4.2**). The acyclic inhibitor **4.1** was 19-fold more potent than the macrocyclic analogue **4.2** in enzyme assays; however, under the conditions for cell assay the macrocycle **4.2** was 30-fold more potent to its acyclic counterpart **4.1**. This indicated that the macrocycle **4.2** had improved resistance to proteolytic degradation and improved cell permeability, which is reflected in the increased efficacy in cell assays.

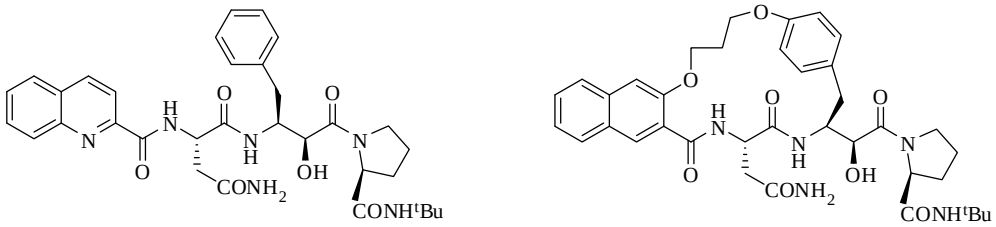

4.1
HIV protease IC_{50} = 0.0011 µM
HIV cell assay EC_{50} = 0.15 µM

4.2
HIV protease IC_{50} = 0.019 µM
HIV cell assay EC_{50} = 0.076 µM

Figure 4.2 Acyclic versus macrocyclic inhibitors of HIV protease[7]

4.1.1 Ring-closing Metathesis

Ring-closing metathesis is currently one of the most widely used methods for new carbon-carbon bond formation and has found application in the design of conformationally constrained peptidomimetics.[8] It is a powerful, reliable reaction that can tolerate a number of functional groups.[9] For these reasons, ring-closing metathesis was deemed to be the most efficient way of synthesizing β-strand constrained inhibitors. Further, 'in house' knowledge of this methodology for incorporation into protease inhibitors made ring-closing metathesis a useful tool.

The mechanism of ring-closing metathesis, in which a new carbon-carbon bond is formed, is outlined in **Figure 4.2**.[10] The acyclic diene is reacted with the carbine catalyst [M] (often Grubbs' second generation catalyst), forming the key metallacyclobutane intermediate, which undergoes cycloreversion towards the cycloalkene with release of

ethene. The forward reaction for ring-closing metathesis is driven by the production and removal of ethene.

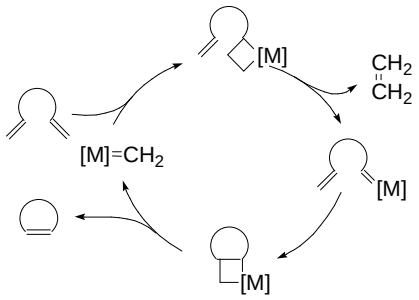

Figure 4.2 Mechanism of ring-closing metathesis. [M] is used to denote the carbine catalyst and attached ligands.[10]

This chapter describes the synthesis of carbon to carbon macrocyclic inhibitors to conformationally constrain tripeptides into a β-strand conformation. The generic structure of these compounds comprises three parts: an address region, the macrocyclic backbone and the warhead as shown in **Figure 4.3**. Definitions of the address region and warhead moieties can be found in **Chapter One**. The macrocyclic backbone has the same function as the recognition region of acyclic cysteine protease inhibitors (see **Chapter One**) and contains tripeptides with amino acids chosen to fit the target enzyme binding pockets.

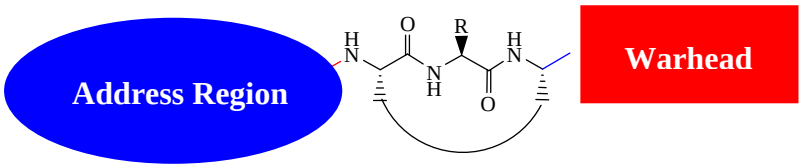

Figure 4.3 Generic structure of macrocyclic β-strand inhibitors

4.2 DESIGN AND SYNTHESIS OF A MACROCYCLIC ALDEHYDE AS A CYSTEINE PROTEASE INHIBITOR

4.2.1 Design of a Macrocyclic Cysteine Protease Inhibitors

The macrocyclic compounds **4.3** and **4.4** (see **Figure 4.4**) were designed as cysteine protease inhibitors. Subseqeunt docking of **4.3** and **4.4** into the rigid μ-calpain model and Boltzmann weighted conformational analysis was used to determine if the macrocycles could adopt a β-strand conformation in water.[†] The structure of a specific conformer was determined using numerical methods to assign it as a β-strand or not. The determining factor for each of these conformers was the distance between the NH group of the first amino acid and the carbonyl oxygen group of the central amino acid (shown in **Figure 4.4**) as previously published[11] where an optimal β-strand is defined by a measured distance of approximately 2.5Å. Utilisation of these methods suggested the alcohol **4.3** existed as a β-strand 67% of the time in water; similarly the aldehyde **4.4** existed as a β-strand 98% of the time.

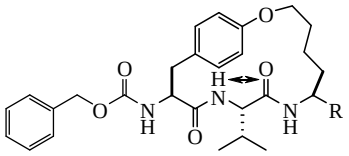

4.3 R = CH_2OH
4.4 R = CHO

Figure 4.4: Measurement used to define a β-sheet conformation

The following sections outline the synthesis of the macrocyclic aldehyde **4.4** and the application of the semicarbazone, cyanohydrin, α-ketotetrazole and azide warheads to an analogous, available macrocyclic aldehyde. The above mentioned warheads were selected on the basis of potency, observed selectivity and availability of materials.

[†] The Boltzmann distribution calculations were performed by Stephen McNabb of the University of Canterbury. Conformational searches were conducted using the Monte Carlo multiple minimum (MCMM) method

4.2.2 Synthesis of a Macrocyclic Aldehyde

The synthesis of the 17-membered ring macrocyclic aldehyde **4.4** is shown in **Scheme 4.1**. The methodology used for synthesizing the macrocyclic aldehyde **4.4** was developed and optimised by co-workers[‡] at Canterbury University. Commercial *N*-Boc-*O*-allyltyrosine **4.5** was reacted with *L*-valine methyl ester using standard HATU methodology to give the dipeptide **4.6** in an 86% yield. Hydrolysis of the ester **4.6** with lithium hydroxide and subsequent coupling to *L*-allylglycine methyl ester gave the diene **4.8**, which was purified by flash chromatography on silica (1:4 ethyl acetate: pet ether to yield a white solid (83%). *L*-Allylglycine methyl ester **4.9** was prepared from acid-catalysed esterification of *L*-allylglycine in the presence of methanol in quantitative yield. Ring-closing metathesis was performed using Grubbs' second generation catalyst under optimised conditions (microwave irradiation, 3 × 10 mol% Grubb's second generation catalyst, 1,1,2-trichloroethanol and chlorodicyclohexyl borane) to give the ring closed alkene **4.10** in the *trans* form[§] as a brown solid (only one isomer was apparent by ^{1}H NMR, see **Chapter 7** for more detail). The brown colour was due to residual ruthenium from the Grubbs' second generation catalyst; however, recrystallisation from methanol gave *trans* alkene macrocycle **4.10** as a white solid in 65% yield. The cyclic olefin **4.10** was hydrogenated at atmospheric pressure and room temperature with palladium on carbon to give saturated macrocycle **4.11** in quantitative yield. Cleavage of the *N*-Boc group of the macrocycle **4.11** with trifluoroacetic acid gave the free amine **4.12**, which was immediately reacted without purification with benzylchloroformate to give the benzyloxycarbonyl protected ester **4.13**. The crude ester **4.13** was recyrstallised from ethyl acetate to give the pure **4.13** as a white solid in 86% yield. The ester **4.13** was subsequently reduced in the presence of lithium aluminium hydride to give the crude alcohol **4.3**. Recrystallisation from methanol gave the pure alcohol **4.3** in 84% yield. The primary alcohol **4.3** was oxidised utilising sulfur trioxide-pyridine[12] to give the macrocyclic aldehyde **4.4** in good yield (79%). No further purification was necessary.

[‡] Matthew Jones and Steve Aitken

[§] Under the conditions used (microwave heating and the addition of chlorodicyclohexyl borane) only one isomer was apparent by ^{1}H NMR. This was assumed to be the *trans* form, based on the crystal structure of a similar macrocyclic diene synthesised under the same conditions by Andrew Muscroft-Taylor.

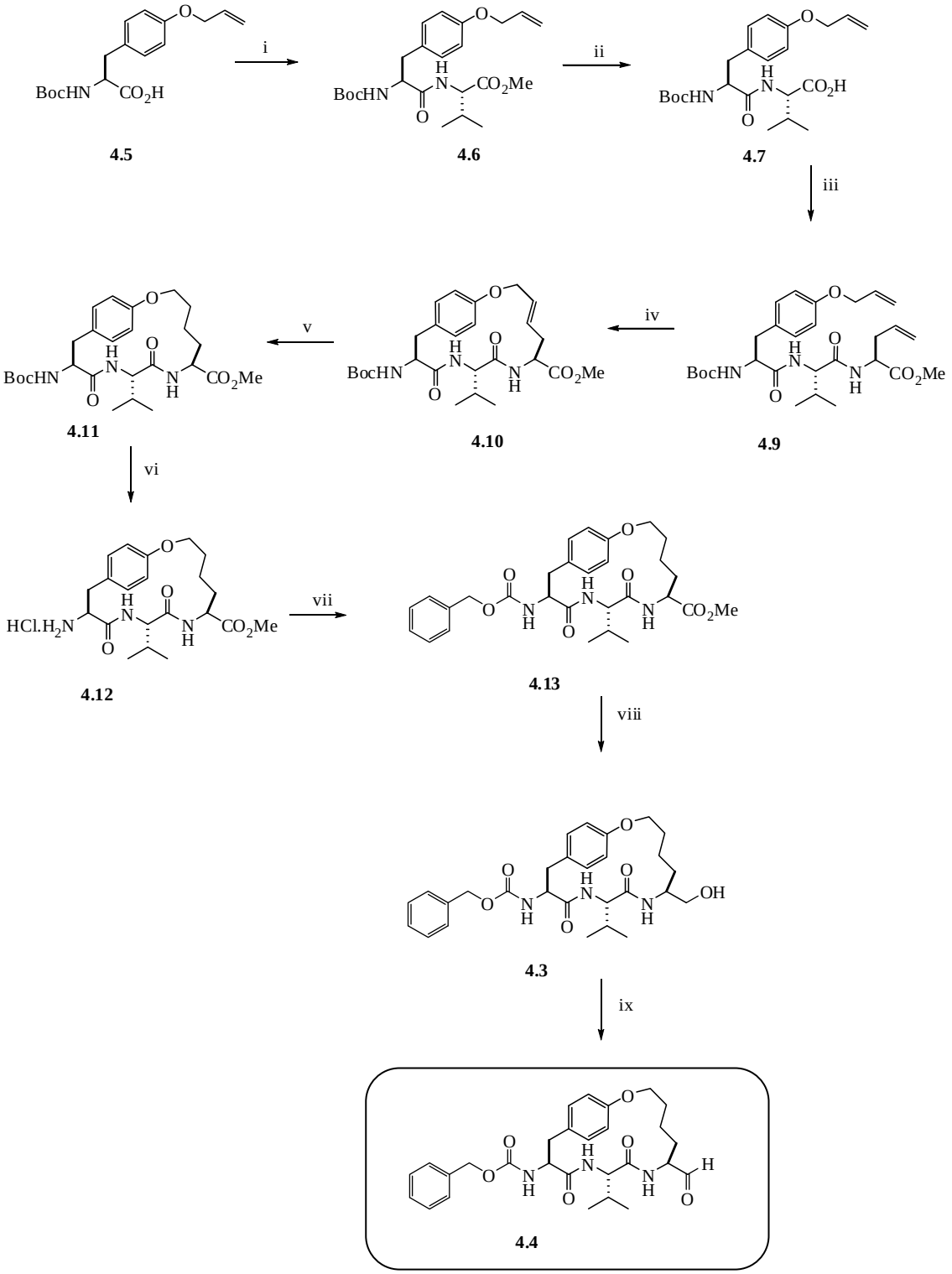

Scheme 4.1 *Reagents and Conditions:* i) HATU, DIPEA, *L*-Val-OMe, DMF, (86%); ii) LiOH, THF, H_2O, (97%); iii) HATU, DIPEA, *L*-allyl-Gly-OMe, DMF, (83%); iv) 3 x 10 mol% Grubb's second generation catalyst, 1,1,2-TCE, chlorodicyclohexyl borane, microwave (89%); v) H_2, 20 mol% Pd/C, MeOH, EtOAc, (100%) vi) TFA, DCM; vii) CbzCl, DIPEA, H_2O, THF (82%); viii) $LiAlH_4$, THF, 0 °C (75%); ix) SO_3-pyr, DMSO, DIPEA, DCM (79%)

4.3 SYNTHESIS OF MACROCYCLIC CYSTEINE PROTEASE INHIBITORS WITH ALTERNATIVE WARHEADS

The macrocyclic aldehyde **4.14**[**] was synthesised at Canterbury University. The aldehyde **4.14** was chosen for further derivatisation as it is an excellent cysteine protease inhibitor (see **Figure 4.5**). Docking of the aldehyde **4.14** into the μ-calpain model suggested that it binds to calpain in a β-strand conformation defined by the hydrogen bonds A, B and C; an additional hydrogen bond between the benzyloxycarbonyl carbonyl oxygen group and Lys_{347} was also suggested to occur. The aldehyde **4.14** is currently being tested *in vivo* for the treatment of cataract in sheep as a topical ointment. However due to the reactive nature of the aldehyde it is not an ideal drug candidate.

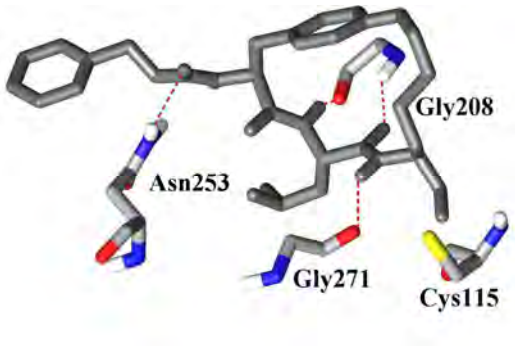

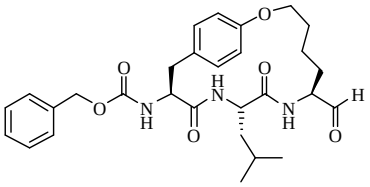

4.14

IC_{50} = 30 nM (m-calpain)
= 220 nM (μ-calpain)
= 70 nM (cathepsin B)
> 50000 nM (papain)

Figure 4.5 The in-house macrocyclic inhibitor **4.14**

[**] Matthew Jones and Andrew Muscroft-Taylor

4.3.1 Synthesis of a Macrocyclic Semicarbazone

A sample of the macrocyclic aldehyde **4.14** was reacted with semicarbazone hydrochloride to give the macrocyclic semicarbazone **4.15** as outlined in **Scheme 4.2**. Recrystallisation of crude **4.15** from ethyl acetate gave the purified product as a white solid in good yield (63%).

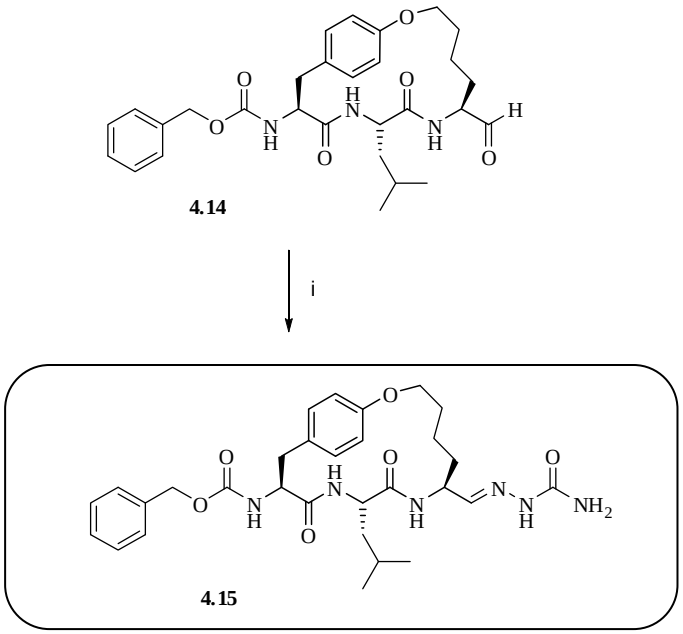

Scheme 4.2 *Reagents and Conditions*: i) semicarbazide hydrochloride, NaOAc, 1:1 THF:MeOH (87%)

^{1}H NMR analysis of the pure product showed the characteristic singlet peak at 9.3 ppm of the semicarbazone NH group and doublet peak at 7.5 ppm of the imine CH group (see **Figure 4.6**), which were unamibiguously assigned through 2D COSY NMR.

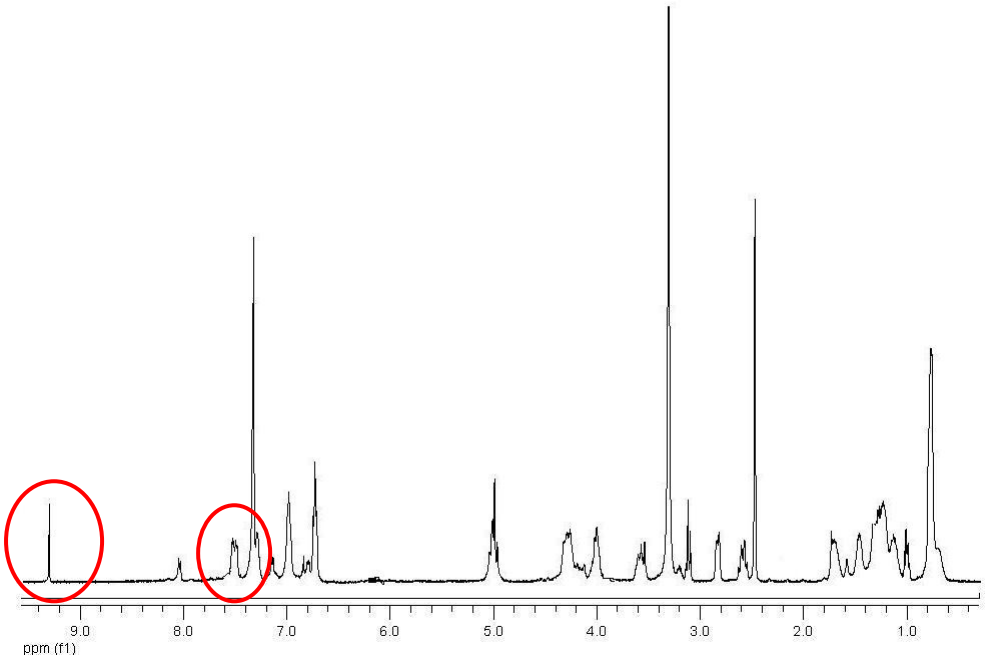

Figure 4.6 ^{1}H NMR of the macrocyclic semicarbazone **4.15** showing the characteristic peaks of the semicarbazone moiety

4.3.2 Attempted Synthesis of a Macrocyclic α-Ketotetrazole

The macrocyclic aldehyde **4.14** was reacted with sodium hydrogen sulfite and potassium cyanide at low temperatures to give the cyanohydrin **4.16** as a 1:1 mixture of diastereoisomers (see **Scheme 4.3**). Recrystallisation from methanol gave the 1:1 mixture of diastereoisomers of **4.16** as a white solid in 81% yield. ^{1}H NMR analysis confirmed the presence of two diastereoisomers, with the characteristic doublet peaks of the β carbon hydrogen atom of the cyanohydrin being observed at 6.5 and 6.6 ppm (see **Figure 4.7**) The fact that six doublet peaks were observed for the amide hydrogen atoms was further evidence that two diastereoisomers were present. 2D NMR (Cosy) was used to confirm these peaks as being the amide hydrogen and cyanohydrin β hydrogen.

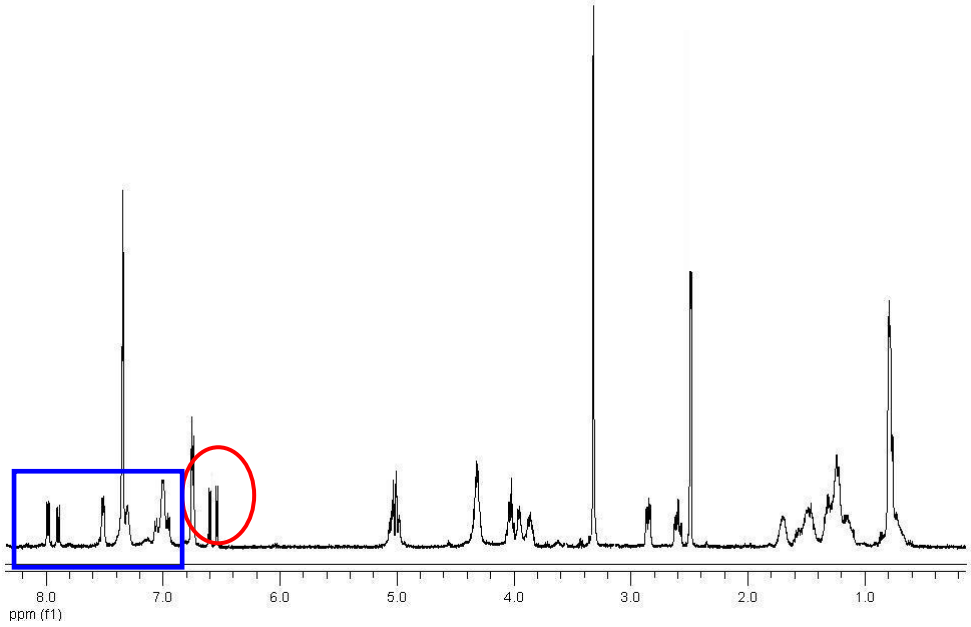

Figure 4.7 ^{1}H NMR of the macrocylic cyanohydrin **4.16**, isolated as a 1:1 mixture of diastereoisomers. The β carbon hydrogen peaks of the two diastereoisomers are circled; the two NH peaks of each of the three amino acids in the backbone lie within the boxed area

The cyanohydrin **4.16** was reacted with sodium azide and triethylamine hydrochloride applying the same methodology used for formation of the acyclic α-hydroxytetrazoles **2.43** and **2.55** (see **Scheme 4.3**). The cyanohydrin **4.16** and the reagents were suspended in toluene and heated at reflux for 24 h, after which an intractable dark orange solid was observed. Analysis by thin layer chromatography showed trace amounts of the desired α-hydroxytetrazole **4.17**; however, the orange solid obtained was not suitable for column chromatography due to low solubility in organic solvent. Recrystallisation from methanol was attempted, but returned a mixture of products by mass spectrometry. The intractable orange solid was determined by mass spectrometry to contain a mixture of the starting cyanohydrin **4.16**, triethylamine hydrochloride, the desired α-hydroxytetrazole product **4.17** and unidentified side products.

Due to the limited inhibition activity of the acyclic α-hydroxytetrazoles **2.43** and **2.55** (see **Chapter Six**) it was not expected that the macrocyclic α-hydroxytetrazole analogue would show much activity against the cysteine proteases tested. Thus, the synthesis of the macrocylic α-hydroxytetrazole analogue **4.18** was abandoned.

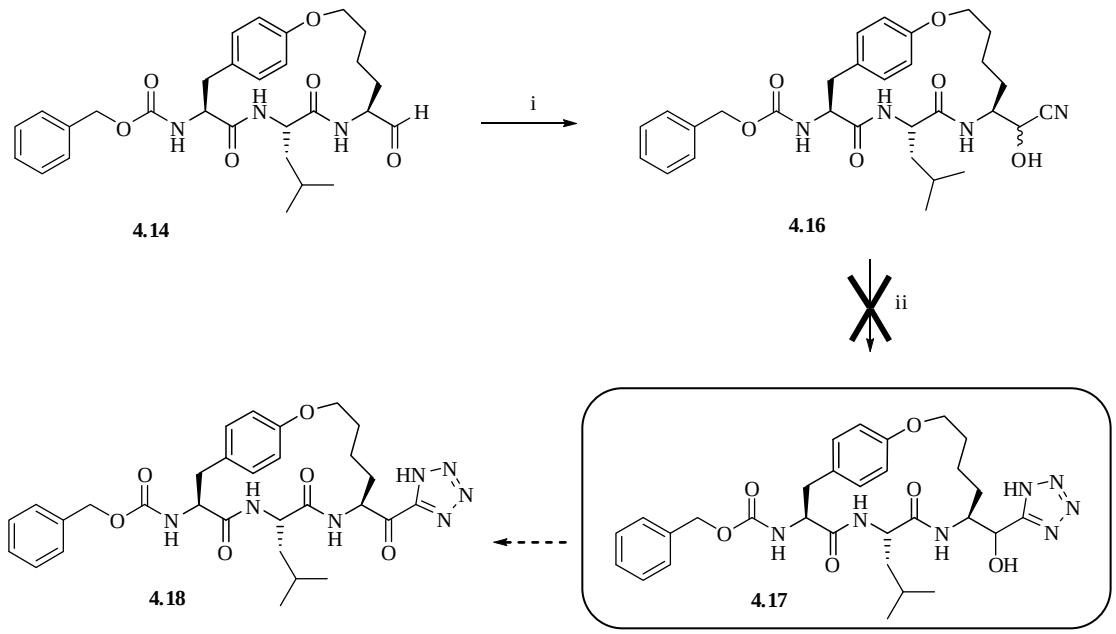

Scheme 4.3 *Reagents and Conditions*: i) $NaHSO_3$, KCN, MeOH, H_2O, EtOAc (82%); ii) $Et_3N.HCl$, NaN_3, toluene, reflux

4.3.3 Synthesis of a Macrocyclic Azide

The analogous acyclic azide **2.62** was shown to be a weak inhibitor of cysteine proteases (see **Chapter Six**). Incorporation of the azide moiety onto a macrocyclic scaffold will provide further opportunity to assess the effect of constraint of the inhibitor backbone on binding affinity.

The macrocyclic alcohol **4.19** was reacted with mesyl chloride followed by sodium azide to give the macrocyclic azide **4.20**. S_N2 displacement of the mesylate with sodium azide occurred without isolation of the intermediate mesylate (see **Scheme 4.5**). Recrystallisation of crude **4.20** from ethyl acetate gave the pure azide **4.20** as a white solid in 49% yield.

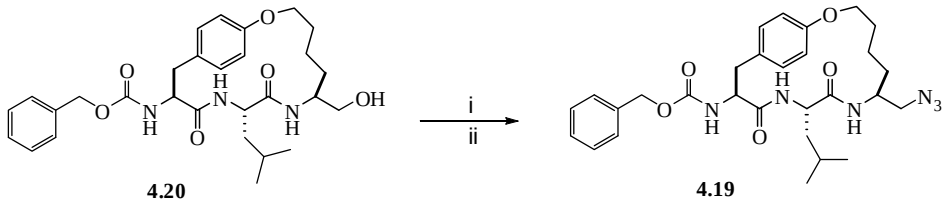

4.20 **4.19**

Scheme 4.5 *Reagents and Conditions*: i) Et_3N, mesyl chloride, DCM; ii) DMF, NaN_3 (53%)

4.4 CONCLUSION AND FUTURE WORK

The synthesis of the macrocyclic compounds **4.3**, **4.4**, **4.15-4.19** provided a range of peptidomimetic inhibitors. The assay results and structure-activity relationships are discussed in **Chapter Six**.

It is envisaged that future work would involve optimisation of the *N*-terminal group (A), amino acid sidechain (R_1) and warhead (R_2) on **Figure 4.8** below, for fine-tuning of the potency, selectivity and solubility of such macrocyclic inhibitors. Alternative warheads, especially those non-reactive in nature, of interest are listed below. The University of Canterbury is currently in the process of provisional patenting compounds of this nature with an application for topical treatment of cataracts.

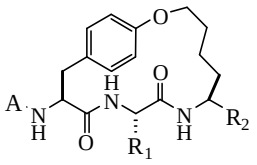

Figure 4.8 Future compounds will be of this formula or a pharmaceutically acceptable salt, solvate, hydrate or prodrug thereof.

Wherein:

A is $–C(=O)R_3$ or $–S(=O)_2R_4$;

R_3 is optionally substituted aryl, heteroaryl, aryloxy, heteroaryloxy, arylalkoxy or heteroarylalkoxy; and

R_4 is optionally substituted aryl, heteroaryl, aryloxy, heteroaryloxy, arylalkoxy or heteroarylalkoxy;

R_1 is a side chain of a natural or non-natural α-amino acid;

R_2 is $–CH_2OH$, $–CH_2OR_5$, $–CH_2NR_6R_7$, $–CH(OH)R_8$, –CHO, $–C(=O)C(=O)NHR_9$ or $–C(=O)R_{10}$;

R_5 is C_1-C_6 alkyl, aryl or arylalkyl;

R_6 is hydrogen, C_1-C_6 alkyl, aryl or arylalkyl;

R_7 is hydrogen, C_1-C_6 alkyl, aryl or arylalkyl;

R_8 is C_1-C_6 alkyl, alkoxy, thioalkoxy, aryl, arylalkyl, heteroaryl or heteroarylalkyl;

R_9 is C_1-C_6 alkyl, hdroxyalkyl, aryl or arylalkyl; and

R_{10} is C_1-C_6 alkyl, aryl, arylalkyl, heteroaryl or heteroarylalkyl.

4.5 REFERENCES FOR CHAPTER FOUR

(1) Lipinski, C. A.; Lombardo, F.; Dominy, B. W.; Feeney, P. J. *Advanced Drug Delivery Reviews* **1996**, *23*, 3-25.

(2) Tyndall, J. D. A. R., R.C.; Tyssen, D.P.; Jardine, D.K.; Todd, B.; Passmore, M.; March, D.R.; Pattenden, L.K.; Bergman, D.A.; Alewood, D.; Hu, S-H.; Alewood, P.F.; Birch, C.J.; Martin, J.L.; Fairlie, D.P. *Journal of Medicinal Chemistry* **2000**, *43*, 3495-3504.

(3) Fairlie, D. P.; Tyndall, J. D. A.; Reid, R. C.; Wong, A. K.; Abbenante, G.; Scanlon, M. J.; March, D. R.; Bergman, D. A.; Chai, C. L. L.; Burkett, B. A. *Journal of Medicinal Chemistry* **2000**, *43*, 1271-1281.

(4) Tyndall, J. D. A. N., T.; Fairlie, D.P. *Chemical Reviews* **2005**, *105*, 973-999.

(5) Loughlin, W. A.; Tyndall, J. D. A.; Glenn, M. P.; Fairlie, D. P. *Chemical Reviews* **2004**, *104*, 6085-6117.

(6) Berger, A.; Schechter, I. *Biochemical & Biophysical Research Communications* **1967**, *27*, 157-162.

(7) Chen, J. J.; Coles, P. J.; Arnold, L. D.; Smith, R. A.; MacDonald, I. D.; Carriere, J.; Krantz, A. *Bioorganic & Medicinal Chemistry Letters* **1996**, *6*, 435-438.

(8) Ersmark, K.; Nervall, M.; Gutierrez-de-Teran, H.; Hamelink, E.; Janka, L. K.; Clemente, J. C.; Dunn, B. M.; Gogoll, A.; Samuelsson, B.; Aqvist, J.; Hallberg, A. *Bioorganic & Medicinal Chemistry* **2006**, *14*, 2197-2208.

(9) Gradillas, A.; Perez-Castells, J. *Angewandte Chemie International Edition* **2006**, *45*, 6086-6101.

(10) Grubbs, R. H.; Carr, D. D.; Hoppin, C.; Burk, P. L. *Journal of the American Chemical Society* **1976**, *98*, 3478-3483.

(11) Aitken, S. G., University of Canterbury, 2006.

(12) Parikh, J. R.; Doering, W. v. E. *Journal of the American Chemical Society* **1967**, *89*, 5505-5507.

CHAPTER FIVE

Assay Protocols

5.1 INTRODUCTION TO PROTEASE INHIBITION ASSAYS

The biological activity of the cysteine protease inhibitors reported in this thesis were determined by measuring the inhibition constants (IC_{50}) in an ***in vitro*** assay. IC_{50} indicates the concentration of inhibitor required to decrease the activity of the target protease by 50%. It should be noted that the irreversible inhibitors of **Chapter Three** were assayed in an identical manner to the reversible inhibitors of **Chapters Two and Four** to allow comparison of the warheads. This chapter will cover the assay protocols that were established for each protease

5.2 THE BODIPY-CASEIN FLUORESCENCE ASSAY FOR CALPAIN

Collaboration with Lincoln University allowed access to the materials required for the biological assay of cysteine protease inhibitors. An established assay protocol for the determination of m-calpain inhibition based on a fluorogenic methodology used by Thompson and co-workers[1] was used. This assay protocol utilises casein, a water soluble protein, labelled with the fluorophore 4,4-difluoro-5,7-dimethyl-4-bora-3a,4a-diaza-*s*-indacene-3-propionic acid (BODIPY). The principle behind this methodology is shown schematically in **Figure 5.1**. Fluorescence increases as proteolysis of the substrate (casein) occurs. Without proteolysis, fluorescence is not observed as adjacent intramolecular fluorophores cause auto-quenching of fluorescence. Thus the inhibitory activity of a proposed inhibitor can be measured by calculating the change in fluorescence over a known period of time.

m-Calpain and μ-calpain were partially purified from sheep lung by ion-exchange chromatography and diluted to give a linear response over the course of the assay.[*] The BODIPY-FL labelled casein was prepared by Lincoln University students according to the protocol set out by Jones ***et al.***[2] The substrate solution (0.0005% BODIPY-FL casein in 10

[*] Calpain was provided courtesy of Matthew Muir of Lincoln University

mM TRIS-HCl, pH 7.5 containing 10 mM $CaCl_2$, 0.1 mM NaN_3, and 0.1% mercaptoethanol) was prepared fresh each day.

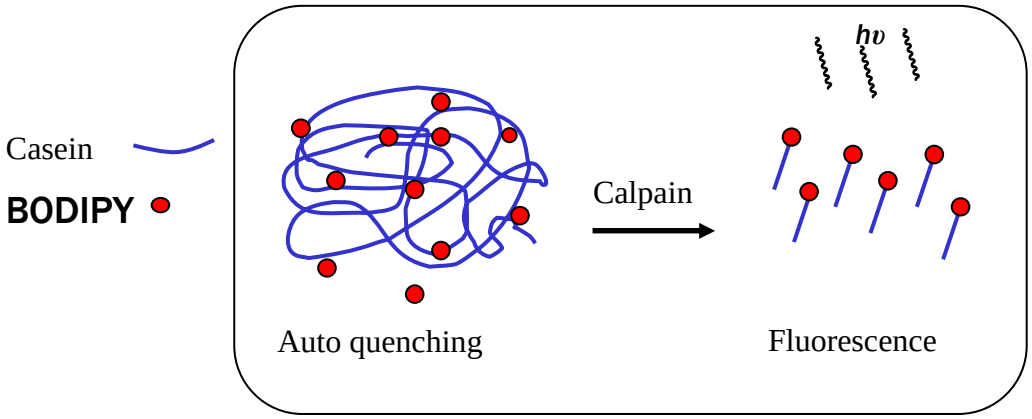

Figure 5.1: Schematic illustration of calpain IC_{50} assay

The assays were performed in 96-well black *Whatman* plates. Two types of blank controls were utilised, a calcium blank and an EDTA blank. The calcium blanks contained 100 µL of 100 mM calcium chloride, and the EDTA blanks 25 µL of 10 mM EDTA solution, 25 µL distilled water and 50 µL of the enzyme. Calpain control assays contained 50 µL calpain (m- or µ-) in sample buffer (20 mM TRIS-HCl, pH 7.5 containing 1 mM EDTA, 1 mM EGTA, and 2 mM dithiothreitol) and 50 µL distilled water (see **Figure 5.2** for a schematic layout). The reaction was initiated by the addition of 100 µL of substrate solution at 25 °C and the progress followed for 10 min in a BMG Fluostar with excitation of 485 nm and emission of 530 nm. For the inhibitor assays the sample buffer was replaced by 50 µL of inhibitor diluted in distilled water.[†] The percentage inhibition was determined as 100 times the activity with inhibitor present divided by the activity of the control assay. Assays were performed in triplicate with serial dilutions of inhibitor concentrations from 50 µM to 50 nM (see **Appendix A1** for a raw data and IC_{50} calculation).

[†] This will be discussed in more detail in **Section 5.2**

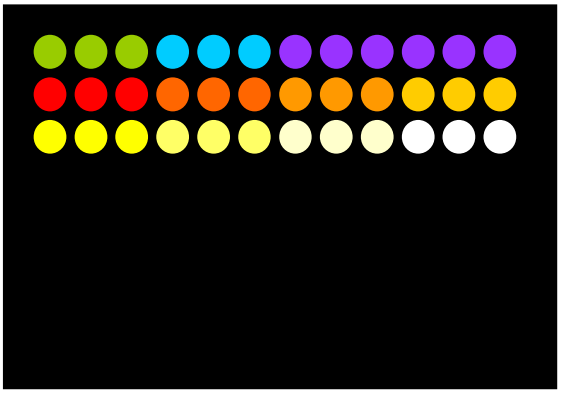

Calcium blank

100 µL 10 mM $CaCl_2$
100 µL BODIPY-casein

EDTA blank

25 µL 100 mM EDTA
25 µL H_20
50 µL calpain
100 µL BODIPY-casein

Enzyme activity blank

50 µL H_20
50 µL calpain
100 µL BODIPY-casein

Inhibitor samples

50 µL inhibitor
50 µL calpain
100 µL BODIPY-casein

Figure 5.2 Schematic diagram of a 96 well plate and the layout of a calpain (m- or µ-) assay run.

5.2.1 Validation of the BODIPY-casein Assay Protocol

The aldehyde **2.3** (see **Table 5.1**) was used as a reference compound to validate the assay protocol. Repeated assay of **2.3** with the BODIPY-casein protocol above mentioned gave an average value of 80 ± 10 nM;[‡] comparable to the IC_{50} obtained by Inoue (78 nM).[3] The difference in the IC_{50} values of **2.3** obtained against µ-calpain with this fluorogenic assay (134 nM) and the value reported by Inoue[3] (7 nM) is attributed to the assay protocol. The Coomassie Blue colorimetric assay[4] that Inoue[3] *et al* utilised can only detect 5-10 µg of calpain, making it a less sensitive and less reliable assay than the BODIPY-casein used herein (under these conditions it is possible to detect 50-100 ng of calpain).[1,5] A similar trend was seen in the µ-calpain IC_{50} values compared for the aldehyde **2.27**; the difference

[‡] SJA6017 was assayed over 20 times against m-calpain and µ-calpain

being attributed to the sensitivity and reliability of the two methods used. The aldehyde **2.27** was found to have an IC_{50} value of 60 nM under the BODIPY-casein assay conditions, significantly different from the value of 350 nM reported by Inoue.[3] Again, the difference is attributed to the greater accuracy of the BODIPY-casein assay in comparison with the less reliable Coomassie Blue conditions. The IC_{50} values for the aldehydes **2.3** and **2.27** obtained herein for μ-calpain are therefore thought be more accurate than those reported in the literature.

Compound		**IC_{50} (nM)**			
		m-calpain		**μ-calpain**	
		Reported	Calc[d]	Reported	Calc[d]
2.3	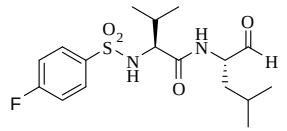	78[3]	80	8[3]	134
2.27	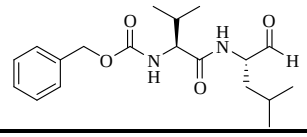	-	145	29[6]	375

Table 5.1 Comparison of IC_{50} values for aldehyde **2.3** against m-calpain and mu-calpain

Once the BODIPY-casein assay was validated for both m- and μ-calpain and reproducibility of IC_{50} results demonstrated for **2.3**, attention turned to finding a suitable assay system for the proteases papain, cathepsin B, α-chymotrypsin and pepsin.

5.3 MODIFICATION OF THE FLUORESCENCE ASSAY TO ACCOMMODATE OTHER PROTEASES

A number of points for consideration arise regarding the modification of the BODIPY-casein assay for use with other proteases:

- Will the alternative enzymes recognise BODIPY-casein as a substrate?
- Will the assays be comparable?
- Calpains are the only enzymes that require calcium for activation – both the blanks and the substrate contain calcium so modification is needed

5.3.1 Turnover of BODIPY-casein by Other Proteases

From observations of the change in the IC_{50} value of SJA6017, it was noted that the optimum activity of m- and µ- calpain was represented by a change in fluorescence of between 600-1200 FU (where FU denotes arbitrary fluorescence units), see **Table 5.2**. When the enzyme has minimal activity (change in fluorescence of 200 units or less) over 10 min, the calculated IC_{50} is far below the value it should be. This highlights the importance of maintaining the activity of the enzyme above a certain threshold in order to obtain meaningful results.

m-calpain		**µ-calpain**	
Change in Fluorescence	**IC_{50} of SJA6017 (nM)**	**Change in Fluorescence**	**IC_{50} of SJA6017 (nM)**
204	9	150	15
650	77	637	134
856	80	1265	130
1235	83	1504	164

Table 5.2 Effect of enzyme activity on the calculated IC_{50} value of SJA6017 against m- and µ- calpain

Papain, cathepsin B, α-chymotrypsin and pepsin were tested for their turnover of BODIPY-casein. The results of this are summarised in **Table 5.3** and show that BODIPY-casein is a suitable substrate for papain, α-chymotrypsin and pepsin. This primary testing utilised the proteases at 1 mg/ml and the resulting change in fluorescence values show that the concentration of each enzyme must be optimised (according to the observations made in **Table 5.2**). This optimisation also allows comparison of potency across the range of proteases tested. The optimised concentrations of each enzyme were found to be the following: papain, 2 mg/ml; pepsin, 0.2 mg/ml; α-chymotrypsin, 0.05 mg/ml. These concentrations were found by observing enzyme activity, as determined in **Figure 5.3** and **Table 5.4**.

Enzmye	**Fluorescence at t_0 (FU)**	**Fluorescence at t_{10} (FU)**	**Change in Fluorescence**
m-calpain	1051	1872	821
μ-calpain	878	1881	1003
papain	459	569	110
pepsin	937	2658	1721
α-chymotrypsin	2352	5115	2763
cathepsin B	300	310	10

Table 5.3 Activity of proteases over 10 min. Concentration of each enzyme is 1 mg/ml; fluorescence is given in arbitrary fluorescence units (FU)

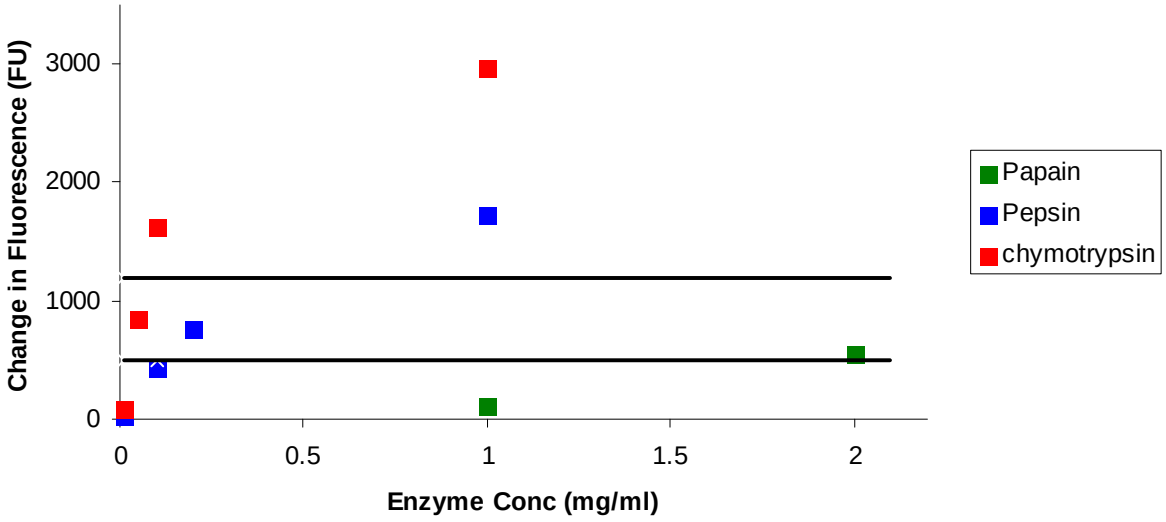

Figure 5.3 Graph of change in fluorescence versus enzyme concentration, the lines represent fluorescence at 500 and 1200 FU. Enzyme concentration must correspond to a change in fluorescence between these two values.

Enzyme	Concentration (mg/ml)	Fluorescence at t_0	Fluorescence at t_{10}	Change in Fluorescence
Papain	**2.00**	**216**	**758**	**542**
	1.00	459	569	110
Pepsin	1.00	937	2658	1721
	0.20	**549**	**1305**	**756**
	0.10	443	852	424
	0.01	390	393	3
α-Chymo	1.00	2677	5642	2965
	0.10	1830	3458	1628
	0.05	**749**	**1593**	**844**
	0.01	1005	1083	78

Table 5.4 Determining the optimal concentration of papain, pepsin and α-chymotrypsin for assay

5.3.2 Adjustment of the Substrate Solution

The calpain assay protocol as described above uses the BODIPY-casein substrate in a solution containing: 0.0005% BODIPY-FL casein in 10 mM TRIS-HCl (pH 7.5), 10 mM $CaCl_2$, 0.1 mM NaN_3, and 0.1% mercaptoethanol. This is unnecessary for papain, α-chymotrypsin and pepsin as they do not require calcium for activation. A simplified solution of 1% BODIPY-casein in distilled water was substituted for the original solution; use of this solution gave similar results for enzyme activity. Only 10 µL of this substrate solution was used in each assay well because of its increased concentration (for calpain assays, 100 µL of the original substrate solution containing 0.0005% BODIPY-casein was used per assay well).

Adjustment of buffer solutions

Each enzyme has different requirements for stabilisation in solution, thus optimised buffer solutions were found. These were: 10 mM HCl (pH 2.0) for pepsin; 10 mM TRIS-HCl (pH 7.8) for α-chymotrypsin; 10 mM MES (pH 6.2) for papain as identified by the CalBiochem catalogue.

The modified enzyme assays were performed in black 96-well *Whatman* plates. Blank control assays contained 190 µL of appropriate buffer (10 mM MES, 10 mM HCl or 10 mM TRIS-HCl). The control assays contained 10 µL of the protease (papain, pepsin or α-chymotrypsin) in 180 µL of appropriate buffer (see **Figure 5.3** for a schematic plate layout) and the inhibitor assays 130 µL of appropriate buffer, 50 µL inhibitor solution and 10 µL of the protease solution. The reaction was initiated by the addition of 10 µL of substrate solution at 25 °C and the progress of the reaction followed for 10 min in a BMG Fluostar with excitation of 485 nm and emission of 530 nm. For the inhibitor assays the sample buffer was replaced by 50 µL of inhibitor diluted in distilled water[§]. The percentage inhibition was determined as 100 times the activity with inhibitor present divided by the activity of the control assay. Assays were performed in triplicate with serial dilutions of inhibitor concentrations from 50 µM to 50 nM.

[§] This will be discussed in more detail in **Section 5.2**

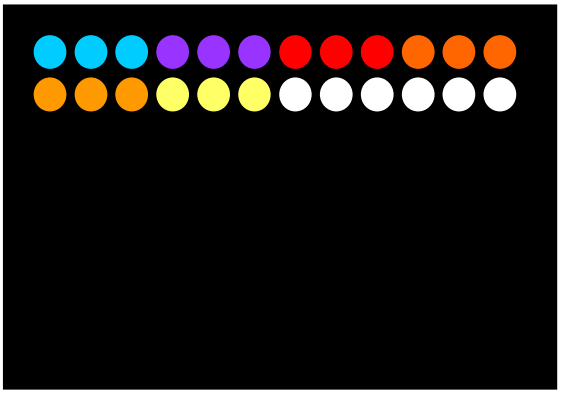

Blank

190 µL buffer
10 µL BODIPY-casein

Enzyme Activity

180 µL buffer
10 µL enzyme
10 µL BODIPY-casein

Inhibitor Assay

130 µL buffer
10 µL enzyme
10 µL BODIPY-casein

Figure 5.3 Schematic diagram of a 96 well plate and the layout of a papain, pepsin or α-chymotrypsin assay run

5.3.3 Cathepsin B Assay Protocol

Cathepsin B showed a change of only 10 fluorescence units over 10 min when tested against the BODIPY-casein substrate (refer to **Table 5.3**), indicating that the BODIPY-casein was not a suitable substrate (optimal change in fluorescence units between 500-1200 is required). Angliker[7] and co-workers described a fluorescent assay protocol for cathepsin B, where the cathepsin B was at a concentration of 1 mg/ml, the buffer 10 mM sodium acetate (pH 5.4) and the substrate used was benzyloxycarbonyl-Phe-Arg-7-amido-4-methyl coumarin (10 µM final concentration). Repeating the activity tests using these conditions showed this to be a viable assay protocol for cathepsin B (see **Table 5.5**). Cathepsin B was tested at concentrations of 0.1 mg/ml, 0.05 mg/ml and 0.02 mg/ml to determine the optimal concentration of the enzyme. The optimal concentration of cathepsin B was found to be 0.02 mg/ml, this having a change in fluorescence units of 664 over 10 min.

Enzyme Concentration (mg/ml)	Fluorescence at t_0 (FU)	Fluorescence at t_{10} (FU)	Change in Fluorescence (FU)
0.1	704	4519	3815
0.05	267	1654	1626
0.02	220	884	664

Table 5.5 Determining the optimal concentration of cathepsin B for assay.

The modified cathepsin B assays were performed in black 96-well *Whatman* plates. The blank control assays contained 190 μL of 10 mM sodium acetate (pH 5.4) buffer. The enzyme control assays contained 10 μL of the cathepsin B 0.02 mg/mL solution and 180 μL of 10 mM sodium acetate buffer (pH 5.4) (see **Figure 5.4** for a schematic plate layout), while the inhibitor assays contained 130 μL of 10 mM sodium acetate buffer (pH 5.4), 50 μL of inhibitor solution and 10 μL of. The reaction was initiated by the addition of 10 μL of 200 μM Cbz-Phe-Arg-7-amido-4-methyl coumarin solution at 25 °C and the progress of the reaction followed for 10 min in a BMG Fluostar with excitation of 360 nm and emission of 460 nm. The percentage inhibition was determined as 100 times the activity with inhibitor present divided by the activity of the control assay. Assays were performed in triplicate with serial dilutions of inhibitor concentrations from 50 μM to 50 nM.

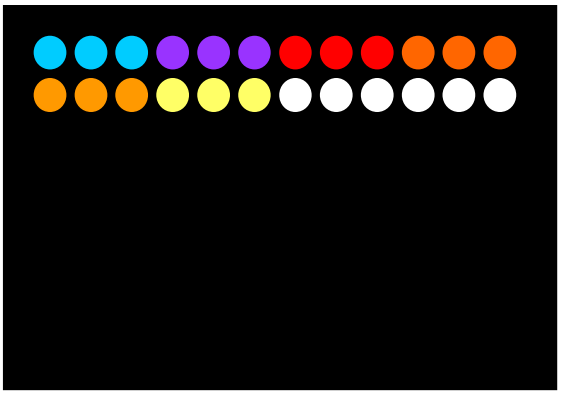

Blank

190 µL NaOAc buffer
10 µL BODIPY-casein

Enzyme Activity

180 µL NaOAc buffer
10 µL cathepsin B
10 µL BODIPY-casein

Inhibitor Assay

130 µL NaOAc buffer
10 µL cathepsin B
10 µL BODIPY-casein

Figure 5.4 Schematic diagram of a 96 well plate and the layout of a cathepsin B assay run

5.3.4 Validation of the Modified Assay Protocols

Known inhibitors of pepsin, α-chymotrypsin and cathepsin B were used to validate the modified assays. The aspartic acid inhibitor pepstatin A[**] **5.1** was used for validation of the pepsin assay; correspondingly an in-house boronic acid[††] **5.2** was used for validation of the α-chymotrypsin assay. The structures of these compounds are pictured in **Figure 5.2**. Comparison of previously reported potency with the IC_{50} values calculated herein show that the modified assays are viable (see **Table 5.6**). The inhibition of pepsin by pepstatin observed correlated well with the results of Marchiniszyn[8] (100% inhibition of pepsin at inhibitor concentration of 120 nM versus 96% inhibition at inhibitor concentration of 100 nM). Similarly, the boronic ester was shown to have an IC_{50} of 1100 nM under the modified assay conditions as compared to a value of 1200 nM in independent assay. The aldehyde **2.3** was used for validation of the cathepsin B assay protocol. Previously, Inoue[3] *et al* had reported an IC_{50} value of 16 nM for **2.3** against cathepsin B; the IC_{50} value of 22 nM obtained with this assay protocol correlated well.

[**] isovaleryl-Val-Val-Sta-Ala-Sta, where Sta is 4-amino-3-hydroxy-6-methylheptanoic acid

[††] Synthesised and independently assayed by David Pearson

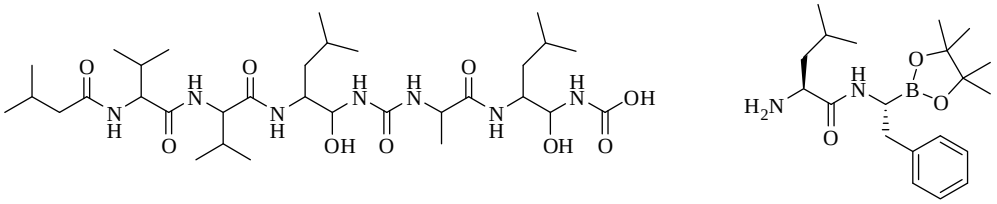

5.1 **5.2**

Figure 5.5 The structures of a) pepstatin A **5.1** and b) a boronic acid **5.2**. These are inhibitors of Pepsin and α-chymotrypsin respectively

Enzyme	Inhibitor	Reported potency (IC_{50})	Calculated potency
Pepsin	**5.1**	100% at 120 nM[8]	96% at 100 nM
α-Chymotrypsin	**5.2**	1200 nM[9]	1100 nM
Cathepsin B	**2.3**	16 nM[3]	22 nM

Table 5.6 Comparison of known inhibitors for validation of modified enzyme assays. Potency given as IC_{50} values unless otherwise stated.

The inhibitors synthesised in **Chapters Two-Four** were not expected to show inhibition against pepsin or α-chymotrypsin as they were designed as cysteine protease inhibitors; thus the validation of the pepsin and α-chymotrypsin assay protocols was necessary to ensure that any lack of inhibition observed was a real observation and not a false negative result.

5.4 SOLVENT EFFECTS ON PROTEASE ACTIVTY

Biological assay of the inhibitors herein synthesised required solutions containing known concentrations of these inhibitors. Ideally, the same buffer solution used in making stock solutions of the enzymes would be utilised; however, due to the limited solubility of most organic compounds in aqueous media, an organic solvent was utilised. Dimethyl sulfoxide was the solvent of choice because its high boiling point ensured that no evaporation of the solvent occurred over the course of the assay. Further, dimethyl sulfoxide is water miscible, a requirement for the solvent used in the assays due to the presence of aqueous based media such a buffers.

Before calculating and reporting IC_{50} values, a study was performed on the effect dimethyl sulfoxide had on the assay protocol. This study entailed running enzyme control assays against enzyme assays containing a variable amount of dimethyl sulfoxide (50 µL to 0 µL). The enzyme control assays are as described above for calpain, cathepsin B and other proteases. Results shown in **Table 5.7** and **Figure 5.6** below provide evidence that dimethyl sulfoxide above 5% of the total well volume does adversely affect the activity of the enzyme with m-calpain, µ-calpain, papain, cathepsin B and pepsin all showing an activity less than half of their natural activity. α-Chymotrypsin gave anomalous results for higher concentrations of dimethyl sulfoxide, with the enzyme activity shown being greater than it should be (over 100%). However, at lower concentrations of dimethyl sulfoxide, activity was restored to normal. This same trend was observed in an independent assay performed at Canterbury University.[10] One suggestion for this trend is that the dimethyl sulfoxide partly denatures α-chymotrypsin which promotes its activity.

The inhibitors were made up as 1 mM solutions in dimethyl sulfoxide and subsequently diluted by the addition of distilled water to give a range of concentrations. The highest concentration of inhibitor used in determining IC_{50} values was 50 µM, corresponding to a 200 µM solution of inhibitor. To achieve this the initial 1 mM solution of the inhibitor was diluted 5-fold with distilled water, resulting in the solution being 20% dimethyl sulfoxide. Further dilution of this solution occurs when setting up the assay wells, as the 50 µL of inhibitor solution makes up only a quarter of the total volume. Thus the final amount of dimethyl sulfoxide present comes to 5% of the total well volume (10 µL out of 200 µL)

and so no solvent effect will be observed. This means that 50 µM is the highest concentration at which inhibition can be reliably measured.

Volume DMSO (µL)	Protease activity (%)					
	m-calpain	µ-calpain	cat B	papain	pepsin	α-chymotrypsin
50	5	2	16	40	20	140
30	45	47	55	66	59	118
10	**95**	**98**	**96**	**92**	**98**	**97**
2	**100**	**100**	**96**	**97**	**100**	**99**

Table 5.7 Effect of DMSO on the activity of enzymes.

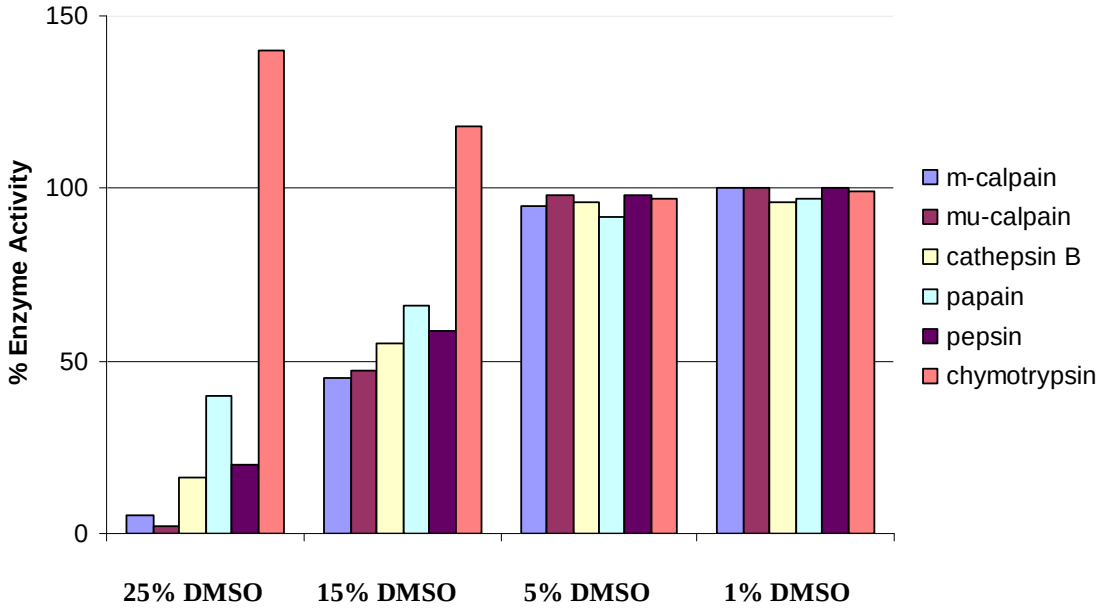

Figure 5.6 Visual representation of the effect of DMSO on the activity of proteases. The amount of DMSO is relative to a total well volume of 200 µL

5.5 CONCLUSION AND FUTURE WORK

The optimised conditions for biological testing of inhibitors against each of the proteases m-calpain, μ-calpain, papain, cathepsin B, pepsin and α-chymotrypsin using a fluorogenic assay system are summarised in **Table 5.8** below. General considerations were:

- The maximum amount of dimethylsulfoxide present in any well of the assay must be no greater than 5% of the total well volume

- The enzyme concentration must correspond to a change in fluorescence between 500-1200 units for consistent results

- Inhibitor samples were serially diluted: 50 μM, 10 μM, 2 μM, 0.4 μM, 0.2 μM, 0.1 μM and 0.05 μM

- The substrate solutions used were as follows:

BODIPY A	**BODIPY B**	**AMC**
8440 μL distilled H_2O	60 μL BODIPY stock	200 μM solution of Cbz-Phe-Arg-AMC in NaOAc buffer (pH 5.4)
1000 μL 10 mM $CaCl_2$	540 μL distilled water	
500 μL digestion buffer[‡‡]		
50 μL BODIPY stock		
10 μL β-mercaptoethanol		

- Assays using either BODIPY A or B as the substrate required excitation of 485 nm and emission of 530 nm for fluorescence measurement; however, use of AMC as a substrate required excitation of 360 nm and emission of 460 nm

[‡‡] Where Digestion buffer: 2 mL 100 mM tris(hydroxymethyl) methylamine
2 mL 10 mM sodium azide
Adjust pH to 7.8 and make up to 10 mL with H_2O

Enzyme	Concentration	Buffer	Assay Protocol		
			Blanks	**Enyme activity**	**Inhibitor assay**
m and μ-calpain	used as provided by Lincoln University	distilled water	calcium blank 100 μL 10 mM $CaCl_2$ 100 μL BODIPY A EDTA blank 25 μL 100 mM EDTA 25 μL water 50 μL enzyme 100 μL BODIPY A	50 μL water 50 μL enzyme 100 μL BODIPY A	50 μL inhibitor 50 μL enzyme 100 μL BODIPY A
papain	2.0 mg/ml in buffer	10 mM MES buffer (pH 6.2)	190 μL buffer 10 μL BODIPY B	180 μL buffer 10 μL enzyme 10 μL BODIPY B	130 μL buffer 50 μL inhibitor 10 μL enzyme 10 μL BODIPY B
pepsin	0.2 mg/ml in buffer	10 mM HCl buffer (pH 2.0)	190 μL buffer 10 μL BODIPY B	180 μL buffer 10 μL enzyme 10 μL BODIPY B	130 μL buffer 50 μL inhibitor 10 μL enzyme 10 μL BODIPY B
α-chymotrypsin	0.05 mg/ml in buffer	10 mM TRIS-HCl buffer (pH 7.8)	190 μL buffer 10 μL BODIPY B	180 μL buffer 10 μL enzyme 10 μL BODIPY B	130 μL buffer 50 μL inhibitor 10 μL enzyme 10 μL BODIPY B
cathepsin B	0.02 mg/ml in buffer	10 mM NaOAc buffer (pH 5.4)	190 μL buffer 10 μL AMC	180 μL buffer 10 μL enzyme 10 μL AMC	130 μL buffer 50 μL inhibitor 10 μL enzyme 10 μL AMC

Table 5.8 Summary of the optimised conditions for each assay protocol established

5.6 REFERENCES FOR CHAPTER FIVE

(1) Thompson, V. F.; Saldana, S.; Cong, J.; Goll, D. E. *Analytical Biochemistry* **2000**, *279*, 170-178.

(2) Jones, L. J.; Upson, R. H.; Haugland, R. P.; Panchuk-Voloshina, N.; Zhou, M.; Haugland, R. P. *Analytical Biochemistry* **1997**, *251*, 144-152.

(3) Inoue, J.; Nakamura, M.; Cui, Y.-S.; Sakai, Y.; Sakai, O.; Hill, J. R.; Wang, K. K. W.; Yuen, P.-W. *Journal of Medicinal Chemistry* **2003**, *46*, 868-871.

(4) Buroker-Kilgore, M.; Wang, K. K. W. *Analytical Biochemistry* **1993**, *208*, 387-392.

(5) Wang, K. K. W.; Yuen, P.-W. In *Calpain: Pharmacology and Toxicology of Calcium-Dependent Protease*; Taylor and Francis: London, 1999, p 1-448.

(6) Iqbal, M.; Messina, P. A.; Freed, B.; Das, M.; Chatterjee, S.; Tripathy, R.; Tao, M.; Josef, K. A.; Dembofsky, B. *Bioorganic & Medicinal Chemistry Letters* **1997**, *7*, 539-544.

(7) Angliker, H.; Wikstrom, P.; Rauber, R.; Shaw, E. *Biochemical Journal* **1987**, *241*, 871-875.

(8) Marchiniszyn, J., Jr.; Hartsuck, J.A.; Tang, J. *The Journal of Biological Chemistry* **1976**, *251*, 7088-7094.

(9) Pearson, D. S., Personal Communication.

(10) Alexander, N. A., Personal Communication.

CHAPTER SIX

Assay Results and Structure-Activity Relationships of Synthesised Inhibitors

6.1 INTRODUCTION TO INHIBITOR STRUCTURE-ACTIVITY RELATIONSHIPS

The only cysteine protease inhibitors that have proceeded to clinical development to date are those that target caspases, cathepsin K, cruzain or rhinovirus.[1,2] Of these the cathepsin K inhibitors are undergoing clinical trials for the treatment of osteroperosis.[1,3] Recent reviews[1,2] of clinical protease inhibitors highlight target selectivity as a major problem in the development of new drugs and state that "attaining selectivity between members of cysteine proteases belonging to the same family is of the utmost concern".[2] The aim of this chapter is to show that selectivity can be conferred upon cysteine protease inhibitors through the choice of warhead.*

The inhibitors synthesised within this thesis (see **Chapters Two-Four**) were assayed according to the protocols established in **Chapter Five** with a view to establishing structure-activity relationships with regard to selectivity. What follows is a discussion of structure-activity relationships for the different warheads. Special mention is made of selectivity for cathepsin B over the other cysteine proteases tested due its role in human diseases such as tumour metastasis (see **Chapter One** for more detail).[4]

The peptidyl backbone and the *N*-protecting group were retained as common structural features in all the synthesised inhibitors (see **Tables 6.1-6.20**) while the warhead was changed. This allowed both the effect of the warhead on inhibitor potency and structure-activity relationships to be studied. The two generic families of synthesised inhibitors were based on the scaffolds shown in **Figure 6.1**, these being a) 4-fluorobenzenesulfonyl-Val-Leu-warhead and b) benzyloxycarbonyl-Val-Leu-warhead respectively. These scaffolds were chosen to allow comparison to literature inhibitors and also because both the 4-fluorbenzyesulfonyl-Val-Leu dipeptide and the benzyloxycarbonyl-Val-Leu dipepetide are known to provide the basis of potent inhibitors of cysteine proteases.

* The term 'warhead' is used to define the part of the inhibitor that interacts with the active site cysteine thiol. More detail can be found in **Chapter One**.

a) **b)**

Figure 6.1 The two scaffolds used for establishing structure-activity relationships of warheads a) 4-fluorobenzenesulfonyl-Val-Leu-warhead and b) benzyloxycarbonyl-Val-Leu-warhead

6.2 REVERSIBLE CYSTEINE PROTEASE INHIBITORS: ASSAY RESULTS AND DISCUSSION

6.2.1 Peptidyl Alcohols and Aldehydes

Over the last decade non-covalent moieties have become increasingly significant as protease inhibitor 'warheads'[5] due to the increased drug-like properties and *in vivo* selectivity such inhibitors. Non-covalent warheads include alcohol, methylene amine and azidomethylene moieties like those shown in **Figure 6.2**. Most non-covalent inhibitors target serine and aspartic acid proteases, with few examples targeting cysteine proteases.[5] Hence the alcohols **2.6**, **2.26**, **2.29**, **2.30**, **2.34**, and **2.35** and the corresponding aldehydes **2.3**, **2.27**, **2.19**, **2.2**, **2.21** and **2.22** respectively (as prepared in **Chapter Two**), were assayed against the cysteine proteases. The results of these assays are shown in **Table 6.1**.

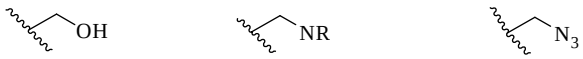

a b c

Figure 6.2 Three non-covalent warheads utilised in protease inhibitors: a) alcohol; b) methylene amine and c) azidomethylene groups

Compound		IC_{50} (μM) m-calpain	μ-calpain	cathepsin B	papain
2.6	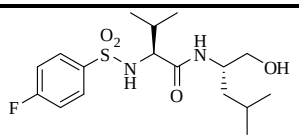	>50	50	9.2	>50
2.3	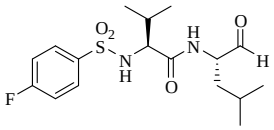	0.080	0.13	0.022	0.023
2.26	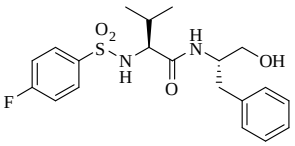	2.3	1.5	0.075	6.3
2.27	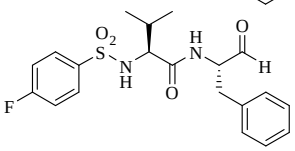	0.072	0.012	0.016	0.033

Compound		IC_{50} (μM)			
		m-calpain	μ-calpain	cathepsin B	papain
2.29	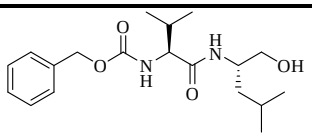	>50	>50	26	>50
2.19	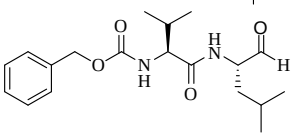	0.15	0.38	0.042	0.66
2.30	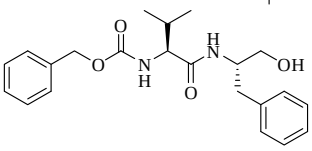	22	28	1.2	>50
2.2	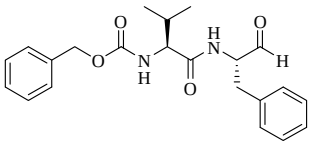	0.060	0.027	0.027	1.1
2.35	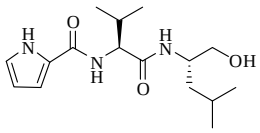	>50	>50	12	>50
2.21	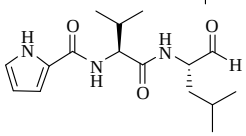	0.32	0.65	0.032	0.053
2.36	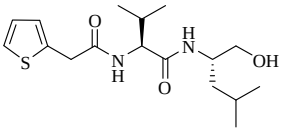	>50	>50	23	>50
2.22	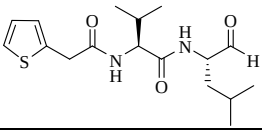	0.25	1.1	0.016	0.040

Table 6.1 Comparison of IC_{50} values of aldehydes and corresponding alcohols

The alcohols **2.26** and **2.30** (see **Figure 6.3**) are noteworthy as the only members of the alcohol series that display significant inhibition of cathepsin B (IC_{50} = 0.075 μM and 1.2 μM respectively). Alcohol **2.26** also shows significant potency against the other cysteine proteases tested {IC_{50} = 2.3 μM (m-calpain), 1.5 μM (μ-calpain) and 6.3 μM (papain)}. The analogous alcohol **2.30**, which differs only in the *N*-protecting group (benzyloxycarbonyl instead of 4-fluorobenzenesulfonyl), is less potent than **2.26**, with IC_{50} values greater than 20 μM against m-calpain, μ-calpain and papain (see **Table 6.1**). These results suggest that having an alcohol moiety at the *C*-terminus and the 4-fluorobenzenesulfonyl moiety as the *N*-terminal protecting group is a significant combination towards the design and synthesis of a potent, cathepsin B specific inhibitor.

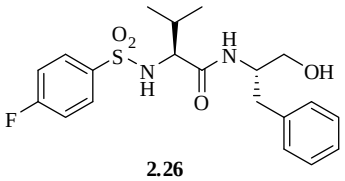

2.26

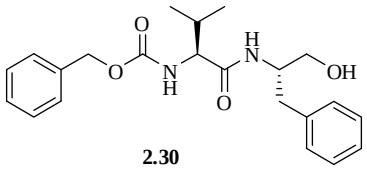

2.30

IC_{50} Values:		
m-calpain	2.3 µM	22 µM
µ-calpain	1.5 µM	28 µM
cathepsin B	0.075 µM	1.2 µM
papain	6.3 µM	>50 µM

Figure 6.3 The alcohol **2.26** is a novel, potent inhibitor of cysteine proteases.

The alcohols **2.26** and **2.30** both contain the dipeptide Val-Phe, indicating that the large aromatic hydrophobic side chain of Phe may be more favourable in the P_1 position than smaller hydrophobic side chains such as Leu or Val (compare with IC_{50} values of alcohols **2.6** and **2.29**). The corresponding Val-Phe aldehydes **2.27** and **2.2** are similarly more potent cysteine proteases inhibitors than the Val-Leu analogues **2.3** and **2.19** (up to 40-fold difference in potency over the cysteine proteases tested). These results refine the previous suggestion by Currier *et al*[6] that Leu and Phe were equally favourable in the P_1 position for µ-calpain

The remainder of the alcohols (**2.6**, **2.29**, **2.35**, and **2.36**) are significantly weaker cysteine protease inhibitors than **2.26** and **2.27**; however, the Leu-Val backbone still provides between 2- to 5-fold specificity for cathepsin B (IC_{50} = 9.2 µM, 26 µM, 12 µM and 23 µM respectively) over the other cysteine proteases tested.

The aldehydes **2.3**, **2.27**, **2.19**, **2.2**, **2.21** and **2.22** were assayed against the cysteine proteases: m-calpain, µ-calpain, cathepsin B and papain. The resulting IC_{50} values (see **Table 6.1**) show that all the aldehydes are broad spectrum cysteine proteases (IC_{50} values <0.70 µM). The aldehydes are, however, specific for cysteine protease being inactive against pepsin and α-chymotrypsin (see **Appendix A2**). The broad cysteine protease specificity observed for the aldehydes **2.3**, **2.27**, **2.19**, **2.2**, **2.21** and **2.22** compares well with the aldehyde examples **2.1-2.5**, which are also non-specific cysteine protease inhibitors (discussed in **Chapter Two**, **Table 2.2**).

The alcohol **2.6** and aldehyde **2.3** (see **Chapter Two**) were modelled to allow direct comparison to literature[7] and to provide representative data for related compounds. Both of these structures were docked into the rigid μ-calpain model and the best poses are shown in **Figure 6.4**.[†] The molecular modelling results suggest that the both alcohol **2.6** and aldehyde **2.3** adopt a β-strand conformation that is known to be important for binding to cysteine proteases (the β-strand is defined by hydrogen bonds A, B and C, see **Chapter One** for more detail). The alcohol **2.6** is suggested to form an additional hydrogen bond between the alcohol oxygen group and Gly_{271}, which is not observed in the case of aldehyde **2.3**. Since both of these compounds appear to bind in a similar region of the active site and form similar hydrogen bonds, the difference in activity {**2.3** IC_{50} = 0.080 μM (m-calpain), 0.13 μM (μ-calpain), 0.022 μM (cathepsin B) and 0.023 μM (papain) versus **2.6** IC_{50} = 50 μM (m-calpain), 50 μM (μ-calpain), 9.2μM (cathepsin B) and 50 μM (papain)} is attributable to the reactivity of the aldehyde moiety over the non-reactive alcohol moiety. The differences in potency between the alcohol **2.6** and aldehyde **2.3** are similar to those observed between the other alcohol and aldehyde pairings, with the exception of alcohols **2.26** and **2.30** (as previously discussed).

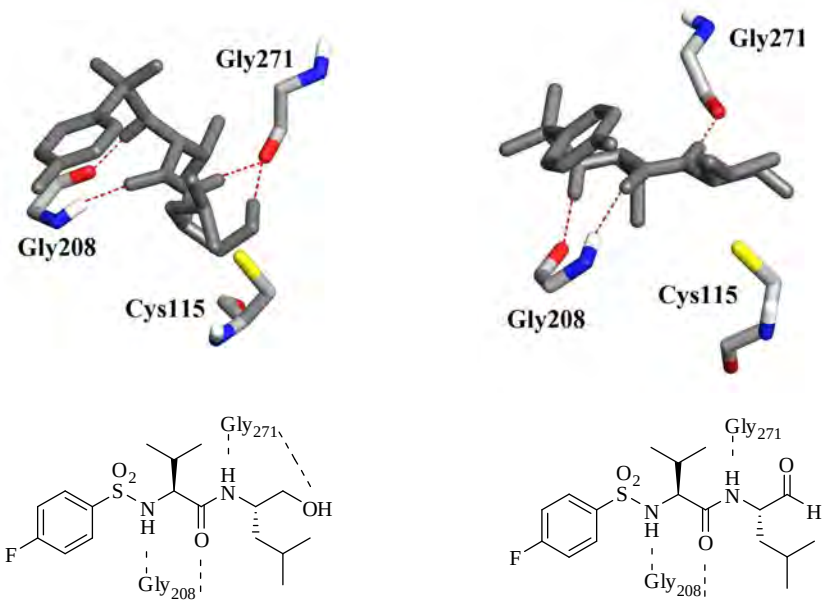

a) **b)**

Figure 6.4 Molecular modelling results comparing the hydrogen bonds of a) alcohol **2.6** and b) aldehyde **2.3**

[†] See **Chapter Two** for details of molecular modelling

A systematic search of the literature reveals few examples of non-covalent cathepsin B specific inhibitors. Fairlie *et al*[5] synthesised cathepsin B inhibitor **6.1** utilising the non-covalent azide moiety in place of a warhead (see **Chapter Two** for details). Conroy *et al*[8] reported the cyclohexanone based cathepsin B inhibitors **6.2** and **6.3** (see **Figure 6.5**), which were designed to bridge the active site by means of interactions between the Orn residue and the S_2 subsite and the Pro residue and the S_2' subsite. The free acid of the Pro forms hydrogen bonds to the His_{110} and His_{111} of the protease. These two active site bridging inhibitors, however, show only weak inhibition of cathepsin B (**6.2**, K_i = 6600 µM; **6.3**, K_i = 6100 µM). Yamamoto *et al*[9] designed the non-covalent inhibitor **6.4** (see **Figure 6.5**) that was a potent cathepsin B inhibitor (IC_{50} <0.10 µM); however, specificity was not addressed. The alcohol **2.26** appears to be an unprecedented example of a potent non-covalent cathepsin B specific inhibitor.

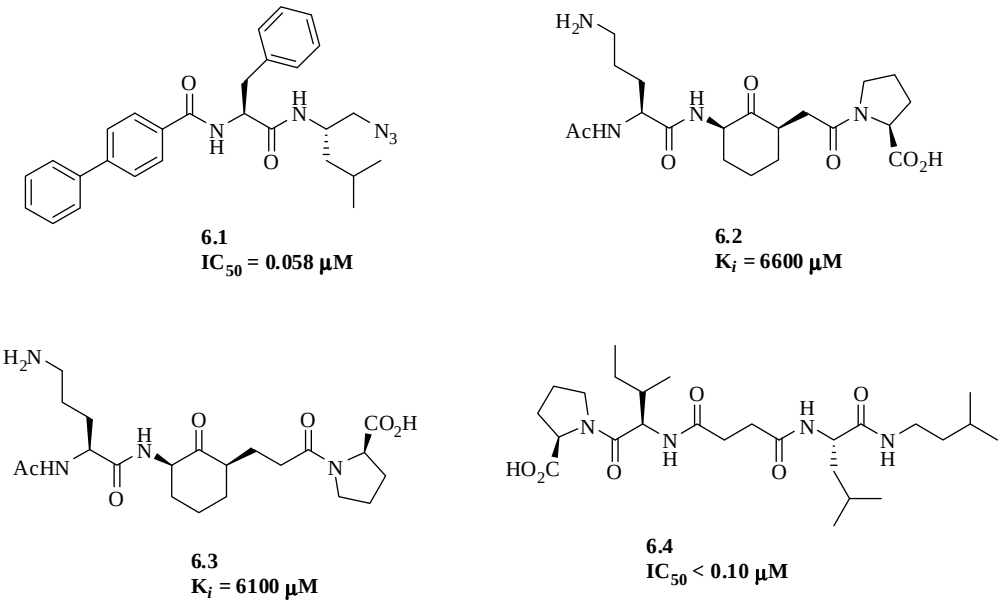

Figure 6.5 The non-covalent cathepsin B azide **6.4**[5]; active site bridging inhibitors **6.2** and **6.3**[8] and the amide **6.4**[9]

6.2.2 Semicarbazone Inhibitors

The semicarbazones **2.37-2.40** exhibited inhibitory activity against m-calpain, µ-calpain, cathepsin B and papain (IC_{50} values in the low µM range) (see **Table 6.2**). At concentrations of 50 µM the semicarbazones **2.37-2.40** were inactive against pepsin and α-

chymotrypsin. The semicarbazone **2.37** {IC_{50} = 1.1 μM (μ-calpain)} is a literature compound synthesised by Senju Pharmaceuticals[10] {reported IC_{50} = 0.68 μM (μ-calpain)}; the 1.6-fold difference in IC_{50} values being attributed to the increased sensitivity of the BODIPY-casein protocol used herein (see **Chapter Five** for details). Selectivity within the papain superfamily has not previously been studied for semicarbazone **2.37**.

The semicarbazones **2.37-2.40** were all significantly less potent than the aldehyde **2.3** (refer to **Table 6.1**); which agrees with trends observed in the literature (see **Chapter Two, Section 2.2.1**[11]). The semicarbazones **2.37-2.40** are between 12- and 190-fold less potent against m-calpain and μ-calpain respectively than the parent aldehyde **2.3**. Activity against papain and cathepsin B was also reduced, but to a lesser degree (between 7- and 40-fold); however, the resulting IC_{50} values of all the semicarbazones **2.37-2.40** remained sub-μM.

The nature of the semicarbazone substituent adjacent to its carbonyl group (extending into the S' pocket) does not seem to have a significant influence on inhibitory activity, with the IC_{50} values of **2.37**, **2.39** and **2.40** being similar against papain (0.92 μM, 0.96 μM and 0.96 μM respectively), m-calpain (1.5 μM, 1.5 μM and 3.8 μM respectively), μ-calpain (1.1 μM, 3.5 μM and 4.8 μM respectively) and cathepsin B (0.69 μM, 0.24 μM and 0.32 μM respectively). The semicarbazones **2.37**, **2.39** and **2.40** display up to 4-fold selectivity for cathepsin B over the other cysteine proteases tested. The thiosemicarbazone **2.38** was significantly more potent than the semicarbazone **2.37** against cathepsin B (0.69 μM and 0.16 μM respectively) and papain (0.92 μM and 0.19 μM respectively).

Compound		IC_{50} (μM) m-calpain	μ-calpain	cathepsin B	papain
2.3	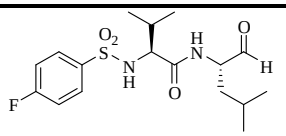	0.080	0.13	0.022	0.023
2.37	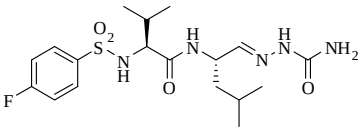	1.5	1.1	0.69	0.92
2.38	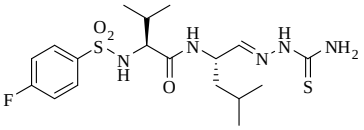	1.6	1.6	0.16	0.19
2.39	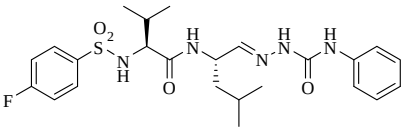	1.5	3.5	0.24	0.96
2.40	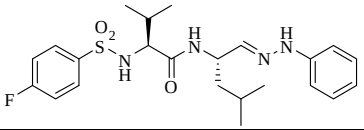	3.8	4.8	0.32	0.96

Table 6.2 Inhibition of cysteine proteases by semicarbazones **2.37-2.40**.

The synthesised compounds **2.37-2.40** containing semicarbazone warheads are potent inhibitors of the cysteine proteases tested (IC_{50} < 4.8 μM). 4-Phenylsemicarbazone **2.39** is the most specific inhibitor within this series, showing greater than 4-fold selectivity for cathepsin B over the other cysteine proteases tested. A structural difference between the $S_{1'}$ pockets of cathepsin B and papain is highlighted by the presence of a phenyl group at the $P_{1'}$ position; both the 4-phenylsemicarbazone **2.39** and phenylhydrazine **2.40** are significantly more potent against cathepsin B (IC_{50} = 0.24 μM and 0.32 μM respectively) than papain (IC_{50} = 0.96 μM and 0.96 μM respectively); the semicarbazone **2.37** and thiosemicarbazone **2.38** (which have a free amide and thioamide respectively) have similar potencies (only 1.2-fold difference) against cathepsin B (IC_{50} = 0.69 μM and 0.16 μM respectively) and papain (IC_{50} = 0.92 μM and 0.19 μM respectively).

The mechanism by which semicarbazones are thought to inhibit cysteine proteases has recently been revised. Adkison[11] and co-workers co-crystallised semicarbazone inhibitors (see **Chapter Two**) with cathepsin K. The majority of these X-crystal structures contained only the parent aldehyde, leading to the hypothesis that the active inhibitor is the parent aldehyde, while the semicarbazone moiety acts only as a pro-drug. This was investigated

using a ^{13}C labelled semicarbazone inhibitor. A ^{13}C NMR which showed enhanced resonances at 150 ppm for the imine carbon and also at 92 ppm (smaller) for the corresponding hydrate. The labelled inhibitor was then added to cathepsin K and a ^{13}C NMR spectrum revealed enhanced resonances at 91 ppm (hydrate) and 204 ppm. The latter resonance, on comparison with the ^{13}C NMR spectrum of the parent aldehyde, was found to represent the aldehyde carbonyl carbon; hence Adkison concluded that the semicarbazone moiety most likely functioned as a pro-drug. On this basis, it is proposed that the semicarbazones **2.37-2.40** also act as pro-drugs ('masked' aldehydes) such that each example then gives a similar IC_{50} value.

6.2.3 Oxadiazole Inhibitors and Precursors

Two dipeptidyl carboxylic acids (**2.7** and **2.46**) and the corresponding methyl esters **2.44** and **2.45** were assayed against m-calpain, μ-calpain, cathepsin B and papain (results in **Table 6.3**). The acid **2.7** and corresponding ester **2.44** are potent and selective cathepsin B specific inhibitors (IC_{50} = 0.39 μM, selectivity 127-fold; 1.4 μM, selectivity 35-fold respectively); while inhibition of the other cysteine proteases was not observed at an inhibitor concentration of 50 μM. The analogous acid **2.46** and ester **2.45** are over 14-fold less potent inhibitors of cathepsin B (IC_{50} = 15 μM and 19 μM respectively) than the methyl esters **2.44** and **2.45**.

As highlighted previously (see **Section 6.2.1**), the 4-fluorobenzenesulfonyl *N*-protecting group is favoured over the benzyloxycarbonyl group for inhibition of cathepsin B. This is reflected in the acid **2.7** (IC_{50} = 0.39 μM) being 40-fold more potent than the corresponding acid **2.46** (IC_{50} = 15 μM) and the methyl ester **2.44** (IC_{50} = 1.4 μM) being 13-fold more potent than the corresponding methyl ester **2.45** (IC_{50} = 19 μM).

	Compound	IC$_{50}$ (μM) m-calpain	μ-calpain	cathepsin B	papain
2.44	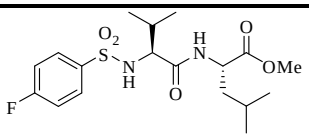	>50	>50	1.4	>50
2.7	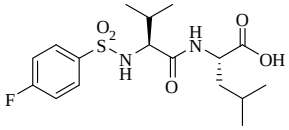	>50	>50	0.39	>50
2.48	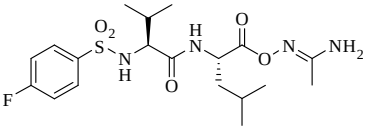	50	50	>50	>50
2.41	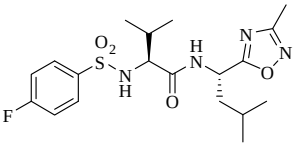	>50	>50	18	50
2.45	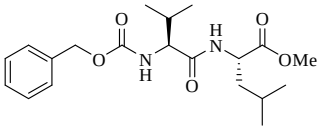	>50	>50	19	>50
2.46	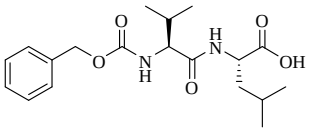	>50	>50	15	>50
2.49	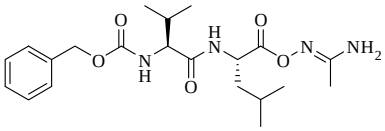	>50	>50	>50	>50
2.50	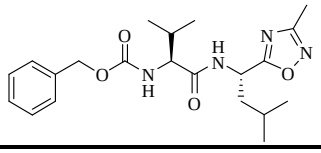	>50	>50	23	>50

Table 6.3 Potency of 1,2,4-oxadiazoles **2.41** and **2.50** and corresponding precursors

The amidoximes **2.48** and **2.49** were inactive against m-calpain, μ-calpain, cathepsin B and papain at a concentration of 50 μM (see **Table 6.3**); however, the corresponding oxadiazoles **2.41** and **2.50** were weak and selective inhibitors of cathepsin B (IC$_{50}$ = 18 μM and 23 μM respectively); inhibition of m-calpain, μ-calpain and papain was not observed.

This selectivity for cathepsin B may be due to the 1,2,4-oxadiazole acting as a bioisostere of carboxylic acids and esters.[12,13] Evidence for this is seen on comparison of the assay results of the oxadiazoles **2.41** and **2.50** with the methyl esters **2.44** and **2.45** and carboxylic acids **2.7** and **2.46**. All six of these inhibitors are cathepsin B specific (IC$_{50}$ = 18

μM, 23 μM, 1.4 μM, 19 μM, 0.39 μM and 15 μM respectively); inhibition of m-calpain, μ-calpain and papain was not observed (see **Table 6.3**).

Bioisosteres are defined as "groups or molecules which have chemical and physical properties producing broadly similar biological properties" and is usually on the basis of two compounds having an atom or a group of atoms with the same number of valence electrons;[14] this can be reflected in similar hydrogen bonding patterns of the two groups to an enzyme active site. The carboxylic acid and the 1,2,4-oxadiazole moieties have the potential to form the same hydrogen bonding patterns within cysteine protease active sites due to the presence the hydrogen bond accepting oxygen atom within both moieties (see **Figure 6.6**).

a **b**

Figure 6.6 The carboxylic acid moiety (a) and the oxadiazole moiety (b) are bioisosteres due to the similar chemical and physical properties of the two groups of atoms

Cathepsin B acts as both an endopeptidase and an exopeptidase.[15] This dual property is largely due a unique structural feature of the enzyme referred to as the occluding loop (see **Chapter One**) located near the active site. The occluding loop contains two positively charged His_{111} and His_{110} residues which can form hydrogen bonds with carboxylate anions (or bioisosteres of these).[16,17] Two modes of binding of the carboxylic acids **2.7** (see **Figure 6.7**) have been proposed but further molecular modelling is required to determine which occurs. These investigations could be extended to include the acid **2.46** and the oxadiazoles **2.41** and **2.50**.

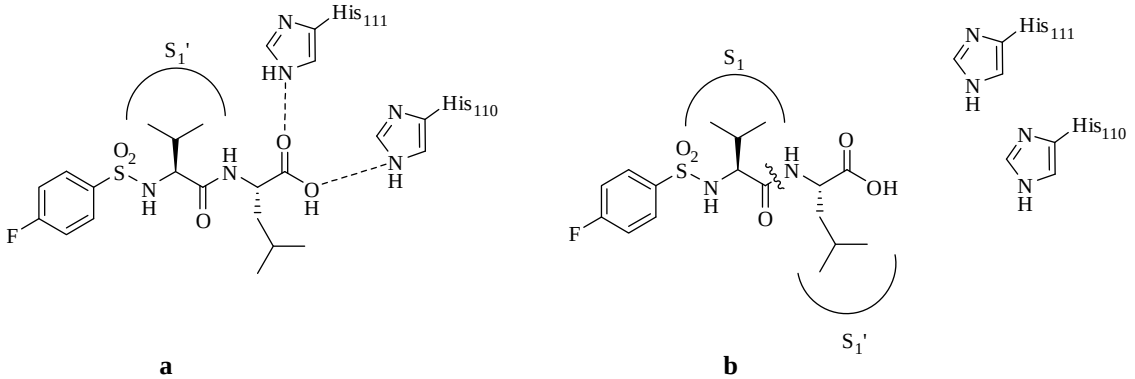

Figure 6.7 The two proposed modes of binding of the acid **2.7** to cathepsin B a) the carboxylic acid forms hydrogen bonds to the His_{110} and His_{111} of the occluding loop, effectively blocking the active site or b) the acid **2.7** with Val in the S_1 subsite and Leu in the S_1' subsite with cleavage occurring at the indicated amide bond

Notably, a literature search reveals an absence of potent cysteine protease inhibitors that incorporate a 1,2,4-oxadiazole warhead. This suggests that 1,2,4-oxadiazole warheads have had limited success or have not been investigated as potent inhibitors of cysteine proteases. Several patents[18-20] have been filed regarding inhibitors with oxadiazole moieties as warheads for the use of cysteine protease inhibition; however, the inhibitors specified in these patents contain α-keto-1,3,4-oxadiazole warheads with P_1' substitution at the 2' position of the oxadiazole (see **Figure 6.8a**) or α-keto-1,2,4-oxadiazole warheads[18] with substitution at the 3' position of the oxadiazole (see **Figure 6.8b**). The potency of the α-ketooxadiazole moiety appears due to it being an α-ketoamide bioisostere (the potency of α-ketoamides is discussed in **Chapter Two**).

Figure 6.8 The structure of the oxadiazole warheads that have been included in patents for use as cysteine protease inhibitors a) α-keto-1,2,4-oxadiazoles, substituted at the 3 position and b) α-keto-1,3,4-oxadiazoles, substituted at the 2 position[18]

As discussed above 1,2,4-oxadiazoles **2.41** and **2.50** are only weak cathepsin B inhibitors; however, a modification that could enhance the potency of these 1,2,4-oxadiazoles would be the insertion of a carbonyl group between the P_1 Leu and the 1,2,4-oxadiazole, making the resulting inhibitors α-ketoamide bioisosteres rather than carboxylic acid bioisosteres. Palmer *et al*[21] reported **6.5a-d** as the first potent cathepsin K specific inhibitors that

incorporated an α-keto-1,3,4-oxadiazole warhead (see **Table 6.4**). Palmer also showed that the nature of the oxadiazole substituent, especially its size and electronics was important for both potency and selectivity between cathepsins; these properties could be exploited for the design of potent specific inhibitors of the papain superfamily.

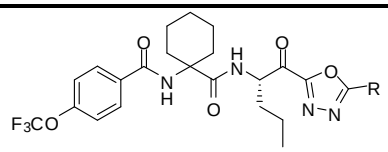

6.5a-d

		K_i (μM)			
	R	**Cathepsin K**	**Cathepsin B**	**Cathepsin L**	**Cathepsin S**
6.5a		0.029	73	19	45
6.5b	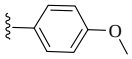	0.037	2.1	7.5	10
6.5c	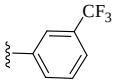	0.054	1.1	1.4	3.3
6.5d		0.033	0.093	0.16	0.32

Table 6.4 Literature examples of potent cathepsin K inhibitors with keto-1,3,4-oxadiazole warheads[21]

6.2.4 α-Ketoheterocycles and Precursors

α-Ketooxazolines and α-ketotetrazoles are thought to inhibit calpain by similar mechanisms. The carbonyl carbon adjacent to the ring in each case is δ^+ and reacts with the δ^- active site cysteine thiol to form a thiohemiacetal.[22] Binding to the active site is further enhanced by hydrogen bonds between the oxygen in the oxazoline ring (δ^-) or the nitrogen in the tetrazole ring and the positively charged histidine residue of the catalytic triad (see **Chapter Two** for the hydrogen bonds suggested to form).

The α-hydroxytetrazoles **2.53** and **2.54** are potent cathepsin B inhibitors (IC_{50} = 2.1 μM and 1.3 μM respectively) that have greater than 18-fold specificity for cathepsin B over the

other cysteine proteases tested (IC_{50} >25 μM; see **Table 6.5**). The α-ketotetrazoles **2.43** and **2.55** are selective inhibitors of papain (IC_{50} = 6.0 μM and 20 μM respectively); inhibition of calpain and cathepsin B was not observed at inhibitor concentrations of 50 μM. The α-hydroxytetrazole moiety appears to be a better fit within the active site of cathepsin B than the α-ketotetrazole moiety, as evidenced by the α-hydroxytetrazole **2.53** (IC_{50} = 2.1 μM) being 24-fold more potent than the α-ketotetrazole **2.43** (IC_{50} = >50 μM); and α-hydroxytetrazole **2.54** (IC_{50} = 1.3 μM) 38-fold more potent than α-ketotetrazole **2.55** (IC_{50} = >50 μM). A suggestion for this difference in activity is that the α-hydroxytetrazoles might be stabilised by the oxyanion hole of cathepsin B; however, further molecular modelling studies are required to confirm this.

The α-ketotetrazole **2.43** (IC_{50} = 6.0 μM) is 8-fold more potent against papain than the corresponding α-hydroxytetrazole **2.53** (IC_{50} = 50 μM); while the α-ketotetrazole **2.55** (IC_{50} = 20 μM) has similar potency to its corresponding α-hydroxytetrazole **2.54** (IC_{50} = 25 μM). These results suggest that the carbonyl oxygen of the α-ketotetrazole moiety is better positioned than the alcohol of the α-hydroxytetrazole for hydrogen bonding to the active site cleft. The *N*-protecting group again plays an important role in binding of the inhibitor to the active site, with the 4-fluorobenzenesulfonyl *N*-protected α-ketotetrazole **2.43** being 4-fold more potent than the corresponding benzyloxycarbonyl *N*-protected **2.53**.

There are few literature examples of potent cysteine protease inhibitors containing α-ketotetrazole warheads. Tao ***et al***[23] designed and evaluated a series of peptidyl α-ketoheterocycles for the inhibition of μ-calpain that included the α-ketotetrazole **6.6** (see **Figure 6.9**); subsequent assay against μ-calpain showed it to be a weak inhibitor only (11% inhibition at a concentration of 10 μM). The activity of α-ketotetrazole **6.6** was not reported against any other cysteine proteases, nor was its α-hydroxytetrazole precursor tested as a potential cysteine protease inhibitor. The analogous α-ketotetrazole **2.55** (see **Table 6.5**), which differs only in the P_2 residue (Val rather than Leu as in **6.6**) shows a similar potency against μ-calpain (IC_{50} > 50 μM). Thus the α-ketotetrazole moiety does not appear to inhibit calpains; α-hydroxytetrazoles could be used as the warhead for selective cathepsin B inhibitors and α-ketotetrazoles the warhead for papain selective inhibitors.

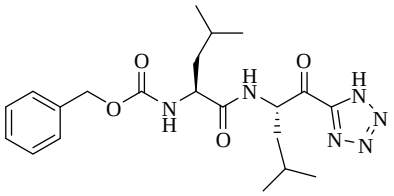

6.6

Figure 6.9 The α-ketotetrazole **6.6** designed for the inhibition of μ-calpain

Compound		IC_{50} (μM) m-calpain	μ-calpain	cathepsin B	papain
2.53	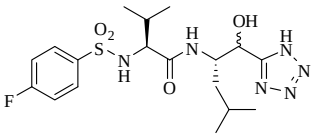	37	>50	2.1	50
2.43	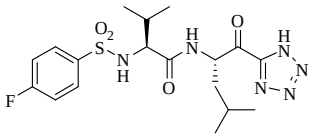	>50	>50	>50	6.0
2.54	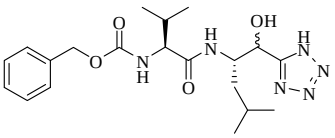	50	>50	1.3	25
2.55	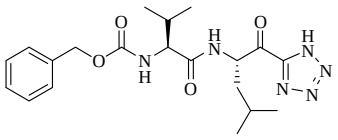	>50	>50	>50	20
2.56	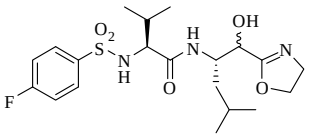	27	>50	26	11
2.42	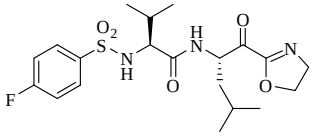	1.2	3.2	0.20	1.2
2.57	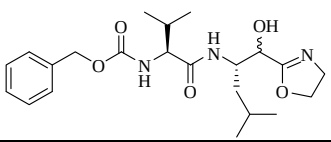	21	>50	40	14

Compound		IC_{50} (μM)			
		m-calpain	μ-calpain	cathepsin B	papain
2.58	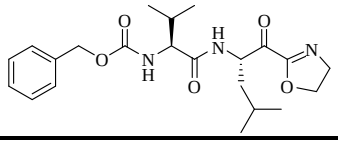	26	>50	29	37

Table 6.5 Inhibition constants for α-hydroxy and α-ketoheterocycles

The α-hydroxyoxazolines **2.56** and **2.57** are broad spectrum cysteine protease inhibitors (IC_{50} = 27 μM, 21 μM (m-calpain); 50 μM; 50 μM (μ-calpain); 26 μM, 40 μM (cathepsin B) and 11 μM, 14 μM (papain) respectively) (see **Table 6.5**). The α-ketooxazoline **2.58** {IC_{50} = 26 μM (m-calpain); >50 μM (μ-calpain); 29 μM (cathepsin B) and 37 μM (papain)} is similarly potent to its corresponding α-hydroxyoxazoline **2.57**. The α-ketooxazoline **2.42** {IC_{50} = 1.2 μM (m-calpain), 3.2 μM (μ-calpain), 0.20 μM (cathepsin B) and 1.2 μM (papain)}, however, is at least 12-fold more potent than its corresponding α-hydroxyoxazoline **2.56** across all cysteine proteases tested (see **Table 6.5**). The *N*-protecting group again plays a pivotal role in the potency of the inhibitors as the 4-fluorobenzenesulfonyl *N*-protected α-ketooxazoline **2.42** is at least 15-fold more potent than the corresponding benzyloxycarbonyl *N*-protected α-ketooxazoline **2.58**. The 4-fluorobenzenesulfonyl *N*-protecting group in conjunction with the α-ketooxazoline warhead thus provide the basis of potent and selective cathepsin B inhibition.

The most potent cathepsin B inhibitor within the heterocyclic series is the α-ketooxazoline **2.42** (IC_{50} = 0.20 μM), showing at least 6-fold selectivity for cathepsin B over the other cysteine proteases tested.

6.2.5 Nitrogen-Containing Warheads

The cyanohydrins **2.51** and **2.52** are potent broad spectrum cysteine protease inhibitors {IC_{50} = 0.34 μM, 0.34 μM (m-calpain); 0.55 μM, 1.2 μM (μ-calpain); 0.086 μM, 0.14 μM (cathepsin B) and 0.030 μM and 1.6 μM (papain)} (see **Table 6.6**). Comparison of the cyanohydrins **2.51** and **2.52** with the corresponding parent aldehydes (**2.3** and **2.19**

respectively, refer to **Table 6.1**) shows that the cyanohydrins are approximately 3-fold less potent (over all enzymes assayed) than the aldehydes **2.3** and **2.19**.

Compound		IC_{50} (μM)			
		m-calpain	μ-calpain	cathepsin B	papain
2.51	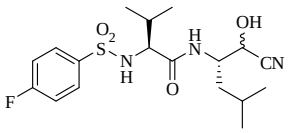	0.34	0.55	0.086	0.030
2.52	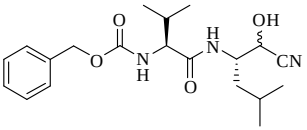	0.34	1.2	0.14	1.6
2.60	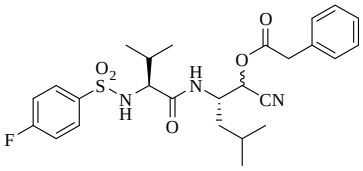	7.5	22	0.35	>50
2.61	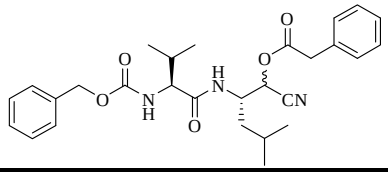	25	50	2.4	>50

Table 6.6 Inhibition constants of the nitriles synthesised against a range of proteases.

The *O*-protected cyanohydrins **2.60** and **2.61** are at least 2.5-fold less active than the corresponding free cyanohydrins **2.51** and **2.52**; however, the presence of a large aryl group capable of extending into the P' subsites appears to be favourable for binding to cathepsin B. This was evidenced by the assay results of the *O*-protected cyanohydrins **2.60** and **2.61**, which are potent cathepsin B inhibitors (IC_{50} = 0.35 μM and 2.5 μM respectively) that show more than 10-fold selectivity for cathepsin B over the other cysteine proteases tested. Selectivity observed for cathepsin B is presumably due its wider active site cleft in comparison to that of calpain and papain (see **Chapter One** for diagrams) and possible stabilisation of the thioimidate-like intermediate through interactions with the oxyanion hole of cathepsin B.

The cyanohydrin moiety appears to be an unprecedented warhead for the inhibition of cysteine proteases, as a literature search reveals few examples of cysteine protease

inhibitors containing nitrogen based warheads. Closely related peptidyl nitriles such as **6.7** (see **Figure 6.10**) are potent cathepsin B inhibitors (IC_{50} = 0.0018 μM);[16] although a comprehensive study of the specificity of peptidyl nitriles against proteases of the papain superfamily does not appear to have been performed to date.

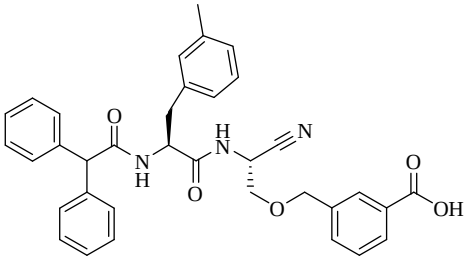

6.7
IC_{50} = 0.0018 μM (cat B)

Figure 6.10 The peptidyl nitrile **6.7**, a potent cathepsin B inhibitor

6.2.6 Azide Inhibitor

The azide **2.62** (see **Table 6.7**) is a weak cysteine protease inhibitor {IC_{50} >50 μM (m-calpain); >50 μM (μ-calpain); 22 μM (cathepsin B) and 25 μM (papain)}. The azide moiety is a non-covalent warhead which relies on hydrophobic interactions and hydrogen bonds between the inhibitor and the target protease to block the active site from the binding of substrate.[5]

	Compound	IC_{50} (μM)			
		m-calpain	**μ-calpain**	**cathepsin B**	**papain**
2.62	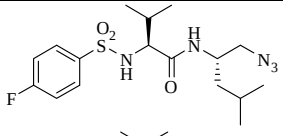	>50	>50	22	25
2.6	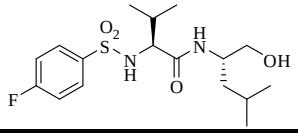	>50	>50	9.2	>50

Table 6.7 Potency of an azide against cysteine proteases

The alcohol **2.6** is a direct analogue of the azide **2.62**, the two inhibitors differing only at the 'warhead' position (an alcohol and azide group respectively, see **Table 6.7**). Both the

azide **2.62** and the alcohol **2.6** are weak inhibitors of m-calpain, μ-calpain and papain (IC_{50} >50 μM); however, the alcohol **2.6** (IC_{50} = 9.2 μM) is 4-fold more potent against cathepsin B than the azide **2.62**. Docking of the alcohol **2.6** and the azide **2.62** into the rigid μ-calpain model suggests that both inhibitors adopt an extended β-strand (see **Figure 6.11**); however, the alcohol **2.6** is suggested to from an additional hydrogen bond between the alcohol oxygen group and Gly_{271}; for the azide **2.61** this is a mismatched hydrogen bond and so is not observed. Thus the increased inhibition of alcohol **2.6** in comparison with azide **2.62** against cathepsin B may be due to an additional hydrogen bond that affords greater stability of the alcohol **2.6** within the protease active site.

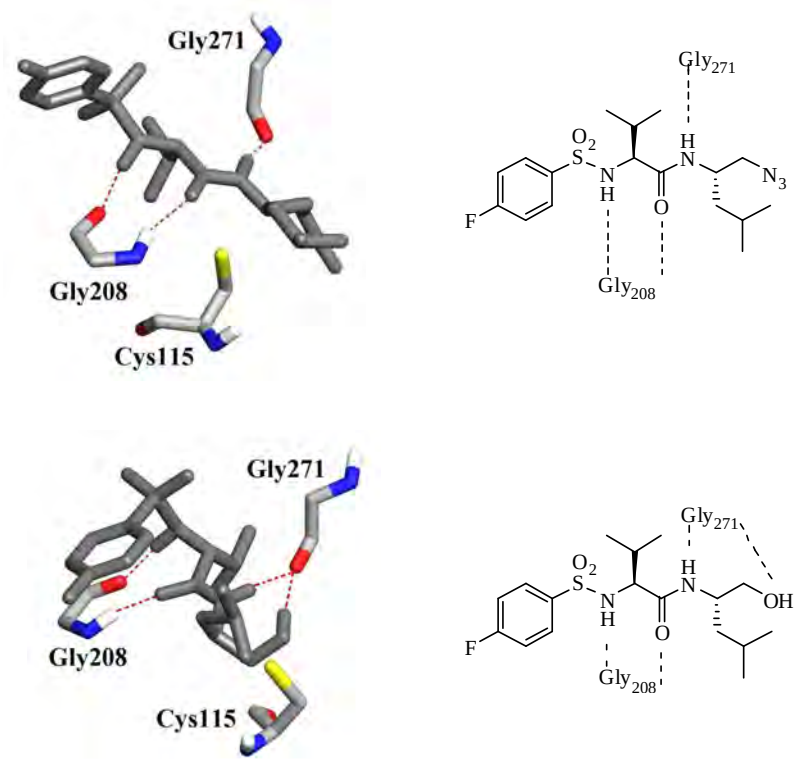

Figure 6.11 Molecular modelling suggests the hydrogen bonds shown between the μ-calpain active site residues and azide **2.62** (top); between the μ-calpain active site residues and alcohol **2.6** (bottom)

6.3 IRREVERSIBLE CYSTEINE PROTEASE INHIBITORS: ASSAY RESULTS AND DISCUSSION

6.3.1 α,β-Unsaturated Carbonyl Inhibitors

The α,β-unsaturated carbonyls **3.14-3.17** are weak inhibitors of m-calpain and μ-calpain (IC_{50} values greater than 47 μM; see **Table 6.8**); but are more potent against cathepsin B and papain {IC_{50} = 20 μM, 27 μM, 21 μM and 24 μM (cathepsin B) and 14 μM, 37 μM, 18 μM and >50 μM (papain), respectively}.

Michael acceptor warheads are characterised by a double bond that is activated by an electrophilic substituent. The double bond of both **3.14** and **3.16** appears to be activated to a greater degree by the methyl ester substituent than that of **3.15** and **3.17** which are substituted with an ethyl ester group. This is reflected by the α,β-unsaturated methyl esters **3.14** (IC_{50} = 14 μM) and **3.16** (IC_{50} = 18 μM) being approximately 3-fold more potent than the corresponding α,β-unsaturated ethyl esters **3.15** (IC_{50} = 37 μM) and **3.17** (IC_{50} >50 μM). The nature of the *N*-protecting group does not appear to be as important for binding affinity as it is for the alcohol and α-ketooxazoline series previously discussed (see **Section 6.2** for details) as the 4-fluorobenzenesulfonyl *N*-protected **3.14** and **3.15** have a similar potency to that of the benzyloxycarbonyl *N*-protected **3.16** and **3.17** against the cysteine proteases tested.

The most potent inhibitor within this series is the α,β-unsaturated aldehyde **3.18** {IC_{50} = 2.0 μM (m-calpain); 2.1 μM (μ-calpain), 0.13 μM (cathepsin B) and 1.6 μM (papain)}; which is at least 9-fold more potent than the α,β-unsaturated carbonyls **3.14-3.17** across all the cysteine proteases tested. α,β-Unsaturated aldehyde **3.18** has a 12-fold selectivity for cathepsin B over the other cysteine proteases tested.

	Compound	IC_{50} (μM) m-calpain	μ-calpain	cathepsin B	papain
3.14	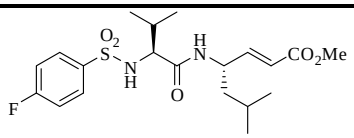	>50	>50	20	14
3.15	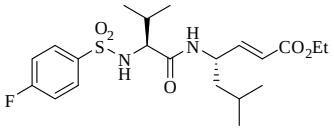	>50	>50	27	37
3.16	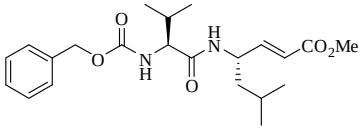	47	>50	21	18
3.17	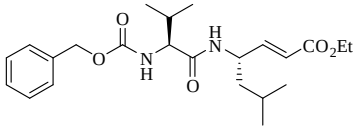	>50	>50	24	>50
3.18	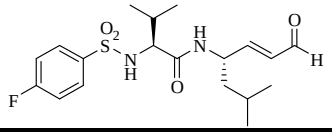	2.0	2.1	0.13	1.6

Table 6.8 Inhibition constants for α,β-unsaturated carbonyls

The two most potent inhibitors within this series (**3.18** and **3.14**) were docked into the rigid μ-calpain model and the best poses shown in **Figure 6.11**. The molecular modelling suggests that both the α,β-unsaturated aldehyde **3.18** and α,β-unsaturated ester **3.14** adopt a β-strand conformation, and have an additional hydrogen bond between the dienyl carbonyl oxygen group and His_{272} (see **Figure 6.12**). Thus, the increased potency of α,β-unsaturated aldehyde **3.18**, in comparison with the α,β-unsaturated carbonyls **3.14-3.17**, is attributed to the reactive aldehyde moiety present in **3.18**.

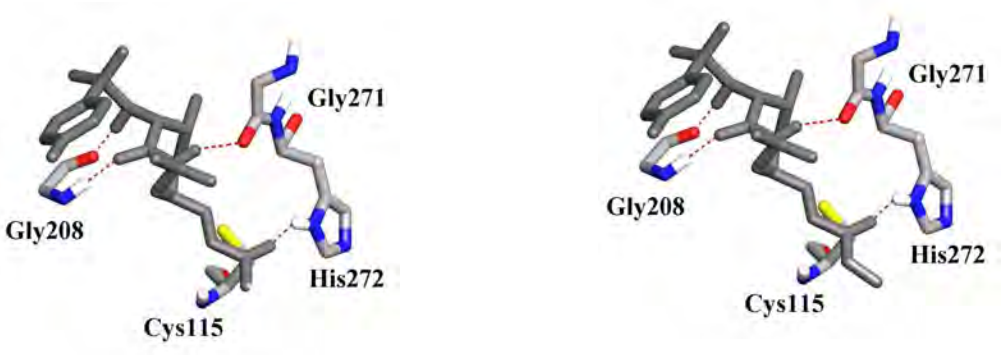

a) **b)**

Figure 6.12 Molecular modelling results of a) α,β-unsaturated aldehyde **3.18** and b) α,β-unsaturated ester **3.14** showing the same proposed hydrogen bonding pattern

The α,β-unsaturated aldehyde **3.18** {IC_{50} = 2.0 μM (m-calpain); 2.1 μM (μ-calpain), 0.13 μM (cathepsin B) and 1.6 μM (papain)}is less potent than its parent aldehyde **2.3** {IC_{50} = 0.080 μM (m-calpain); 0.13 μM (μ-calpain); 0.022 μM (cathepsin B) and 0.023 μM (papain)}. The reduced potency of the α,β-unsaturated aldehyde **3.18** in comparison with the aldehyde **2.3** is attributable to the reduced electrophilic nature of the double bond carbon of **3.18** (compared to the carbonyl carbon of **2.3**). The double bond carbon of the α,β-unsaturated aldehyde **3.18** forms an irreversible covalent bond to the active site cysteine thiol, and is activated for this reaction by the presence of the electrophilic aldehyde moiety. In comparison, it is the aldehyde moiety of aldehyde **2.3** that directly reacts with the active site cysteine thiol to give a thiohemicacetal species.

The α,β-unsaturated aldehyde **3.18** is a potent and specific inhibitor of cathepsin B (IC_{50} = 0.13 μM, selectivity 12-fold).

6.3.2 Vinyl Sulfone Inhibitors

The vinyl sulfones **3.20**-**3.23** are more potent (by 2-fold) against cathepsin B (IC_{50} = 1.9 μM, 5.9 μM, 21 μM and 27 μM respectively) than m-calpain (IC_{50} = 25 μM, >50 μM, >50 μM and >50 μM respectively), μ-calpain (IC_{50} = 22 μM, >50 μM, >50 μM and >50 μM respectively) and papain (IC_{50} = 30 μM, 21 μM, >50 μM and >50 μM respectively; see **Table 6.9**). The vinyl sulfones **3.20** and **3.21** are at least 5-fold more potent against cathepsin B than vinyl sulfones **3.22** and **3.23**, suggesting that the 4-fluorobenezenesulfonyl *N*-protecting group is favoured over the benzyloxycarbonyl (see **Sections 6.2** and **6.3.1** for more examples that show the same trend).

Vinyl sulfone **3.20** (IC_{50} = 1.9 μM, selectivity 11-fold) is the most potent cathepsin B within this series.

Leu appears to be favoured over Phe in the S_1 pocket of cathepsin B. This is supported by the Val-Leu vinyl sulfones **3.20** and **3.22** being 1.5-fold and 3-fold more potent than the corresponding Val-Phe vinyl sulfones **3.21** and **3.23** respectively and is the reverse of that observed within the alcohol series (see **Section 6.2.1**) where Val-Phe alcohol **2.26** (IC_{50} =

0.075 μM) was 120-fold more favourable for cathepsin B than the Val-Leu alcohol **2.6** (IC_{50} = 9.2 μM). These results suggest that potent non-covalent inhibition of cathepsin B requires the hydrophobic interactions and hydrogen bonds between the P_2 and P_1 residues and the S_2 and S_1 pockets to be optimised. Potent covalent inhibition of cathepsin B (whether reversible or irreversible), however, is more dependent on the warhead being in close enough proximity to react with the active site cysteine thiol; although the amino acid residues must still be those favourable for binding affinity to cathepsin B

	Compound	IC_{50} (μM) m-calpain	μ-calpain	cathepsin B	papain
3.20	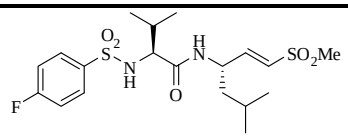	25	22	1.9	30
3.21	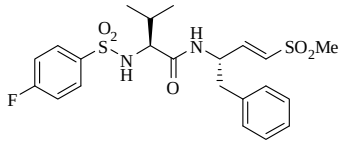	>50	>50	5.9	21
3.22	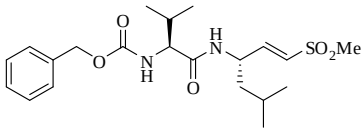	>50	>50	21	>50
3.23	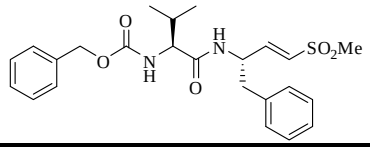	>50	>50	27	>50

Table 6.9 Inhibition constants for vinyl sulfones synthesised; comparison to parent aldehydes.

The vinyl sulfones **3.20** and **3.21** (with IC_{50} = 1.9 μM and 21 μM against cathepsin B respectively, see **Table 6.9**) are more potent than the α,β-unsaturated carbonyls **3.14-3.17** (IC_{50} >20 μM against cathepsin B, see **Table 6.8**). This increased potency is attributable to a sulfone being more electrophilic than an ester; thus a sulfone group will activate the double bond carbon for the formation of a covalent bond with the active site cysteine thiol to a greater degree than an ester group.

Vinyl sulfone warheads have previously been incorporated into cysteine protease inhibitors. Gotz[24] and co-workers synthesised a range of allyl and vinyl sulfones **6.8a-c** (see **Table 6.10**) and assayed these against μ-calpain, papain and cathepsin B. The allyl sulfone **6.8b** was over 5-fold more potent than the corresponding vinyl sulfone **6.8c**.

Interestingly, inhibition of cathepsin B was not observed in Gotz's study.[24] By comparison the vinyl sulfone inhibitors **3.20**-**3.23** synthesised in this thesis are selective cathepsin B inhibitors, suggesting that the nature of the P_1' substituent of the sulfone moiety (for **3.20**-**3.23** this is a methyl group; for **6.8a-c** it was a phenyl group) can affect the selectivity of the inhibitor.

Compound		K_i ($M^{-1}s^{-1}$) μ-calpain	papain	cathepsin B
6.8a	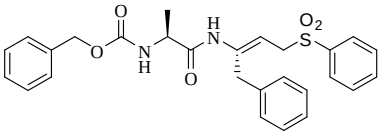	3	9	-
6.8b	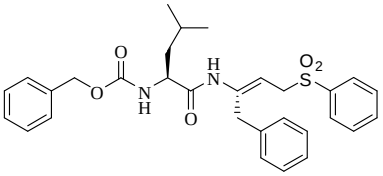	23	49	-
6.8c	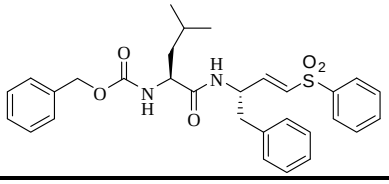	550	10	-

Table 6.10 Allyl and vinyl sulfones reported to inhibit cysteine proteases[24]

6.3.3 Diazoketone Inhibitors

Diazoketones **3.25** and **3.26** (see **Table 6.11**) are potent inhibitors of cathepsin B (with IC_{50} = 1.1 μM and 0.23 μM respectively); but are less potent against m-calpain (IC_{50} = >50 μM and 11 μM); μ-calpain (IC_{50} >50 μM and 21 μM); and papain (IC_{50} = 28 μM and 13 μM).

	Compound	IC_{50} (μM) m-calpain	μ-calpain	cathepsin B	papain
3.25	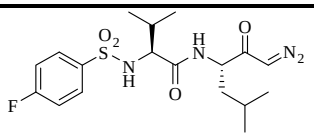	>50	>50	1.1	28
3.26	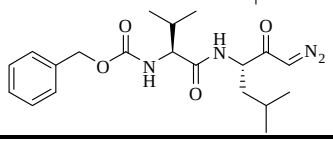	11	21	0.23	13

Table 6.11 Inhibition constants of the diazoketones **3.11** and **3.12**

The benzyloxycarbonyl *N*-protected diazoketone **3.26** is at least 2-fold more potent than the corresponding 4-fluorobenzenesulfonyl *N*-protected diazoketone **3.25** across all of the cysteine proteases tested (see **Table 6.11**). This differs from the previous observation that the 4-fluorobenzenesulfonyl moiety is favoured over the benzyloxycarbonyl group (see previous **Sections 6.2.1-6.3.2**). Subsequent docking of the diazoketones **3.25** and **3.26** into the rigid μ-calpain model (see **Figure 6.13**) suggests that the benzyloxycarbonyl moiety is in a more extended conformation than the 4-fluorobenzenesulfonyl moiety, thus it may be a better fit within the active site of the proteases. This could account for the increased potency of the benzyloxycarbonyl protected **3.26** in comparison with **3.25**.

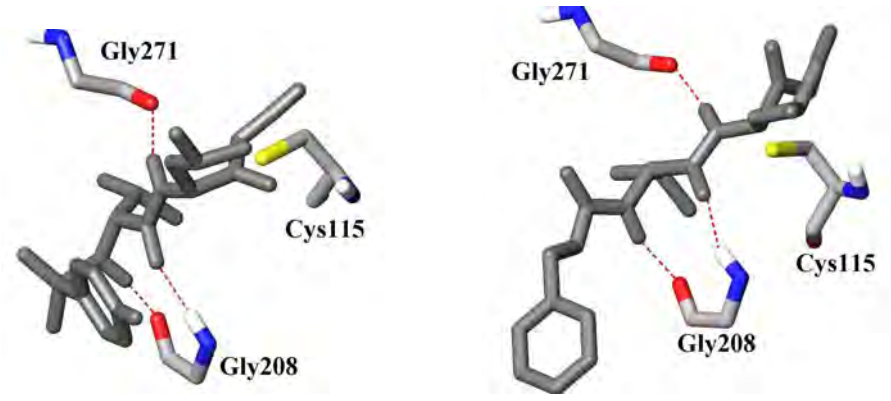

a) **b)**

Figure 6.13 Molecular modelling results of a) diazoketone **3.25** and b) diazoketone **3.26** with the suggesting hydrogen bond pattern shown.

Compounds containing diazoketone warheads are reported in the literature as potent inhibitors of papain and the cathepsins B and L;[17] however, to date this type of inhibitor has not been tested for selectivity between cysteine proteases of the papain superfamily.

The results presented in **Table 6.11** show that the diazoketones **3.25** and **3.26** are both potent and selective cathepsin B inhibitors (IC_{50} = 1.1 μM, selectivity 25-fold; and 0.23 μM, selectivity 48-fold respectively).

6.3.4 α-Bromomethyl Ketone Inhibitors and Precursors

The α-bromomethyl ketones **3.28** and **3.29** are potent cathepsin B inhibitors (IC_{50} = 0.025 μM and 0.077 μM respectively; see **Table 6.12**); but are less potent against m-calpain (IC_{50} = >50 μM and 29 μM respectively) and μ-calpain (IC_{50} = 33 μM and 36 μM respectively) papain (IC_{50} = 0.40 μM and 0.18 μM respectively). The 4-fluorobenezenesulfonyl *N*-protected **3.28** is 3-fold more potent than the benzyloxycarbonyl *N*-protected **3.29**, suggesting that the 4-fluorobenezenesulfonyl moiety has better binding affinity to the active site cleft than the benzyloxycarbonyl (see **Section 6.2** for further examples).

The enantiomerically pure[‡] α-bromomethyl 3*R*-alcohols[§] **3.30** and **3.31** inhibit the cysteine proteases tested as follows: IC_{50} = 30 μM and >50 μM (m-calpain); 23 μM and >50 μM (μ-calpain); 9.9 μM and 9.8 μM (cathepsin B); and 15 μM and 50 μM (papain) respectively (see **Table 6.12**). The diastereomeric α-bromomethyl 3-*S/R*-alcohols **3.32** and **3.33** inhibit the cysteine proteases tested as follows: IC_{50} = 31 μM and >50 μM (m-calpain); 27 μM and 27 μM (μ-calpain); 0.76 μM and 0.39 μM (cathepsin B); and 7.1 μM and 1.2 μM (papain) respectively (see **Table 6.12**).

The α-bromomethyl ketones **3.28** and **3.29** are over 30-fold more potent than the α-bromomethyl alcohols **3.30-3.33**. This is attributed to the carbonyl carbon of the ketone being more electrophilic than the β-carbon of the alcohol, thus the formation of a covalent bond with the cysteinyl thiol is more likely to occur.

[‡] A discussion of the absolute configuration of the α-bromomethyl alcohols **3.30-3.33** can be found in **Chapter Three**

[§] Where 3*R* denotes the third carbon stereocentre, counting in the P_3 to $P_{1'}$ direction

Compound		IC_{50} (μM) m-calpain	μ-calpain	cathepsin B	papain
3.28	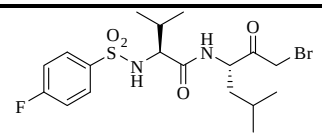	>50	33	0.025	0.40
3.30	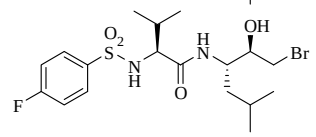	30	23	9.9	15
3.32	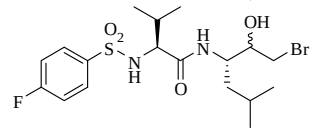	31	27	0.76	7.1
3.29	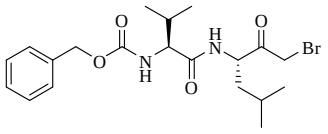	29	36	0.077	0.18
3.31	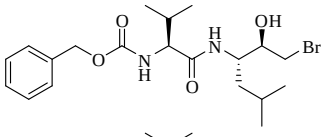	>50	>50	9.8	>50
3.33	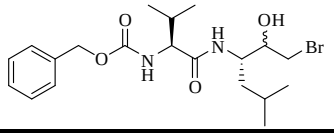	>50	27	0.39	1.2

Table 6.12 Assay results for α-bromomethyl ketones and alcohols

The absolute configuration of the alcohol group at C3 is important for binding affinity to cysteine proteases; this is evidenced by the diastereomeric 3-*R/S*-alcohols **3.32** and **3.33** (IC_{50} = 0.76 and 0.39 μM respectively) being 13-fold and 25-fold more potent than the enantiomerically pure 3*R*-alcohols **3.30** and **3.31** (IC_{50} = 9.9 and 9.8 μM respectively). Separate docking of the two diastereoisomers (1S,2S,3R and 1S,2S,3S) of α-bromomethyl alcohol **3.32** (see **Figure 6.14**) into the rigid μ-calpain model suggests that the 3*S*-alcohol forms only two of the three hydrogen bonds required for a β-sheet conformation (hydrogen bonds A and B), plus another hydrogen bond between the 3*S*-alcohol oxygen group and Cys_{115}. The 3*R*-alcohol is suggested to adopt a β-sheet conformation and also form additional hydrogen bonds between the sulfonamide oxygen group and Ser_{251} and the 3*R*-alcohol oxygen group and Gly_{113}. The assay results (see **Table 6.12**) and the predicted hydrogen bonding pattern suggest that the 3*S*-alcohol would be more potent against cathepsin B than the 3*R*-alcohol and further supports the hypothesis that cysteine proteases bind substrates in an extended β-strand conformation.

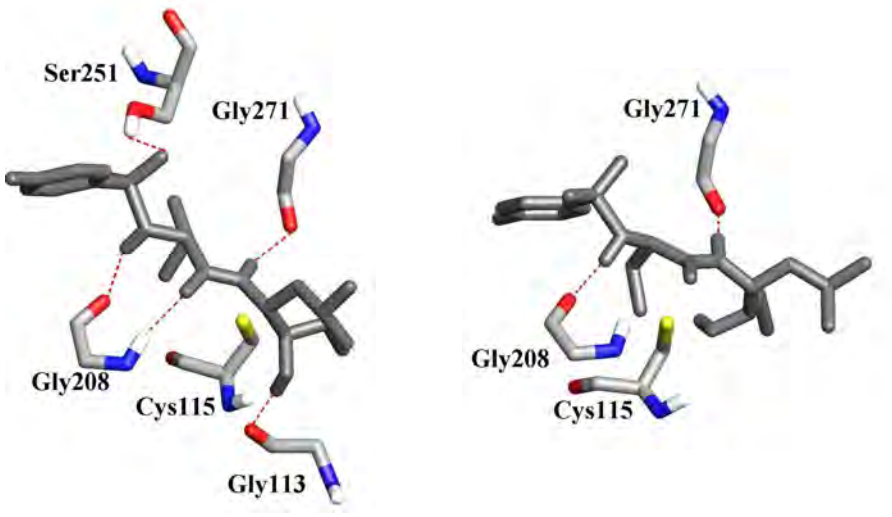

a) **b)**

Figure 6.14 Comparison of the purported hydrogen bond pattern between a) α-bromomethyl C_3-*R*-alcohol **3.32** and b) α-bromomethyl C_3-*S*-alcohol **3.32**

6.3.5 Epoxide Inhibitors

The epoxides **3.27**, **3.34-3.36** are significantly more potent against cathepsin B (IC_{50} = 12 µM, 0.49 µM, 19 µM and 5.7 µM respectively) compared to m-calpain, µ-calpain and papain (all IC_{50} values >50 µM; see **Table 6.13**). The 3*R*-epoxides[**] **3.27** and **3.34** (IC_{50} = 12 µM and 0.49 µM) are 1.5-fold and 11-fold more potent than the corresponding diastereomeric 3-*R/S*-epoxides **3.35** and **3.36** (IC_{50} = 19 µM and 5.7 µM respectively).

Like the α-bromomethyl alcohol series (see **Section 6.3.4**), where the absolute configuration of the 3C-alcohol was important for binding affinity, the absolute configuration of the 3C-epoxide is also important for binding affinity. The 3*R*-epoxides **3.27** and **3.34** (IC_{50} = 12 µM and 0.49 µM respectively) are 2-fold and 116-fold more potent than the corresponding diastereomeric 3-*S*/*R*-mixed epoxides **3.35** and **3.36** (IC_{50} = 19 µM and 5.7 µM respectively). Molecular modelling suggests this difference in potency is attributable to the 3*S*-epoxide adopting the β-strand conformation required for binding to

[**] The absolute configuration of the peptidyl epoxides **3.33-3.36** is based on that of the α-bromomethyl alcohol used in its preparation. A discussion of this can be found in **Chapter Three**

cysteine proteases; while the 3*R*-epoxide only forms hydrogen bonds A and C of the three (A, B and C) hydrogen bonds that define a β-strand conformation (refer back to **Chapter Three**, **Section 3.3.2**).

The epoxides **3.34** and **3.36** are more potent (by 25-fold and 3-fold respectively) against cathepsin B than the corresponding epoxides **3.27** and **3.35**, suggesting that the benzyloxycarbonyl *N*-protecting group is a better fit within the active site cleft of cathepsin B than the 4-fluorobenzenesulfonyl moiety (this agrees with the results observed earlier for the diazoketones **3.25** and **3.26**; see **Section 6.3.3**).

	Compound	IC_{50} (μM)			
		m-calpain	μ-calpain	cathepsin B	papain
3.27	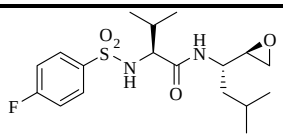	>50	>50	12	>50
3.34	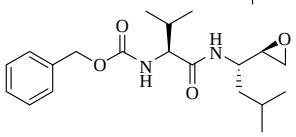	>50	>50	0.49	>50
3.35	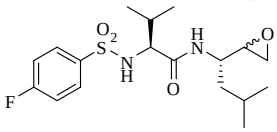	50	>50	19	>50
3.36	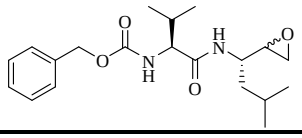	>50	>50	5.7	>50

Table 6.13 Assay results for the amino epoxides **3.27**, **3.34-3.36**

6.4 β-STRAND CONSTRAINED INHIBITORS: ASSAY RESULTS AND DISCUSSION

Proteases (including cysteine, serine, aspartic and metallo proteases) are known to recognise and bind substrates in an extended β-strand conformation, with over 99% of known substrates and inhibitors binding in such a manner[25] (see **Chapter Four** for more details).

Acyclic peptidyl inhibitors, while being able to adopt a β-strand conformation, are conformationally flexible and exist as random conformations in aqueous solution.[26] Inhibitors that are in a fixed β-strand conformation are thought to have increased binding affinity to protease active sites in comparison to flexible inhibitors.[27] One method of fixing or constraining protease inhibitors into a β-strand conformation is by restricting flexibility through cyclisation of the peptidyl backbone of the inhibitor. Macrocyclic protease inhibitors[††] are thus of increasing interest due to having a rigid β-strand conformation and showing increased resistance to degradation over acyclic protease inhibitors (see **Chapter Four** for an example).

Macrocycles have been described[28] as "excellent mimics of the β-strand required for binding to aspartic, serine and metallo proteases… but have yet to be described for cysteine proteases." A literature search confirms that macrocyclic inhibitors have been designed for the inhibition of serine and aspartic acid proteases (particularly the Hepatitis C Virus (HCV)[29] and Human Immunodeficiency Virus (HIV-1) protease[30]; see **Figure 6.15** for representative inhibitors) but no examples of macrocyclic compounds for the inhibition of cysteine proteases were found.

[††] Where the term macrocycle refers to a ring size of 7 atoms or larger; generally macrocycles are synthesised utilizing ring-closing metathesis (see **Chapter Four**)

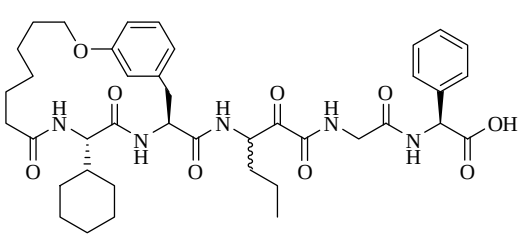

6.9
K_i = 0.16 mM (HCV NS3)

a)

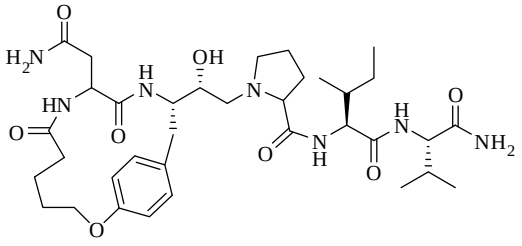

6.10
K_i = 0.008 mM (HIV-1)

b)

Figure 6.15 Two β-strand constrained inhibitors: a) macrocycle **6.9** a potent inhibitor of HCV and b) macrocycle **6.10**, a potent inhibitor of HIV-1 protease

The macrocyclic inhibitors: alcohol **4.3**, aldehyde **4.4**, methyl ester **4.13**, aldehyde **4.14**, semicarbazone **4.15**, cyanohydrin **4.16** and azide **4.19** (see **Figure 6.15**) all of which adopt a β-strand conformation,[‡‡] are unprecedented examples of cysteine protease inhibitors.

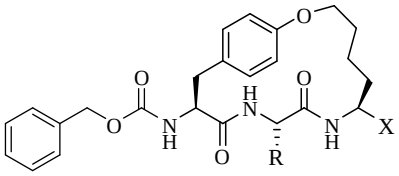

4.3 R = Val, X = CH_2OH
4.4 R = Val, X = CHO
4.13 R = Val, X = CO_2Me
4.14 R = Leu, X = CHO
4.15 R = Leu, X = $CH{=}NNHC(O)NH_2$
4.16 R = Leu, X = CH(OH)CN
4.19 R = Leu, X = CH_2N_3

Figure 6.15 The macrocyclic inhibitors synthesised in this thesis are unprecedented cysteine protease inhibitors

6.4.1 Macrocyclic Aldehydes and Precursors

The macrocyclic ester **4.13**, alcohol **4.3** and aldehydes **4.4** and **4.14** were assayed for activity against m-calpain, μ-calpain, cathepsin B and papain in order to determine the effect of the macrocyclic constraint on cysteine protease inhibition. The macrocyclic inhibitors **4.13**, **4.3**, **4.4** and **4.14** are also compared with the closely related acyclic

[‡‡] For a discussion of how a β-strand conformation is determined see **Chapter Four**

analogues **2.45**, **2.29** and **2.19** to determine relationships between potency and selectivity of the macrocyclic and acyclic series.

The macrocyclic aldehydes **4.4** and **4.14** are broad spectrum cysteine protease inhibitors {IC_{50} = 0.24 μM and 0.03 μM (m-calpain); 2.7 μM and 0.22 μM (μ-calpain); 0.23 μM and 0.070 μM (cathepsin B) and 0.61 μM and >50 μM (papain)}. This lack of specificity is similar to that observed for the acyclic aldehydes **2.3**, **2.27**, **2.19**, **2.2**, **2.21** and **2.22** (see **Section 6.2.1**). The similar potency of the macrocyclic and acyclic aldehydes suggests that the presence of a highly reactive warhead (such as an aldehyde) is the determining factor of potency rather than the conformation of the inhibitor backbone.

The P_2-Leu macrocyclic aldehyde **4.14** is at least 3-fold more potent than the P_2-Val containing aldehyde **4.4** against m-calpain, μ-calpain and cathepsin B which suggests that Leu is favoured over Val in the S_2 pocket for these three cysteine proteases. Iqbal[31] reported that μ-calpain possesses a strict requirement for Leu in the S_2 pocket; this is supported by the macrocyclic aldehyde **4.14** (IC_{50} = 0.22 μM) being 12-fold more potent than macrocyclic aldehyde **4.4** (IC_{50} = 2.7 μM) against μ-calpain.

Compound		IC_{50} (μM) m-calpain	μ-calpain	cathepsin B	Papain
4.13	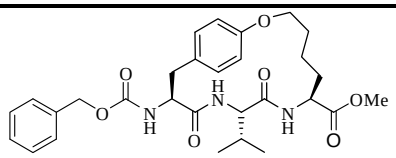	>50	>50	16	>50
4.3	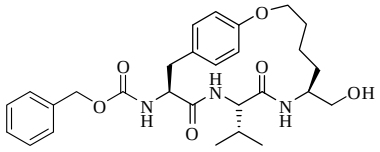	1.6	5.2	19	28
4.4	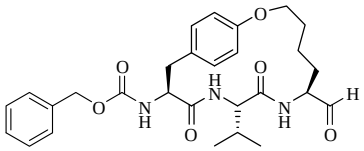	0.24	2.7	0.23	0.61
4.14	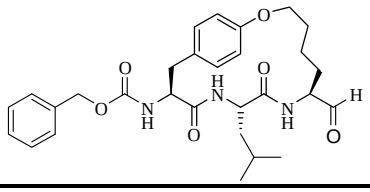	0.03	0.22	0.070	>50

Table 6.14 Assay results of a macrocyclic alcohol and aldehyde.

Comparison of the acyclic and macrocyclic methyl esters (**2.45** and **4.13**) and alcohols (**2.6** and **4.3**) (see following discussion) provides more insight into the effect of β-strand constraint as the methyl ester is less reactive than the aldehyde warhead and the alcohol is a non-covalent 'warhead'; therefore hydrophobic interactions and hydrogen bonds between the active site cleft and the inhibitor backbone become the important determining factors of binding affinity to the protease and thus potency of the inhibitor (see **Section 6.3.2** for more evidence).

The macrocyclic ester **4.13** is more potent (by 3-fold) against cathepsin B (IC_{50} = 16 μM) than against m-calpain (IC_{50} = >50 μM); μ-calpain (IC_{50} >50 μM) and papain (IC_{50} >50 μM). These results are similar to those observed for the acyclic ester **2.45**, which is also a selective inhibitor of cathepsin B (IC_{50} = 19 μM, selectivity 3-fold; see **Table 6.3**). The 1.2-fold increase in potency of the macrocyclic ester **4.13** compared to the acyclic ester **2.45** suggests that constraining the inhibitor into a β-strand conformation does improve

binding affinity to the active site of cathepsin B and this is reflected in an increased potency against cathepsin B.

The macrocyclic alcohol **4.3** {IC_{50}: 1.6 μM (m-calpain), 5.2 μM (μ-calpain), 19 μM (cathepsin B), 28 μM (papain)} is over 2-fold more potent than the acyclic alcohol **2.29** {IC_{50}: >50 μM (m-calpain), >50 μM (μ-calpain), 26 μM (cathepsin B), >50 μM (papain)} which again suggests that the conformational constraint of the macrocyclic inhibitors increases binding affinity to the cysteine proteases tested (see **Table 6.14** and **Table 6.1**).

The alcohol **4.3** and the aldehydes **4.4** and **4.14** are selective for m-calpain over μ-calpain (3-fold, 11-fold and 7-fold respectively). Selectivity between m-calpain and μ-calpain will be discussed in the following **Section 6.5**.

6.4.2 Macrocyclic Warhead Derivatives

Section 6.4.1 establishes β-strand constrained non-covalent cysteine protease inhibitors as being more potent than the acyclic analogues (this increase in potency is assumed to be due to better binding affinity within the active site of the proteases); however, the macrocyclic aldehydes **4.4** and **4.14** had potency similar to that of the acyclic aldehyde series (see above). The macrocyclic inhibitors **4.15**, **4.16** and **4.19** (see **Table 6.15**) were assayed against m-calpain, μ-calpain, cathepsin B and papain to further determine the effect β-strand constraint has on warhead potency and selectivity in comparison with acyclic analogues (see **Sections 6.2** and **6.3**). Four warheads utilised in the acyclic series (see **Chapters Two** and **Three**) were chosen as warheads for macrocyclic inhibitors: the semicarbazone, cyanohydrin, α-ketotetrazole and azide moieties; the rationale for each of these choices being the following:

Semicarbazone warhead: The acyclic semicarbazone series **2.37-2.40** are broad spectrum cysteine protease inhibitors (IC_{50} values < 4.8 μM; see **Section 6.2.2**); the semicarbazone warhead of **2.37** was chosen as it gave the highest yield of product in the acyclic series (see **Chapter Two**) and its solubility was compatible with that of the macrocycle **4.14**.

Cyanohydrin Warhead: acyclic cyanohydrins **2.60** and **2.61** are also broad spectrum cysteine protease inhibitors (IC_{50} < 1.2 μM), further the cyanohydrin is the intermediate in the formation of the α-ketotetrazole and α-ketooxazoline warheads; thus the cyanohydrin of **4.14** was synthesised.

α-Ketotetrazole Warhead: the acyclic α-ketotetrazoles **2.43** and **2.55** were selective inhibitor of papain (IC_{50} = 6.0 μM and 20 μM); the α-ketotetrazole moiety was chosen for use as a macrocyclic warhead in order to determine the effect of β-strand constraint on selectivity. The limited solubility of the macrocycle **4.14** was also considered; the reaction conditions for synthesis of α-ketooxazoline rings (see **Chapter Two**) were not compatible with the solubility of the macrocycle.

Non-covalent Azide: The azide moiety was chosen for application to a macrocycle because of the increased potency of the non-covalent macrocycles **4.13** and **4.3** in comparison with the acyclic analogues **2.45** and **2.29** (see above **Section 6.4.1**). It was thought that constraint of the backbone into a β-strand would increase the potency against cysteine proteases.

These four moieties (semicarbazone, cyanohydrin, α-ketotetrazole and azide) were utilised as warheads on the macrocycle **4.14**[§§] as it is more potent than the macrocycle **4.4** and is currently being trialled as a topical drug for the treatment of cataract.

[§§] See **Chapter Four** for further rationale behind the used of macrocycle **4.14** for the application of various warheads

Compound		IC_{50} (μM) m-calpain	μ-calpain	cathepsin B	papain
4.15	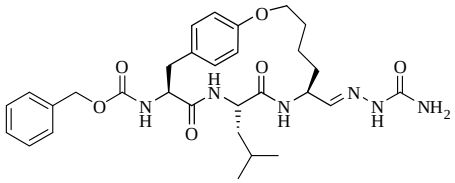	0.16	1.3	3.7	2.0
4.16	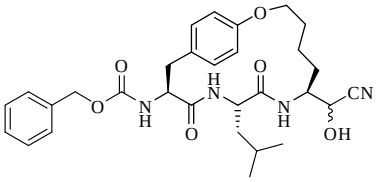	8.9	35	2.4	12
4.19	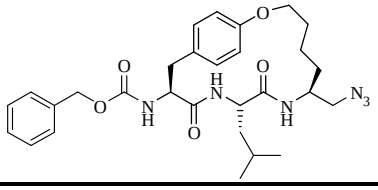	>50	>50	>50	>50

Table 6.15 Potency of macrocycles with a variety of warheads.

The macrocyclic semicarbazone **4.15** is a potent cysteine protease inhibitor {IC_{50}: 0.16 μM (m-calpain), 1.3 μM (μ-calpain), 3.7 μM (cathepsin B), 2.0 μM (papain); see **Table 6.15**}. Similarly, the acyclic semicarbazone **2.37** is also a broad spectrum cysteine protease {IC_{50}: 1.5 μM (m-calpain), 1.1 μM (μ-calpain), 0.69 μM (cathepsin B), 0.92 μM (papain)

The macrocyclic semicarbazone **4.15** is 9-fold more potent against m-calpain than its acyclic analogue **2.37**; has a similar potency against μ-calpain (IC_{50} = 1.3 μM) in comparison with the acyclic semicarbazone **2.37** (IC_{50} = 1.1 μM); and is less potent against cathepsin B and papain (by 2- to 5-fold) than the acyclic semicarbazone **2.37**. These observations suggest that m-calpain has a much more stringent requirement for a β-strand conformation than μ-calpain, cathepsin B and papain; this is attributable to the narrow active site cleft of m-calpain (in comparison with that of cathepsin B and papain; see **Chapter One**). A rigid β-strand appears to be a promising conformation for the design of inhibitors selective for m-calpain.

The macrocyclic cyanohydrin **4.16** is a more potent inhibitor of cathepsin B (IC_{50} = 2.4 μM) than of m-calpain (IC_{50} = 8.9 μM); μ-calpain (IC_{50} = 35 μM) and papain (IC_{50} = 12 μM). The acyclic cyanohydrin analogue **2.52** is more potent than the macrocyclic

cyanohydrin **4.16** {IC_{50} = 0.34 μM (m-calpain); 1.2 μM (μ-calpain); cathepsin B (IC_{50} = 0.14 μM) and 1.6 μM (papain); see **Table 6.6**}. A proposed explanation of the reduced potency of the macrocyclic cyanohydrin **4.16** in comparison to the acyclic cyanohydrin **2.52** is attributed to the increased length of the macrocyclic cyanohydrin (tripeptide backbone) in comparison with the acyclic cyanohydrin (dipeptide backbone). The insertion of an amino acid into the backbone means the alcohol group of the macrocyclic cyanohydrin may no longer be in close proximity to the oxyanion hole (see **Chapter One** for detail) of the cysteine proteases (m-calpain, μ-calpain, cathepsin B and papain), thus hydrogen bonds between the oxygen of the secondary alcohol group and the oxyanion hole cannot form; the acyclic cyanohydrin **2.51**, which is proposed to form hydrogen bonds to the oxyanion hole, is more stabilised within the active site of the proteases than the macrocyclic **4.16**.

Several failed attempts were made to synthesise the macrocyclic α-ketotetrazole **4.18** (see **Figure 6.16** and **Chapter Four**). Synthesis of the macrocyclic α-ketotetrazole **4.18** for this thesis was abandoned due to time constraints; future work will include the examination of suitable reaction conditions for the successful synthesis of this macrocyclic α-ketotetrazole.

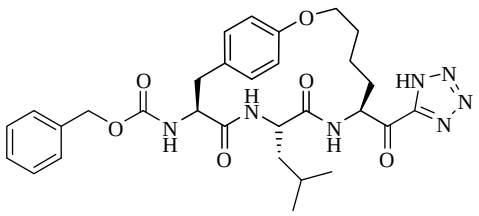

4.18

Figure 6.16 The proposed macrocyclic α-ketotetrazole **4.18**; synthesis was abandoned

Azide **4.19** is a weak cysteine protease inhibitor (IC_{50} > 50 μM for all cysteine proteases tested; see **Table 6.15**). Comparison of the macrocyclic azide **4.19** with the acyclic analogue **2.62** shows a similar trend of low potency (refer to **Table 6.7**). It was envisaged that the application of the azide moiety to the constrained β-strand conformation of the macrocycle would result in improved inhibition against cysteine proteases of the papain superfamily; however, this was not the case, as seen by the lack of inhibition against m-calpain, μ-calpain, cathepsin B and papain. A suggestion for this lack of activity is that the

orientation of the azide moiety precludes any interaction with the oxyanion hole of the proteases and is thus not stabilised within the active site cleft.

The β-strand constrained macrocycles **4.3**, **4.4**, **4.13**-**4.16** and **4.19** are unprecedented examples of cysteine protease inhibitors. The macrocyclic semicarbazone **4.15** is a potent and selective inhibitors of m-calpain (IC_{50} = 0.16 μM, selectivity 8-fold); the macrocyclic cyanohydrin **4.16** is a potent and selective inhibitor of cathepsin B (IC_{50} = 2.4 μM, selectivity 4-fold).

6.5 SELECTIVITY BETWEEN m-CALPAIN AND μ-CALPAIN

Structural features of m-calpain and μ-calpain that have been reported to date are remarkably similar. Both m-calpain and μ-calpain are polypeptides made up of a large subunit (around 80 kDa) and a small subunit (around 30 kDa); other properties include cellular distribution and the requirement of calcium for activation (see **Table 6.16** for a summary).[32] The one difference that has been clearly identified between m- and μ-calpain is the level of calcium required for activation (mM and μM respectively), but structural evidence for this difference has so far eluded researchers.[33]

Structural Feature	**m-calpain**	**μ-calpain**
Size of large subunit	80 kDa	80 kDa
Size of small subunit	30 kDa	30 kDa
Ca^{2+} level required for activation	400-800 μM	3-50 μM
Optimum pH	7.2-8.2	7.2-8.2
Occurrence	Mammals and plants	Mammals and plants
Distribution	Intracellular	Intracellular

Table 6.16 Known properties and structural features m-calpain and μ-calpain[32]

The physiological roles of m-calpain and μ-calpain appear to be identical (see **Chapter One** for a detailed discussion) and m-calpain and μ-calpain have similar subsite specificities, thus it is assumed that these two calpains have virtually identical overall structures.[34,35] This implies that the structure of the active sites of m-calpain and μ-calpain are also very similar; however, if this were the case, compounds that are designed as potent m-calpain inhibitors should show similar potency against μ-calpain (and vice versa).

Within this thesis, however, 11 inhibitors are observed to be selective[***] for m-calpain over μ-calpain (see **Table 6.17**). The potency and selectivity of these inhibitors for m-calpain are as follows: aldehyde **2.3** (IC_{50} = 0.080 μM, selectivity 2-fold); aldehyde **2.19** (IC_{50} = 0.15 μM, selectivity 3-fold); aldehyde **2.21** (IC_{50} = 0.32 μM, selectivity 2-fold); aldehyde **2.22** (IC_{50} = 0.25 μM, selectivity 4-fold); semicarbazone **2.37** (IC_{50} = 1.5 μM, selectivity 8-fold); cyanohydrin **2.51** (IC_{50} = 7.5 μM, selectivity 3-fold); diazoketone **3.26** (IC_{50} = 11 μM, selectivity 2-fold); macrocyclic alcohol **4.3** (IC_{50} = 1.6 μM, selectivity 3-fold); macrocyclic aldehyde **4.4** (IC_{50} = 0.24 μM, selectivity 11-fold); aldehyde **4.14** (IC_{50} = 0.03 μM, selectivity 7-fold) and macrocyclic semicarbazone **4.16** (IC_{50} = 1.6 μM, selectivity 8-fold). Additionally, over 90% of the inhibitors assayed have at least a 1.2-fold difference in potency against m-calpain and μ-calpain (see **Tables 6.1-6.20**).

	Compound	IC_{50} (μM) m-calpain	μ-calpain	Selectivity Ratio (m/μ)
2.3	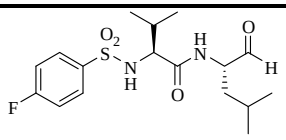	0.080	0.13	2
2.19	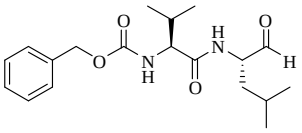	0.15	0.38	3
2.21	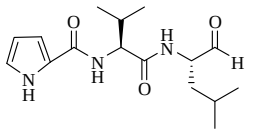	0.32	0.65	2
2.22	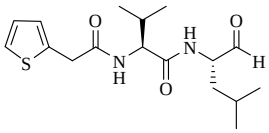	0.25	1.1	4
2.37	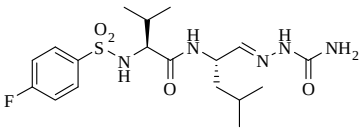	1.5	11	8

[***] Where the term selective refers to a difference in potency of at least 2-fold

Compound		IC_{50} (μM) m-calpain	μ-calpain	Selectivity Ratio (m/ μ)
2.51	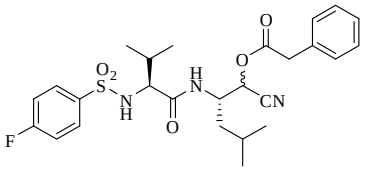	7.5	22	3
3.26	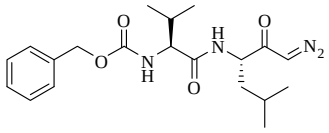	11	21	2
4.3	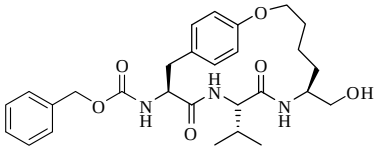	1.6	5.2	3
4.4	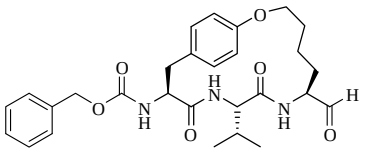	0.24	2.7	11
4.14	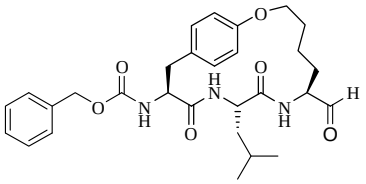	0.030	0.22	7
4.15	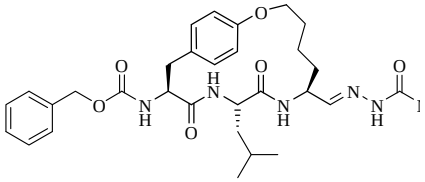	0.16	1.3	8

Table 6.17 Synthesised inhibitors that show selectivity for m-calpain over μ-calpain

Only two inhibitors, the aldehydes **2.27** and **2.2** show selectivity for μ-calpain over m-calpain (by 6-fold and 2-fold respectively) as shown in **Table 6.18** below. Both of the aldehydes **2.27** and **2.2** contain the dipeptide Val-Phe; the acyclic inhibitors that are selective for m-calpain over μ-calpain all contain the dipeptide Val-Leu (see **Table 6.17**), thus indicating that the S_1 pocket of μ-calpain may be larger and more hydrophobic than

that of m-calpain. The dipeptide Val-Phe thus provides a basis for the design of specific μ-calpain inhibitors.

	Compound	IC_{50} (μM) m-calpain	μ-calpain	Selectivity Ratio (μ/m)
2.27	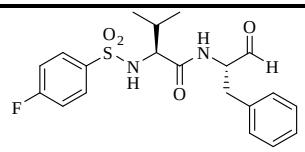	0.072	0.012	6
2.2	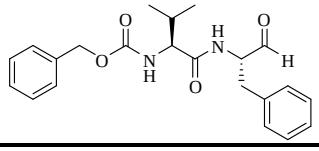	0.060	0.027	2

Table 6.18 The two synthesised inhibitors that show selectivity for μ-calpain over m-calpain

The overwhelming number of inhibitors within this thesis that show selectivity between the calpains suggest that a structural difference between the active sites of m-calpain and μ-calpain does exist; numerous journal articles also present assay data for inhibitors that are selective between m-calpain and μ-calpain, further strengthening this argument.[7,36,37] One example is that of the literature aldehyde **2.3**[7] (see **Figure 6.17**) which is reported as being 10-fold more potent against μ-calpain (IC_{50} = 0.008 μM) than m-calpain (IC_{50} = 0.080 μM). As a note: the assays utilised within thesis are based on a fluorogenic substrate (see **Chapter Five** for details); the majority of IC_{50} values reported in the literature were obtained using colorimetric assays that have been shown to be less sensitive than fluorogenic assays;[38] hence an absolute comparison of the IC_{50} values obtained herein with those found in the literature must be undertaken with caution because of the dependency of the results on the conditions used. The literature aldehyde **2.3** was thus used as a reference compound in the validation of the assay protocols (see **Chapter Five**).

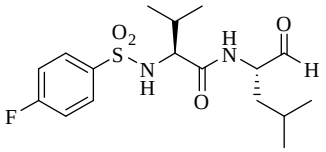

2.3

IC_{50} = 0.080 μM (m-calpain)
IC_{50} = 0.008 μM (μ-calpain)

Figure 6.17 The literature IC_{50} values of aldehyde **2.3** show a 10-fold selectivity for μ-calpain

The results presented in **Tables 6.17** and **6.18** thus suggest that a structural difference exists between the active site clefts of m-calpain and μ-calpain that can be exploited for the design of specific calpain inhibitors. Further investigation is required, however, to define the active sites of m-calpain and μ-calpain unambiguously.

6.6 SELECTIVITY FOR CATHEPSIN B

6.6.1 Selectivity Between Cathepsin B and Papain

Identifying selective inhibitors of papain proved problematic. Nine inhibitors have IC_{50} values of less than 1.0 μM against papain, these are: aldehyde **2.3** (IC_{50} = 0.023 μM); aldehyde **2.21** (IC_{50} = 0.053 μM); aldehyde **2.22** (IC_{50} = 0.040 μM); aldehyde **2.27** (IC_{50} = 0.033 μM); thiosemicarbazone **2.38** (IC_{50} = 0.19 μM); phenylhydrazine **2.39** (IC_{50} = 0.96 μM); cyanohydrin **2.51** (IC_{50} = 0.030 μM); α-bromomethyl ketone **3.27** (IC_{50} = 0.18 μM) and macrocyclic aldehyde **4.4** (IC_{50} = 0.61 μM; see **Table 6.19**); however, eight of these nine inhibitors are up to 3-fold more potent against cathepsin B than papain.

The one inhibitor that shows selectivity for papain is cyanohydrin **2.51** (IC_{50} = 0.030 μM), which is at least 3-fold more potent against papain than against cathepsin B). A suggested reason for the cyanohydrin **2.50** being selective for papain over cathepsin B is that the alcohol of the cyanohydrin moiety is positioned such that it cannot be stabilised by the oxyanion hole of cathepsin B. This is supported by the fact that the cyanohydrin is the only potent inhibitor of papain that contains an alcohol group (see **Table 6.19**).

The main structural difference between the active sites of cathepsin B and papain is the large occluding loop unique to cathepsin B that endows it with exopeptidase properties (see **Section 6.2.3** and **Chapter One** for a discussion of the occluding loop). The overall structures of papain and cathepsin B are highly conserved, and peptidyl substrates are proposed to bind in the active site of cathepsin B in a manner analogous to that of papain,[39] explaining the similar potency of many inhibitors (see **Tables 6.1-6.15**) assayed against these two proteases. However, this lack of distinction is not overly troublesome as cathepsin B is a mammalian protease while papain is exclusively found in plants.

	Compound	IC_{50} papain (μM)	Selectivity for papain
2.3	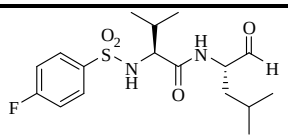	0.023	-
2.21	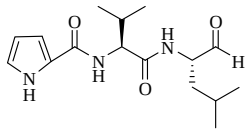	0.053	-2
2.22	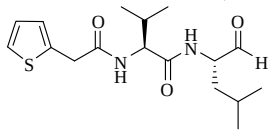	0.040	-3
2.27	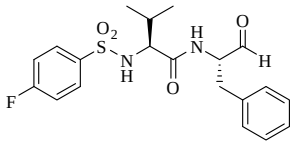	0.033	-2
2.38	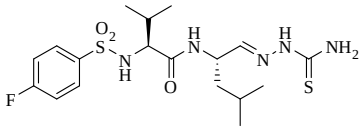	0.19	-
2.39	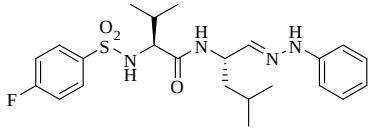	0.96	-2
2.51	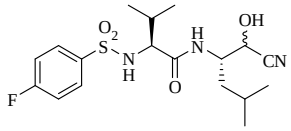	0.030	3
3.27	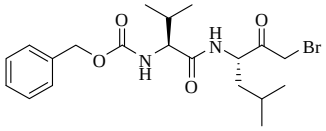	0.18	-2
4.4	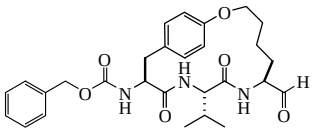	0.61	-3

Table 6.19 Potent papain inhibitors: only compounds with IC_{50} values lower than 1.0 μM were included. Negative selectivity values indicate that the inhibitor is more selective for cathepsin B than papain. A dash indicates that there was no selectivity observed

6.6.2 Warhead Rankings for Cathepsin B

Many of the inhibitors discussed above (see **Sections 6.2-6.4**) are both highly potent and selective for cathepsin B; for this reason the following **Table 6.20** lists all of inhibitors synthesised within this thesis of the skeleton: 4-fluorobenzenesulfonyl-Val-Leu-warhead, in order of most potent to least potent against cathepsin B. The use of this fixed scaffold for the **Tables 6.20** and **6.21** allows for a direct comparison of the potency and selectivity for each of the warheads (aldehyde, alcohol, semicarbazone, methyl ester, carboxylic acid, amidoxime, 1,2,4-oxadiazole, α-hydroxytetrazole, α-ketotetrazole, α-hydroxyoxazoline, α-ketooxazoline, cyanohydrin, *O*-protected cyanohydrin, azide, α,β-unsaturated methyl ester, α,β-unsaturated ethyl ester, α,β-unsaturated aldehyde, vinyl sulfone, diazoketone, α-bromomethyl ketone, α-bromomethyl-3*R*-alcohol, α-bromomethyl-3-*S/R*-alcohol, 3*R*-epoxide and 3-*S/R*-epoxide). **Table 6.21** contains the same set of inhibitors but listed according to the selectivity shown for cathepsin B.

Sixteen of the compounds listed in **Table 6.20** are potent cathepsin B inhibitors (IC_{50} <5.0 μM). These are the: aldehyde **2.3** (IC_{50} = 0.022 μM); α-bromomethyl ketone **3.28** (IC_{50} = 0.075 μM); cyanohydrin **2.51** (IC_{50} = 0.086 μM); α,β-unsaturated aldehyde **3.18** (IC_{50} = 0.13 μM); thiosemicarbazone **2.40** (IC_{50} = 0.16 μM); α-ketooxazoline **2.42** (IC_{50} = 0.20 μM); 4-phenylsemicarbzone **2.38** (IC_{50} = 0.24 μM); phenylhydrazone **2.39** (IC_{50} = 0.32 μM); *O*-protected cyanohydrin **2.60** (IC_{50} = 0.35 μM); carboxylic acid **2.7** (IC_{50} = 0.39 μM); semicarbazone **2.37** (IC_{50} = 0.69 μM); α-bromomethyl-3-*S/R*-alcohol **3.32** (IC_{50} = 0.76 μM); diazoketone **3.25** (IC_{50} = 1.1 μM); methyl ester **2.44** (IC_{50} = 1.4 μM); vinyl sulfone **3.20** (IC_{50} = 1.9 μM) and α-hydroxytetrazole **2.53** (IC_{50} = 2.1 μM).

The remaining compounds (IC_{50} >5.0 μM) are: alcohol **2.6** (IC_{50} = 9.2 μM); α-bromomethyl-3*R*-alcohol **3.30** (IC_{50} = 9.9 μM); 3*R*-epoxide **3.27** (IC_{50} = 12 μM); 1,2,4-oxadiazole **2.41** (IC_{50} = 18 μM); 3-*S/R*-epoxide **3.35** (IC_{50} = 19 μM); α,β-unsaturated methyl ester **3.14** (IC_{50} = 20 μM); azide **2.62** (IC_{50} = 22 μM); α-hydroxyoxazoline **2.56** (IC_{50} = 24 μM); α,β-unsaturated methyl ester **3.15** (IC_{50} = 27 μM); α-ketotetrazole **2.43** (IC_{50} >50 μM) and amidoxime **2.48** (IC_{50} >50 μM).

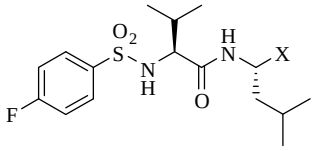

Compound	X	IC_{50} (μM)	Ranking
2.3	CHO	0.022	1
3.28	$C(O)CH_2Br$	0.075	2
2.51	CH(*S*,*R*-OH)CN	0.086	3
3.18	CH=CHCHO	0.13	4
2.38	$CH=NNHC(S)NH_2$	0.16	5
2.42	CO-oxz	0.20	6
2.39	CH=NNHC(O)NHPh	0.24	7
2.40	CH=NNHPh	0.32	8
2.60	$CH(S,R\text{-}CN)OC(O)CH_2Ph$	0.35	9
2.7	COOH	0.39	10
2.37	$CH=NNHC(O)NH_2$	0.69	11
3.31	$CH(S,R\text{-}OH)CH_2Br$	0.76	12
3.25	$C(O)CHN_2$	1.1	13
2.44	CO_2Me	1.4	14
3.20	$CH=CHSO_2Me$	1.9	15
2.53	CH(*S*,*R*-OH)-tet	2.1	16
2.6	CH_2OH	9.2	17
3.30	$CH(3R\text{-}OH)CH_2Br$	9.9	18
3.27	3*S*-epox	12	19
2.41	oxd	18	20
3.35	3-*S*/*R*-epox	19	21
3.14	$CH=CHCO_2Me$	20	22
2.62	CH_2N_3	22	23
2.56	CH(*S*,*R*-OH)-oxz	24	24
3.15	$CH=CHCO_2Et$	27	25
2.43	CO-tet	>50	26
2.48	$C(O)ONCH(CH_3)NH_2$	>50	27

Table 6.20 Ranking of warheads according to potency. Where epox = epoxide ring; oxd = oxadiazole ring; tet = tetrazole ring and oxz = oxazoline ring.

Twenty-seven compounds were synthesised within this thesis that contain the 4-fluorobenzenesulfone-Val-Leu-warhead scaffold; of these, fifteen are at least 2-fold more selective for cathepsin B than m-calpain, μ-calpain or papain (see **Table 6.21**). These are: carboxylic acid **2.7** (IC_{50} = 0.39 μM, selectivity 127-fold); methyl ester **2.44** (IC_{50} = 1.4 μM, selectivity 35-fold); diazoketone **3.25** (IC_{50} = 1.1 μM, selectivity 25-fold); *O*-protected cyanohydrin **3.60** (IC_{50} = 0.35 μM, selectivity 22-fold); α-hydroxytetrazole **2.53** (IC_{50} = 2.1 μM, selectivity 18-fold); α-bromomethyl ketone **3.28** (IC_{50} = 0.075 μM, selectivity 16-fold); α,β-unsaturated aldehyde **3.18** (IC_{50} = 0.13 μM, selectivity 13-fold); vinyl sulfone **3.20** (IC_{50} = 1.9 μM, selectivity 12-fold); α-bromomethyl-3-*S/R*-alcohol **3.32** (IC_{50} = 0.76 μM, selectivity 9-fold); α-ketooxazoline **2.42** (IC_{50} = 0.20 μM, selectivity 6-fold); alcohol **2.6** (IC_{50} = 9.2 μM, selectivity 5-fold); 4-phenylsemicarbazone **2.39** (IC_{50} = 0.24 μM, selectivity 4-fold); 3*R*-epoxide **3.27** (IC_{50} = 0.12 μM, selectivity 4-fold); phenylhydrazine **2.40** (IC_{50} = 0.32 μM, selectivity 3-fold) and semicarbazone **2.37** (IC_{50} = 0.69 μM, selectivity 2-fold).

The remaining twelve compounds are not significantly selective for cathepsin B (selectivity lower than 1.5-fold): 3-*S/R*-epoxide **3.35** (IC_{50} = 19 μM); α-bromomethyl-3*R*-alcohol **3.29** (IC_{50} = 9.9 μM); α,β-unsaturated ethyl ester **3.15** (IC_{50} = 27 μM); thiosemicarbazone **2.38** (IC_{50} = 0.16 μM); aldehyde **2.3** (IC_{50} = 0.022 μM); cyanohydrin **2.51** (IC_{50} = 0.086 μM); 1,2,4-oxadiazle **2.41** (IC_{50} = 18 μM); α,β-unsaturated methyl ester **3.14** (IC_{50} = 20 μM); azide **2.62** (IC_{50} = 22 μM); α-hydroxyoxazoline **2.56** (IC_{50} = 24 μM); amidoxime **2.48** (IC_{50} >50 μM) and α-ketotetrazole **2.43** (IC_{50} >50 μM).

The choice of warhead plays a major role in the design of potent and selective cathepsin B inhibitors, as the above results indicate (refer to **Tables 6.20** and **6.21**). The outstanding compound is the carboxylic acid **2.7**, which is not only a potent cathepsin B (IC_{50} = 0.39 μM) inhibitor but also has 125-fold selectivity for cathepsin B.

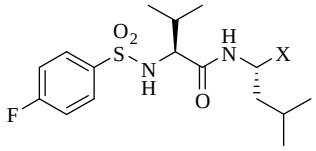

Compound	X	Selectivity†††	Activity Ranking	IC_{50} (μM)
2.7	COOH	127-fold	10	0.39
2.44	CO_2Me	35-fold	14	1.4
3.25	$C(O)CHN_2$	25-fold	13	1.1
2.60	CH(*S*,*R*-CN)OC(O)CH_2Ph	22-fold	9	0.35
2.53	CH(*S*,*R*-OH)-tet	18-fold	16	2.1
3.28	$C(O)CH_2Br$	16-fold	2	0.075
3.18	CHCHCHO	13 fold	4	0.13
3.20	$CH=CHSO_2Me$	12-fold	22	1.9
3.32	CH(*S*,*R*-OH)CH_2Br	9-fold	12	0.76
2.42	CO-oxz	6-fold	6	0.20
2.6	CH_2OH	5-fold	17	9.2
2.38	CH=NNHC(O)NHPh	4-fold	7	0.24
3.27	*S*-epox	4-fold	19	12
2.39	CH=NNHPh	3-fold	8	0.32
2.37	$CH=NNHC(O)NH_2$	2-fold	11	0.69
3.35	(*S*,*R*)-epox	1.5-fold	21	19
3.29	CH(*R*-OH)CH_2Br	1.5-fold	18	9.9
3.15	$CH=CHCO_2Et$	1.5-fold	25	27
2.40	$CH=NNHC(S)NH_2$	1.2 fold	5	0.16
2.3	CHO	-	1	0.022
2.51	CH(*S*,*R*-OH)CN	-	3	0.086
2.41	oxd	-	20	18
3.14	$CH=CHCO_2Me$	-	22	20
2.62	CH_2N_3	-	23	22
2.56	CH(*S*,*R*-OH)-oxz	-	24	24
2.48	$C(O)ONCH(CH_3)NH_2$	-	27	>50
2.43	CO-tet	-	26	>50

Table 6.21 Ranking of warheads according to selectivity for cathepsin B. Where epox = epoxide ring; oxd = oxadiazole ring; tet = tetrazole ring and oxz = oxazoline ring.

††† Where selectivity is calculated according to the difference between IC_{50} for cathepsin B and the nearest IC_{50} value of the other cysteine proteases and is at least as selective as shown.

6.7 INHIBITION OF α-CHYMOTRYPSIN AND PEPSIN

For screening purposes, all inhibitors were initially assayed against m-calpain, μ-calpain, cathepsin B, papain, pepsin and α-chymotrypsin at a concentration of 50 μM. Compounds with inhibition greater than 50% were diluted further to determine an IC_{50} value; while those with inhibition under 50% were disqualified from further assay (see **Appendix A2** for a table of % inhibition of synthesised compounds at a concentration of 50 μM). The previous **Sections 6.2-6.6** discuss the inhibition of the cysteine proteases: m-calpain, μ-calpain, cathepsin B and papain; this section discusses inhibition that was observed against α-chymotrypsin and pepsin.

6.7.1 Inhibition of α-Chymotrypsin

The compounds synthesised within this thesis (see **Chapters Two-Four**) showed no inhibition of α-chymotrypsin (percentage inhibition at 50 μM between 0% and 40%; see **Appendix A2**). This lack of inhibition of α-chymotrypsin was expected as the dipeptide Val-Leu and Val-Phe comprising the inhibitors were selected for specific cysteine protease inhibition; whereas α-Chymotrypsin strictly favours large hydrophobic residues such as Phe, Try and Leu in the P_1 position[40] and the S_2 and S_3 subsites display little specificity.[41] Arg and Lys are favoured at the $P_{1'}$ position of α-chymotrypsin due to interactions with nearby Asp residues along the active site cleft.[41]

6.7.2 Inhibition of Pepsin

Most of the compounds synthesised in this thesis (see **Chapters Two-Four**) were inactive against pepsin at a concentration of 50 μM. However, seven compound showed inhibition greater than or equal to 50% at an inhibitor concentration of 50 μM (see **Table 6.22**). These compounds are: aldehyde **2.2** (IC_{50} = 32 μM); cyanohydrin **2.51** (IC_{50} = 25 μM); α-ketotetrazole **2.55** (IC_{50} = 11 μM); α-hydroxyoxazoline **2.57** (IC_{50} = 37 μM); *O*-protected cyanohydrin **2.61** (IC_{50} = 1.6 μM); 3-*R/S*-expoxide **3.35** (IC_{50} = 50 μM) and macrocyclic aldehyde **4.4** (IC_{50} = 16 μM).

	Compound	% Inhibition at 50 µM	IC_{50} (µM)
2.2	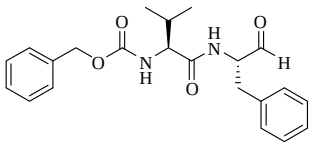	60	32
3.35	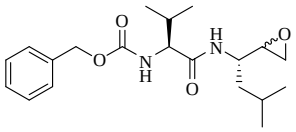	50	50
2.52	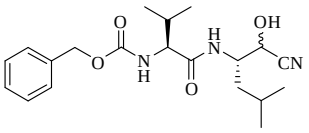	63	25
2.61	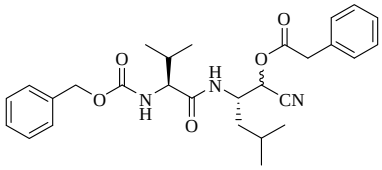	69	1.6
2.55	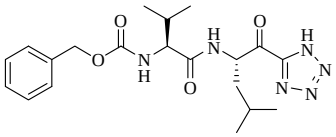	78	11
4.4	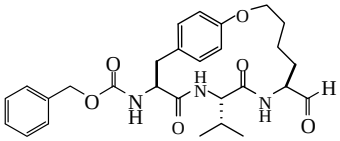	90	16
2.57	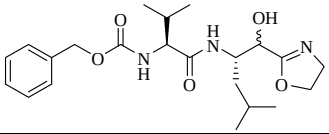	57	37

Table 6.22 Compounds that exhibited some inhibitory potency against pepsin

To explain why these seven compounds are inhibitors of pepsin, the mechanism of substrate hydrolysis employed by pepsin is shown in **Figure 6.18**. Aspartic acid proteases, such as pepsin, have an 'acid-base' mechanism of hydrolysis. The scissile amide bond undergoes nucleophilic attack by an activated water molecule that has been deprotonated by an aspartic acid residue in the active site. A charged species (b) is formed as the intermediate. This collapses to give the cleaved products (c). Typical inhibitors of aspartic acid proteases are of the nature shown in **Figure 6.19** and include hydroxyethylene, hydroxyethylurea and reduced amides as mimics of the tetrahedral intermediate. Pepsin

hydrolyses peptide bonds that connect bulky hydrophobic and aromatic residues such as Phe, Trp and Tyr. Residues that show favourable binding in the active site are: hydrophobic residues at P_3 and $P_{3'}$; Ala or Val at $P_{2'}$.[42,43]

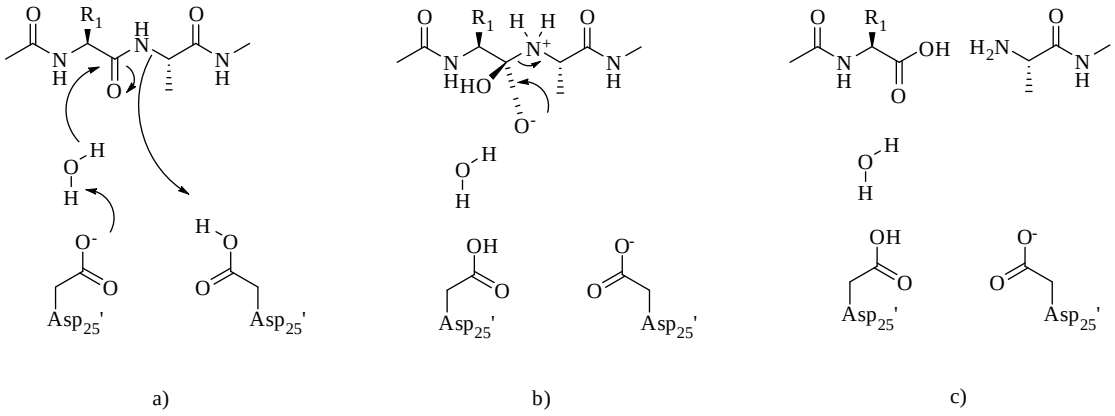

Figure 6.18 The catalytic mechanism of substrate hydrolysis by aspartic acid proteases; a) nucleophilic attack on the scissile bond by an activated water molecule followed by b) protonation of the amide nitrogen to give a charged species which collapses c) to give the cleaved products.

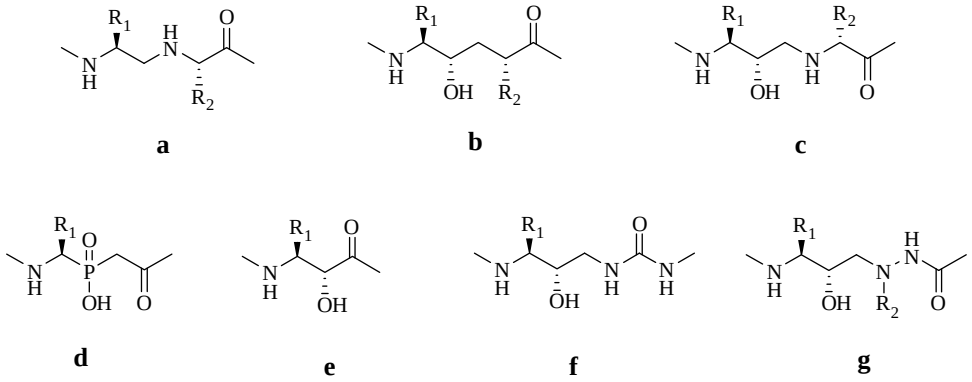

Figure 6.19 Transition state analogues for aspartic acid proteases: a) reduced amide; b) hydroxyethylene; c) hydroxyethylamine; d) phosphonic; e) α-hydroxy-β-amino acid; f) hydroxyethylurea; g) hydroxyethyl hydrazide moieties

A key structural element of aspartic acid protease inhibitors is the presence of a hydroxyl or hydroxyl-like moiety that can bind to the two aspartic acid residues in the active site (refer to **figure 6.15**).[44] It is thus suggested that the warhead of inhibitors **2.2**, **3.35**, **2.52**, **2.60**, **2.55**, **2.57** and **4.4** mimics a hydroxyl moiety. The aldehydes **2.2** and **4.4** can exist as hemiacetals, the cyanohydrin **2.51** is similar in nature to an aminoalcohol analogue (see

Figure 6.16) and the epoxide is not active unless it has been protonated (for example by a water molecule). The exception is the *O*-protected cyanohydrin **2.60**, which shows good inhibition of pepsin (IC_{50} = 1.6 μM). The *O*-protected cyanohydrin **2.60** shows at least 1.5-fold selectivity for pepsin over any of the cysteine proteases {IC_{50} values: 25 μM (m-calpain), 50 μM (μ-calpain), 20 μM (cathepsin B) and >50 μM (papain)}.

Noteworthy also is the observation that the inhibitors **2.2**, **2.52**, **2.55**, **2.57**, **2.61**, **3.36** and **4.4** in **Table 6.21** all have benzyloxycarbonyl as the *N*-protecting group. The 4-fluorobenzenesulfonyl protected analogues (**2.27**, **2.51**, **2.43**, **2.56** and **3.35**) are inactive against pepsin at a concentration of 50 μM. This suggests that the benzyloxycarbonyl is a better fit in the active site cleft of pepsin than the 4-fluorobenezenesulfonyl. Further, the alcohol, aldehyde, ester, carboxylic acid, 1,2,4-oxadiazole, α-ketotetrazole, α-ketooxazoline, cyanohydrin and Michael accepter series of inhibitors with the 4-fluorobenezenesulfonyl moiety as the *N*-protecting group are more potent against m-calpain, μ-calpain, cathepsin B and papain than those within the same series containing the benzyloxycarbonyl *N*-protecting group. The 4-fluorobenzenesulfonyl group is thus an essential *N*-protecting group for the design protease inhibitors that are selective for cysteine proteases over serine or aspartic acid proteases.

6.8 CONCLUSION AND FUTURE WORK

6.8.1 Summary of Inhibitors with Reversible Warheads

The assay results of the acyclic aldehydes **2.3**, **2.27**, **2.19**, **2.2**, **2.21** and **2.22** against the papain superfamily of cysteine proteases agreed with trends observed in the literature; with the aldehydes being potent and broad spectrum cysteine protease inhibitors.

The alcohol **2.26** is an unprecedented example of a non-covalent inhibitor of cathepsin B. It is a highly potent and specific inhibitor of cathepsin B (IC_{50} = 0.075 μM; selectivity 85-fold over m-calpain, μ-calpain and papain). Future work would involve the investigation of other non-covalent warheads on the 4-fluorobenezenesulfonyl-Val-Phe scaffold to examine the effect of both potency and selectivity on cathepsin B and other proteases of the papain superfamily

The semicarbazones **2.37-2.40** were between 5- and 100-fold less potent than the parent aldehyde **2.3** against m-calpain, μ-calpain, cathepsin B and papain. The most potent inhibitor within this series was the thiosemicarbazone **2.38** {IC_{50} = 1.6 μM (m-calpain); 1.6 μM (μ-calpain); 0.16 μM (cathepsin B) and 0.19 μM (papain)}. All the semicarbazones **2.37-2.40** were selective for cathepsin B by 1.2- to 4-fold.

The oxadiazoles **2.41** and **2.50** were weak inhibitor of all the cysteine proteases tested (IC_{50} values >18 μM). The α-hydroxytetrazoles **2.53** and **2.54** were potent and selective inhibitors of cathepsin B (IC_{50} = 2.1 μM, selectivity 18-fold and 1.3 μM, selectivity19-fold respectively). The α-ketotetrazoles **2.43** was a potent and selective inhibitor of papain (IC_{50} = 6.0 μM, selectivity 8-fold). The outstanding inhibitor within the heterocyclic series was α-ketooxazoline **2.42**, which was a potent, selective inhibitor of cathepsin B (IC_{50} = 0.20 μM, selectivity 6-fold).

The cyanohydrins **2.51** and **2.52** were potent and broad spectrum cysteine protease inhibitors (IC_{50} values < 1.6 μM). The *O*-protected cyanohydrins **2.60** and **2.61** were potent and selective inhibitors of cathepsin B (IC_{50} = 0.35 μM, selectivity 22-fold and 2.4

μM, 10-fold respectively). The cyanohydrins **2.51**, **2.52**, **2.60** and **2.61** appear to be unprecedented cysteine protease inhibitors. Azide **2.62** was a weak inhibitor of cathepsin B and papain only (IC_{50} = 22 μM and 23 μM respectively).

Table 6.23 summarises the best reversible inhibitors synthesised for each of the proteases tested, these being chosen for potency and selectivity against individual proteases. Where no selective inhibitors were found, the most potent against that protease was chosen and the lack of specificity denoted by a dash.

The reversible inhibitors that met the above criteria were: cyanohydrin **2.52** (m-calpain, IC_{50} = 0.34 μM), cyanohydrin **2.51** (μ-calpain, IC_{50} = 0.55 μM), acid **2.7** (cathepsin B, IC_{50} = 0.39, selectivity 127-fold), α-ketotetrazole **2.53** (papain, IC_{50} = 6.0 μM, selectivity 8-fold) and *O*-protected cyanohydrin **2.61** (pepsin, IC_{50} = 1.6 μM, selectivity 1.5-fold). Inhibition against α-chymotrypsin was not observed.

Enzyme	Compound		IC_{50} (μM)	Selectivity
m-calpain	**2.52**	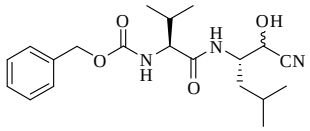	0.34	-
μ-calpain	**2.51**	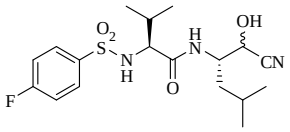	0.55	-
cathepsin B	**2.7**	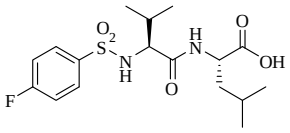	0.39	127
papain	**2.53**	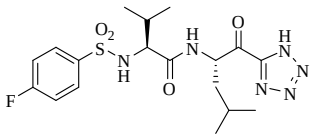	6.0	8
pepsin	**2.61**	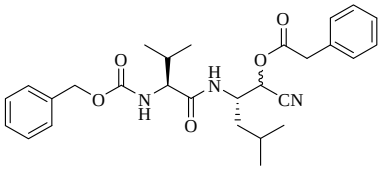	1.6	1.5
α-chymotrypsin	-	-	-	-

Table 6.23 Summary of the best reversible inhibitor synthesised (balance of potency and selectivity) for each enzyme tested.

6.8.2 Summary of Inhibitors with Irreversible Warheads

The α,β-unsaturated carbonyls **3.14-3.17** and the vinyl sulfones **3.19-3.21** were between 5- to 12-fold weaker inhibitors of the calpains and papain (IC_{50} > 14 μM); than of cathepsin B {IC_{50} = 20 μM (**3.14**); 27 μM (**3.15**); 21 μM (**3.16**); 24 μM (**3.17**); 1.9 μM (**3.20**); 5.9 μM (**3.21**); 21 μM (**3.22**); 27 μM (**3.23**)}. The α,β-unsaturated aldehyde **3.18** was a potent and selective inhibitor of cathepsin B (IC_{50} = 0.13 μM, selectivity 4-fold) within the Michael acceptor series.

Diazoketones **3.25** and **3.26** were potent and selective inhibitors of cathepsin B (IC_{50} values of 1.1 μM and 0.22 μM respectively). The α-bromomethyl ketones **3.28** and **3.29** were potent and selective inhibitors of cathepsin B (IC_{50} = 0.025 μM, selectivity 16-fold and 0.077 μM, selectivity 2-fold respectively). The α-bromomethyl alcohols **3.30-3.33** were less potent against cathepsin B than the α-bromomethyl ketones **3.28** and **3.29** by at least 3.5-fold. It was also suggested that the absolute configuration of the hydroxyl group is important for binding affinity and potency (the 3*S*-alcohol was preferred). The epoxides **3.27**, **3.34-3.36** were cathepsin B specific; the absolute configuration of the epoxide was suggested to be important for binding affinity (the 3*R*-epoxide being the preferred).

Table 6.24 summarises the best irreversible inhibitors synthesised for each of the proteases tested, these being chosen for potency and selectivity against individual proteases. Where no selective inhibitors were found, the most potent against that protease was chosen, the lack of specificity denoted by a dash.

The irreversible inhibitors that met the above criteria were: diazoketone **3.26** (m-calpain, IC_{50} = 1.0 μM), α,β-unsaturated aldehyde **3.18** (μ-calpain, IC_{50} = 2.1 μM), diazoketone **3.26** (cathepsin B, IC_{50} = 0.23, selectivity 49-fold) and α,β-unsaturated ester **3.14** (papain, IC_{50} = 14 μM, selectivity 1.4-fold). Inhibition against pepsin and α-chymotrypsin was not observed.

Enzyme	Compound		IC_{50} (μM)	Selectivity
m-calpain	**3.26**	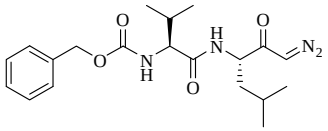	1.0	-
μ-calpain	**3.18**	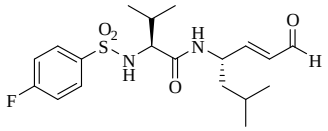	2.1	-
cathepsin B	**3.26**	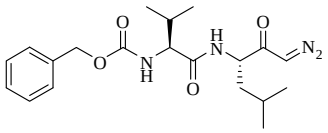	0.23	49
papain	**3.14**	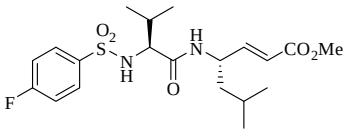	14	1.4
pepsin	-	-	-	-
α-chymotrypsin	-	-	-	-

Table 6.24 Summary of the best irreversible inhibitors synthesised (balance of potency and selectivity) against each of the proteases tested

6.8.3 Summary of β-Sheet Constrained Inhibitors

The macrocyclic aldehyde **4.4** was a potent broad spectrum cysteine protease, a characteristic in common with the acyclic range of aldehydes **2.3**, **2.27**, **2.19**, **2.2**, **2.21** and **2.22** tested. Constraining the backbone into a β-strand was suggested to increase the binding affinity of the inhibitors, as evidenced by the macrocyclic alcohol **4.3** showing increased potency of the cysteine proteases tested in comparison to the acyclic alcohols **2.6**, **2.29**, **2.30**, **2.34** and **2.35**, which showed little inhibition of m-calpain, μ-calpain and papain.

The macrocyclic semicarbazone **4.15** was a potent and selective inhibitor of m-calpain (IC_{50} = 0.16 μM, selectivity 8-fold). The macrocyclic cyanohydrin **4.16** was a potent and selective inhibitor of cathepsin B (IC_{50} = 2.4 μM, selectivity 4-fold). The macrocyclic azide **4.19** was a very weak cysteine protease inhibitor (IC_{50} values >50 μM).

Table 6.25 summarises the best irreversible inhibitors synthesised for each of the proteases tested, these being chosen for potency and selectivity against individual proteases. Where no selective inhibitors were found, the most potent against that protease was chosen, the lack of specificity denoted by a dash.

The irreversible inhibitors that met the above criteria were: macrocyclic semicarbazone **4.15** (m-calpain, IC_{50} = 0.16 μM, selectivity 8-fold), macrocyclic semicarbazone **4.15** (μ-calpain, IC_{50} = 1.3 μM), macrocyclic cyanohydrin **4.16** (cathepsin B, IC_{50} = 2.4, selectivity 4-fold), macrocyclic semicarbazone **4.15** (papain, IC_{50} = 3.7 μM) and macrocyclic aldehyde **4.4** (pepsin, IC_{50} = 16 μM). Inhibition against α-chymotrypsin was not observed.

The macrocyclic compounds **4.3**, **4.4**, **4.13**, **4.14**-**4.16** and **4.19** are unprecedented examples of cysteine protease inhibitors.

Enzyme	Compound		IC_{50} (μM)	Selectivity
m-calpain	**4.15**	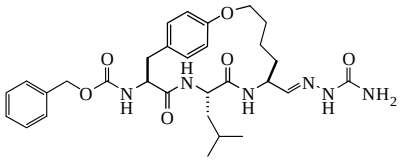	0.16	8.0
μ-calpain	**4.15**	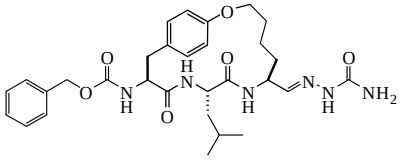	1.2	-
cathepsin B	**4.16**	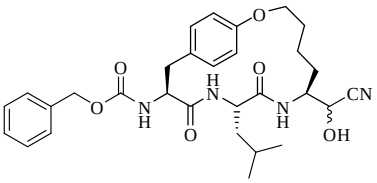	2.4	3.7
papain	**4.15**	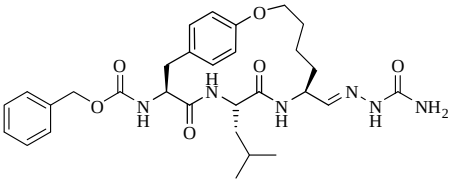	2.0	-
pepsin	**4.4**	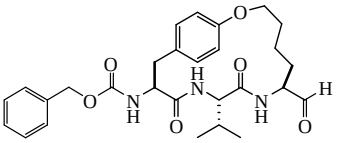	16	-
α-chymotrypsin	-	-	-	-

Table 6.25 Summary of the best macrocyclic inhibitors synthesised (balance of potency and selectivity) against each of the proteases tested.

6.8.4 Summary of Findings

This thesis, through the design, synthesis and biological assay of cysteine protease inhibitors has shown that the nature of the warhead has a significant effect on the potency and selectivity of inhibitors against cysteine proteases of the papain superfamily (clan CA).

Through comparison of the IC_{50} values of the synthesised inhibitors it was possible to identify structure-activity relationship. Twenty seven compounds had the scaffold of 4-fluorobenezenesulfonyl-Val-Leu-warhead and were inhibitors of cathepsin B. Ranking of these compounds in terms of potency and selectivity against cathepsin B allowed for a comparison of warhead effect. The top ten most potent warheads were (in order of most potent to least potent): aldehyde, α-bromomethyl ketone, cyanohydrin, α,β-unsaturated aldehyde, thiosemicarbazone, 4-phenylsemicarbazone, phenyl hydrazone, esterified cyanohydrin, carboxylic acid and semicarbazone (see **Figure 6.20**). These warheads on the 4-fluorobenzenesulfonyl-Val-Leu-warhead scaffold were potent cathepsin B inhibitors (IC_{50} values from 0.022 to 0.69 μM).

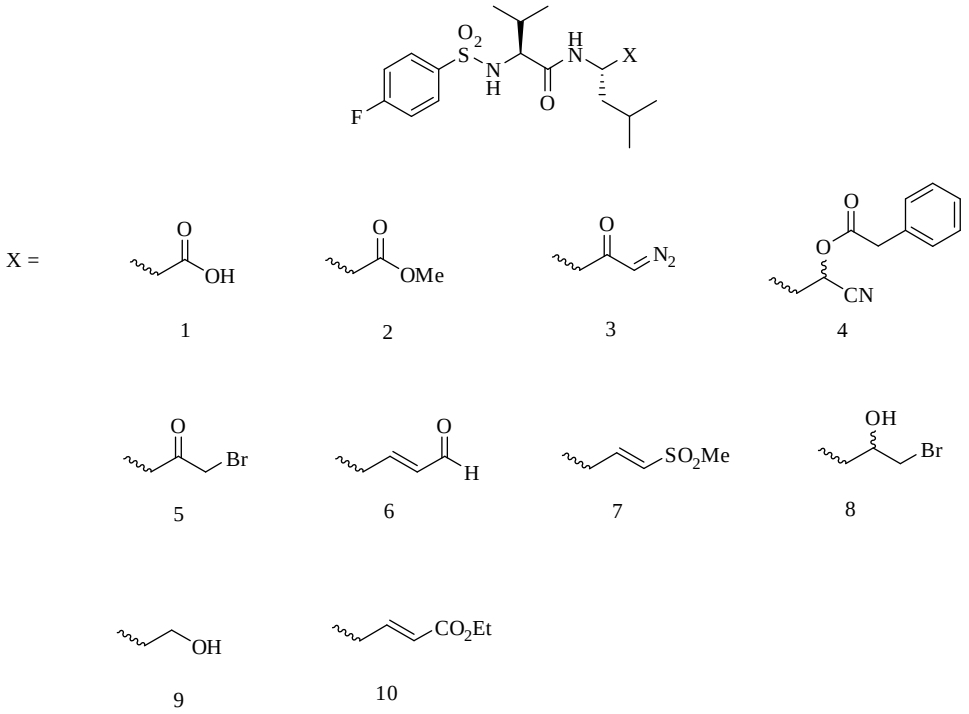

Figure 6.20 The top ten most selectivity warheads for cathepsin B based on the 4-fluorobenzenesulfonyl-Val-Leu-X scaffold: 1) carboxylic acid; 2) methyl ester; 3) diazoketone; 4) *O*-protected cyanohydrin; 5) α-bromomethyl ketone; 6) α,β-unsaturated aldehyde; 7) vinyl sulfone; 8) α-bromomethyl-(*S*,*R*)-alcohol; 9) alcohol and 10) α,β-unsaturated ethyl ester

Further ranking of the warheads in terms of selectivity for cathepsin B gave the top ten most selective warheads: carboxylic acid, methyl ester, diazoketone, esterified cyanohydrin, α-bromomethyl ketone, α,β-unsaturated aldehyde, vinyl sulfone, α-

bromomethyl (*S,R*)-alcohol, alcohol and α,β-unsaturated ethyl ester (see **Figure 6.13**). The selectivity of these warheads was between 5- and 130-fold for cathepsin B.

Using potency and selectivity in combination, the best inhibitors for cathepsin B were the α,β-unsaturated aldehyde **3.18**, α-bromomethyl ketone **3.25** and the esterified cyanohydrin **3.60** (see **Figure 6.21**)

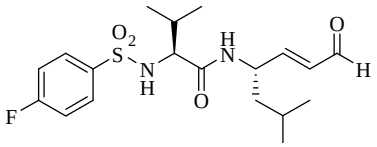

3.18
IC_{50} = 0.025 µM
Selectivity 16-fold

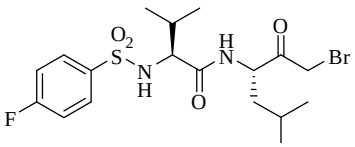

3.25
IC_{50} = 0.13 µM
Selectivity 13-fold

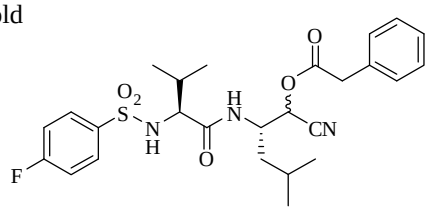

3.60
IC_{50} = 0.35 µM
Selectivity 22-fold

Figure 6.21 The three best inhibitors of cathepsin B, based on a balance of potency and selectivity.

6.9 REFERENCES FOR CHAPTER SIX

(1) Fairlie, D. P.; Abbenante, G. *Medicinal Chemistry* **2005**, *1*, 71-104.

(2) Leung-Toung, R.; Zhao, Y.; Li, W.; Tam, T. F.; Karimian, K.; Spino, M. *Current Medicinal Chemistry* **2006**, *13*, 547-581.

(3) http://www.hgsi.com/news/press/02-07-16_cathespin_gsk.html (Access Date: 22 Mar 2007).

(4) Lim, I. T.; Meroueh, S. O.; Lee, M.; Heeg, M. J.; Mobashery, S. *Journal of the American Chemical Society* **2004**, *126*, 10271-10277.

(5) Le, G. T.; Abbenante, G.; Madala, P. K.; Hoang, H. N.; Fairlie, D. P. *Journal of the American Chemical Society* **2006**, *128*, 12396-12397.

(6) Cuerrier, D.; Moldoveanu, T.; Davies, P. L. *The Journal of Biological Chemistry* **2005**, *280*, 40632-40641.

(7) Inoue, J.; Nakamura, M.; Cui, Y.-S.; Sakai, Y.; Sakai, O.; Hill, J. R.; Wang, K. K. W.; Yuen, P.-W. *Journal of Medicinal Chemistry* **2003**, *46*, 868-871.

(8) Conroy, J. L.; Abato, P.; Ghosh, M.; Austermuhle, M. I.; Kiefer, M. R.; Seto, C. T. *Tetrahedron Letters* **1998**, *39*, 8253-8256.

(9) Yamamoto, A.; Tomoo, K.; Matsugi, K.-i.; Hara, T.; In, Y.; Murata, M.; Kitamura, K.; Ishida, T. *Biochimica et Biophysica Acta, Protein Structure and Molecular Enzymology* **2002**, *1597*, 244-251.

(10) Nakamura, M.; Inoue, J. *Bioorganic & Medicinal Chemistry Letters* **2002**, *12*, 1603-1606.

(11) Adkison, K. K.; Barrett, D. G.; Deaton, D. N.; Gampe, R. T.; Hassell, A. M.; Long, S. T.; McFadyen, R. B.; Miller, A. B.; Miller, L. R.; Payne, J. A.; Shewchuk, L. M.; Wells-Knecht, K. J.; Willard, D. H. J.; Wright, L. L. *Bioorganic & Medicinal Chemistry Letters* **2006**, *16*, 978-983.

(12) Lee, C.-S.; Liu, W.; Sprengeler, P. A.; Somoza, J. R.; Janc, J. W.; Sperandio, D.; Spencer, J. R.; Green, M. J.; McGrath, M. E. *Bioorganic & Medicinal Chemistry Letters* **2006**, *16*, 4036-4040.

(13) Diana, G. D.; Volkots, D. L.; Nitz, T. J.; Bailey, T. R.; Long, M. A.; Vescio, N.; Aldous, S.; Pevear, D. C.; Dutko, F. J. *Journal of Medicinal Chemistry* **1994**, *37*, 2421-2436.

(14) Cannon, J. G. In *Burger's Medicinal Chemistry and Drug Discovery. Volume I: Principles and Practice*; 5th ed.; Wolff, M. E., Ed.; John Wiley & Sons: New York, 1995; Vol. 1.

(15) Illy, C.; Quraishi, O.; Wang, J.; Purisima, E.; Vernet, T.; Mort, J. S. *The Journal of Biological Chemistry* **1997**, *272*, 1197-1202.

(16) Frlan, R.; Gobec, S. *Current Medicinal Chemistry* **2006**, *13*, 2309-2327.

(17) Otto, H.-H.; Schirmeister, T. In *Chemical Reviews (Washington, D. C.)* 1997; Vol. 97, p 133-171.

(18) Ohmoto, K.; Kawabata, K.; (Ono Pharmaceutical Co., Ltd., Japan). 2002, p 369.

(19) Ohmoto, K.; Itagaki, I.; (Ono Pharmaceutical Co., Ltd., Japan). 2001, p 424.

(20) Spruce, L. W.; Gyorkos, A. C.; Cheronis, J. C.; Goodfellow, V. S.; Leimer, A. H.; Young, J. M.; Gerrity, J. I.; (Cortech, Inc., USA). 1998, p 84

(21) Palmer, J. T.; Hirschbein, B. L.; Cheung, H.; McCarter, J.; Janc, J. W.; Yu, W.; Wesolowski, G. *Bioorganic & Medicinal Chemistry Letters* **2006**, *16*, 2909-2914.

(22) Chan, A. W. E.; Golec, J. M. C. *Bioorganic & Medicinal Chemistry* **1996**, *4*, 1673-1677.

(23) Tao, M.; Bihovsky, R.; Kauer, J. C. *Bioorganic & Medicinal Chemistry Letters* **1996**, *6*, 3009-3012.

(24) Gotz, M. G.; Caffrey, C. R.; Hansell, E.; McKerrow, J. H.; Powers, J. C. *Bioorganic & Medicinal Chemistry* **2004**, *12*, 5203-5211.

(25) Tyndall, J. D. A. N., T.; Fairlie, D.P. *Chemical Reviews* **2005**, *105*, 973-999.

(26) Milner-White, E. J. *Trends in Pharmacological Sciences* **1989**, *10*, 70-74.

(27) Loughlin, W. A.; Tyndall, J. D. A.; Glenn, M. P.; Fairlie, D. P. *Chemical Reviews* **2004**, *104*, 6085-6117.

(28) Leung-Toung, R.; Li, W.; Tam, T. F.; Karimian, K. *Current Medicinal Chemistry* **2002**, *9*, 979-1002.

(29) Chen, K. X.; Njoroge, F. G.; Pichardo, J.; Prongay, A.; Butkiewicz, N.; Yao, N.; Madison, V.; Girijavallabhan, V. *Journal of Medicinal Chemistry* **2005**, *48*, 6229-6235.

(30) Abbenante, G.; Bergman, D. A.; Brinkworth, R. I.; March, D. R.; Reid, R. C.; Hunt, P. A.; James, I. W.; Dancer, R. J.; Barnham, B.; Stoermer, M. L. *Bioorganic & Medicinal Chemistry Letters* **1996**, *6*, 2531-2536.

(31) Iqbal, M.; Messina, P. A.; Freed, B.; Das, M.; Chatterjee, S.; Tripathy, R.; Tao, M.; Josef, K. A.; Dembofsky, B. *Bioorganic & Medicinal Chemistry Letters* **1997**, *7*, 539-544.

(32) Goll, D. E.; Thompson, V. F.; Li, H.; Wei, W.; Cong, J. *Physiological Reviews* **2003**, *83*, 731-801.

(33) Khorchid, A.; Ikura, M. *Nature Structural Biology* **2002**, *9*, 239-241.

(34) Sorimachi, H.; Ishiura, S.; Suzuki, K. *Journal of Biochemistry* **1997**, *328*, 721-732.

(35) Sorimachi, H.; Suzuki, K. *Journal of Biochemistry* **2001**, *129*, 653-664.

(36) Nakamura, M.; Yamaguchi, M.; Sakai, O.; Inoue, J. *Bioorganic & Medicinal Chemistry* **2003**, *11*, 1371-1379.

(37) Nakamura, M.; Miyashita, H.; Yamaguchi, M.; Shirasaki, Y.; Nakamura, Y.; Inoue, J. *Bioorganic & Medicinal Chemistry* **2003**, *11*, 5449-5460.

(38) Thompson, V. F.; Saldana, S.; Cong, J.; Goll, D. E. *Analytical Biochemistry* **2000**, *279*, 170-178.

(39) Katunuma, N.; Suzuki, K.; Travis, J.; Fritz, H. In *The Refined X-Ray Crystal Structure of Human and Rat Liver Cathepsin B*; Japan Scientific Societies Press: Japan, 1994, p 274.

(40) Leung, D.; Abbenante, G.; Fairlie, D. P. *Journal of Medicinal Chemistry* **2000**, *43*, 305-341.

(41) Hedstrom, L. *Chemical Reviews* **2002**, *102*, 4501-4525.

(42) Kageyama, T. *Biochemistry* **2004**, *43*, 15122-15130.

(43) Cooper, J. B. *Current Drug Targets* **2002**, *3*, 155-173.

(44) Bursavich, M. G.; Rich, D. H. *Journal of Medicinal Chemistry* **2002**, *45*, 541-558.

CHAPTER SEVEN

Experimental Methods

7.1 GENERAL METHODS AND EXPERIMENTAL PROCEDURES

7.1.1 General Practice

Infrared Spectroscopy

Infrared spectra were obtained using a Shimadzu 9201PC series FTIR interfaced with an Intel 486 PC operating Shimadzu's HyperIR software. Diffuse reflectance spectra were obtained in a solid KBr matrix.

Nuclear Magnetic Resonance

Proton detected NMR spectra were obtained on a Varian Inova or Varian Unity spectrometer operating at 500 MHz or 300 MHz respectively. Carbon detected NMR spectra were obtained on a Varian Unity 300 spectrometer operating at 75 MHz with a delay (D_1) of 1 s. Unless otherwise stated, all spectra were obtained at 23 °C. Two-dimensional cosy experiments were obtained on the Inova 500 spectrometer at 500 MHz.

Solvents used in NMR analysis (reference peak listed) included $CDCl_3$ ($C\mathbf{H}Cl_3$ at δ_H 7.26 ppm, $\mathbf{C}DCl_3$ at δ_C 77.0 ppm); CD_3OD ($C\mathbf{H}D_2OD$ at δ_H 3.31 ppm, $\mathbf{C}D_3OD$ at δ_C 49.05 ppm); $(CD_3)_2SO$ ($(C\mathbf{H}D_2)_2SO$ at δ_H 2.50 ppm, $(\mathbf{C}D_3)_2SO$ at δ_C 49.43 ppm).

Small Molecule Mass Spectrometry

Electron impact (EI) mass spectra were obtained on a Kratos MS80 RFA mass spectrometer operating at 4000V (accelerating potential) and 70 eV (ionization energy). The source temperature was 200-250^o C. Electrospray ionization (ESI) mass spectra were detected on a micromass LCT TOF mass spectrometer, with a probe voltage of 3200V, temperature of 150^o C and a source temperature of 80 ^{o}C. Direct ionization used 10μL of a 10μg mL^{-1} solution, using a carrier solvent of 50% acetonitrile/water at a flow rate of 20μL min^{-1}. Ionization was assisted by the addition of 0.5% formic acid.

Microanalysis

Microanalysis was performed at the University of Otago Microanalytical Laboratory. All reported values are within ±0.4% of the calculated value.

Melting Points

Melting points were taken on an Electrothermal apparatus and are uncorrected. Melting points are not reported for diastereomeric mixtures, oils or glassy solids.

Optical Rotary Dispersion

Optical rotation measurements were performed on a Perkin Elmer polarimeter Model 341 with 100 mm path length. Measurements were taken at 20 °C in HPLC grade methanol or chloroform at λ = 589 nm. $[\alpha]_D$ values are given in units of °.mL/g.dm and the sample concentration given in units of 10 mg/mL. Optical rotation measurements were not performed for diastereomeric mixtures.

Molecular Modelling

All molecular modelling experiments were conducted by Wanting Jiao and Steven McNabb with the Schrödinger suite 2005. Conformational searches were carried out with MacroModel 9.0 to generate an ensemble of low energy conformers to establish a suitable starting conformation of each compound for the docking. The searches were conducted with the MCMM method using a GB/SA water model and either the OPLS2001 force field or MM2 force field. The minimisation was stopped with the default gradient convergence threshold of δ = 0.05 kJ/(mol*Å). The default Polak-Ribiere Conjugate Gradient method was used for all minimisations. The crystal structure of mini mu-calpain (pdb code 1KXR) was prepared by: deleting water and ions, adding hydrogen atoms, mutation of $Ser_{115} \Rightarrow Cys_{115}$, deprotonation of Cys_{115}, and protonation of His_{272}. This structure was minimised using the OPLS2001 force field with a GB/SA water model over 500 iterations. All residues within a 5 Å distance to the calcium ions of the crystal structure were kept frozen during this minimisation. The RMSD of the minimised structure to the crystal structure was 0.96 Å for the heavy atoms (C, N, O, S). The centre of the docking grid was defined as the centroid of the residues Cys_{115}, Gly_{208}, and Gly_{271} and was generated with GLIDE

3.5 using default settings. The centre of the docked ligands was defined within a 12 Å box. The docking of flexible ligands to the rigid receptor model with GLIDE was performed with the following parameters: OPLS2001 force filed, extra precision mode, 90000 poses per ligand for the initial docking, scoring window for keeping initial poses: 5000, keep best 1000 poses per ligand for energy minimisation, energy minimisation with a distance dependent dielectric constant of two and a maximum of 5000 conjugate gradient steps. Ten poses per ligand were saved for evaluation. The amino acids Cys_{115} and His_{272} were uncharged in the induced fit calpain model. The centroid of Cys_{115}, Gly_{208}, Gly_{271}, Glu_{349} and Asn_{253} was chosen for the docking grid generation and the size of the box was chosen by default van der Waals radii of the ligand and the protein atoms were scaled to 0.5. The side chain of Lys_{347} was removed for the docking and the 20 best poses of this initial docking were retained. All protein residues with a 5 Å of the respective ligand pose were refined with PRIME 1.2, including Lys_{347}. The ligands were re-docked with a van der Waals radius of 0.8 to the newly generated protein structures if within 30 kcal/mol of the best protein structure and only if within the top 20 structures. For each of these protein structures, one ligand pose was kept for evaluation.

Reagents and Solvents

Oven-dried glassware was used in all reactions performed under an inert atmosphere (either dry nitrogen or argon). All starting materials and reagents were obtained commercially and used without further purification unless otherwise stated.

Concentration *in vacuo* refers to the removal of solvents "under reduced pressure" by rotary evaporation (low vacuum pump) followed by application of high vacuum (oil pump) for a minimum of thirty minutes.

Analytical thin layer chromatography (TLC) was performed on plastic-backed Merck Kieselgel $KG60F_{254}$ silica plates. Visualisation was achieved using short wave ultraviolet light, potassium permanganate or vanillin dip. Flash chromatography was performed using 230-400 mesh Merck Silica gel 60 either under a positive pressure of dry nitrogen or using the Buchi sepacore flash chromatography system.

All reagents were purified by established techniques. THF and diethyl ether were distilled from sodium benzophenone ketyl under an inert atmosphere immediately prior to use. Dichloromethane, petroleum ether,* ethyl acetate, benzene, toluene, triethylamine and 1,1,2-trichloroethane were distilled from calcium hydride under an inert atmosphere. Anhydrous *N,N*-dimethylformamide was obtained from commercial sources.

Cooled Solutions

The cooled solutions comprise the following: 5 °C refers to the reaction taking place in a controlled 5 °C refrigerated room; -78 °C using a mixture of CO_2(s) acetone; -30 °C, -25 °C and -10 °C using mixtures of methanol/water.

Sonication

Contained solutions were sonicated in a water trough at rt for 15 min using a Branson 2510 sonicator.

7.1.2 General Procedures

General Procedure A: Amide bond formation from an acid chloride

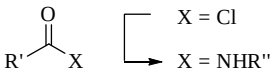

To a stirred solution of the acid chloride (1.0 equiv) in dry *N,N*-dimethylformamide was added the amine (1.0 equiv) and DIPEA (2.0 equiv) and the resulting solution stirred at rt overnight. The reaction mixture was diluted with ethyl acetate and washed successively with 1M aqueous HCl, saturated aqueous sodium bicarbonate and brine. The organic phase was separated and dried over $MgSO_4$. Concentrating *in vacuo* gave a colourless oil that was purified by column chromatography, details are given with individual compounds.

* Where petroleum ether refers to the fractions distilled between 50-70 °C

General Procedure B: HATU mediated peptide coupling

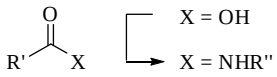

To an anhydrous solution of *N,N*-dimethylformamide was added the acid (1.0 equiv), amine (1.1 equiv) and HATU (1.1 equiv). The reaction mixture was stirred for 10 min at rt followed by the addition of DIPEA (4.0 equiv) and subsequently stirred at rt for 18 h. The reaction mixture was partitioned between ethyl acetate and 1M aqueous HCl. The organic phase was separated and washed sequentially with 1M aqueous HCl and brine. The organic phase was dried over $MgSO_4$, filtered and concentrated *in vacuo*. If required, products were purified by flash chromatography on silica.

General Procedure B2: Modified HATU mediated peptide coupling

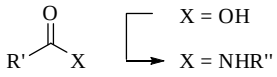

To a stirred solution of the acid (1.0 equiv) in dry *N,N*-dimethylformamide was added the amino alcohol (1.0 equiv), DIPEA (2.5 equiv), and HATU (1.2 equiv). The solution was stirred at rt overnight then diluted with ethyl acetate and washed with water and brine. The organic phase was separated, then dried over $MgSO_4$ and the solvent removed *in vacuo* to give a colourless oil. Purification by column chromatography afforded the desired product.

General Procedure C: EDCI mediated peptide coupling

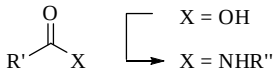

To an anhydrous solution of *N,N*-dimethylformamide was added the acid (1.0 equiv), EDCI (1.1 equiv), $HOBt.H_2O$ (1.1 equiv) and the amine (1.5 equiv). The reaction mixture was stirred for 10 min at rt followed by the addition of DIPEA (4.0 equiv) and subsequent stirring at rt for a further 18 h. The reaction mixture was partitioned between ethyl acetate

and 1M aqueous HCl. The organic phase was separated and sequentially washed with 1M aqueous HCl and brine. The organic phase was dried over $MgSO_4$, filtered and concentrated *in vacuo* to yield the dipeptide. Purification details are given with individual compounds.

General Procedure C2: Modified EDCI mediated peptide coupling

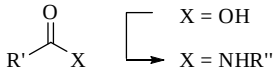

To an anhydrous solution of dichloromethane:*N,N*-dimethylformamide (9:1) at -10 °C was added the acid (1.0 equiv), EDCI (1.2 equiv), HOBt.H_2O (1.2 equiv) and *N*-hydroxyacetamidine (1.2 equiv). The reaction mixture was stirred for 30 min at -10 °C followed by the addition of DIPEA (1.2 equiv) and subsequently stirred at rt for a further 1.5 h. The solvents were concentrated *in vacuo* and the residue dissolved in ethyl acetate. The organic phase was separated and washed sequentially with saturated aqueous sodium bicarbonate, water, 0.5 M aqueous potassium hydrogen sulfate and brine. The organic phase was dried over $MgSO_4$, filtered and concentrated *in vacuo* to yield the product. Purification details are given with individual compounds.

General Procedure D: *N*-hydroxysuccinimide mediated peptide coupling

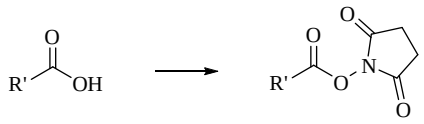

To a solution of *N*-hydroxysuccinimide ester (1.0 equiv) and amine (1.3 equiv) in dichloromethane was added DIPEA (1.5 equiv) and the resulting reaction mixture stirred at rt for 2 h. The reaction mixture was partitioned between dichloromethane and 1M aqueous HCl. The organic phase was separated and sequentially washed with saturated aqueous sodium bicarbonate and brine, dried over $MgSO_4$, filtered and the solvent removed under reduced pressure to give a white solid. Recrystallisation from ethyl acetate/petroleum ether gave the pure product.

General Procedure E: *N*-Boc cleavage

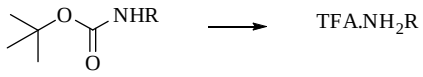

The *N*-Boc protected compound was dissolved in dichloromethane and 10% trifluoroacetic acid (v/v) added. The reaction mixture was stirred at rt for 18 h, then concentrated *in vacuo* to give the free amine as the trifluoroacetate salt.

General Procedure F: *N*-Boc protection of amino acids

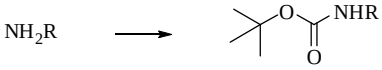

The amino acid was dissolved in a 1:1 biphasic mixture of water and dichloromethane. To this was added triethylamine (2.8 equiv) and di-*tert*-butyl dicarbonate (1.2 equiv). The reaction mixture was stirred at rt for 18 h then concentrated *in vacuo*. The residue was partitioned between ethyl acetate and 10% (w/w) aqueous citric acid. The organic phase was separated and the aqueous phase was extracted twice more with ethyl acetate. The combined organic phases were washed with brine, dried over $MgSO_4$, filtered and concentrated *in vacuo*.

General Procedure G: Ester hydrolysis with base

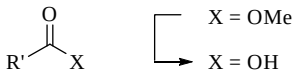

The ester was dissolved in a 3:1 mixture of methanol and water. Lithium hydroxide (5.0 equiv) was added and the mixture stirred at rt for 18 h. The reaction mixture was concentrated *in vacuo* and the resulting residue partitioned between ethyl acetate and 1M aqueous HCl. The organic phase was separated and the aqueous phase extracted twice more with ethyl acetate. The combined organic extracts were washed with brine, dried over

$MgSO_4$, filtered and concentrated *in vacuo*. Purification details are given with individual compounds.

General Procedure H: Esterification of acids

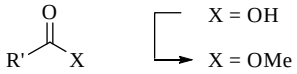

The carboxylic acid was suspended in ice-cold methanol and 20% (v/v) thionyl chloride was added in portions until the carboxylic acid was completely soluble. The ice-cold solution of the reaction mixture was stirred 1 h, followed by a further 18 h at rt before being concentrated *in vacuo* to give a white solid. No purification was necessary.

General Procedure I: Cyanohydrin formation

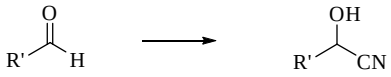

To a cooled solution (5 °C) of the aldehyde (1.0 equiv) in methanol was added a cooled (5 °C) aqueous solution of sodium hydrogen sulfite (1.0 equiv). The solution was stirred for 16 h at 4 °C then potassium cyanide (1.0 equiv) in ethyl acetate added. The biphasic reaction mixture was stirred for 4 h at rt. The organic layer was separated and the aqueous phase was extracted (x 2) with ethyl acetate. The separated organic phases were combined, washed with distilled water, dried over $MgSO_4$ and the solvent removed to yield the cyanohydrin as a mixture of diastereoisomers (1:1). Purification details are given with individual compounds.

General Procedure J: *Horner-Emmons-Wadsworth* reaction of aldehydes

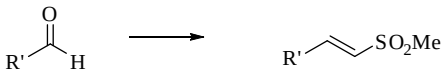

Ethylmethanesulfonylmethylphosphinoyl ethane (1.0 equiv) was dissolved in tetrahydrofuran and cooled to -78 °C. 15% butyllithium in tetrahydrofuran was added over 10 min and the reaction mixture stirred for 20 min at -78 °C. The aldehyde in tetrahydrofuran was added to the reaction mixture and subsequently stirred for a further 2 h at -78 °C. The solvent was removed *in vacuo* and the residue partitioned between water and ethyl acetate. The aqueous phase was separated and extracted twice more with ethyl acetate. The combined organic phases were successively washed with saturated aqueous sodium bicarbonate and brine, dried over $MgSO_4$, filtered and the solvent removed under reduced pressure to give the crude product. Purification was achieved by either column chromatography or recrystallisation; details are given with individual compounds.

General Procedure K: Reduction via lithium aluminium hydride

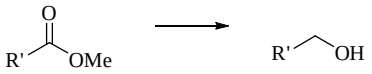

A solution of the methyl ester (1.0 equiv) tetrahydrofuran was cooled in an ice bath and 1M lithium aluminium hydride in diethyl ether (1.1 equiv) added. The ice cold reaction mixture was stirred for 1 h then warmed to rt and stirred for a further 17 h, after which methanol was added to quench the reaction. The reaction mixture was stirred at rt for 10 min then concentrated *in vacuo*. The resulting residue was partitioned between ethyl acetate and 1M aqueous potassium hydrogen sulfate. The aqueous phase was separated and extracted twice more with chloroform. The combined organic phases were washed with brine, dried over $MgSO_4$, filtered and concentrated *in vacuo*. Purification details are given with individual compounds.

General Procedure L: Oxidation via sulfur trioxide-pyridine (Parikh-Doering)[1]

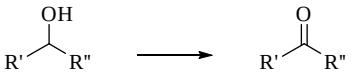

A solution of the alcohol in a 1:3 mixture dimethylsulfoxide and dichloromethane was cooled over an ice bath, followed by the addition of DIPEA (4.3 equiv). To this ice-cold reaction mixture a solution of SO_3.Pyr complex (4.5 equiv) dissolved in dimethylsulfoxide was added. The reaction mixture was maintained at a low temperature for a further 2 h (or until TLC indicated complete consumption of the starting alcohol). The reaction mixture was diluted with ethyl acetate and partitioned between ethyl acetate and 1M aqueous HCl. The organic phase was washed with saturated aqueous sodium bicarbonate and brine, dried over $MgSO_4$, filtered and concentrated *in vacuo*. Purification details are given with individual compounds.

General Procedure M: Oxidation via TEMPO-NaOCl[2]

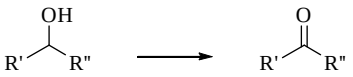

A buffered solution of sodium hypochlorite (5.25%, 9.7 mL commercial bleach, 15.3 mL distilled water) was prepared by addition of solid $NaHCO_3$ (*ca.* 300 mg) until the pH lay within the range 8.6-9.5.[†]

To a solution of the alcohol (1.0 equiv) in ice-cold dichloromethane (35 mL/mmol) was added KBr (0.2 equiv) and TEMPO (0.1 equiv). Buffered NaOCl (0.5 mL/mL dichloromethane) was added drop-wise and the reaction mixture stirred rapidly for 2 h over ice. The bi-phasic mixture was diluted with ethyl acetate and the organic phase separated, then washed with brine, dried over $MgSO_4$, filtered and concentrated *in vacuo*. Further purification of the crude product was achieved by recrystallisation or column chromatography; details are given with individual compounds.

[†] The required pH range for HOCl distribution between both phases

General Procedure M2: Modified Oxidation via TEMPO-NaOCl[3]

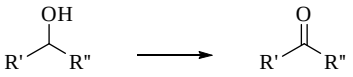

To an ice-cold solution of the alcohol (1.0 equiv) in dichloromethane (12.5 mL/mmol) was added buffered aqueous NaOCl solution (2.6%, 0.35 M, pH 8.6), (1.25 equiv), aqueous KBr solution (50 mM, 0.1 equiv) and TEMPO (0.01 equiv) in dichloromethane (400 µM). The ice-cold bi-phasic mixture was rapidly stirred for 2 h, diluted with a 4 x volume of ethyl acetate, washed with water then brine, dried over $MgSO_4$, filtered and concentrated *in vacuo*. Further purification of the crude product was achieved by recrystallisation or column chromatography; details are given with individual compounds.

General Procedure N: Preparation of diazomethane

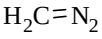

Aqueous potassium hydroxide (3.00 g in 10 ml) was added to dimethyl digol (20 ml) at 75 °C in one arm of a two-armed distillation apparatus. The biphasic mixture was stirred vigorously throughout the addition of Diazald (10.75 g) in ether (50 ml) over 40 min. The yellow ethereal diazomethane solution was collected over ice-cold potassium hydroxide. **WARNING**: diazomethane is explosive. Avoid contact with broken glass, ground glass joints and rough surfaces. No purification was needed.

General Procedure O: Semicarbazone reaction of aldehydes

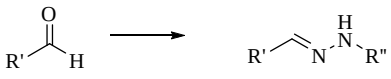

To an aqueous solution of sodium acetate (1.1 equiv) and semicarbazone (1.1 equiv) was added the aldehyde dissolved in a water miscible solvent. The reaction mixture was stirred for 20 h at rt, then water added until precipitation occurred. Ethyl acetate was added, the

organic phase separated, dried over $MgSO_4$, filtered and solvent removed to give the semicarbazone as a coloured solid. If purification was required the solid was recrystallised; details are given with individual compounds.

General Procedure P: *Wittig* Reaction of aldehydes

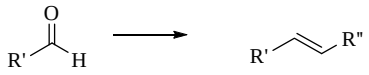

To a solution of the aldehyde (1.0 equiv) in dichloromethane was added the ylide (1.0 equiv). The reaction mixture was stirred at rt for 16 h then the solvent removed *in vacuo*. The resulting white solid was purified by column chromatography (diethyl ether) to remove the triphenylphosphine oxide by-product.

General Procedure Q: Epoxidation of bromomethyl alcohols

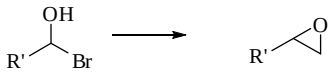

To a solution of the bromomethyl alcohol (1.0 equiv) in anhydrous methanol was added potassium carbonate (2.0 equiv). The reaction mixture was stirred for 1 h at rt then solvent removed *in vacuo*. The resulting residue was dissolved in ethyl acetate and successively washed with water and brine, dried over $MgSO_4$ and solvent removed *in vacuo* to give the epoxide. Purification details are given with individual compounds.

General Procedure R: Oxazoline ring formation

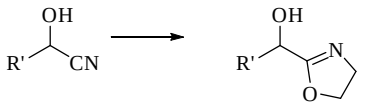

A solution of anhydrous methanol (19.0 equiv) in chloroform was cooled over an ice bath, after which acetyl chloride (16.0 equiv) was added dropwise. The reaction mixture was stirred for 15 min at low temperature then the cyanohydrin (1.0 equiv) in chloroform added. The reaction mixture was stirred for 16 h with gradual return to rt. The solvent and volatiles were removed *in vacuo* to give the intermediate imidate as an oily residue. The imidate was dissolved in dichloromethane along with ethanolamine (1.0 equiv) and triethylamine (1.0 equiv). The reaction mixture was stirred at rt for 16 h then diluted with ethyl acetate. The organic phase was washed with 1M aqueous sodium hydroxide and brine, dried over $MgSO_4$, filtered and the solvent removed *in vacuo* to give the crude product. Further purification was achieved using column chromatography; details are given with individual compounds.

General Procedure S: Tetrazole ring formation

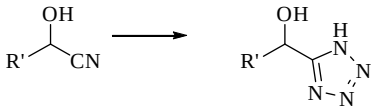

Triethylamine hydrochloride was prepared by the careful addition of triethylamine (3 mL) to hydrogen chloride in ether (10.5 mL) and subsequent removal of excess solvent.

The cyanohydrin (1.0 equiv), triethylamine hydrochloride (2.0 equiv) and sodium azide (2.0 equiv) were suspended in toluene. The reaction mixture was heated at reflux for 20 h. Upon cooling to rt, the reaction mixture was diluted with toluene and extracted with water (3 x 200 mL). The combined aqueous phases were acidified to pH 2 with 1M aqueous HCl. The resulting white precipitate was extracted with ethyl acetate (2 x 200 mL). The combined organic phases were washed with brine, dried over $MgSO_4$ and concentrated *in vacuo* to give the product as a colourless glassy solid. If purification was necessary,

recrystallisation from a minimal amount of ethyl acetate gave the pure product; details are given with individual compounds.

General Procedure T: Hydrogenation of a double bond

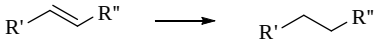

The olefin was dissolved in methanol and 20% (w/w) of 10% palladium on carbon catalyst added. The mixture was subjected to hydrogenation at rt and atmospheric pressure for 18 h. The resulting black suspension was filtered through celite and concentrated *in vacuo*. Recrystallisation from ethyl acetate afforded the pure product.

7.2 EXPERIMENTAL WORK AS DESCRIBED IN CHAPTER TWO

7.2.1 Synthesis of Peptidyl Aldehydes

Preparation of 2*S*-(4-fluorobenzenesulfonylamino)-3-methylbutyric acid (2.24)

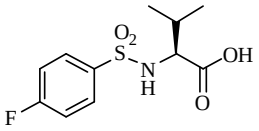

L-Valine (2.11 g, 18.0 mmol) and 1M aqueous sodium hydroxide (18 mL) were dissolved in an ice cold solution of 1:1 water:tetrahydrofuran. 1M aqueous sodium hydroxide (18 mL) and 4-fluorobenzenesulfonyl chloride **2.23** (3.05 g, 15.7 mmol) were added and the reaction mixture stirred at rt for 24 h. The reaction mixture was cooled over an ice bath and partitioned between ethyl acetate and 1M aqueous HCl. The organic phase was separated and washed with brine, dried over $MgSO_4$, filtered and solvent removed *in vacuo* to give the crude product. Purification was achieved by rinsing the crude product with 5% EtOAc in petroleum ether to give the pure product as a white solid (2.41g, 57%).

mp = 125-126 °C;

Spectral properties are in agreement with the literature.[4]

^{1}H NMR δ($CDCl_3$) 7.88-7.84 (2H, m, Ar**H** (Fps)), 7.19-7.14 (2H, m, Ar**H** (Fps)), 5.36 (1H, m, N**H**), 3.78 (1H, dd, *J* = 4.7 and 10.1 Hz, C**H**CH$(CH_3)_2$), 2.14-2.08 (1H, m, CHC**H**$(CH_3)_2$), 0.96 (3H, d, *J* = 6.8 Hz, CHCH(C**H$_3$**)$_2$), 0.87 (3H, d, *J* = 6.8 Hz, CHCH(C**H$_3$**)$_2$);

^{13}C NMR δ($CDCl_3$) 176.44, 165.16 (d, *J* = 255.4 Hz), 135.55 (d, *J* = 3.2 Hz), 130.00 (d, *J* = 9.4 Hz), 116.24 (d, *J* = 22.6 Hz), 60.7, 31.26, 18.98, 17.05;

$[\alpha]_D$ = +42.0 (c = 0.1 in $CHCl_3$);

HRMS (ES) 276.0697 (MH^+) $C_{11}H_{15}FNO_4S$ requires 276.0706;

ν_{max} (KBr) 3250 (SO_2NH), 1699 (CO_2H).

Preparation of 2*S*-(4-fluorobenzenesulfonylamino)-3-methylbutyric acid 2,5-dioxo-pyrrolidin-1-yl ester (2.25)

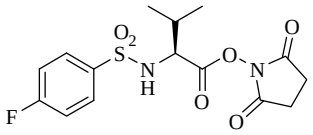

The *N*-terminal protected acid **2.24** (2.31 g, 8.39 mmol) and *N*-hydroxysuccinimide (1.16 g, 10.30 mmol) were dissolved in tetrahydrofuran (25 ml) and cooled over an ice bath. A solution of EDCI (2.01 g, 10.48 mmol) in dichloromethane (20 ml) was added dropwise to the reaction mixture at a low temperature. The reaction mixture was warmed to rt and stirred for a further 4 h then the solvent removed *in vacuo*. The resulting residue was dissolved in ethyl acetate. The organic phase was washed successively with 1M aqueous HCl, saturated aqueous sodium bicarbonate and brine, dried over $MgSO_4$, filtered and solvent removed *in vacuo* to give the crude product. Purification was achieved by rinsing the crude product with 5% ethyl acetate in petroleum ether to give the pure product as a white solid (2.99 g, 96%).

mp = 166-167 °C;

Spectral properties are in agreement with the literature.[4]

^{1}H NMR δ($CDCl_3$) 7.87-7.83 (2H, m, Ar**H** (Fps)), 7.20-7.15 (2H, m, Ar**H** (Fps)), 5.30 (1H, d, *J* = 10.3 Hz, N**H**), 4.22 (1H, dd, *J* = 4.6 and 10.3 Hz, C**H**CH(CH_3)$_2$), 2.77 (4H, s, C**H$_2$**C**H$_2$**), 2.38-2.27 (1H, m, CHC**H**(CH_3)$_2$), 1.10 (3H, d, *J* = 6.8 Hz, CHCH(C**H$_3$**)$_2$), 0.98 (3H, d, *J* = 6.8 Hz, CHCH(C**H$_3$**)$_2$);

^{13}C NMR δ($CDCl_3$) 168.23, 167.21, 165.25 (d, *J* = 255.0 Hz), 135.42 (d, *J* = 3.1 Hz), 129.71 (d, *J* = 9.6 Hz), 116.62 (d, *J* = 22.8 Hz), 59.24, 32.08, 25.45, 18.79, 16.77;

$[\alpha]_D$ = +10.0 (c = 0.1 in $CHCl_3$);

HRMS (ES) 373.0859 (MH^+) $C_{15}H_{18}FN_2O_6S$ requires 373.0870;

ν_{max} (KBr) 3290 (SO_2NH), 1741 (C=O), 1591 (C=O(Suc)).

Preparation of 2*S*-(4-fluorobenzenesulfonylamino)-*N*-(1*S*-hydroxymethyl-3-methyl-butyl)-3-methylbutyramide (2.6)

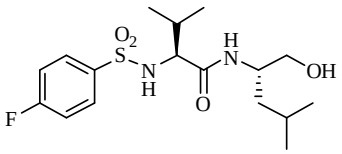

The ester **2.25** (1.28 g, 3.44 mmol) was coupled to *L*-leucinol (0.48 mL, 4.47 mmol) according to **General Procedure D** to afford the alcohol **2.6** as a white solid. No purification was required (0.80 g, 62 %).

mp >300 °C;

Spectral properties are in agreement with the literature.[4]

^{1}H NMR δ(CD_3OD) 7.91-7.87 (2H, m, Ar**H** (Fps)), 7.27-7.23 (2H, m, Ar**H** (Fps)), 3.76-3.71 (1H, m, C**H**$CH_2CH(CH_3)_2$), 3.55 (1H, d, *J* = 6.2 Hz, C**H**$CH(CH_3)_2$), 3.37 (1H, dd, *J* = 5.2 and 10.9 Hz, C**H$_2$**OH), 3.33 (1H, dd, *J* = 5.5 and 10.9 Hz, C**H$_2$**OH), 1.26-1.20 (2H, m, CHC**H$_2$**$CH(CH_3)_2$ and $CHCH_2$C**H**$(CH_3)_2$), 1.17-1.11 (1H, m, CHC**H$_2$**$CH(CH_3)_2$), 0.94 (3H, d, *J* = 6.8 Hz, $CHCH(C\mathbf{H_3})_2$), 0.88 (3H, d, *J* = 6.8 Hz, $CHCH(C\mathbf{H_3})_2$), 0.85 (3H, d, *J* = 6.2 Hz, $CHCH_2CH(C\mathbf{H_3})_2$), 0.77 (3H, d, *J* = 6.0 Hz, $CHCH_2CH(C\mathbf{H_3})_2$);

^{13}C NMR δ(CD_3OD) 172.57, 166.33 (d, *J* = 252.1 Hz), 138.49 (d, *J* = 3.3 Hz), 131.18 (d, *J* = 9.4 Hz), 117.10 (d, *J* = 22.8 Hz), 65.29, 63.23, 50.54, 41.03, 33.12, 25.54, 23.65, 22.38, 19.49, 18.20;

$[\alpha]_D$ = +8.0 (c = 0.1 in CH_3OH);

HRMS (ES) 397.1577 (MNa^+) $C_{17}H_{27}FN_2O_4$ SNa requires 397.1573;

ν_{max} (KBr) 3609 (CH_2OH), 3280 (SO_2NH), 2974 (C(O)NH).

Preparation of 2*S*-(4-fluorobenzenesulfonylamino)-*N*-(1*S*-formyl-3-methylbutyl)-3-methylbutyramide (2.3)

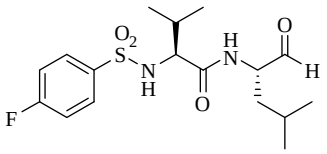

The alcohol **2.6** (0.40 g, 1.06 mmol) was oxidised according to **General procedure L** to afford the product as a white solid. Purification was not necessary (0.32 g, 82 %).

mp = 127-129 °C;

Spectral properties are in agreement with the literature.[4]

^{1}H NMR δ($CDCl_3$) 9.39 (1H, s, C**H**O), 7.88-7.85 (2H, m, Ar**H** (Fps)), 7.16-7.11 (2H, m, Ar**H** (Fps)), 6.72 (1H, d, *J* = 7.4 Hz, N**H**), 5.90 (1H, d, *J* = 8.8 Hz, N**H**), 4.32-4.28 (1H, m, C**H**$CH_2CH(CH_3)_2$), 3.63 (1H, dd, *J* = 5.7 and 8.8 Hz, C**H**$CH(CH_3)_2$), 2.08-2.04 (1H, m, CHC**H**$(CH_3)_2$), 1.55-1.47 (1H, m, CHC**H$_2$**$CH(CH_3)_2$), 1.42-1.35 (1H, m, CHC**H$_2$**$CH(CH_3)_2$), 1.30-1.23 (1H, m, $CHCH_2$C**H**$(CH_3)_2$), 0.93 (3H, d, *J* = 6.8 Hz, $CHCH_2CH(CH_3)_2$), 0.88 (3H, d, *J* = 6.6 Hz, $CHCH(CH_3)_2$), 0.85 (3H, d, *J* = 6.8 Hz, $CHCH_2CH(CH_3)_2$), 0.83 (3H, d, *J* = 6.6 Hz, $CHCH(CH_3)_2$);

^{13}C NMR δ($CDCl_3$) 199.30, 170.58, 164.27 (d, *J* = 255.2 Hz), 136.06 (d, *J* = 3.2 Hz), 129.43 (d, *J* = 9.3 Hz), 115.45 (d, *J* = 22.5 Hz), 61.43, 56.56, 36.60, 31.25, 23.86, 22.58, 21.00, 18.86, 16.94;

$[\alpha]_D$ = +16.0 (c = 0.1 in $CHCl_3$);

HRMS (ES) 373.1613 (MH^+) $C_{17}H_{26}FN_2O_4S$ requires 373.1597;

ν_{max} (KBr) 3260 (SO_2NH), 2968 (CONH), 1730 (CHO).

Preparation of *N*-(1*S*-benzyl-2-hydroxyethyl)-2*S*-(4-fluorobenzenesulfonylamino) -3-methylbutyl)-3-methylbutyramide (2.26)

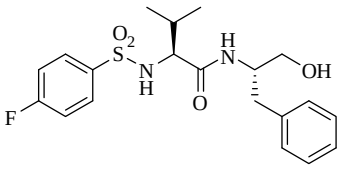

The ester **2.25** (1.28 g, 3.44 mmol) was couple to *L*-phenylalaninol (0.68 g, 4.47 mmol) according to **General Procedure D** to afford the crude alcohol **2.26**. Recrystallisation from ethyl acetate/petroleum ether gave the pure product as a white solid (1.28 g, 91 %).

mp = 125-126 °C;

Spectral properties are in agreement with the literature.[4]

^{1}H NMR δ(CD_3OD) 7.86-7.82 (2H, m, Ar**H** (Fps)), 7.81 (1H, d, *J* = 8.2 Hz, N**H**), 7.28-7.25 (2H, m, Ar**H** (Fps)), 7.22, 7.17 (5H, m, Ar**H** (Phe)), 3.90-3.93 (1H, m, C**H**CH_2C), 3.52 (1H, d, *J* = 6.4 Hz, C**H**$CH(CH_3)_2$), 3.37 (2H, d, *J* = 5.0 Hz, CHC**H$_2$**C), 2.73 (1H, dd, *J* = 7.4 and 13.7 Hz, C**H$_2$**OH), 2.50 (1H, dd, *J* = 7.2 and 13.7 Hz, C**H$_2$**OH), 1.91-1.84 (1H, m, CHC**H**$(CH_3)_2$), 0.82 (6H, dd, *J* = 6.9 and 7.7 Hz, CHCH(C**H$_3$**)$_2$);

^{13}C NMR δ(CD_3OD) 172.86, 166.37 (d, *J* = 252.4 Hz), 139.67, 138.32 (d, *J* = 3.2 Hz), 131.18 (d, *J* = 9.4 Hz), 130.32, 129.49, 127.46, 117.07 (d, *J* = 22.9 Hz), 63.79, 63.39, 54.35, 37.79, 32.73, 19.71, 18.29;

$[\alpha]_D$ = -20.0 (c = 0.1 in CH_3OH);

HRMS (ES) 409.1586 (MH^+) $C_{20}H_{26}FN_2O_4S$ requires 409.1597;

ν_{max} (KBr) 3600 (CH_2OH), 3277 (SO_2NH), 2966 (C(O)NH).

Preparation of *N*-(1*S*-benzyl-2-oxoethyl)-2*S*-(4-fluorobenzenesulfonylamino)-3-methylbutyramide (2.27)

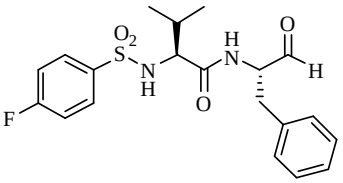

The alcohol **2.26** (1.28 g, 3.13 mmol) was oxidised according to **General procedure L** to afford the product as a white solid. Purification was not necessary (1.02 g, 79 %).

mp = 154-155 °C;

Spectral properties are in agreement with the literature.[4]

^{1}H NMR δ((CD$_3$)$_2$CO) 9.33 (1H, s, C**H**O), 7.90-7.84 (2H, m, Ar**H** (Fps)), 7.31-7.16 (7H, m, Ar**H** (Fps and Phe)), 6.58 (1H, d, *J* = 9.4 Hz, N**H**), 4.33-4.27 (1H, m, C**H**CH$_2$C), 3.80-3.78 (1H, m, C**H**CH(CH$_3$)$_2$), 3.09 (1H, dd, *J* = 5.4 and 14.3 Hz, CHC**H$_2$**C), 2.87 (1H, dd, *J* = 8.4 and 14.3 Hz, CHC**H$_2$**C), 2.02-1.94 (1H, m, CHC**H**(CH$_3$)$_2$), 0.87 (3H, d, *J* = 6.8 Hz, CHCH(C**H$_3$**)$_2$), 0.82 (3H, d, *J* = 6.8 Hz, CHCH(C**H$_3$**)$_2$);

^{13}C NMR δ((CD$_3$)$_2$CO) 206.33, 199.30, 171.52, 165.59 (d, *J* = 251.6 Hz), 138.05 (d, *J* = 5.6 Hz), 130.89 (d, *J* = 9.4 Hz), 130.00, 129.24, 127.41, 116.68 (d, *J* = 22.7 Hz), 62.20, 60.99, 34.81, 32.34, 19.58, 17.56;

[α]$_D$ = +37.0 (c = 0.1in CHCl$_3$);

HRMS (ES) 407.1444 (MH$^+$) $C_{20}H_{23}FN_2O_4S$ requires 407.1441;

ν$_{max}$ (KBr) 3261 (SO$_2$NH), 2968 (C(O)NH), 1732 (CHO)

Preparation of [1*S*-(1*S*-hydroxymethyl-3-methylbutylcarbamoyl)-2-methylpropyl]-carbamic acid benzyl ester (2.29)

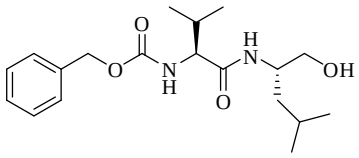

Cbz-*L*-valine **2.28** (2.00 g, 8.36 mmol) was coupled to *L*-leucinol (1.07 mL, 8.36 mmol) according to **General procedure B2** to give the crude alcohol **2.29**. Flash chromatography (60:40 ethyl acetate:petroleum ether) gave the pure product as a white solid (2.11 g, 72%).

mp = 119-120 °C;

Spectral properties are in agreement with the literature.[5]

^{1}H NMR δ(CD$_3$OD) 7.37-7.28 (5H, m, Ar**H** (Cbz)), 5.12 (1H, d, *J* = 12.5 Hz, CC**H$_2$**O), 5.06 (1H, d, *J* = 12.5 Hz, CC**H$_2$**O), 4.01-3.96 (1H, m, C**H**CH$_2$CH(CH$_3$)$_2$), 3.90-3.87 (1H, m, C**H**CH(CH$_3$)$_2$), 3.49-3.41 (2H, m, C**H$_2$**OH), 2.06-2.00 (1H, m, CHC**H**(CH$_3$)$_2$), 1.70-1.62 (1H, m, CHC**H$_2$**CH(CH$_3$)$_2$), 1.44-1.33 (2H, m, CHC**H$_2$**CH(CH$_3$)$_2$ and CHCH$_2$C**H**(CH$_3$)$_2$), 0.96-0.88 (12H, m, CHCH(C**H$_3$**)$_2$ and CHCH$_2$CH(C**H$_3$**)$_2$);

^{13}C NMR δ(CD$_3$OD) 173.92, 158.50, 138.19, 129.44, 128.98, 128.80, 67.63, 65.57, 62.38, 50.66, 41.03, 31.83, 25.79, 23.84, 22.29, 19.82, 18.65;

[α]$_D$ = -23.0 (c = 0.1 in CH$_3$OH);

HRMS (ES) 351.2278 (MH^+) $C_{19}H_{31}N_2O_4$ requires 351.2284;

ν_{max} (KBr) 3330 (CH_2OH), 2976 (CONH), 1693 (OC=O).

Preparation of [1*S*-(1*S*-formyl-3-methylbutylcarbamoyl)-2-methylpropyl]carbamic acid benzyl ester (2.19)

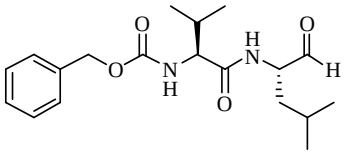

The alcohol **2.29** (2.00 g, 5.71 mmol) was oxidised according to **General procedure L** to give the pure product as a white solid. Purification was not necessary (1.83 g, 91%).

mp = 136-138 °C;

Spectral properties are in agreement with the literature.[5]

^{1}H NMR δ($CDCl_3$) 9.56 (1H, s, C**H**O), 7.38-7.32 (5H, m, Ar**H** (Cbz)), 6.34 (1H, d, *J* = 7.3 Hz, N**H**), 5.36 (1H, d, *J* = 8.7 Hz, N**H**), 5.41 (2H, s, CC**H$_2$**O), 4.57-4.53 (1H, m, C**H**$CH_2CH(CH_3)_2$), 4.05 (1H, t, *J* = 8.3 Hz, C**H**$CH(CH_3)_2$), 2.18-2.12 (1H, m, CHC**H**$(CH_3)_2$), 1.75-1.66 (2H, m, CHC**H$_2$**$CH(CH_3)_2$), 1.47-1.40 (1H, m, $CHCH_2$C**H**$(CH_3)_2$), 0.99 (3H, d, *J* = 6.8 Hz, $CHCH_2CH(C$**H$_3$**$)_2$), 0.94 (9H, m, $CHCH(C$**H$_3$**$)_2$ and $CHCH_2CH(C$**H$_3$**$)_2$);

^{13}C NMR δ($CDCl_3$) 199.11, 171.49, 156.38, 128.53, 128.20, 127.97, 67.07, 60.33, 57.27, 37.72, 30.97, 24.72, 23.00, 21.84, 21.84, 19.19, 17.76;

$[\alpha]_D$ = +12.0 (c = 0.1 in $CHCl_3$);

HRMS (ES) 349.2119 (MH^+) $C_{19}H_{28}N_2O_4$ requires 349.2127;

ν_{max} (KBr) 2958 (CONH), 1732 (CHO), 1693 (OC=O).

Preparation of [1*S*-(1*S*-hydroxymethyl-2-phenylethylcarbamoyl)-2-methylpropyl]-carbamic acid benzyl ester (2.30)

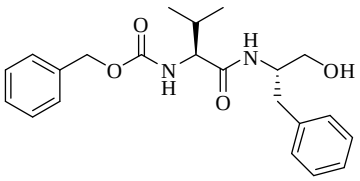

Cbz-*L*-valine **2.28** (1.00 g, 4.18 mmol) was coupled to *L*-phenylalaninol (0.63 g, 4.18 mmol) according to **General procedure B2**. The crude alcohol **2.30** was recrystallised from ethyl acetate/petroleum ether to afford the pure product (1.32 g, 82%).

mp = 108-110 °C;

^{1}H NMR δ((CD$_3$)$_2$CO) 7.39-7.18 (10H, m, Ar**H** (Cbz and Phe)), 6.93 (1H, d, *J* = 9.2 Hz, N**H**), 5.09 (2H, bs, CC**H$_2$**O), 4.16-4.10 (1H, m, C**H**CH$_2$C), 3.89-3.83 (1H, m, C**H**CH(CH$_3$)$_2$), 3.50 (2H, d, *J* = 5.3 Hz, CHC**H$_2$**OH), 2.91 (1H, dd, *J* = 6.1 and 13.5 Hz, CHC**H$_2$**C), 2.72 (1H, dd, *J* = 8.6 and 13.5 Hz CHC**H$_2$**C), 2.01-1.91 (1H, CHC**H**(CH$_3$)$_2$), 0.88-0.83 (6H, m, CHCH(C**H$_3$**)$_2$);

^{13}C NMR δ((CD$_3$)$_2$CO) 207.39, 207.20, 140.92, 130.98, 130.112, 129.99, 129.90, 129.73, 129.39, 127.55, 67.35, 64.27, 62.28, 54.46, 38.36, 32.52, 20.62, 19.30;

$[\alpha]_D$ = -11.0 (c = 0.1 in CH$_3$OH);

HRMS (ES) 407.1947 (MNa$^+$) C$_{22}$H$_{28}$N$_2$O$_4$Na requires 407.1947;

ν_{max} (KBr) 3278 (CH$_2$OH), 2961 (C(O)NH), 1691 (OC=O).

Preparation of [1*S*-(1*S*-benzyl-2-oxoethylcarbamoyl)-2-methylpropyl]carbamic acid benzyl ester (2.2)

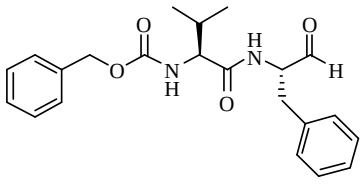

The alcohol **2.30** (1.26 g, 3.74 mmol) was oxidised according to **General procedure L** to give the pure product as a white solid. Purification was not necessary (1.30 g, 91%).

mp = 112-113 °C;

Spectral properties are in agreement with the literature.[6]

^{1}H NMR δ((CD$_3$)$_2$CO) 9.61 (1H, s, C**H**O), 7.70 (1H, d, *J* = 8.6 Hz, N**H**), 7.38-7.35 (5H, m, Ar**H** (Cbz)), 7.27-7.23 (5H, m, Ar**H** (Phe)), 6.34 (1H, d, *J* = 9.2 Hz, N**H**), 5.10 (1H, d, *J* = 12.5 Hz, CC**H$_2$**O), 5.07 (1H, d, *J* = 12.5 Hz, CC**H$_2$**O) , 4.55-4.51 (1H, m, C**H**CH$_2$C), 4.10-4.06 (1H, m, C**H**CH(CH$_3$)$_2$), 3.25 (1H, dd, *J* = 5.1 and 14.2 Hz, CHC**H$_2$**C), 2.97 (1H, dd, *J* = 8.8 and 14.2 Hz, CHC**H$_2$**C), 2.15-2.06 (1H, m, CHC**H**(CH$_3$)$_2$), 0.93 (3H, d, *J* = 6.8 Hz, CHCH(C**H$_3$**)$_2$), 0.89 (3H, d, *J* = 6.8 Hz, CHCH(C**H$_3$**)$_2$);

^{13}C NMR δ((CD$_3$)$_2$CO) 207.20, 200.94, 173.55, 158.14, 139.25, 139.13, 131.13, 130.18, 129.61, 129.57, 128.30, 67.79, 62.11, 61.98, 35.88, 32.57, 20.71, 19.02;

$[\alpha]_D$ = -6.0 (c = 0.1 in CH$_3$OH);

HRMS (ES) 383.1979 (MH$^+$) $C_{22}H_{26}N_2O_4$ requires 383.1971;

ν_{max} (KBr) 2966 (CONH), 1730 (CHO), 1639 (OC=O).

Preparation of [1*S*-(1*S*-hydroxymethyl-3-methylbutylcarbamoyl)-2-methylpropyl]-carbamic acid *tert*-butyl ester (2.32)

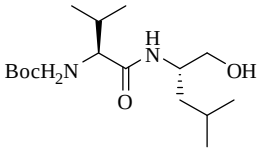

N-Boc-*L*-valine **2.31** (4.63 g, 21.35 mmol) was coupled to *L*-leucinol (2.73 mL, 21.35 mmol) according to **General Procedure B2**. The crude material was purified by flash chromatography on silica using a gradient of EtOAc and (50/70) pet ether to yield a white solid (2.30 g, 68%).

mp = 54-56 ºC ;

^{1}H NMR δ(CDCl$_3$) 6.24 (1H, d, *J* = 7.9 Hz, N**H** Leu), 5.10 (1H, d, *J* = 7.32 Hz, N**H** Val), 3.99–4.06 (1H, m, C**H**CH$_2$CH(CH$_3$)$_2$), 3.80 (1H, dd, *J* = 7.3 and 7.3 Hz, C**H**CH(CH$_3$)$_2$), 3.65 (1H, dd, *J* = 3.2 and 11.1 Hz, C**H$_2$**OH), 3.50 (1H, dd *J* = 5.6Hz and 11.1 Hz, C**H$_2$**OH), 2.06-2.16 (1H, m, CHC**H**(CH$_3$)$_2$), 1.58-1.62 (1H, m, CHCH$_2$C**H**(CH$_3$)$_2$), 1.43 (9H, s, C(C**H$_3$**)$_3$), 0.88-0.97 (12H, m, CHCH$_2$CH(C**H$_3$**)$_2$ and CHCH(C**H$_3$**)$_2$);

^{13}C NMR δ(CD$_3$OD) 172.95, 163.32, 79.20, 64.31, 60.74, 49.32, 39.80, 30.45, 27.48, 24.46, 22.69, 21.05, 18.56, 17.32;

HRMS (ES) 317.2249 (MH$^+$) $C_{16}H_{32}N_2O_4$ requires 317.2240.

Preparation of 2*S*-amino-*N*-(1*S*-hydroxymethyl-3-methylbutyl)-3-methylbutyr-amide trifluoroacetate salt (2.33)

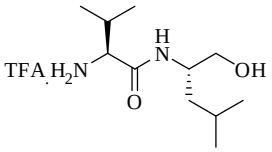

N-Boc protected compound **2.32** (2.30 g, 7.23 mmol) was deprotected using **General Procedure E** to afford a white solid. Purification was not necssary (1.57 g, 100%).

mp = 64-66 ºC;

^{1}H NMR δ((CD$_3$)$_2$SO) 8.13 (2H, bs, N**H$_2$**) 4.72-4.77 (1H, m, C**H**CH$_2$CH(CH$_3$)$_2$), 3.79-3.87 (1H, m, C**H**CH(CH$_3$)$_2$) 3.52-3.56 (1H, m, C**H$_2$**OH), 3.26 (1H, dd, *J* = 6.0 and 16.0 Hz, C**H$_2$**OH), 2.02-2.08 (1H, m, CHC**H**(CH$_3$)$_2$), 1.60-1.68 (1H, m, CHCH$_2$C**H**(CH$_3$)$_2$), 1.30-1.33 (2H, m, CHC**H$_2$**CH(CH$_3$)$_2$), 0.85-0.94 (12H, m, CHCH$_2$CH(C**H$_3$**)$_2$ and CHCH(C**H$_3$**)$_2$);

^{13}C NMR δ((CD$_3$)$_2$SO) 167.19 63.43, 57.35, 49.25, 29.71, 23.94, 23.33, 21.97, 18.21, 17.90;

HRMS (ES) 217.1910 (MH$^+$) C$_{11}$H$_{24}$N$_2$O$_2$ requires 217.1916.

Preparation of 1*H*-pyrrole-2-carboxylic acid [1*S*-(1*S*-hydroxymethylbutyl-carbamoyl)-2-methylpropyl]amide (2.35)

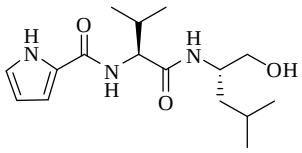

Reaction of the free amine **2.33** (0.70 g, 2.77 mmol) with 2-pyrrole carboxylic acid (0.31 g, 2.77 mmol) according to **General procedure C** gave **2.35** as an orange solid (0.73 g, 85%).

mp = 110-112 ºC ;

^{1}H NMR δ(CD$_3$OD) 7.85 (1H, d, *J* = 9.8 Hz, N**H**), 7.60 (1H, d, *J* = 9.8 Hz, N**H**), 6.86-6.87 (1H, m, C**H**CHCH), 6.91-6.92 (1H, m, C**H**CHCH), 6.16-6.17 (1H, m, CHC**H**CH), 4.26 (1H, dd, *J* = 9.8 and 2.1 Hz, C**H**CH(CH$_3$)$_2$), 3.98-4.02 (1H, m, C**H**CH$_2$CH(CH$_3$)$_2$), 3.43-3.48 (2H, m, C**H$_2$**OH), 2.11-2.12 (1H, m, C**H**(CH$_3$)$_2$), 1.55-1.59 (1H, m,

$CH_2C\mathbf{H}(CH_3)_2$), 1.35-1.40 (2H, m, $C\mathbf{H_2}CH(CH_3)_2$), 0.97-1.00 (6H, m, $CHCH_2CH(C\mathbf{H_3})_2$), 0.89 (3H, d, *J* = 7.2 Hz, $CHCH(C\mathbf{H_3})_2$), 0.86 (3H, d, *J* = 7.2 Hz, $CHCH(C\mathbf{H_3})_2$);

^{13}C NMR δ(CD_3OD) 174.21, 163.67, 126.76, 123.56, 112.82, 110.60, 65.83, 60.62, 51.09, 41.32, 31.94, 26.15, 24.03, 22.69, 20.26, 19.48;

HRMS (ES) 310.2134 (MH^+) $C_{16}H_{28}N_3O_3$ requires 310.2131;

ν_{max} (KBr) 3415 (CH_2OH), 2648 (CONH).

Preparation of 1*H*-pyrrole-2-carboxylic acid [1*S*-(1*S*-formyl-3-methylbutyl-carbamoyl)-2-methylpropyl]amide (2.21)

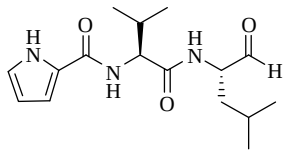

Oxidation of **2.35** (0.37 g, 1.18 mmol) according to **General procedure L** gave the pure product **2.21** as a colourless crystalline solid (0.26 g, 84%).

mp = 165-167 ºC;

^{1}H NMR δ(CD_3OD) 11.45 (1H, s, N**H**), 9.36 (1H, s, C**H**O), 8.40 (1H, d, *J* = 9.4 Hz, N**H**), 7.92 (1H, d, *J* = 9.1 Hz, N**H**), 6.85-6.87 (1H, m, C**H**CHCH), 6.83-6.85 (1H, m, C**H**CHCH), 6.03-6.05 (1H, m, C**H**CHCH), 4.30 (1H, m, $C\mathbf{H}CH(CH_3)_2$), 4.02-4.07 (1H, m, $C\mathbf{H}CH_2CH(CH_3)_2$), 2.10-2.15 (1H, m, $C\mathbf{H}(CH_3)_2$), 1.53-1.56 (1H, m, $CH_2C\mathbf{H}(CH_3)_2$), 1.33-1.38 (2H, m, $C\mathbf{H_2}CH(CH_3)_2$), 0.89 (3H, d, *J* = 12.0 Hz, $CHCH_2CH(C\mathbf{H_3})_2$), 0.87 (3H, d, *J* = 12.0 Hz, $CHCH_2CH(C\mathbf{H_3})_2$), 0.81 (3H, d, *J* = 11.5 Hz, $CHCH(C\mathbf{H_3})_2$), 0.79 (3H, d, *J* = 10.5 Hz, $CHCH(C\mathbf{H_3})_2$);

^{13}C NMR δ($(CD_3)_2SO$) 201.36, 172.08, 160.53, 125.91, 121.60, 111.23, 108.76, 57.99, 56.89, 36.41, 30.34, 23.28, 21.42, 19.44, 18.80, 18.72;

HRMS (ES) 308.1961 (MH^+) $C_{16}H_{26}N_3O_3$ requires 308.1974;

ν_{max} (KBr) 1741 (CHO), 1651 (CONH).

Preparation of *N*-(1*S*-hydroxymethyl-3-methylbutyl)-3-methyl-2*S*-(2-thiophen-2-ylacetylamino)butyramide (2.36)

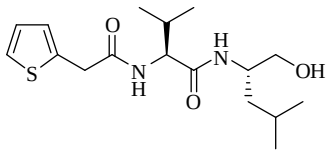

Reaction of the free amine **2.33** (0.70 g, 2.77 mmol) with 2-thiophene acetyl chloride according to **General procedure A** gave **2.36** as an orange solid. Flash chromatography on silica (1:1 ethyl acetate/petroleum ether) gave the pure product (0.46 g, 49%).

mp = 158-160 ºC;

^{1}H NMR δ(CD_3OD), 8.03 (1H, d, *J* = 9.3 Hz, N**H**), 7.75 (1H, d, *J* = 9.4 Hz, N**H**), 7.25 (1H, d, *J* = 5.5 Hz, C**H**CHCH), 6.93-6.94 (2H, m, CHC**H**CH), 4.11 (1H, t, *J* = 7.5 Hz, C**H**CH(CH_3)$_2$), 3.96-3.97 (1H, m, C**H**CH_2CH(CH_3)$_2$), 3.73-3.81 (2H, m, C**H$_2$**C(O)NH), 3.39-3.47 (2H, m, C**H$_2$**OH), 2.00-2.05 (1H, m, C**H**(CH_3)$_2$), 1.59-1.61 (1H, m, CH_2C**H**(CH_3)$_2$), 1.33-1.37 (2H, m, C**H$_2$**CH(CH_3)$_2$), 0.93 (3H, d, *J* = 7.2 Hz, CHCH_2CH(C**H$_3$**)$_2$), 0.91 (3H, d, *J* = 7.2 Hz, CHCH_2CH(C**H$_3$**)$_2$), 0.88 (3H, d, *J* = 7.0 Hz, CHCH(C**H$_3$**)$_2$), 0.85 (3H, d, *J* = 7.0 Hz, CHCH(C**H$_3$**)$_2$);

^{13}C NMR δ(CD_3OD), 173.5, 173.0, 138.4, 128.1, 127.9, 126.0, 65.9, 60.9, 51.1, 38.0, 32.1, 30.1, 26.0, 24.1, 22.5, 20.0, 19.0;

HRMS (ES) 341.1893 (MH^+) $C_{17}H_{29}N_2O_3S$ requires 341.1899;

ν_{max} (KBr) 3350 (CH_2OH), 1647 (CONH).

Preparation of *N*-(1*S*-formyl-3-methylbutyl)-3-methyl-2*S*-(2-thiophen-2-ylacetyl-amino)butyramide (2.22)

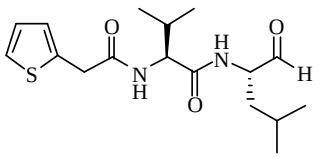

Oxidation of **2.36** (0.40 g, 1.17 mmol) according to **General procedure L** gave **2.22** as a colourless crystalline solid (0.26 g, 84%).

mp = 134-136 °C;

^{1}H NMR δ((CD$_3$)$_2$SO) 8.51 (1H, d, *J* = 6.5 Hz, N**H**), 8.28 (1H, d, *J* = 9.0 Hz, N**H**), 7.42-7.44 (1H, m, C**H**CHCH), 7.02-7.04 (1H, m, C**H**CHCH), 6.99-7.01 (2H, m, CHC**H**CH), 4.32 (1H, t, *J* = 8.5 Hz, C**H**CH(CH$_3$)$_2$), 4.19-4.21 (1H, m, C**H**CH$_2$CH(CH$_3$)$_2$), 3.73-3.81 (2H, dd, *J* = 38.0 and *J* = 15.5 Hz, C**H$_2$**C(O)NH), 2.07-2.09 (1H, m, C**H**(CH$_3$)$_2$), 1.60-1.62 (1H, m, CH$_2$C**H**(CH$_3$)$_2$), 1.50-1.53 (2H, m, C**H$_2$**CH(CH$_3$)$_2$), 0.98 (3H, d, *J* = 6.5 Hz, CHCH$_2$CH(C**H$_3$**)$_2$), 0.94 (3H, d, *J* = 8.3 Hz, CHCH$_2$CH(C**H$_3$**)$_2$), 0.93 (3H, d, *J* = 7.4 Hz, CHCH(C**H$_3$**)$_2$), 0.91 (3H, d, *J* = 10.3 Hz, CHCH(C**H$_3$**)$_2$);

^{13}C NMR δ((CD$_3$)$_2$SO) 18.20, 19.32, 21.44, 23.18, 24.16, 30.73, 36.38, 39.02, 56.88, 57.65, 124.87, 126.01, 126.69, 138.04, 169.25, 171.58, 201.24;

HRMS (ES) 339.1753 (MH$^+$) C$_{17}$H$_{27}$N$_2$O$_3$S requires 339.1742;

ν_{max} (KBr) 1726 (CHO), 1638 (CONH);

7.2.2 Synthesis of Semicarbazones

Preparation of 2*S*-(4-fluorobenzenesulfonylamino)-*N*-(1*S*-semicarbazone-3-methylbutyl)-3-methylbutyramide (2.37)

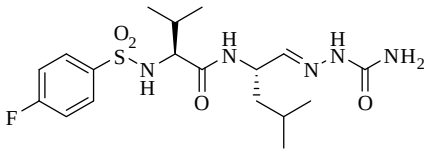

The aldehyde **2.3** (0.10 g, 0.268 mmol) in 1:1 tetrahydrofuran:water was reacted with semicarbazide hydrochloride (0.033 g, 0.295 mmol) according to **General Procedure O** to give the product as a white solid (0.10 g, 90%)

mp = 104-106 °C (lit.[7] mp = 100-102 °C);

^{1}H NMR δ((CD$_3$)$_2$SO) 9.86 (1H, s, CH=NN**H**C(O)NH$_2$), 7.92 (1H, d, *J* = 8.0 Hz, CHC**H**=N), 7.83-7.80 (2H, m, Ar**H** (Fps)), 7.38-7.34 (2H, m, Ar**H** (Fps)), 7.00 (1H, d, *J* = 4.1 Hz, N**H**), 6.23 (1H, bs, N**H$_2$**), 4.23-4.16 (1H, m, C**H**CH$_2$CH(CH$_3$)$_2$), 3.58-3.52 (1H, m, C**H**CH(CH$_3$)$_2$), 1.85-1.77 (1H, m, CHC**H**(CH$_3$)$_2$), 1.24-1.12 (2H, m, CHC**H$_2$**CH(CH$_3$)$_2$ and CHCH$_2$C**H**(CH$_3$)$_2$), 1.07-0.98 (1H, m, CHC**H$_2$**CH(CH$_3$)$_2$), 0.81-0.77 (9H, m, CHCH(C**H$_3$**)$_2$ and CHCH$_2$CH(C**H$_3$**)$_2$), 0.72 (3H, d, *J* = 5.7 Hz, CHCH(C**H$_3$**)$_2$);

^{13}C δ((CD$_3$)$_2$SO) 169.19, 162.91, 161.35 (d, *J* = 256.3 Hz), 156.69, 141.86, 137.63 (d, *J* = 3.0 Hz), 129.44 (d, *J* = 9.4 Hz), 115.82 (d, *J* = 22.9 Hz), 61.29, 47.69, 41.65, 31.15, 23.74, 22.58, 21.95, 19.08, 18.08;

HRMS (ES) 430.1935 (MH$^+$) $C_{18}H_{29}FN_5O_4S$ requires 430.1924;

$[\alpha]_D$ = +6.0 (c = 0.1 in (CH$_3$)$_2$SO);

Preparation of 2*S*-(4-fluorobenzenesulfonylamino)-*N*-(1*S*-thiosemicarbazone-3-methylbutyl)-3-methylbutyramide (2.28)

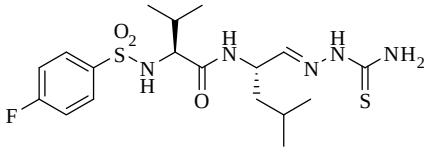

The aldehyde **2.3** (0.10 g, 0.268 mmol) in 1:1 tetrahydrofuran:water was reacted with thiosemicarbazone hydrochloride (0.027 g, 0.295 mmol) according to **General Procedure O** to give the product as a yellow solid (0.067 g, 54%)

mp = 101-103 °C;

^{1}H NMR δ((CD$_3$)$_2$SO) 9.13 (1H, s, CH=NN**H**C(O)NH$_2$), 7.96 (1H, d, *J* = 4.9 Hz, N**H**), 7.95 (1H, d, *J* = 6.1 Hz, CHC**H**=N) 7.83-7.80 (2H, m, Ar**H** (Fps)), 7.37-7.33 (2H, m, Ar**H** (Fps)), 7.26 (1H, d, *J* = 4.1 Hz, N**H**), 5.57 (1H, bs, N**H$_2$**), 4.30-4.23 (1H, m, C**H**CH$_2$CH(CH$_3$)$_2$), 4.06-4.03 (1H, m, C**H**CH(CH$_3$)$_2$), 1.87-1.77 (1H, m, CHC**H**(CH$_3$)$_2$), 1.20-1.11 (2H, m, CHC**H$_2$**CH(CH$_3$)$_2$ and CHCH$_2$C**H**(CH$_3$)$_2$), 1.07-1.00 (1H, m, CHC**H$_2$**CH(CH$_3$)$_2$), 0.84-0.73 (12H, m, CHCH(C**H$_3$**)$_2$ and CHCH$_2$CH(C**H$_3$**)$_2$);

^{13}C δ((CD$_3$)$_2$SO) 162.98, 156.79 (d, *J* = 250.8 Hz), 137.68, 128.79 (d, *J* = 3.3 Hz), 121.63 (d, *J* = 9.4 Hz), 107.5 (d, *J* = 22.9 Hz), 53.80, 32.96, 23.26, 15.96, 13.50, 12.87, 10.17, 8.68;

$[\alpha]_D$ = +66.0 (c = 0.1 in (CH$_3$)$_2$SO);

HRMS (ES) 446.1695 (MH$^+$) $C_{18}H_{29}FN_5O_3S_2$ requires 446.1696;

ν_{max} (KBr) 3269 (SO_2NH), 2959 (C(O)NH), 1593 (NHS=C).

Preparation of 2*S*-(4-fluorobenzenesulfonylamino)-*N*-[1*S*-(4-phenylsemicarbazone)-3-methylbutyl]-3-methylbutyramide (2.39)

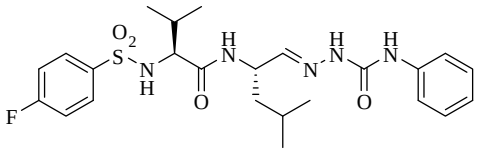

The aldehyde **2.3** (0.10 g, 0.268 mmol) in methanol was reacted with 4-phenyl semicarbazide hydrochloride (0.055 g, 0.295 mmol) according to **General Procedure O** to give the product as a brown solid (0.11 g, 82%)

mp = 200-201 °C;

^{1}H NMR δ((CD$_3$)$_2$SO) 10.40 (1H, s, NN**H**C(O)NHPh), 8.60 (1H, s, NNHC(O)N**H**Ph), 8.10 (1H, d, *J* = 8.6 Hz, N**H**), 7.96 (1H, d, *J* = 9.4 Hz, N**H**), 7.85-7.82 (2H, m, Ar**H** (Fps)), 7.55 (2H, d, *J* = 7.6 Hz, Ar**H** (Ph)), 7.39-7.36 (2H, m, Ar**H** (Fps)), 7.27 (2H, t, *J* = 7.6 Hz, Ar**H** (Ph)), 7.13 (1H, d, *J* = 4.1 Hz, CHC**H**=NNHC(O)NHPh), 6.99 (1H, t, *J* = 7.6 Hz, Ar**H**(Ph)), 4.36-4.31 (1H, m, C**H**CH$_2$CH(CH$_3$)$_2$), 3.63-3.60 (1H, m, C**H**CH(CH$_3$)$_2$), 1.89-1.83 (1H, m, CHC**H**(CH$_3$)$_2$), 1.27-1.22 (1H, m, CHCH$_2$C**H**(CH$_3$)$_2$), 1.19-1.13 (1H, m, CHC**H$_2$**CH(CH$_3$)$_2$), 1.10-1.05 (1H, m, CHC**H$_2$**CH(CH$_3$)$_2$), 0.84 (3H, d, *J* = 6.5 Hz, CHCH(C**H$_3$**)$_2$), 0.81 (3H, d, *J* = 3.0 Hz, CHCH$_2$CH(C**H$_3$**)$_2$), 0.79 (3H, d, *J* = 3.0 Hz, CHCH$_2$CH(C**H$_3$**)$_2$), 0.75 (3H, d, *J* = 6.5 Hz, CHCH(C**H$_3$**)$_2$);

^{13}C NMR δ((CD$_3$)$_2$SO) 169.29, 168.07 (d, *J* = 252.4 Hz), 162.97, 152.97, 152.90, 143.42, 138.94 (d, *J* = 2.0 Hz), 129.45 (d, *J* = 9.4 Hz), 128.59, 122.40, 119.14, 115.88 (d, *J* = 22.5 Hz), 61.30, 47.71, 41.90, 31.30, 23.83, 22.75, 21.86, 19.15, 18.04;

$[\alpha]_D$ = +3.0 (c = 0.1 in (CH$_3$)$_2$SO);

HRMS (ES) 506.2242 (MH$^+$) C$_{24}$H$_{33}$FN$_5$O$_4$S requires 506.2237;

ν_{max} (KBr) 3499 (C(O)NH$_2$), 3283 (SO$_2$NH), 2963 (C(O)NH), 2503 (C=NNH).

Preparation of 2*S*-(4-fluorobenzenesulfonylamino)-3-methyl-*N*-[3-methyl-1*S*-(phenyl-hydrazono)butyl]butyramide (2.40)

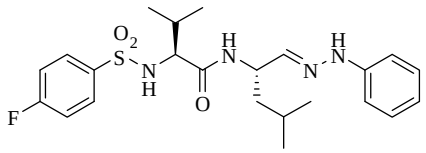

The aldehyde **2.3** (0.10 g, 0.268 mmol) in methanol was reacted with phenylhydrazine hydrochloride (0.043 g, 0.295 mmol) according to **General Procedure O** to give the product as a brown solid (0.097 g, 80%)

mp = 176-178 °C;

^{1}H NMR δ((CD$_3$)$_2$SO) 9.79 (1H, s, CH=NN**H**Ph), 8.06 (1H, d, *J* = 7.8 Hz, C**H**=NNHPh), 7.85-7.79 (2H, m, Ar**H** (Fps)), 7.70 (2H, d, *J* = 6.9 Hz, Ar**H** (Ph)), 7.37-7.33 (2H, m, Ar**H** (Fps)), 7.06 (2H, t, *J* = 6.9 Hz, Ar**H** (Ph)), 6.66-6.62 (1H, m, Ar**H** (Ph)), 4.12-4.07 (1H, m, C**H**CH$_2$CH(CH$_3$)$_2$), 3.61 (1H, dd, *J* = 6.6 and 9.4 Hz, C**H**CH(CH$_3$)$_2$), 1.86-1.78 (1H, m, CHC**H**(CH$_3$)$_2$), 1.34-1.19 (3H, m, CHC**H$_2$**CH(CH$_3$)$_2$ and CHCH$_2$C**H**(CH$_3$)$_2$), 0.86 (3H, d, *J* = 6.1 Hz, CHCH(C**H$_3$**)$_2$), 0.81 (3H, d, *J* = 6.8 Hz, CHCH$_2$CH(C**H$_3$**)$_2$), 0.78 (3H, d, *J* = 6.8 Hz, CHCH$_2$CH(C**H$_3$**)$_2$), 0.75 (3H, d, *J* = 6.1 Hz, CHCH(C**H$_3$**)$_2$);

^{13}C NMR δ((CD$_3$)$_2$SO) 171.381, 169.68, 163.92 (d, *J* = 248.7 Hz), 149.06, 137.45 (d, *J* = 3.0 Hz), 129.57 (d, *J* = 9.9 Hz), 128.51, 118.34, 115.81 (d, *J* = 22.48 Hz), 112.04, 60.80, 49.30, 40.77, 31.23, 23.92, 22.62, 21.90, 19.08, 17.96;

$[\alpha]_D$ = +9.0 (c = 0.1 in (CH$_3$)$_2$SO);

HRMS (ES) 463.2174 (MH$^+$) $C_{23}H_{32}FN_4O_3S$ requires 463.2179;

ν_{max} (KBr) 3260 (SO_2NH), 2963 (C(O)NH), 2365 (C=NNH).

7.2.3 Synthesis of Heterocycles

Preparation of 2*S*-[-2*S*-(4-fluorobenzenesulfonylamino)-3-methylbutyrylamino]-4-methylpentanoic acid methyl ester (2.44)

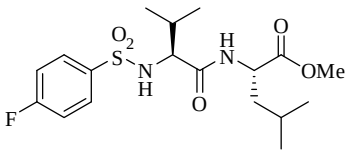

The acid **2.24** (1.00 g, 3.63 mmol) was coupled to *L*-leucine methyl ester hydrochloride (0.727 g, 4.00 mmol) according to **General Procedure B** to give the crude product which was purified by flash chromatography on silica (1:4 ethyl acetate:petroleum ether). The pure product was isolated as a white solid (1.25 g, 86%).

mp = 110-111 °C;

Spectral properties are in agreement with the literature.[8]

^{1}H NMR δ($CDCl_3$) 7.83-7.89 (2H, m, Ar**H** (Fps)), 7.10-7.16 (2H, m, Ar**H** (Fps)), 6.16 (1H, d, *J* = 8.1 Hz, N**H**), 5.63 (1H, d, *J* = 8.8 Hz, N**H**), 4.35-4.44 (1H, m, C**H**$CH_2CH(CH_3)_2$), 4.11 (1H, dd, *J* = 7.1 and 8.1 Hz, C**H**$CH(CH_3)_2$), 3.69 (3H, s, $CO_2C\mathbf{H_3}$), 1.99-2.08 (1H, m, $CHC\mathbf{H}(CH_3)_2$), 1.41-1.54 (1H, m, $CHCH_2C\mathbf{H}(CH_3)_2$), 1.21-1.37 (2H, m, $CHC\mathbf{H_2}CH(CH_3)_2$), 0.94 (3H, d, *J* = 6.8 Hz, $CHCH(C\mathbf{H_3})_2$), 0.84 (3H, d, *J* = 6.8 Hz, $CHCH(C\mathbf{H_3})_2$), 0.84 (3H, d, *J* = 6.5 Hz, $CHCH_2CH(C\mathbf{H_3})_2$), 0.80 (3H, d, *J* = 6.5 Hz, $CHCH_2CH(C\mathbf{H_3})_2$);

^{13}C NMR δ($CDCl_3$) 172.83, 170.18, 164.93 (d, *J* = 252.3 Hz), 132.88 (d, *J* = 3.4 Hz) 130.98 (d, *J* = 9.4 Hz), 115.70 (d, *J* = 23.1 Hz), 61.49, 52.22, 50.64, 41.12, 31.86, 24.48, 22.43, 21.54, 19.02, 17.04;

$[\alpha]_D$ = +3.4 (c = 0.1 in $CHCl_3$);

HRMS (ES) 403.1706 ($MH^{+)}$ $C_{18}H_{28}FN_2O_5S$ requires 403.1703;

ν_{max} (KBr) 3273 (SO_2NH), 2961 (C(O)NH), 1720 (CO_2Me).

Preparation of 2*S*-[-2*S*-(4-fluorobenzenesulfonylamino)-3-methylbutyrylamino]-4-methylpentanoic acid (2.7)

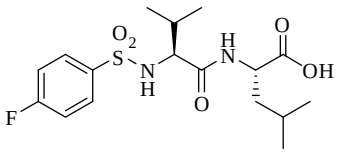

The methyl ester **2.44** (1.00 g, 2.49 mmol) was hydrolysed according to **General Procedure G2** to give the pure product **2.7** as a white solid (0.93 g, 96%).

mp = 167-168 °C;

Spectral properties are in agreement with the literature.[9]

^{1}H NMR δ(CD_3OD) 7.81-7.78 (2H, m, Ar**H** (Fps)), 7.31 (1H, d, *J* = 5.8 Hz, N**H**), 7.11-7.08 (2H, m, Ar**H** (Fps)), 4.20-4.16 (1H, m, C**H**$CH_2CH(CH_3)_2$), 3.51 (1H, d, *J* = 5.7 Hz, C**H**$CH(CH_3)_2$), 1.97 (1H, m, CHC**H**$(CH_3)_2$), 1.48-1.42 (1H, m, $CHCH_2$C**H**$(CH_3)_2$), 1.31-1.21 (2H, m, CHC**H$_2$**$CH(CH_3)_2$), 0.90 (3H, d, *J* = 6.5 Hz, $CHCH_2CH(C$**H$_3$**$)_2$), 0.82 (3H, d, *J* = 2.4 Hz, $CHCH(C$**H$_3$**$)_2$), 0.81 (3H, d, *J* = 2.4 Hz, $CHCH(C$**H$_3$**$)_2$), 0.75 (3H, d, *J* = 6.5 Hz, $CHCH_2CH(C$**H$_3$**$)_2$);

^{13}C NMR δ(CD_3OD) 175.53, 172.81, 166.30 (d, *J* = 252.1 Hz), 138.57 (d, *J* = 3.2 Hz), 131.22 (d, *J* = 9.4 Hz), 117.05 (d, *J* = 22.8 Hz), 62.86, 51.92, 41.70, 33.11, 25.73, 23.24, 22.01, 19.80, 18.28;

$[\alpha]_D$ = -8.0 (c = 0.1 in CH_3OH);

HRMS (ES) 389.1543 (MH^+) $C_{23}H_{34}N_2O_6$ requires 389.1546;

ν_{max} (KBr) 3344 (COOH), 3184 (SO_2NH), 2968 (C(O)NH).

Preparation of *N*-hydroxyacetamidine (2.47)

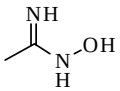

A 50% aqueous hydroxylamine solution (3.7 mL, 56 mmol) was added to acetonitrile (30 mL) and heated at for 24 h. After cooling to rt the solvent was removed *in vacuo* to yield a glassy solid (2.45 g, 59%).

Spectral properties are in agreement with the literature.[10]

^{1}H NMR δ($CDCl_3$) 4.55 (3H, bs, O**H**N**H** and C=N**H**), 1.86 (3H, s, C**H$_3$**);

Preparation of 2*S*-[-2*S*-(4-fluorobenzenesulfonylamino)-3-methylbutyrylamino]-4-methylpentanoic-*N*-hydroxyacetamidine (2.48)

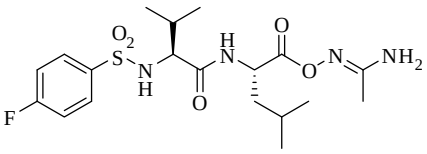

The acid **2.44** (0.50 g, 1.29 mmol) was coupled to *N*-hydroxyacetamidine **2.47** (0.17 g, 1.54 mmol) according to **General Procedure E2** to give the crude product as a glassy solid. Recrystallisation from a minimal amount of ethyl acetate gave the pure product as a colourless glassy solid (0.47 g, 82 %).

^{1}H NMR δ($CDCl_3$) 7.90-7.85 (2H, m, Ar**H** (Fps)), 7.19-7.14 (2H, m, Ar**H** (Fps)), 6.36 (1H, d, *J* = 8.2 Hz, N**H**), 5.61 (1H, d, *J* = 8.6 Hz, N**H**), 4.53-4.48 (1H, m, C**H**$CH_2CH(CH_3)_2$), 3.55 (1H, dd, *J* = 5.1 and 8.6 Hz, C**H**$CH(CH_3)_2$), 2.08-2.03 (1H, m, CHC**H**$(CH_3)_2$), 1.96 (3H, s, N=C(NH_2)C**H$_3$**), 1.62-1.53 (2H, m, CHC**H$_2$**$CH(CH_3)_2$ and $CHCH_2$C**H**$(CH_3)_2$), 1.46-1.36 (1H, m, CHC**H$_2$**$CH(CH_3)_2$), 0.92-0.86 (12H, m, $CHCH(CH_3)_2$ and $CHCH_2CH(CH_3)_2$);

^{13}C NMR δ($CDCl_3$) 173.72, 172.04, 165.61 (d, *J* = 255.1 Hz), 137.18 (d, *J* = 3.5 Hz), 130.55 (d, *J* = 9.4 Hz), 116.82, 116.58 (d, *J* = 22.6 Hz), 62.84, 52.49, 45.43, 40.93, 32.43, 25.21, 22.92, 21.84, 19.45, 17.89, 16.27;

$[\alpha]_D$ = -10.0 (c = 0.1 in $CHCl_3$);

HRMS (ES) 445.1923 (MH^+) $C_{19}H_{30}FN_4O_5S$ requires 445.1921.

Preparation of 2*S*-(4-fluorobenzenesulfonylamino)-3-methyl-*N*-[3-methyl-1*S*-(3-methyl-[1,2,4]oxadiazole-5-yl)-butyl]butyramide (2.41)

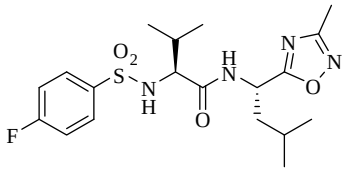

Sodium acetate (0.20 g, 0.25 mmol, 1.1 equiv) dissolved in water was added to a stirred solution of **2.48** (0.10 g, 0.23 mmol, 1.0 equiv) in ethanol and the resulting mixture heated at reflux for 5 h. The solution was allowed to cool to rt, then the solvents were removed *in vacuo* to give a colourless residue. The residue was partitioned between ethyl acetate and water. The aqueous layer was extracted and the subsequent organic layer dried over $MgSO_4$, filtered and solvent removed under reduced pressure to give the crude product. Recrystallisation from ethyl acetate/petroleum ether gave the pure product as a colourless glassy solid (0.06 g, 58%).

^{1}H NMR δ($CDCl_3$) 7.89-7.84 (2H, m, Ar**H** (Fps)), 7.17-7.13 (2H, m, Ar**H** (Fps)), 6.50 (1H, bs, N**H**), 5.69 (1H, bs, N**H**), 5.16-5.12 (1H, m, C**H**$CH_2CH(CH_3)_2$), 3.62-3.59 (1H, m, C**H**$CH(CH_3)_2$), 2.35 (3H, s, NC(=N)C**H$_3$**), 2.04-2.01 (1H, m, CHC**H**$(CH_3)_2$), 1.64-1.60 (1H, m, CHC**H$_2$**$CH(CH_3)_2$), 1.56-1.48 (1H, m, CHC**H$_2$**$CH(CH_3)_2$), 1.35-1.29 (1H, m, $CHCH_2$C**H**$(CH_3)_2$), 0.91-0.88 (6H, m, $CHCH_2CH(CH_3)_2$), 0.83-0.81 (3H, m, $CHCH(CH_3)_2$);

^{13}C NMR δ($CDCl_3$) 179.62, 171.88, 167.63, 165.53 (d, *J* = 254.0 Hz), 137.02 (d, *J* = 3.1 Hz), 130.48 (d, *J* = 22.6 Hz), 116.55 (d, *J* = 9.3 Hz), 62.08, 45.34, 42.02, 32.30, 24.85, 22.61, 21.92, 19.40, 17.81, 11.52;

$[\alpha]_D$ = -30.0 (c = 0.1 in $CHCl_3$);

HRMS (ES) 427.1813 (MH^+) $C_{19}H_{28}FN_4O_4S$ requires 427.1815.

Preparation of 2*S*-(2*S*-benzyloxycarbonylamino-3-methylbutyrylamino)-4-methyl-pentanoic acid methyl ester (2.45)

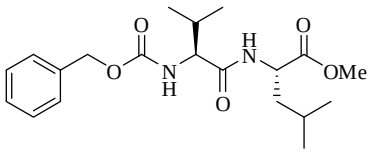

Cbz-*L*-valine **2.28** (2.00 g, 7.96 mmol) was coupled to *L*-leucine methyl ester hydrochloride (1.59 g, 8.76 mmol) according to **General Procedure B** to give the crude product which was purified by flash chromatography on silica (1:5 ethyl acetate:petroleum ether). The pure product was isolated as a white solid (2.66 g, 88%).

mp = 99-100 °C;

Spectral properties are in agreement with the literature.[8]

^{1}H NMR δ($CDCl_3$) 7.35 (5H, m, Ar**H** (Cbz)), 6.53 (1H, d, *J* = 7.8 Hz, N**H**), 5.51 (1H, d, *J* = 8.9 Hz, N**H**), 5.13-5.07 (2H, m, CC**H$_2$**O), 4.63-4.59 (1H, m, C**H**$CH_2CH(CH_3)_2$), 4.09-4.06 (1H, m, C**H**$CH(CH_3)_2$), 3.72 (3H, s, CO_2C**H$_3$**), 2.13-2.07 (1H, m, C**H**$CH(CH_3)_2$), 1.67-1.60 (2H, m, CHC**H$_2$**$CH(CH_3)_2$ and $CHCH_2$C**H**$(CH_3)_2$), 1.54-1.52 (1H, m, CHC**H$_2$**$CH(CH_3)_2$), 0.97 (3H, d, *J* = 6.7 Hz, $CHCH_2CH(C$**H$_3$**$)_2$), 0.94-0.91 (9H, m, $CHCH_2CH(C$**H$_3$**$)_2$);

^{13}C NMR δ($CDCl_3$) 174.24, 174.16, 158.28, 138.04, 129.36, 128.88, 128.67, 67.50, 61.67, 52.58, 51.97, 41.23, 32.00, 25.73, 23.31, 21.89, 19.69, 18.70;

$[\alpha]_D$ = -12.5 (c = 0.1 in $CHCl_3$);

HRMS (ES) 379.2236 (MH^+) $C_{20}H_{31}N_2O_5$ requires 379.2233;

ν_{max} (KBr) 2962 (C(O)NH), 22428 (C(O)NH), 1751 (CO_2Me).

Preparation of 2*S*-(2*S*-benzyloxycarbonylamino-3-methylbutyrylamino)-4-methyl-pentanoic acid (2.46)

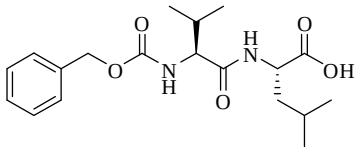

The methyl ester **2.45** (1.00 g, 2.64 mmol) was hydrolysed according to **General Procedure G2** to give the pure product **2.46** as a white solid (0.98 g, 92%).

mp = 137-139 °C (lit[11] mp = 138-139 °C)

^{1}H NMR δ($CDCl_3$) 7.36-7.28 (5H, m, Ar**H** (Cbz)), 6.97 (1H, d, *J* = 7.8 Hz, N**H**), 5.99 (1H, d, *J* = 9.1 Hz, N**H**), 5.08 (2H, s, CC**H$_2$**O), 4.61-4.57 (1H, m, C**H**$CH_2CH(CH_3)_2$), 4.08-4.05 (1H, m, C**H**$CH(CH_3)_2$), 2.05-2.01 (1H, m, CHC**H**$(CH_3)_2$), 1.71-1.62 (2H, m, CHC**H$_2$**$CH(CH_3)_2$), 1.58-1.55 (1H, m, $CHCH_2$C**H**$(CH_3)_2$), 0.94-0.89 (12H, m, $CHCH(CH_3)_2$ and $CHCH_2CH(CH_3)_2$);

^{13}C NMR δ($CDCl_3$) 175.70, 174.18, 158.42, 138.11, 129.42, 128.93, 128.72, 67.60, 61.80, 51.92, 41.57, 32.06, 25.85, 23.43, 21.90, 19.77, 18.66;

$[\alpha]_D$ = -25.0 (c = 0.1 in CH_3OH);

HRMS (ES) 365.2074 (MH^+) $C_{19}H_{29}N_2O_5$ requires 365.2076;

ν_{max} (KBr) 3352 (COOH), 2961 (C(O)NH), 2872 (C(O)NH).

Preparation of 2*S*-(2*S*-benzyloxycarbonylamino-3-methylbutyrylamino)-4-methyl-pentanoic-*N*-hydroxyacetamidine (2.49)

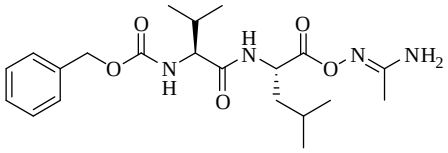

The acid **2.46** (0.50 g, 1.37 mmol) was coupled to *N*-hydroxyacetamidine **2.47** (0.12 g, 1.65 mmol) according to **General Procedure E2** to give the crude product as a glassy solid. Recrystallisation from a minimal amount of ethyl acetate gave the pure product as a colourless glassy solid (0.50 g, 87 %).

^{1}H NMR δ($CDCl_3$) 7.38-7.32 (5H, m, Ar**H** (Cbz)), 6.37 (1H, d, *J* = 7.6 Hz, N**H**), 5.32 (1H, d, *J* = 8.0 Hz, N**H**), 5.10 (2H, s, CC**H$_2$**O), 4.66-4.61 (1H, m, C**H**$CH_2CH(CH_3)_2$), 4.03-4.00

(1H, m, C**H**CH$(CH_3)_2$), 2.17-2.10 (1H, m, CHC**H**$(CH_3)_2$), 1.96 (3H, s, N=CC**H$_3$**), 1.77-1.57 (3H, m, CHC**H$_2$**CH$(CH_3)_2$ and $CHCH_2$C**H**$(CH_3)_2$), 0.97-0.90 (12H, m, CHCH(C**H$_3$**)$_2$ and $CHCH_2$CH(C**H$_3$**)$_2$);

^{13}C NMR δ($CDCl_3$) 171.72, 170.14, 156.86, 156.40, 136.03, 128.76, 128.15, 127.62, 66.96, 60.07, 50.95, 40.75, 30.99, 24.57, 22.50, 21.79, 19.00, 17.71, 16.60;

$[\alpha]_D$ = +2.0 (c = 0.1 in $CHCl_3$)

HRMS (ES) 421.2443 (MH^+) $C_{21}H_{33}N_4O_5$ requires 421.2451;

ν_{max} (KBr) 3449 (N=CNH_2), 3328 (C(O)NH) 2976 (C(O)NH), 1647 (CO_2N=C).

Preparation of [2-methyl-1*S*-(3-methyl-1*S*-[1,2,4]oxadiazol-5-yl-3-methylbutyl-carbamoyl)-propyl]carbamic acid benzyl ester (2.50)

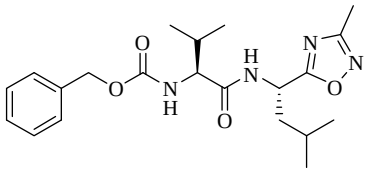

Sodium acetate (0.17 g, 0.21 mmol, 1.1 equiv) dissolved in water was added to a stirred solution of **2.49** (0.08 g, 0.19 mmol, 1.0 equiv) in ethanol and the resulting mixture heated at reflux for 5 h. The solution was allowed to cool to rt, then solvents removed *in vacuo* to give a colourless residue. The residue was partitioned between ethyl acetate and water. The aqueous layer was extracted and the organic layer subsequently dried over $MgSO_4$, filtered and solvent removed under reduced pressure to give the crude product. Recrystallisation from ethyl acetate/petroleum ether gave the pure product as a colourless glassy solid (0.05 g, 61%).

^{1}H NMR δ($CDCl_3$) 7.38-7.33 (5H, m, Ar**H** (Cbz)), 6.87 (1H, d, *J* = 7.5 Hz, N**H**), 5.51 (1H, d, *J* = 8.6 Hz, N**H**), 5.37 (1H, q, *J* = 8.0 Hz, C**H**$CH_2CH(CH_3)_2$), 5.14-5.10 (2H, m, CC**H$_2$**O), 4.09 (1H, t, *J* = 7.6 Hz, C**H**$CH(CH_3)_2$), 2.37 (3H, s, N=C(N)C**H$_3$**), 2.14-2.08 (1H, m, CHC**H**$(CH_3)_2$), 1.81-1.56 (3H, m, CHC**H$_2$**$CH(CH_3)_2$ and $CHCH_2$C**H**$(CH_3)_2$), 0.98-0.90 (12H, m, CHCH(C**H$_3$**)$_2$ and $CHCH_2$CH(C**H$_3$**)$_2$);

^{13}C NMR δ($CDCl_3$) 178.96, 171.33, 167.08, 156.49, 136.03, 128.78, 128.19, 127.60, 67.045, 60.03, 45.69, 44.32, 42.41, 31.00, 24.76, 22.36, 21.75, 18.99, 17.78;

$[\alpha]_D$ = -27.0 (c = 0.1 in $CHCl_3$);

HRMS (ES) 403.2336 (MH^+) $C_{21}H_{31}N_4O_4$ requires 403.2345;

ν_{max} (KBr) 3300 (C(O)NH), 2963 (C(O)NH), 1661 (CHC=NC), 1539 (NC=NO), 1244 (CHCON).

Preparation of *N*-[1*S*-(cyano-(*R*,*S*)-hydroxymethyl)-3-methylbutyl]-2*S*-(4-fluoro-benzenesulfonylamino)-3-methylbutyramide (2.51)

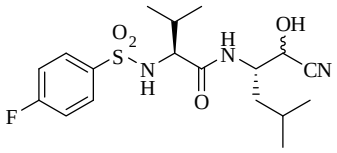

The aldehyde **2.3** (2.73 g, 7.33 mmol) was reacted according to **General Procedure I** to give the cyanohydrin **2.51** as a colourless glassy solid (2.81 g, 96%). No further purification was necessary.

NMR data reported for the mixture of diastereoisomers (1:1).

^{1}H NMR δ($CDCl_3$) 7.91-7.87 (4H, m, Ar**H** (Fps)), 7.24-7.18 (4H, m, Ar**H** (Fps)), 6.49 (1H, d, *J* = 8.7 Hz, N**H**), 6.38 (1H, d, *J* = 8.3 Hz, N**H**), 5.38 (1H d, *J* = 7.3 Hz, N**H**), 5.30 (1H, d, *J* = 6.7 Hz, N**H**), 4.55 (1H, d, *J* = 6.7 Hz, C**H**OH(CN)), 4.49 (1H, d, *J* = 3.0 Hz, C**H**OH(CN)),4.26-4.21 (1H, m, C**H**$CH(CH_3)_2$), 4.08-4.03 (1H, m, C**H**$CH(CH_3)_2$), 3.54 (1H, dd, *J* = 4.4 and 7.2 Hz, C**H**$CH_2CH(CH_3)_2$), 3.47 (1H, dd, *J* = 5.2 and 6.5 Hz, C**H**$CH_2CH(CH_3)_2$), 2.20-2.08 (2H, m, CHC**H**$(CH_3)_2$), 1.68 (2H, bs, CHO**H**(CN)), 1.60-1.39 (6H, m, CHC**H$_2$**$CH(CH_3)_2$ and $CHCH_2$C**H**$(CH_3)_2$), 0.97-0.82 (24H, m, CHCH(C**H$_3$**$)_2$) and $CHCH_2CH$(C**H$_3$**$)_2$);

13C NMR δ($CDCl_3$) 171.30, 171.29, 164.91 (d, *J* = 252.7 Hz), 164.86 (d, *J* = 251.7 Hz), 129.68 (d, *J* = 9.2 Hz), 129.73 (d, *J* = 9.7 Hz), 118.62 (d, *J* = 3.6 Hz), 118.31 (d, *J* = 3.5 Hz), 115.99 (d, *J* = 23.5 Hz), 115.93 (d, *J* = 23.1 Hz), 105.75, 104.66, 62.76, 61.44, 50.35, 48.59, 37.96, 37.84, 37.59, 37.48, 31.74, 31.54, 24.12, 24.05, 22.95, 22.87, 21.21, 21.08, 18.94, 18.87. 16.81, 16.73;

HRMS (ES) 400.1696 (MH^+) $C_{18}H_{27}FN_3O_4S$ requires 400.1706;

ν_{max} (KBr) 3335 (SO_2NH), 2964 (C(O)NH), 2220 (CN).

Preparation of {1*S*-[1*S*-(cyano-(*R,S)*-hydroxymethyl)-3-methylbutylcarbamoyl]-2-methyl-propyl}carbamic acid benzyl ester (2.52)

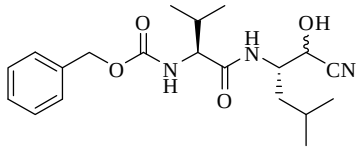

The aldehyde **2.19** (1.18 g, 3.39 mmol) was reacted according to **General Procedure I** to give the cyanohydrin **2.52** as a colourless glassy solid (1.07 g, 84%). No further purification was necessary.

NMR data reported for the mixture of diastereoisomers (1:1)

^{1}H NMR δ($CDCl_3$) 7.36-7.31 (10H, m, Ar**H** (Cbz)), 6.92 (1H, d, *J* = 7.9 Hz, N**H**), 6.80 (1H, d, *J* = 6.9 Hz, N**H**), 5.69 (1H, d, *J* = 8.0 Hz, N**H**), 5.45 (1H, d, *J* = 7.5 Hz, N**H**), 5.17 (1H, d, *J* = 7.3 Hz, **H**CN), 5.13-5.06 (4H, m, CC**H$_2$**O), 5.02 (1H, d, *J* = 6.1 Hz, **H**CN), 4.62-2.57 (1H, m, C**H**$CH_2CH(CH_3)_2$), 4.52-4.47 (1H, m, C**H**$CH_2CH(CH_3)_2$), 4.08-4.03 (1H, m, C**H**$CH(CH_3)_2$), 4.02-3.97 (1H, m, CHC**H**$(CH_3)_2$), 2.15-2.06 (2H, m, CHC**H**$(CH_3)_2$), 1.68-1.51 (5H, m, CHC**H$_2$**$CH(CH_3)_2$ and $CHCH_2$C**H**$(CH_3)_2$), 1.41-1.35 (1H, m, CHC**H$_2$**$CH(CH_3)_2$), 1.02-0.85 (24H, m, $CHCH_2CH(C$**H$_3$**$)_2$ and $CHCH_2CH(C$**H$_3$**$)_2$);

^{13}C NMR δ($CDCl_3$) 174.02, 172.99, 156.65, 156.61, 136.02, 135.85, 128.45, 128.41, 128.15, 128.04, 127.88, 127.72, 118.56, 118.10, 67.24, 67.02, 66.60, 64.46, 60.72, 60.59, 51.70, 51.11, 38.39, 36.85, 30.79, 30.72, 24.60, 24.55, 23.13, 22.84, 21.51, 21.45, 19.17, 19.08;

HRMS (ES) 376.2231 (MH^+) $C_{20}H_{30}N_3O_4$ requires 376.2236.

Preparation of 2*S*-(4-fluorobenzenesulfonylamino)-*N*-{1*S*-[(*R,S)*-hydroxy-(1*H*-tetrazol-5-yl)-methyl]-3-methylbutyl}-3-methylbutyramide (2.53)

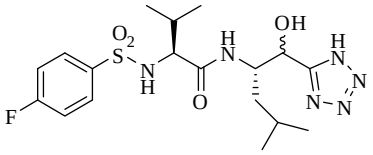

The cyanohydrin **2.51** (0.60 g, 1.60 mmol) was reacted according to **General Procedure S** to yield the α-hydroxy tetrazole as a pale orange glassy solid (0.54 g, 75%).

^{1}H NMR ($(CD_3)_2SO$) 7.84-7.77 (4H, m, Ar**H** (Fbs)), 7.38-7.27 (4H, m, Ar**H** (Fbs)), 4.85 (1H, d, *J* = 3.8 Hz, C**H**OH), 4.76 (1H, d, *J* = 4.1 Hz, N**H**), 4.72 (1H, d, *J* = 4.0 Hz, N**H**),

4.69 (1H, d, *J* = 6.2 Hz, C**H**OH), 4.09-3.97 (2H, m, C**H**$CH_2CH(CH_3)_2$), 3.62 (1H, dd, *J* = 5.0 and 9.1 Hz, C**H**$CH(CH_3)_2$), 3.54 (1H, dd, *J* = 5.0 and 9.2 Hz, C**H**$CH(CH_3)_2$), 1.89-1.77 (2H, m, CHC**H**$(CH_3)_2$), 1.24-0.99 (6H, m, CHC**H$_2$**$CH(CH_3)_2$ and $CHCH_2$C**H**$(CH_3)_2$), 0.77-0.69 (24H, m, $CHCH(CH_3)_2$ and $CHCH_2CH(CH_3)_2$);

^{13}C NMR ($(CD_3)_2SO$) 169.52, 169.43, 163.93 (d, *J* = 250.1 Hz), 137.47 (d, *J* = 3.0 Hz), 137.47 (d, *J* = 3.3 Hz), 129.56 (d, *J* = 15.8 Hz), 129.47 (d, *J* = 15.1 Hz), 115.76 (d, *J* = 22.6 Hz), 115.72 (d, *J* = 22.4 Hz), 67.21, 67.08, 66.49, 66.18, 62.11, 61.82, 60.63, 60.46, 31.21, 30.93, 23.60, 23.46, 23.35, 23.23, 21.26, 21.12, 20.89, 20.72, 19.28, 19.04, 17.26, 16.78;

HRMS (ES) 443.1855 (MH^+) $C_{18}H_{28}FN_6O_4S$ requires 443.1877;

ν_{max} (KBr) 3418 (CH(OH), 3120 (SO_2NH), 2964 (C(O)NH), 2256 (N=N), 2129 (C=N).

Preparation of 2*S*-(4-fluorobenzenesulfonylamino)-3-methyl-*N*-[3-methyl-1*S*-(1*H*-tetrazole-5-carbonyl)butyl]butyramide (2.43)

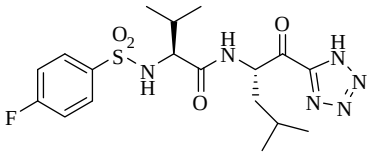

The α-hydroxy tetrazole **2.53** (0.54 g, 1.20 mmol) was oxidised according to **General Procedure M** to give the product as an orange glassy solid. Recrystallisation ethyl acetate/petroleum ether gave the pure **2.43** as an orange glassy solid (0.34 g, 64%).

^{1}H NMR ($(CD_3)_2SO$) 8.15 (1H, d, *J* = 8.4 Hz, N**H**), 8.04 (1H, d, *J* = 7.9 Hz, N**H**), 7.82-7.80 (2H, m, Ar**H** (Fbs)), 7.35-7.32 (2H, m, Ar**H** (Fbs)), 5.22-5.17 (1H, m, C**H**$CH_2CH(CH_3)_2$), 3.67-3.60 (1H, m, C**H**$CH(CH_3)_2$), 1.89-1.84 (1H, m, CHC**H**$(CH_3)_2$), 1.36-1.32 (1H, m, $CHCH_2$C**H**$(CH_3)_2$), 1.27-1.19 (2H, m, CHC**H$_2$**$CH(CH_3)_2$), 0.81-0.72 (12H, m, $CHCH(CH_3)_2$ and $CHCH_2CH(CH_3)_2$);

^{13}C NMR ($(CD_3)_2SO$) 192.39, 169.74, 163.99 (d, *J* = 250.04 Hz), 160.07, 129.61 (d, *J* = 9.3 Hz), 137.86 (d, *J* = 2.9 Hz), 115.86 (d, *J* = 22.7 Hz), 62.29, 60.90, 54.27, 31.22, 24.39, 23.27, 21.10, 19.21, 17.92;

$[\alpha]_D$ = +37.0 (c = 0.1 in $(CH_3)_2SO$);

HRMS (ES) 463.1562 (MNa^+) $C_{18}H_{25}FSN_6O_4Na$ requires 463.1540;

ν_{max} (KBr) 2963 (SO_2NH), 2873 (C(O)NH), 2257 (N=N), 2129 (C=N), 1664 (CHC(O)C).

Preparation of (1S-{1*S*-[(*R,S)*-hydroxy-(1*H*-tetrazol-5-yl)methyl]-3-methylbutyl-carbamoyl}-2-methylpropyl)carbamic acid benzyl ester (2.54)

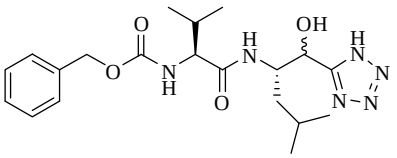

The cyanohydrin **2.52** (0.60 g, 1.60 mmol) was reacted according to **General Procedure S** to yield the α-hydroxy tetrazole as a pale orange glassy solid (0.54 g, 75%).

Spectral data reported for the mixture of diastereoisomers (1:1)

1H NMR δ(CD_3OD) 7.74 (1H, d, *J* = 8.9 Hz, N**H**), 7.57 (1H, d, *J* = 9.2 Hz, N**H**), 7.35-7.30 (10H, m, Ar**H** (Cbz)), 6.76 (1H, d, *J* = 8.6 Hz, N**H**), 6.68 (1H, d, *J* = 8.7 Hz, N**H**), 5.10 (1H, d, *J* = 3.9 Hz, CHC**H**C=N), 5.08-5.07 (4H, m, CC$\mathbf{H_2}$O), 4.99 (1H, d, *J* = 5.45 Hz, CHC**H**C=N), 4.41-4.34 (2H, m, C**H**$CH_2CH(CH_3)_2$), 3.87-3.82 (2H, m, C**H**$CH(CH_3)_2$), 1.99-1.88 (2H, m, CHC**H**$(CH_3)_2$), 1.64-1.53 (2H, m, CHC$\mathbf{H_2}CH(CH_3)_2$), 1.45-1.38 (2H, m, CHC$\mathbf{H_2}CH(CH_3)_2$), 1.31-1.24 (2H, m, $CHCH_2$C**H**$(CH_3)_2$), 0.91-0.77 (24H, $CHCH(C\mathbf{H_3})_2$ and $CHCH_2CH(C\mathbf{H_3})_2$);

13C NMR δ(CD_3OD) 174.07, 173.88, 158.74, 158.64, 154.80, 154.73, 138.16, 138.14, 129.50, 129.46, 129.03, 129.01, 128.87, 128.86, 67.77, 67.70, 62.15, 62.22, 52.96, 52.92, 40.65, 39.69, 31.63, 31.52, 25.83, 25.62, 24.11, 23.75, 22.24, 22.04, 21.72, 21.51, 19.73, 19.70, 18.29, 18.19;

HRMS (ES) 419.2322 (MH^+) $C_{20}H_{31}N_6O_4$ requires 419.2407;

ν_{max} (KBr) 3292 (C(O)NH), 2872 (C(O)NH), 2469 (CHOH), 1692 (N=N), 1649 (N=N).

Preparation of {2-methyl-1*S*-[3-methyl-1*S*-(1*H*-tetrazole-5-carbonyl)butylcarbamoyl]-propyl}carbamic acid benzyl ester (2.55)

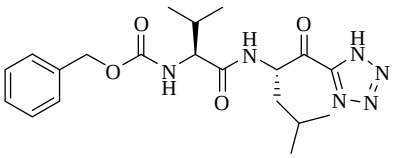

The α-hydroxy tetrazole **2.54** (0.09 g, 0.20 mmol) was oxidised according to **General Procedure M2** to give the product as a colourless glassy solid (0.04 g, 42%).

^{1}H NMR ($(CD_3)_2SO$) 8.11 (1H, d, *J* = 8.4 Hz, N**H**), 8.03 (1H, d, *J* = 7.2 Hz, N**H**), 7.50-7.34 (5H, m, Ar**H** (Cbz)), 5.51-5.45 (1H, m, C**H**$CH_2CH(CH_3)_2$), 5.03 (2H, bs, CC**H$_2$**O), 3.96-3.91 (1H, m, C**H**$CH(CH_3)_2$), 2.02-1.93 (1H, m, CHC**H**$(CH_3)_2$), 1.75-1.65 (1H, m, CHC**H$_2$**$CH(CH_3)_2$), 1.61-1.52 (1H, m, $CHCH_2$C**H**$(CH_3)_2$), 1.47-1.40 (1H, m, CHC**H$_2$**$CH(CH_3)_2$), 0.88-0.74 (12H, m, $CHCH(CH_3)_2$ and $CHCH_2CH(CH_3)_2$);

^{13}C NMR ($(CD_3)_2SO$) 193.02, 171.60, 156.47, 137.32, 128.72, 128.16, 127.88, 65.81, 65.78, 60.45, 54.90, 48.95, 30.73, 24.92, 23.50, 21.43, 19.50, 18.31;

$[\alpha]_D$ = +3.5 (c = 0.2 in $(CH_3)_2SO$);

HRMS (ES) 417.2262 (MH^+) $C_{20}H_{29}N_6O_4$ requires 417.2250;

ν_{max} (KBr) 3429 (C(O)NH), 2964 (C(O)NH), 2254 (N=N), 2128 (C=N), 1658 (C=O)

Preparation of *N*-{1*S*-[(4,5-dihydrooxazol-2-yl)-(*R,S)*-hydroxymethyl]-3-methylbutyl}-2*S*-(4-fluorobenzenesulfonylamino)-3-methylbutyramide (2.56)

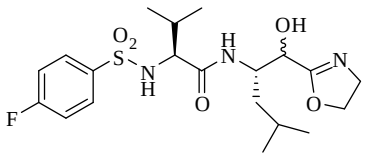

The cyanohydrin **2.51** (0.43 g, 1.09 mmol) was reacted according to **General Procedure R** to give the α-hydroxyoxazoline as a colourless oil. Flash chromatography on silica (2:5 ethyl acetate:dichloromethane) gave the pure product as a colourless oil (0.29 g, 61%).

Spectral data reported for the mixture of diastereoisomers (1:1)

^{1}H NMR δ(CD_3OD) 7.91-7.88 (4H, m, Ar**H** (Fps)), 7.27-7.23 (4H, m, Ar**H** (Fps)), 4.33 (4H, m, C=NC**H$_2$**CH_2O), 4.24 (4H, m, C=NC**H$_2$**CH_2O), 4.18 (2H, bs CHC**H**OH), 4.09-4.04 (2H, m, C**H**$CH_2CH(CH_3)_2$), 3.80-3.73 (4H, m, C=NCH_2C**H$_2$**O), 3.65 (2H, dd, *J* = 2.1 and 5.1 Hz, C**H**$CH(CH_3)_2$), 1.97-1.90 (2H, m, C**H**$CH(CH_3)_2$), 1.26-1.13 (6H, m, CHC**H$_2$**$CH(CH_3)_2$ and $CHCH_2$C**H**$(CH_3)_2$), 0.95-0.94 (6H, m, $CHCH(CH_3)_2$), 0.85-0.78 (18H, m, $CHCH(CH_3)_2$ and $CHCH_2CH(CH_3)_2$);

HRMS (ES) 444.1957 (MH^+) $C_{20}H_{31}FN_3O_5S$ requires 444.1968;

ν_{max} (KBr) 3442 (CH(OH)), 3002 (SO_2NH), 2963 (C(O)NH), 1643 ($COCH_2CH_2$).

Preparation of *N*-[1*S*-(4,5-dihydrooxazole-2-carbonyl)-3-methylbutyl]-2*S*-(4-fluoro-benzenesulfonylamino)-3-methylbutyramide (2.42)

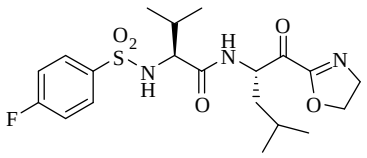

The α-hydroxyoxazoline **2.56** (0.20 g, 0.045 mmol) was according to **General Procedure L** to give the crude product. Column chromatography on silica (2:5 ethyl acetate:dichloromethane) gave the pure product as a colourless oil (0.17 g, 88%)

^{1}H NMR δ($CDCl_3$) 7.87-7.84 (2H, m, Ar**H** (Fps)), 7.17-7.13 (2H, m, Ar**H** (Fps)), 6.33 (1H, d, *J* = 8.5 Hz, N**H**), 5.49 (1H, d, *J* = 8.6 Hz, N**H**), 5.17-5.13 (1H, m, C**H**$CH_2CH(CH_3)_2$), 4.42-4.37 (2H, m, C=NC**H$_2$**CH_2O), 4.13-4.10 (2H, m, C=NCH_2C**H$_2$**O), 3.56 (1H, dd, *J* = 4.7 and 8.5 Hz, C**H**$CH(CH_3)_2$), 2.07-2.01 (1H, m, CHC**H**$(CH_3)_2$), 1.63-1.58 (1H, m, CHC**H$_2$**$CH(CH_3)_2$), 1.34-1.24 (2H, m, CHC**H$_2$**$CH(CH_3)_2$ and $CHCH_2$C**H**$(CH_3)_2$), 0.92 (3H, d, *J* = 6.7 Hz, $CHCH(CH_3)_2$), 0.86-0.85 (6H, m, $CHCH(CH_3)_2$ and $CHCH_2CH(CH_3)_2$) 0.82 (3H, d, *J* = 6.9 Hz, $CHCH_2CH(CH_3)_2$);

^{13}C NMR δ($CDCl_3$) 190.48, 170.06, 165.04 (d, *J* = 254.9 Hz), 159.27, 135.74 (d, *J* = 3.1 Hz), 130.03 (d, *J* = 9.3 Hz), 116.16 (d, *J* = 22.5 Hz), 68.07, 61.59, 55.16, 54.93, 40.89, 31.81, 24.89, 23.01, 21.17, 19.12, 16.95;

$[\alpha]_D$ = +7.0 (c = 0.1 in $CHCl_3$);

HRMS (ES) 442.1829 (MH^+) $C_{20}H_{29}FN_3O_5S$ requires 442.1812.

Preparation of (1*S*-{1*S*-[(4,5-dihydrooxazol-2-yl)-(*R,S)*-hydroxymethyl]-3-methyl-butylcarbamoyl}-2-methylpropyl)carbamic acid benzyl ester (2.57)

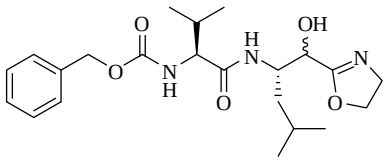

The cyanohydrin **2.52** (0.75 g, 2.00 mmol) was reacted according to **General Procedure R** to give the α-hydroxyoxazoline as a colourless oil. Flash chromatography on silica (2:5 ethyl acetate:dichloromethane) gave the pure product as a colourless oil (0.59 g, 70%).

Spectral data reported for the mixture of diastereoisomers (1:1)

^{1}H NMR δ(CD_3OD) 7.32-7.24 (10H, m, Ar**H** (Cbz)), 5.05 (4H, s, CC**H$_2$**O), 4.29-4.18 (8H, m, C**H**$CH_2CH(CH_3)_2$ and CHC**H**OH and CHC=NC**H$_2$**CH_2O), 3.93-3.90 (2H, m, C**H**$CH(CH_3)_2$), 3.76-3.70 (4H, m, CHC=NCH_2C**H$_2$**O), 2.06-1.98 (2H, m, CHC**H**$(CH_3)_2$), 1.63-1.46 (4H, m, CHC**H$_2$**$CH(CH_3)_2$ and $CHCH_2$C**H**$(CH_3)_2$), 1.35-1.30 (2H, m, $CHCH_2$C**H**$(CH_3)_2$), 0.92-0.80 (24H, m, CHCH(C**H$_3$**)$_2$ and $CHCH_2CH$(C**H$_3$**)$_2$);

^{13}C NMR δ(CD_3OD) 173.89, 170.57, 158.52, 138.23, 129.47, 129.00, 128.83, 70.96, 70.16, 69.41, 69.63, 62.33, 62.27, 54.38, 54.35, 51.45, 51.33, 41.15, 39.70, 31.84, 31.72, 25.82, 25.68, 24.18, 24.66, 22.37, 21.83, 19.92, 19.90, 18.49, 18.41;

HRMS (ES) 420.2480 (MH^+) $C_{22}H_{34}N_3O_5$ requires 420.2498;

ν_{max} (KBr) 3308 (CH(OH)), 2969 (C(O)NH), 1660 ($COCH_2CH_2$), 1578 (OC(O)).

Preparation of {1*S*-[1*S*-(4,5-dihydrooxazole-2-carbonyl)-3-methylbutylcarbamoyl]-2-methylpropyl}carbamic acid benzyl ester (2.58)

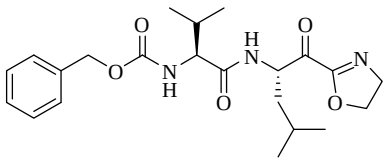

The α-hydroxyoxazoline **2.57** (0.50 g, 0.12 mmol) was oxidised according to **General Procedure L** to give the crude product. Column chromatography on silica (2:5 ethyl acetate:dichloromethane) gave the pure product as a colourless oil (0.037 g, 74%).

^{1}H NMR δ($CDCl_3$) 7.30-7.21 (5H, m, Ar**H** (Cbz)), 6.45 (1H, d, *J* = 5.0 Hz, N**H**), 5.99 (1H, d, *J* = 4.6 Hz, N**H**), 4.98 (2H, s, CC**H$_2$**O), 4.43-4.32 (3H, m, C**H**CH_2CH(CH_3)$_2$ and CHC=NC**H$_2$**CH_2O), 3.98 (1H, dd, *J* = 4.3 and 7.9 Hz, C**H**CH(CH_3)$_2$), 3.82-3.75 (2H, m, CHC=NCH_2C**H$_2$**O), 1.98-1.95 (1H, m, CHC**H**(CH_3)$_2$), 1.67-1.52 (2H, m, CHC**H$_2$**CH(CH_3)$_2$ and CHCH_2C**H**(CH_3)$_2$), 1.39-1.34 (2H, m, CHCH_2C**H**(CH_3)$_2$), 0.98-0.82 (12H, m, CHCH(C**H$_3$**)$_2$ and CHCH_2CH(C**H$_3$**)$_2$);

^{13}C NMR δ($CDCl_3$)

$[\alpha]_D$ = +3.0 (c = 0.1 in $CHCl_3$);

HRMS (ES) 418.2339 (MH^+) $C_{22}H_{33}N_3O_5$ requires 418.2342;

ν_{max} (KBr) 2972 (C(O)NH), 1681 (COCH_2CH_2), 1660 (C=O), 1559 (OC(O)).

7.2.4 Synthesis of Peptidyl Nitriles

Preparation of phenylacetic hydroxysuccinimide (2.59)

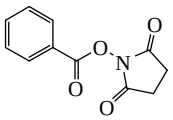

To a solution of phenylacetic acid (1.00 g, 7.34 mmol, 1.0 equiv) in tetrahydrofuran at 0 °C was added *N*-hydroxysuccinimide (1.01 g, 9.55 mmol, 1.3 equiv) and EDCI (1.83 g, 9.55 mmol, 1.3 equiv) in dichloromethane. The reaction mixture was stirred at rt for 3 h after which the solvent was removed. The residue was dissolved in ethyl acetate and washed sequentially with 1M aqueous HCl, saturated aqueous sodium carbonate and brine, dried over $MgSO_4$ and the solvent removed to give the product as a white solid. Recrystallisation from ethyl acetate/petroleum ether gave pure phenylacetic hydroxy-succinimide (1.47 g, 86%).

Spectral properties are in agreement with the literature.[12]

^{1}H NMR δ($CDCl_3$) 7.37 (5H, m, Ar**H** (Ph)), 3.93 (2H, s, CHC**H$_2$**CO), 2.81 (4H, s, C(O)C**H$_2$**C**H$_2$**C(O))

Preparation of phenylacetic acid 1(*R,S)*-cyano-2*S*-[2*S*-(4-fluorobenzenesulfonyl-amino)-3-methylbutyrylamino]-4-methylpentyl ester (2.60)

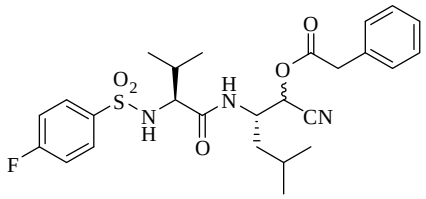

To a stirred solution of **2.59** (0.30 g, 1.32 mmol, 1.0 equiv) in dichloromethane was added cyanohydrin **2.51** (0.53 g, 1.32 mmol, 1.0 equiv) and DIPEA (0.34 mL, 1.98 mmol, 1.5 equiv). The reaction mixture was stirred at rt overnight then diluted with dichloromethane. The organic phase was washed with water and brine, dried over $MgSO_4$ and the solvent removed to give the product as a white solid. Flash chromatography on silica (3:7 ethyl acetate/petroleum ether) afforded the pure product as a 1:1 mixture of diastereoisomers (0.56 g, 82%).

Spectral data given for the mixture of diastereoisomers (1:1)

^{1}H NMR δ($(CD_3)_2SO$) 8.03-7.98 (4H, m, Ar**H** (Fps)), 7.81-7.78 (4H, m, Ar**H** (Fps)), 7.27-7.16 (10H, m, Ar**H** (Ph)), 5.31 (1H, d, *J* = 4.5 Hz, CHC**H**CN), 5.22 (1H, d, *J* = 4.1 Hz, CHC**H**CN), 4.10-4.06 (1H, m, C**H**$CH_2CH(CH_3)_2$), 4.02-4.00 (1H, m, C**H**$CH_2CH(CH_3)_2$), 3.68 (2H, s, OC(O)C$\mathbf{H_2}$Ph), 3.60 (2H, s, OC(O)C$\mathbf{H_2}$Ph), 3.58-3.55 (2H, m, C**H**$CH(CH_3)_2$), 1.87-1.80 (2H, m, CHC**H**$(CH_3)_2$), 1.29-0.99 (6H, m, CHC$\mathbf{H_2}$$CH(CH_3)_2$ and $CHCH_2$C**H**$(CH_3)_2$), 0.88-0.86 (6H, m, $CHCH(CH_3)_2$), 0.78-0.73 (12H, m, $CHCH(CH_3)_2$ and $CHCH_2CH(CH_3)_2$), 0.60 (3H, d, *J* = 5.8 Hz, $CHCH_2CH(CH_3)_2$), 0.56 (3H, d, *J* = 6.1 Hz, $CHCH_2CH(CH_3)_2$);

^{13}C NMR δ($(CD_3)_2SO$) 170.62, 170.36, 169.78, 169.68, 163.99 (d, *J* = 250.3 Hz), 140.52, 137.53 (d, *J* = 3.0 Hz), 134.45, 133.25, 131.12, 130.33, 129.55 (d, *J* = 9.4 Hz), 129.44, 129.35, 128.43, 128.40, 127.15, 126.29, 115.83 (d, *J* = 22.5 Hz), 64.62, 63.34, 60.82, 60.77, 47.24, 46.92, 37.92, 37.89, 31.47, 23.42, 23.31, 22.97, 20.98, 20.96, 19.24, 19.10, 17.52, 17.41;

HRMS (ES) 518.2122 (MH^+) $C_{26}H_{33}FN_3O_5S$ requires 518.2125;

ν_{max} (KBr) 3366 (SO_2NH), 2974 (C(O)NH), 2417 (CN), 1757 (CHOC(O)).

Preparation of phenylacetic acid 2*S*-(2*S*-benzyloxycarbonylamino-3-methyl-butyrylamino)-1(*R*,*S*)-cyano-4-methylpentyl ester (2.61)

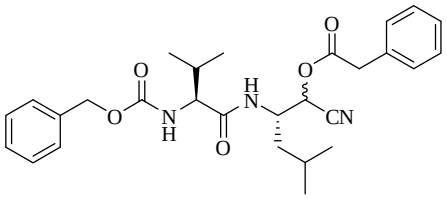

To a stirred solution of **2.59** (0.18 g, 0.79 mmol, 1.0 equiv) in dichloromethane was added cyanohydrin **2.52** (0.30 g, 0.79 mmol, 1.0 equiv) and DIPEA (0.21 mL, 1.19 mmol, 1.5 equiv). The reaction mixture was stirred at rt overnight then diluted with dichloromethane. The organic phase was washed with water and brine, dried over $MgSO_4$ and the solvent removed to give the product as a white solid. Flash chromatography on silica (3:7 ethyl acetate/petroleum ether) afforded the pure product as a 1:1 mixture of diastereoisomers (0.29 g, 74%).

Spectral data given for the mixture of diastereoisomers (1:1)

^{1}H NMR δ((CD$_3$)$_2$SO) 7.36-7.28 (20H, m, Ar**H** (Cbz and Ph)), 5.52 (1H, d, *J* = 5.4 Hz, CHC**H**CN), 5.46 (1H, d, *J* = 4.5 Hz, CHC**H**CN), 5.06-5.02 (6H, m, CC**H$_2$**O and N**H**), 4.40-4.29 (2H, m, C**H**CH$_2$CH(CH$_3$)$_2$), 3.98-3.93 (2H, m, C**H**CH(CH$_3$)$_2$), 3.81-3.80 (2H, m, OC(O)C**H$_2$**Ph), 3.75-3.74 (2H, m, OC(O)C**H$_2$**Ph), 2.05-1.97 (2H, m, CHC**H**(CH$_3$)$_2$), 1.71-1.59 (2H, m, CHCH$_2$C**H**(CH$_3$)$_2$), 1.57-1.47 (2H, m, CHC**H$_2$**CH(CH$_3$)$_2$), 1.32-1.24 (2H, m, CHC**H$_2$**CH(CH$_3$)$_2$), 0.95-0.86 (18H, m, CHCH(C**H$_3$**)$_2$ and CHCH$_2$CH(C**H$_3$**)$_2$), 0.79-0.77 (6H, m, CHCH$_2$CH(C**H$_3$**)$_2$);

^{13}C NMR δ((CD$_3$)$_2$SO) 171.93, 171.78, 169.80, 169.72, 156.12, 156.10, 137.09, 137.06, 133.27, 133.22, 129.53, 129.46, 129.40, 129.36, 128.40, 128.36, 128.29, 128.25, 127.68, 127.54, 127.51, 127.10, 127.06, 115.99, 115.86, 65.33, 65.30, 63.43, 63.32, 60.39, 60.21, 47.42, 47.09, 37.89. 37.79, 30.22, 30.12, 23.71, 23.21, 23.10, 20.94, 20.30, 20.19, 19.18, 19.11, 18.10, 18.00;

HRMS (ES) 482.2664 (MH$^+$) $C_{27}H_{36}N_3O_5$ requires 482.2655;

ν_{max} (KBr) 3281 (C(O)NH), 2968 (C(O)NH), 2230 (CN), 1753 (CHOC(O)).

Preparation of *N*-(1*S*-azidomethyl-3-methylbutyl)-2*S*-(4-fluorobenzenesulfonyl-amino)-3-methylbutyramide (2.62)

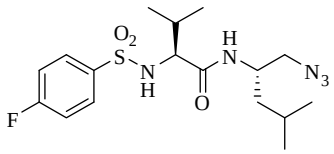

To the alcohol **2.6** (0.10 g, 0.26 mmol, 1.0 equiv) in dichloromethane was added triethylamine (0.10 mL, 0.67 mmol, 2.5 equiv) and mesyl chloride (0.02 mL, 0.26 mmol, 1.0 equiv). The reaction mixture was stirred at rt overnight, then the solvent removed *in vacuo*. The residue was dissolved in *N*,*N*-dimethylformamide and sodium azide (0.02 g, 0.26 mmol, 1.0 equiv) added and the reaction mixture stirred at rt for 4 h after which it was diluted with ethyl acetate. The organic phase was separated and washed with brine, dried over $MgSO_4$ and solvent removed under reduced pressure to give the crude material. Recrystallisation from ethyl acetate/petroleum ether afforded the product as a white solid (0.065 g, 63%)

^{1}H NMR δ($CDCl_3$) 7.87-7.85 (2H, m, Ar**H** (Fps)), 7.16-7.12 (2H, m, Ar**H** (Fps)), 5.26 (1H, d, *J* = 9.7 Hz, N**H**), 4.11 (1H, dd, *J* = 8.1 and 9.2 Hz, CHC**H$_2$**N_3), 3.88-3.81 (1H, m, C**H**$CH_2CH(CH_3)_2$), 3.79 (1H, dd, *J* = 5.1 and 9.5 Hz, C**H**$CH(CH_3)_2$), 3.62-3.59 (1H, m, CHC**H$_2$**N_3), 2.03-1.96 (1H, m, CHC**H**$(CH_3)_2$), 1.59-1.50 (1H, m, $CHCH_2$C**H**$(CH_3)_2$), 1.29-1.24 (1H, m, CHC**H$_2$**$CH(CH_3)_2$), 1.14-1.08 (1H, m, CHC**H$_2$**$CH(CH_3)_2$), 0.99 (3H, d, *J* = 6.8 Hz, $CHCH(CH_3)_2$), 0.89 (3H, d = 6.8 Hz, $CHCH(CH_3)_2$), 0.88-0.85 (6H, m, $CHCH_2CH(CH_3)_2$);

^{13}C NMR δ($CDCl_3$) 189.20, 161.52 (d, *J* = 255.84 Hz), 130.14 (d, *J* = 8.8 Hz), 130.02 (d, *J* = 3.4 Hz), 116.04 (d, *J* = 21.7 Hz), 61.74, 48.12, 47.79, 40.61, 31.97, 24.49, 22.53, 22.04, 19.18, 17.08;

$[\alpha]_D$ = -24.0 (c = 0.1 in CH_3OH)

ν_{max} (KBr) 3297 (SO_2NH), 2976 (C(O)NH), 2100 (CH_2N_3).

7.3 EXPERIMENTAL WORK AS DESCRIBED IN CHAPTER THREE

7.3.1 Synthesis of Michael Acceptors

Preparation of 4*S*-[2*S*-(4-fluorobenzenesulfonylamino)-3-methylbutyrylamino]-6-methylhept-2-enoic acid methyl ester (3.14)

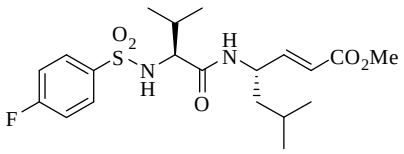

The aldehyde **2.3** (0.40 g, 1.07 mmol) was reacted with methyl(triphenyl-phosphoranylidene) acetate according to **General Procedure P** to give the product as a white solid (0.43 g, 93%).

mp = 147-149 °C;

^{1}H NMR δ($CDCl_3$) 7.88-7.86 (2H, m, Ar**H** (Fps)), 7.18-7.14 (2H, m, Ar**H** (Fps)), 6.74 (1H, dd, *J* = 5.8 and 15.9 Hz, C**H**=CHCO$_2$CH$_3$), 6.08 (1H, d, *J* = 8.0 Hz, N**H**), 5.90 (1H, d, *J* = 15.9 Hz, CH=C**H**CO$_2$CH$_3$), 5.53 (1H, d, *J* = 7.9 Hz, N**H**), 4.53-4.48 (1H, m, C**H**CH(CH$_3$)$_2$), 3.72 (3H, s, CH=CHCO$_2$C**H$_3$**), 3.54 (1H, dd, *J* = 4.7 and 7.9 Hz, C**H**CH$_2$CH(CH$_3$)$_2$), 2.11-2.04 (1H, m, CHC**H**(CH$_3$)$_2$), 1.40-1.22 (3H, m, CHC**H$_2$**CH(CH$_3$)$_2$ and CHCH$_2$C**H**(CH$_3$)$_2$), 0.86 (3H, d, *J* = 6.4 Hz, CHCH(C**H$_3$**)$_2$), 0.83-0.80 (9H, m, CHCH(C**H$_3$**)$_2$ and CHCH$_2$CH(C**H$_3$**)$_2$);

^{13}C NMR δ($CDCl_3$) 169.87, 164.93 (d, *J* = 254.8 Hz), 166.27, 146.22, 135.47, 130.05 (d, *J* = 9.4 Hz), 120.07, 116.24 (d, *J* = 22.5 Hz), 61.80, 61.58, 48.57, 43.20, 32.52, 24.28, 22.49, 20.90, 19.14, 16.85;

$[\alpha]_D$ = -40.0 (c = 0.1 in $CHCl_3$);

HRMS (ES) 429.1845 (MH^+) $C_{20}H_{30}FN_2O_5S$ requires 429.1859;

ν_{max} (KBr) 3364 (SO_2NH), 3082 (C(O)NH), 1726 (CO_2Me), 1649 (CH=CH).

Preparation of 4*S*-[2*S*-(4-fluorobenzenesulfonylamino)-3-methylbutyrylamino]-6-methylhept-2-enoic acid ethyl ester (3.15)

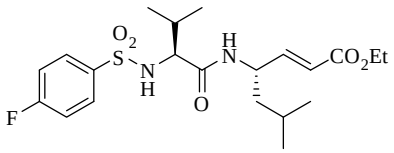

The aldehyde **2.3** (0.40 g, 1.07 mmol) was reacted with ethyl(triphenylphosphoranylidene) acetate according to **General Procedure P** to give the product as a white solid (0.45 g, 95%).

mp = 117-119 °C ;

^{1}H NMR δ($CDCl_3$) 7.88 (2H, m, Ar**H** (Fbs)), 7.17-7.14 (2H, m, Ar**H** (Fbs)), 6.72 (1H, dd, *J* = 5.8 and 15.7 Hz, C**H**=CH), 6.09 (1H, d, *J* = 5.7 Hz, N**H**), 5.87 (1H, d, *J* = 15.6 Hz, CH=C**H**), 5.57 (1H, d, *J* = 6.3 Hz, N**H**), 4.54 (1H, m, C**H**$CH_2CH(CH_3)_2$), 4.17 (2H, t, *J* = 7.1 Hz, C$\mathbf{H_2}CH_3$), 3.55-3.53 (1H, m, C**H**$CH(CH_3)_2$), 2.10-2.03 (1H, m, CHC**H**$(CH_3)_2$), 1.38-1.20 (3H, m, CHC$\mathbf{H_2}CH(CH_3)_2$and $CHCH_2C$**H**$(CH_3)_2$), 1.27 (3H, t, *J* = 7.1 Hz, $CH_2C\mathbf{H_3}$), 0.86-0.80 (12H, m, $CHCH(C\mathbf{H_3})_2$ and $CHCH_2CH(C\mathbf{H_3})_2$);

^{13}C NMR δ($CDCl_3$) 169.77, 165.08 (d, *J* = 255.3 Hz), 166.24, 147.22, 135.46, 130.05 (d, *J* = 9.33 Hz), 121.07, 116.25 (d, *J* = 22.6 Hz), 61.81, 60.58, 48.51, 43.22, 31.52, 24.48, 22.47, 21.90, 19.19, 16.82, 14.14;

$[\alpha]_D$ = -35.0 (c = 0.1 in $CHCl_3$);

HRMS (ES) 443.1935 (MH^+) $C_{21}H_{32}FN_2O_5S$ requires 443.1938;

ν_{max} (KBr) 3358 (SO_2NH), 3082 (C(O)NH), 1717 (CO_2Et), 1651 (CH=CH).

Preparation of 4*S*-(2*S*-benzyloxycarbonylamino-3-methylbutyrylamino)-6-methyl-hept-2-enoic acid methyl ester (3.16)

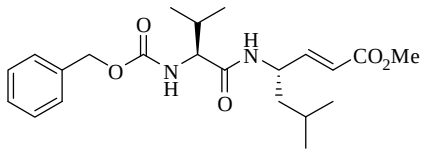

The aldehyde **2.19** (0.40 g, 1.15 mmol) was reacted with methyl(triphenyl-phosphoranylidene) acetate according to **General Procedure P** to give the product as a white solid (0.41 g, 89%).

mp = 109-111 °C;

^{1}H NMR δ($CDCl_3$) 7.36 (5H, s, Ar**H** (Cbz)), 6.81 (1H, dd, *J* = 5.6 and 15.9 Hz, C**H**=CHCO$_2$CH$_3$), 5.90 (1H, d, *J* = 15.9 Hz, CH=C**H**CO$_2$CH$_3$), 5.82 (1H, d, *J* = 8.6 Hz, N**H**), 5.24 (1H, d, *J* = 7.9 Hz, N**H**), 5.11 (2H, s, CC**H$_2$**O), 4.71-4.65 (1H, m, C**H**CH$_2$CH(CH$_3$)$_2$), 3.93 (1H, t, *J* = 6.7 Hz, C**H**CH(CH$_3$)$_2$), 2.20-2.13 (1H, m, CHC**H**(CH$_3$)$_2$), 1.64-1.55 (1H, m, CHCH$_2$C**H**(CH$_3$)$_2$), 1.43-1.40 (2H, m, CHC**H$_2$**CH(CH$_3$)$_2$), 0.97 (3H, d, *J* = 6.7 Hz, CHCH(C**H$_3$**)$_2$), 0.92-0.89 (9H, m, CHCH(C**H$_3$**)$_2$ and CHCH$_2$CH(C**H$_3$**)$_2$);

^{13}C NMR δ($CDCl_3$) 170.85, 166.65, 156.51, 148.10, 136.04, 128.48, 128.14, 127.84, 120.46, 67.02, 60.54, 51.59, 48.35, 43.29, 30.87, 24.66, 22.55, 22.12, 19.33, 17.83

$[\alpha]_D$ = -20.0 (c = 0.1 in $CHCl_3$);

HRMS (ES) 405.2393 (MH^+) $C_{22}H_{33}N_2O_5$ requires 405.2389;

ν_{max} (KBr) 3298 (C(O)NH), 2968 (C(O)NH), 1705 (CO$_2$Me), 1653 (CH=CH).

Preparation of 4*S*-(2*S*-benzyloxycarbonylamino-3-methylbutyrylamino)-6-methyl-hept-2-enoic acid ethyl ester (3.17)

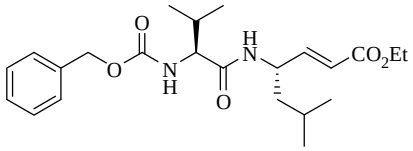

The aldehyde **2.19** (0.40 g, 1.15 mmol) was reacted with methyl(triphenyl-phosphoranylidene) acetate according to **General Procedure P** to give the product as a white solid (0.43 g, 91%).

mp = 86-88 °C;

^{1}H NMR δ($CDCl_3$) 7.37-7.31 (5H, m, Ar**H** (Cbz)), 6.80 (1H, dd, *J* = 5.8 and 15.6 Hz, C**H**=CHCO$_2$CH$_2$CH$_3$), 6.12 (1H, d, *J* = 7.6 Hz, N**H**), 5.90 (1H, d, *J* = 15.7 Hz, CH=C**H**CO$_2$CH$_2$CH$_3$), 5.36 (1H, d, *J* = 7.9 Hz, N**H**), 5.10 (2H, s, CC**H$_2$**O), 4.70-4.64 (1H, m, C**H**CH$_2$CH(CH$_3$)$_2$), 4.17 (2H, dd, *J* = 7.1 and 14.2 Hz, CO$_2$C**H$_2$**CH$_3$) 3.96 (1H, dd, *J* = 6.7 and 8.5 Hz, C**H**CH(CH$_3$)$_2$), 2.16-2.10 (1H, m, CHC**H**(CH$_3$)$_2$), 1.63-1.57 (1H, m, CHCH$_2$C**H**(CH$_3$)$_2$), 1.43-1.39 (2H, m, CHC**H$_2$**CH(CH$_3$)$_2$), 1.27 (3H, t, *J* = 7.1 Hz, CO$_2$CH$_2$C**H$_3$**), 0.96 (3H, d, *J* = 6.7 Hz, CHCH(C**H$_3$**)$_2$), 0.92-0.88 (9H, m, CHCH(C**H$_3$**)$_2$ and CHCH$_2$CH(C**H$_3$**)$_2$);

^{13}C NMR δ($CDCl_3$) 170.87, 166.21, 156.46, 147.85, 136.05, 128.42, 128.05, 127.73, 120.81, 66.91, 60.39, 52.85, 48.27, 43.23, 30.99, 24.61, 22.51, 22.11, 19.28, 17.85, 14.10

$[\alpha]_D$ = -26.0 (c = 0.1 in $CHCl_3$)

HRMS (ES) 419.2552 (MH^+) $C_{23}H_{35}N_2O_5$ requires 419.2546;

ν_{max} (KBr) 3287 (C(O)NH), 2962 (C(O)NH), 1721 (CO$_2$Et), 1649 (CH=CH).

Preparation of 2*S*-(4-fluorobenzenesulfonylamino)-*N*-(1*S*-isobutyl-4-oxobut-2-enyl)-3-methylbutyramide (3.18)

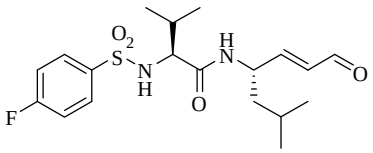

The aldehyde **2.3** (0.40 g, 1.07 mmol) was reacted with triphenylphosphoranylidene acetaldehyde according to **General Procedure P** to give the product as a pale yellow solid (0.29 g, 68%).

mp = 49-51 °C;

^{1}H NMR δ((CD$_3$)$_2$CO) 9.62 (1H, dd, *J* = 2.3 and 7.7 Hz, C**H**O), 8.03 (2H, m, Ar**H** (Fps)), 7.53 (1H, d, *J* = 7.9 Hz, N**H**), 7.42-7.38 (2H, m, Ar**H** (Fps)), 6.94 (1H, m, C**H**=CH), 6.74 (1H, d, *J* = 7.5 Hz, N**H**), 6.19 (1H, m, CH=C**H**), 4.73-4.62 (1H, m, C**H**CH$_2$CH(CH$_3$)$_2$), 3.84-3.78 (1H, m, C**H**CH(CH$_3$)$_2$), 2.17-2.11 (1H, m, CHC**H**(CH$_3$)$_2$), 1.48-1.38 (3H, m, CHC**H$_2$**CH(CH$_3$)$_2$ and CHCH$_2$C**H**(CH$_3$)$_2$), 1.11-0.88 (12H, m, CHCH(C**H$_3$**)$_2$ and CHCH$_2$CH(C**H$_3$**)$_2$);

^{13}C NMR δ((CD$_3$)$_2$CO) 194.98, 171.63, 166.50 (d, *J* = 251.6 Hz), 159.29, 138.94 (d, *J* = 3.0 Hz), 132.64, 131.82 (d, *J* = 9.4 Hz), 117.69 (d, *J* = 22.7 Hz), 63.28, 50.19, 44.28, 33.57, 26.00, 24.00, 22.96, 20.68, 18.40;

$[\alpha]_D$ = -42.0 (c = 0.1 in CHCl$_3$);

HRMS 399.1741 (MH$^+$) $C_{19}H_{28}FN_2O_4S$ requires 399.1754;

ν_{max} (KBr) 2873 (SO_2NH), 2723 (C(O)NH), 1693 (CHO), 1593 (CH=CH).

Preparation of 2*S*-(4-fluorobenzenesulfonylamino)-*N*-(1*S*-isobutyl-3-methanesulfonylallyl)-3-methylbutyramide (3.20)

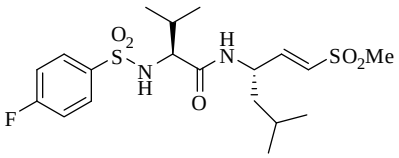

Butyllithium (1.0 M solution, 0.41 mL, 0.40 mmol) was reacted with ethyl-methanesulfonylmethylphosphinoyl ethane **3.24** (0.097 g, 0.44 mmol) and aldehyde **2.3** (0.15 g, 0.40 mmol) according to **General Procedure J** to give the crude product. Recrystallisation from ethyl acetate/petroleum ether afforded the pure product as a white solid (0.16 g, 89%)

mp = 84-86 °C;

^{1}H NMR δ($CDCl_3$) 7.90-7.87 (2H, m, Ar**H** (Fbs)), 7.23-7.20 (2H, m, Ar**H** (Fbs)), 6.82 (1H, dd, *J* = 4.5 and 15.1 Hz, C**H**=CHSO_2CH_3), 6.68 (1H, d, *J* = 15.1 Hz, CH=C**H**SO_2CH_3), 6.42 (1H, d, *J* = 8.5 Hz, N**H**), 5.13 (1H, d, *J* = 6.8 Hz), 4.71-4.66 (1H, m, C**H**CH$(CH_3)_2$), 3.50 (1H, dd, *J* = 4.4 and 7.1 Hz, C**H**CH_2CH$(CH_3)_2$), 2.94 (3H, s, SO_2C**H$_3$**), 2.20-2.14 (1H, m, CHC**H**$(CH_3)_2$), 1.52-1.47 (1H, m, CHC**H$_2$**CH$(CH_3)_2$), 1.42-1.39 (2H, m, CHC**H$_2$**CH$(CH_3)_2$ and $CHCH_2$C**H**$(CH_3)_2$), 0.92 (3H, d, *J* = 6.4 Hz, CHCH(C**H$_3$**)$_2$), 0.87 (3H, d, *J* = 6.4 Hz, CHCH(C**H$_3$**)$_2$), 0.78 (3H, d, *J* = 6.9 Hz, $CHCH_2$CH(C**H$_3$**)$_2$), 0.71 (3H, d, *J* = 6.9 Hz, $CHCH_2$CH(C**H$_3$**)$_2$);

^{13}C NMR δ($CDCl_3$) 170.11, 165.38 (d, *J* = 256.1 Hz), 147.38, 134.59, 130.24 (d, *J* = 9.4 Hz), 129.34, 116.51 (d, *J* = 22.7 Hz), 62.08, 48.01, 42.74, 42.64, 30.87, 24.74, 22.73, 21.54, 19.17, 16.61;

$[\alpha]_D$ = -35.0 (c = 0.1 in CH_3OH);

HRMS (ES) 449.1599 (MH^+) $C_{19}H_{30}FN_2O_5S_2$ requires 449.1580;

ν_{max} (KBr) 3321 (SO_2NH), 2873 (C(O)NH), 1659 (CH=CH), 1304 (O=S=O), 1134 (O=S=O).

Preparation of *N*-(1*S*-benzyl-3-methanesulfonylallyl)-2*S*-(4-fluorobenzene-sulfonylamino)-3-methylbutyramide (3.21)

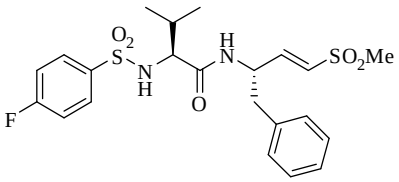

Butyllithium (1.0 M solution, 0.34 mL, 0.34 mmol) was reacted with ethylmethanesulfonylmethylphosphinoyl ethane **3.24** (0.087 g, 0.38 mmol) and aldehyde **2.27** (0.14 g, 0.34 mmol) according to **General Procedure J** to give the crude product. Flash chromatography on silica (1:4 ethyl acetate/petroleum ether) afforded the pure product as a colourless oil (0.14 g, 84%)

^{1}H NMR δ($CDCl_3$) 7.87-7.85 (2H, m, Ar**H** (Fps)), 7.32-7.29 (2H, m, Ar**H** (Fps), 7.24-7.14 (5H, m, Ar**H** (Phe)), 6.92 (1H, dd, *J* = 4.1 and 15.2 Hz, C**H**=CHSO_2CH_3), 6.69 (1H, d, *J* = 15.2 Hz, CH=C**H**SO_2CH_3), 6.33 (1H, d, *J* = 10.6 Hz, N**H**), 5.46 (1H, bs, N**H**), 5.04-4.97 (1H, m, C**H**CH$(CH_3)_2$), 3.42-3.38 (1H, m, C**H**CH_2C), 3.03 (1H, dd, *J* = 3.7 and 11.4 Hz, CHC**H$_2$**C), 2.91 (3H, s, CH=CHSO_2C**H$_3$**), 2.81 (1H, dd, *J* = 3.7 and 13.5 Hz, CHC**H$_2$**C), 2.10 (1H, m, CHC**H**$(CH_3)_2$), 0.51 (3H, d, *J* = 6.4 Hz, CHCH(C**H$_3$**)$_2$), 0.46 (3H, d, *J* = 6.4 Hz, CHCH(C**H$_3$**)$_2$);

^{13}C NMR δ($CDCl_3$) 170.39, 165.29 (d, *J* = 252.4 Hz), 146.13, 136.04, 134.58 (d, *J* = 2.3 Hz), 130.18 (d, *J* = 9.3 Hz), 129.76, 129.06, 128.73, 127.12, 116.34 (d, *J* = 23.4 Hz), 62.48, 50.86, 42.67, 39.66, 30.54, 18.88, 16.50;

$[\alpha]_D$ = -49.0 (c = 0.1 in $CHCl_3$);

HRMS (ES) 483.1428 (MH^+) $C_{22}H_{28}FN_2O_5S_2$ requires 483.1424;

ν_{max} (KBr) 3267 (SO_2NH), 2976 (C(O)NH), 1659 (CH=CH), 1296 (O=S=O), 1155 (O=S=O).

Preparation of [1*S*-(1*S*-isobutyl-3-methanesulfonylallylcarbamoyl)-2-methylpropyl]-carbamic acid benzyl ester (3.22)

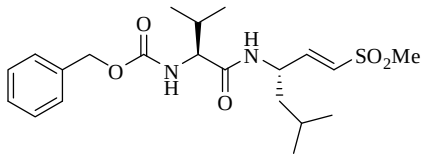

Butyllithium (1.0 M solution, 0.97 mL, 1.55 mmol) was reacted with ethylmethanesulfonylmethylphosphinoyl ethane **3.24** (0.39 g, 1.71 mmol) and aldehyde **2.19** (0.50 g, 1.55 mmol) according to **General Procedure J** to give the crude product. Flash chromatography on silica (2:3 ethyl acetate:petroleum ether) gave the pure product as a white solid. (0.51 g, 78%)

mp = 170-171 °C;

^{1}H NMR δ($CDCl_3$) 7.38-7.32 (5H, m, Ar**H** (Cbz)), 6.80 (1H, dd, *J* = 5.1 and 15.0 Hz, C**H**=$CHSO_2CH_3$), 6.52 (1H, d, *J* = 15.0 Hz, CH=C**H**SO_2CH_3), 6.30 (1H, d, *J* = 8.5 Hz, N**H**), 5.28 (1H, d, *J* = 7.6 Hz, N**H**), 5.11 (2H, s, CC$\mathbf{H_2}$O), 4.76-4.70 (1H, m, C**H**$CH(CH_3)_2$), 3.98 (1H, dd, *J* = 6.2 and 8.1 Hz, C**H**$CH_2CH(CH_3)_2$), 2.91 (3H, s, $CH=CHSO_2C\mathbf{H_3}$), 2.21-2.15 (1H, m, CHC**H**$(CH_3)_2$), 1.65-1.57 (1H, m, $CHCH_2C\mathbf{H}(CH_3)_2$), 1.44-1.41 (2H, m, CHC$\mathbf{H_2}CH(CH_3)_2$), 0.98 (3H, d, *J* = 6.8 Hz, $CHCH(C\mathbf{H_3})_2$), 0.92-0.91 (6H, m, $CHCH(C\mathbf{H_3})_2$ and $CHCH_2CH(C\mathbf{H_3})_2$), 0.89 (3H, d, *J* = 6.5 Hz, $CHCH_2CH(C\mathbf{H_3})_2$);

^{13}C NMR δ($CDCl_3$) 171.18, 156.46, 147.53, 135.90, 129.24, 128.42, 128.07, 127.71, 66.93, 60.49, 47.73, 42.26, 42.40, 30.70, 24.55, 22.53, 21.74, 19.24, 17.71;

$[\alpha]_D$ = -31.0 (c = 0.1 in $CHCl_3$)

HRMS (ES) 425.2116 (MH^+) $C_{21}H_{33}N_2O_5S$ requires 425.2110;

ν_{max} (KBr) 3269 (C(O)NH), 2926 (C(O)NH), 1745 (CH=CH), 1537 (O=S=O).

Preparation of [1*S*-(1*S*-benzyl-3-methansulfonylallylcarbamoyl)-2-methylpropyl]-carbamic acid benzyl ester (3.23)

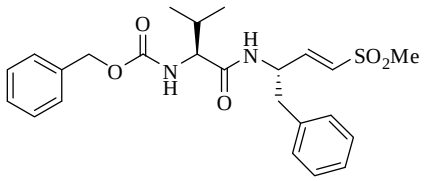

Butyllithium (1.0 M solution, 1.83 mL, 1.83 mmol) was reacted with ethylmethanesulfonylmethylphosphinoyl ethane **3.23** (0.463 g, 2.01 mmol) and aldehyde **2.2** (0.70 g, 1.83 mmol) according to **General Procedure J** to give the crude product. Flash chromatography on silica (1:4 ethyl acetate/petroleum ether) afforded the pure product as a colourless oil (0.55 g, 66%).

^{1}H NMR δ($CDCl_3$) 7.39-7.34 (5H, m, Ar**H** (Cbz)), 7.30-7.21 (3H, m, Ar**H** (Phe)), 7.13 (2H, d, *J* = 7.2 Hz, Ar**H** (Phe)), 6.89 (1H, dd, *J* = 4.4 and 15.0 Hz, CHC**H**=CHSO_2CH_3), 6.43 (1H, d, *J* = 15.0 Hz, CHCH=C**H**SO_2CH_3), 6.13 (1H, d, *J* = 8.3 Hz N**H**,), 5.11 (2H, s, CC**H$_2$**O), 5.03-4.96 (C**H**CH_2Ph), 3.90 (1H, dd, *J* = 5.8 and 7.7 Hz, C**H**$CH(CH_3)_2$), 2.97 (1H, dd, *J* = 6.6 and 13.9 Hz, CHC**H$_2$**Ph), 2.83 (1H, *J* = 8.0 and 13.9 Hz, CHC**H$_2$**Ph), 2.17-2.11 (1H, m, CHC**H**$(CH_3)_2$), 1.58 (3H, s, SO_2CH_3), 0.88 (3H, d, *J* = 6.7 Hz, CHCH(C**H$_3$**)$_2$), 0.74 (3H, d, *J* = 6.7 Hz, CHCH(C**H$_3$**)$_2$);

^{13}C NMR δ($CDCl_3$) 170.95, 146.24, 135.86, 135.62, 130.11, 129.14, 128.75, 128.63, 128.36, 128.10, 127.21, 67.34, 60.77, 50.47, 42.66, 39.87, 30.23, 19.30, 17.34;

$[\alpha]_D$ = +27.0 (c = 0.1 in $CHCl_3$)

HRMS (ES) 459.1958 (MH^+) $C_{24}H_{31}N_2O_5S$ requires 459.1954;

ν_{max} (KBr) 3306 (C(O)NH), 2966 (C(O)NH), 1701 (CH=CH), 1304 (O=S=O), 1240 (O=S=O).

Preparation of (ethylmethanesulfonylmethylphosphinoyl)ethane (3.24)

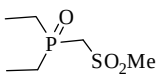

Diethyl(methylthiomethyl) phosphonate (0.90 g, 4.56 mmol, 1.0 equiv) was added to a biphasic mixture of dichloromethane and distilled water (1:2). Benzyltriethylammonium

chloride (0.10 g, 0.46 mmol, 0.1 equiv) and potassium permanganate (1.44 g, 9.12 mmol, 2.0 equiv) were added with vigorous stirring. The purple biphasic solution was stirred vigorously at rt for 20 h. The resulting brown precipitous mixture was filtered and rinsed with dichloromethane. The aqueous phase was separated and extracted twice more with dichloromethane. The combined organic phases were washed with 1% aqueous hydrazine hydrochloride until colourless then brine and dried over $MgSO_4$. The solvent was removed to give the sulfone as a glassy solid (0.80 g, 89%). No purification was necessary.

^{1}H NMR δ($CDCl_3$) 4.21-4.15 (4H, m, C**H**$_2$$CH_3$), 3.58 (2H, d, *J* = 16.5 Hz, C**H**$_2$$CH_3$), 3.15 (3H, s, S($O_2$)C**H**3), 1.32 (6H, t, *J* = 7.1 Hz, C**H**$_3$);

^{13}C NMR δ($CDCl_3$) 63.29 (d, *J* = 6.5 Hz), 51.63 (d, *J* = 138.9 Hz), 42.31, 15.94 (d, *J* = 6.3 Hz);

$[\alpha]_D$ = +3.0 (c = 0.1 in $CHCl_3$);

ν_{max} (KBr) 1306 (SO_2), 1248 (P=O), 1158 (SO_2)

HRMS could not be obtained for this compound as the electrospray conditions did not allow detection.

7.3.2 Diazoketones and Derivatives

Preparation of *N*-[1*S*-(2-diazoacetyl)-3-methylbutyl]-2*S*-(4-fluorobenzenesulfonyl-amino)-3-methylbutyramide (3.25)

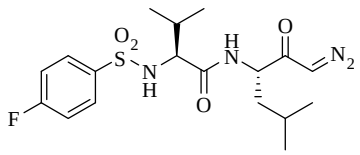

The dipeptidyl acid **2.7** (1.10 g, 2.83 mmol) in tetrahydrofuran was cooled to -25^{o}C. Triethylamine (0.39 mL, 2.83 mmol) and ethyl chloroformate (0.27 mL, 2.83 mmol) were added and the reaction mixture was stirred at -25^{o}C for 20 min until it had a precipitous appearance. The reaction mixture was then cooled over an ice bath and ethereal diazomethane (~1.2 equiv prepared according to **General Procedure N**) added dropwise over 10 min until the solution maintained a consistent yellow colour over 10 min. The reaction mixture was stirred over an ice bath for 2 h followed by a further 16 h at rt. Glacial acetic acid was added to quench the reaction, followed by the addition of enough

1M aqueous sodium hydroxide to result in a basic solution. The reaction mixture was partitioned between ethyl acetate and water. The aqueous phase was separated and extracted twice more with ethyl acetate. The combined organic phases were washed sequentially with saturated aqueous ammonium chloride and brine, dried over $MgSO_4$, filtered and concentrated *in vacuo* to give the crude product. Purification was achieved by column chromatography (1:4 ethyl acetate:petroleum ether) to afford the pure product as a pale yellow solid (0.95 g, 83%).

mp = 136-138 °C;

^{1}H NMR δ($CDCl_3$) 7.89-7.86 (2H, m, Ar**H** (Fbs)), 7.18-7.14 (2H, m, Ar**H** (Fbs)), 6.41 (1H, d, *J* = 8.5 Hz, N**H**), 5.52 (1H, s, C**H**N_2), 5.51 (1H, bs, N**H**), 4.41-4.35 (1H, m, C**H**$CH_2CH(CH_3)_2$), 3.55 (1H, dd, *J* = 4.8 and 8.1 Hz, C**H**$CH(CH_3)_2$), 2.10-2.03 (1H, m, CHC**H**$(CH_3)_2$), 1.50-1.45 (1H, m, CHC**H$_2$**$CH(CH_3)_2$), 1.35-1.28 (2H, m, CHC**H$_2$**$CH(CH_3)_2$ and $CHCH_2$C**H**$(CH_3)_2$), 0.88-0.81 (12H, m, $CHCH(CH_3)_2$ and $CHCH_2CH(CH_3)_2$);

^{13}C NMR δ($CDCl_3$) 193.53, 170.15, 165.10 (d, *J* = 255.3 Hz), 135.47 (d, *J* = 3.4 Hz), 130.09 (d, *J* = 9.3 Hz), 116.22 (d, *J* = 22.5 Hz), 61.84, 54.54, 54.33, 41.44, 31.59, 24.51, 22.89, 21.63, 19.11, 16.98;

$[\alpha]_D$ = -87.0 (c = 0.1 in $CHCl_3$);

HRMS (ES) 435.1467 (MNa^+) $C_{18}H_{26}FN_4O_4$ SNa requires 435.1478;

ν_{max} (KBr) 3267 (SO_2NH), 3084 (C(O)NH), 2102 ($C=N_2$).

Preparation of {1*S*-[1*S*-(2-diazoacetylo)-3-methylbutylcarbamoyl]-2-methylpropyl}-carbamic acid benzyl ester (3.26)

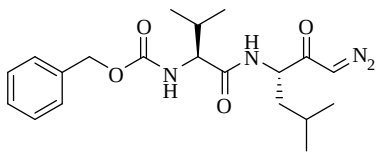

The dipeptidyl acid **2.46** (0.89 g, 2.44 mmol) in tetrahydrofuran was cooled to -25^{o}C. Triethylamine (0.34 mL, 2.44 mmol) and ethyl chloroformate (0.25 mL, 2.44 mmol) were added and the reaction mixture was stirred at -25^{o}C for 20 min until it had a precipitous appearance. The reaction mixture was then cooled over an ice bath and ethereal diazomethane (~1.2 equiv prepared according to **General Procedure N**) added dropwise over 10 min until the solution maintained a consistent yellow colour over 10 min. The

reaction mixture was stirred over an ice bath for 2 h followed by a further 16 h at rt. Glacial acetic acid was added to quench the reaction, followed by the addition of enough 1M aqueous sodium hydroxide to result in a basic solution. The reaction mixture was partitioned between ethyl acetate and water. The aqueous phase was separated and extracted twice more with ethyl acetate. The combined organic phases were washed sequentially with saturated aqueous ammonium chloride and brine, dried over $MgSO_4$, filtered and concentrated *in vacuo* to give the crude product. Purification was achieved by column chromatography (1:4 ethyl acetate:petroleum ether) to afford the pure product as a pale yellow solid (0.58 g, 61%)

mp = 111-112 °C;

^{1}H NMR δ($CDCl_3$), 7.37-7.31 (5H, m, Ar**H** (Cbz), 6.62 (1H, bs, N**H**), 5.48 (1H, bs, N**H**), 5.43 (1H, s, C**H**N_2), 5.11 (2H, s, CC**H$_2$**O), 4.56-5.57 (1H, m, C**H**$CH_2CH(CH_3)_2$), 4.07-4.02 (1H, m, C**H**$CH(CH_3)_2$), 2.16-2.09 (1H, m, CHC**H**$(CH_3)_2$), 1.65-1.57 (2H, m, CHC**H$_2$**$CH(CH_3)_2$ and $CHCH_2$C**H**$(CH_3)_2$), 1.52-1.47 (1H, m, CHC**H$_2$**$CH(CH_3)_2$), 0.96 (3H, d, *J* = 6.8 Hz, $CHCH_2CH$(C**H$_3$**$)_2$), 0.92-0.90 (9H, m, CHCH(C**H$_3$**$)_2$ and $CHCH_2CH$(C**H$_3$**$)_2$);

^{13}C NMR δ($CDCl_3$) 193.50, 171.16, 156.38, 136.14, 128.50, 128.16, 127.96, 67.05, 60.30, 54.40, 54.13, 41.10, 31.04, 24.74, 22.96, 21.84, 19.19, 17.74;

$[\alpha]_D$ = -55.5 (c = 0.1 in $CHCl_3$);

HRMS (ES) 411.1999 (MNa^+) $C_{20}H_{29}N_4O_4Na$ requires 411.2008;

ν_{max} (KBr) 2976 (C(O)NH), 2871 (C(O)NH), 2117 (C=N_2).

Preparation of *N*-[1*S*-(2-bromoacetyl)-3-methylbutyl]-2*S*-(4-fluorobenzenesulfonyl-amino)-3-methylbutyramide (3.28)

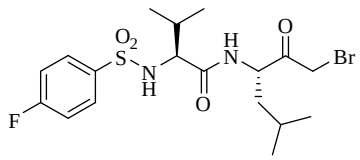

Hydrogen bromide in glacial acetic acid (33%) was added dropwise (~1-2 mL) to a solution of the diazoketone **3.25** (1.89 g, 4.72 mmol) in dichloromethane at rt until the yellow colour disappeared. The solvent was immediately removed *in vacuo* and the

residue rinsed with dichloromethane until no acid was present. The product was isolated as a pale yellow solid, no purification necessary (1.78 g, 81%).

mp = 148-150 °C;

^{1}H NMR δ(CD_3OD) 7.86-7.81 (2H, m, Ar**H** (Fps)), 7.40 (1H, d, *J* = 5.6 Hz, N**H**), 7.19-7.12 (2H, m, Ar**H** (Fps)), 4.50-4.44 (1H, m, C**H**$CH_2CH(CH_3)_2$), 4.04 (1H, d, *J* = 5.6 Hz, C**H$_2$**Br), 3.99 (1H, d, *J* = 5.6 Hz, C**H$_2$**Br), 3.55-3.52 (1H, m, C**H**$CH(CH_3)_2$), 2.01-1.92 (1H, m, CHC**H**$(CH_3)_2$), 1.53-1.46 (1H, m, $CHCH_2$C**H**$(CH_3)_2$), 1.40-1.28 (2H, m, CHC**H$_2$**$CH(CH_3)_2$), 0.89-0.78 (12H, m, $CHCH(CH_3)_2$ and $CHCH_2CH(CH_3)_2$);

^{13}C NMR δ(CD_3OD) 202.00, 173.17, 166.35 (d, *J* = 252.2 Hz), 138.45 (d, *J* = 3.2 Hz), 131.21 (d, *J* = 9.4 Hz), 117.11 (d, *J* = 22.9 Hz), 62.86, 56.08, 40.20, 33.73, 32.98, 25.84, 23.56, 21.69, 19.82, 18.13;

$[\alpha]_D$ = -52.0 (c = 0.1 in CH_3OH);

HRMS (ES) 465.0873 (MH^+) $C_{23}H_{34}N_2O_6$ requires 465.0859;

ν_{max} (KBr) 3283 (SO_2NH), 2874 (C(O)NH), 2446 ($C(O)CH_2$), 1649 (CH_2Br).

Preparation of {1*S*-[1*S*-(2-bromoacetyl)-3-methylbutylcarbamoyl]-2-methylpropyl}-carbamic acid benzyl ester (3.29)

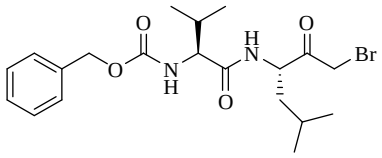

Hydrogen bromide in glacial acetic acid (33%) was added dropwise (~1-2 mL) to a solution of the diazoketone **3.26** (1.06 g, 2.73 mmol) in dichloromethane at rt until the yellow colour disappeared. The solvent was immediately removed *in vacuo* and the residue rinsed with dichloromethane until no acid was present. The product was isolated as a pale yellow solid, no purification necessary (0.96 g, 80%)

mp = 129-130 °C;

^{1}H NMR δ(CD_3OD) 7.38-7.31 (5H, m, Ar**H** (Cbz)), 5.12 (2H, d, *J* = 12.5, CC**H$_2$**O), 5.07 (2H, d, *J* = 12.5, CC**H$_2$**O), 4.67 (1H, dd, *J* = 4.2 and 10.4 Hz, C**H**$CH_2CH(CH_3)_2$), 4.21 (2H, m, C**H$_2$**Br), 3.94 (1H, d, *J* = 7.3 Hz, C**H**$CH(CH_3)_2$), 2.09-2.00 (1H, m, CHC**H**$(CH_3)_2$), 1.74-1.65 (1H, m, $CHCH_2$C**H**$(CH_3)_2$), 1.64-1.55 (2H, m, CHC**H$_2$**$CH(CH_3)_2$), 0.98-0.94 (9H, m, $CHCH(CH_3)_2$ and $CHCH_2CH(CH_3)_2$), 0.91 (3H, d, *J* = 6.4 Hz, $CHCH(CH_3)_2$);

^{13}C NMR δ(CD_3OD) 202.20, 174.71, 138.25, 129.52, 129.06, 128.91, 122.21, 67.73, 62.20, 56.34, 40.10, 33.76, 31.81, 25.98, 23.67, 21.56, 19.82, 18.70;

$[\alpha]_D$ = -51.0 (c = 0.1 in CH_3OH);

HRMS (ES) 441.1396 (MH^+) $C_{20}H_{29}BrN_2O_4$ requires 441.1389;

ν_{max} (KBr) 2961 (C(O)NH), 2872 (C(O)NH), 2411 (C(O)CH_2), 1651 (CH_2Br).

Preparation of *N*-[1*S*-(2-bromo-1*S*-hydroxyethyl)-3-methylbutyl]-2*S*-(4-fluoro-benzenesulfonylamino)-3-methylbutyramide (3.30)

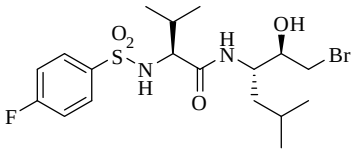

Tri-*tert*-butyllithium aluminium hydride[13] was prepared by the dropwise addition of *tert*-butanol (3.00 mL, 31.50 mmol. 3.15 equiv) to lithium aluminium hydride (10.00 mL, 10.0 mmol, 1.0 equiv) followed by removal of the solvent to give the product as a white solid.

Solid tri-*tert*-butoxylithium aluminium hydride (1.11 g, 4.36 mmol) was cooled to -78 °C. Ethanol:tetrahydrofuran 1:1 (25 mL) was added dropwise and the solution stirred vigorously at -78 °C. A cold (5 °C) solution of α-bromoketone **3.28** in the same solvent (90 mL) was added slowly and the reaction mixture stirred for 1 h at -78 °C after which the reaction was quenched with 1M aqueous HCl (5 mL) and warmed to rt. Solvent was removed *in vacuo* to give a colourless residue that was dissolved in a minimal amount of ethyl acetate. The resulting slushy residue was sonicated for 15 min and the resulting suspension washed sequentially with 1M aqueous HCl and brine, dried over $MgSO_4$ and solvent removed under reduced pressure to give the product as a white solid. No further purification was necessary (0.86 g, 89%).

mp = 149-151°C;

^{1}H NMR δ(CD_3OD) 7.92 (2H, m, Ar**H** (Fps)), 7.77 (1H, d, *J* = 9.1 Hz, N**H**) 7.28-7.24 (2H, m, Ar**H** (Fps), 3.91-3.85 (1H, m, C**H**$CH_2CH(CH_3)_2$), 3.61-3.59 (1H, m, C**H**$CH(CH_3)_2$), 3.42 (1H, dd, *J* = 4.4 and 10.6 Hz, CHC**H$_2$**Br), 3.27 (1H, dd, *J* = 7.5 and 10.6 Hz, CHC**H$_2$**Br), 2.00 (1H, m, CHC**H**$(CH_3)_2$), 1.34-1.29 (2H, m, CHC**H$_2$**$CH(CH_3)_2$), 1.19-1.13 (1H, m, $CHCH_2$C**H**$(CH_3)_2$), 0.93 (3H, d, *J* = 6.8 Hz, $CHCH(CH_3)_2$), 0.85 (3H, d,

J = CHCH(C**H**$_3$)$_2$), 0.83 (d, *J* = 6.9 Hz, CHCH$_2$CH(C**H**$_3$)$_2$), 0.74 (d, *J* = 6.9 Hz, CHCH$_2$CH(C**H**$_3$)$_2$) ;

^{13}C NMR δ(CD$_3$OD) 172.68, 166.85 (d, *J* = 253.5 Hz), 136.90 (d, *J* = 3.1 Hz), 131.43 (d, *J* = 9.5 Hz), 117.57 (d, *J* = 23.1 Hz), 74.99, 62.75, 56.20, 44.13, 32.46, 25.38, 23.01, 22.54, 18.73, 18.25, 17.77;

$[\alpha]_D$ = -30.0 (c = 0.1 in CH$_3$OH);

HRMS (ES) 467.1023 (MH^+) $C_{18}H_{29}BrFN_2O_4S$ requires 467.1015;

ν_{max} (KBr) 3489 (CHOH), 3271 (SO_2NH), 2961 (C(O)NH), 1240 (CH_2Br).

Preparation of {1*S*-[1*S*-(2-bromo-1*S*-hydroxyethyl)-3-methylbutylcarbamoyl]-2-methylpropyl}carbamic acid benzyl ester (3.31)

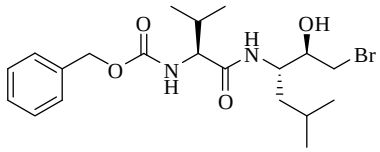

Solid tri-*tert*-butoxylithium aluminium hydride (1.11 g, 4.36 mmol) was cooled to -78 °C. Ethanol:tetrahydrofuran 1:1 (25 mL) was added dropwise and the solution stirred vigorously at -78 °C. A cold (5 °C) solution of α-bromoketone **3.29** in the same solvent (90 mL) was added slowly and the reaction mixture stirred for 1 h at -78 °C after which the reaction was quenched with 1M aqueous HCl (5 mL) and warmed to rt. Solvent was removed *in vacuo* to give a colourless residue that was dissolved in a minimal amount of ethyl acetate. The resulting slushy residue was sonicated for 15 min and the resulting suspension washed sequentially with 1M aqueous HCl and brine, dried over $MgSO_4$ and solvent removed under reduced pressure to give the product as a white solid. No further purification was necessary (0.86 g, 89%).

mp = 165-166 °C;

^{1}H NMR δ(CD$_3$OD) 7.80 (1H, d, *J* = 9.1 Hz, N**H**), 7.37-7.32 (5H, m, Ar**H** (Cbz)), 7.04 (1H, d, *J* =8.2 Hz, N**H**), 5.12 (1H, d, *J* = 12.4 Hz, CC**H$_2$**O), 5.08 (1H, d, *J* = 12.4 Hz, CC**H$_2$**O), 4.07-4.01 (1H, m, C**H**CH$_2$CH(CH$_3$)$_2$), 3.88 (1H, m, CHC**H**OH), 3.67-3.64 (1H, m, C**H**CH(CH$_3$)$_2$), 3.94 (1H, dd, *J* = 4.0 and 10.6 Hz, CHC**H$_2$**Br), 3.33 (1H, dd, *J* = 7.7 and 10.6 Hz, CHC**H$_2$**Br), 2.08-2.01 (1H, m, CHC**H**(CH$_3$)$_2$), 1.66-1.58 (1H, m, CHCH$_2$C**H**(CH$_3$)$_2$), 1.51-1.40 (1H, m, CHC**H$_2$**CH(CH$_3$)$_2$), 0.97 (3H, d, *J* = 6.8 Hz,

$CHCH_2CH(C\mathbf{H_3})_2$), 0.95 (3H, d, *J* = 6.8 Hz, $CHCH_2CH(C\mathbf{H_3})_2$), 0.91 (3H, d, *J* = 6.6 Hz, $CHCH(C\mathbf{H_3})_2$), 0.86 (3H, d, *J* = 6.6 Hz, $CHCH(C\mathbf{H_3})_2$);

^{13}C NMR δ(CD_3OD) 172.68, 157.30, 137.89, 129.02, 128.49, 128.36, 74.29, 66.57, 61.82, 51.09, 37.09, 30.98, 24.89, 24.11, 21.59, 21.48, 19.61, 18.42;

$[\alpha]_D$ = -28.0 (c = 0.1 in CH_3OH);

HRMS (ES) 443.1547 (MH^+) $C_{20}H_{32}BrN_2O_4$ requires 443.1545;

ν_{max} (KBr) 3275 (CHOH), 2959 (C(O)NH), 2872 (C(O)NH), 1246 (CH_2Br).

Preparation of *N*-[1*S*-(2-bromo-1(*R*,*S*)-hydroxyethyl)-3-methylbutyl]-2*S*-(4-fluoro-benzenesulfonylamino)-3-methylbutyramide (3.32)

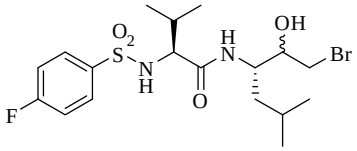

Solid sodium borohydride (0.11 g, 2.83 mmol) was cooled to -78 °C and tetrahydrofuran added dropwise to give a slurry that was stirred vigorously at -78 °C. A cold (5 °C) solution of the α-bromoketone **3.28** (0.66 g, 1.41 mmol) in tetrahydrofuran was added dropwise. The reaction mixture was stirred at -78 °C for 1.5 h after which time the reaction was quenched with 1M aqueous HCl (5 mL) and warmed to rt. The solvent was removed *in vacuo* and the residue sonicated in ethyl acetate. The resulting suspension was diluted with ethyl acetate then sequentially washed with 1M aqueous HCl and brine, dried over $MgSO_4$, filtered and solvent removed to give the crude material. Recrystallisation from ethyl acetate gave the product, a white solid, as a mixture of diastereoisomers (1:1) (0.48 g, 73%).

Spectral data reported for the diastereomeric mixture (1:1).

^{1}H NMR δ(CD_3OD) 7.92-7.89 (4H, m, Ar**H** (Fbs)), 7.77 (1H, d, *J* = 8.8 Hz, N**H**), 7.56 (1H, d, *J* = 9.3 Hz, N**H**), 7.28-7.24 (4H, m, Ar**H** (Fbs)), 4.04-3.99 (1H, m, $C\mathbf{H}CH_2(CH_3)_2$), 3.91-3.84 (1H, m, $C\mathbf{H}CH_2CH(CH_3)_2$), 3.72-3.69 (1H, m, $C\mathbf{H}CH(CH_3)_2$), 3.62 (1H, dd, *J* = 5.0 and 10.0 Hz, CHC**H**OH), 3.60-3.58 (2H, m, $C\mathbf{H}CH(CH_3)_2$ and CHC**H**OH), 3.42 (1H, dd, *J* = 4.4 and 10.6 Hz, $CHC\mathbf{H_2}Br$), 3.32-3.25 (2H, m, $CHC\mathbf{H_2}Br$), 3.20 (1H, dd, *J* = 7.2 and 10.2 Hz, $CHC\mathbf{H_2}Br$), 2.00-1.93 (2H, m, $CHC\mathbf{H}(CH_3)_2$), 1.37-1.27 (4H, m, $CHC\mathbf{H_2}CH(CH_3)_2$), 1.21-1.12 (2H, m, $CHCH_2C\mathbf{H}(CH_3)_2$), 0.93 (3H, d, *J* = 4.2 Hz,

$CHCH_2CH(C\mathbf{H_3})_2$), 0.92 (3H, d, *J* = 4.2 Hz, $CHCH_2CH(C\mathbf{H_3})_2$), 0.86-0.83 (18H, m, $CHCH(C\mathbf{H_3})_2$ and $CHCH_2CH(C\mathbf{H_3})_2$), 0.80 (3H, d, *J* = 6.1 Hz, $CHCH(C\mathbf{H_3})_2$), 0.74 (3H, d, *J* = 6.1 Hz, $CHCH(C\mathbf{H_3})_2$);

^{13}C NMR δ(CD_3OD) 170.06, 169.71, 164.68 (d, *J* = 252.7 Hz), 164.20 (d, *J* = 250.5 Hz), 137.54 (d, *J* = 2.7 Hz), 136.07 (d, *J* = 2.3 Hz), 129.99 (d, *J* = 5.8 Hz), 129.75 (d, *J* = 5.8 Hz), 116.63 (d, *J* = 22.8 Hz), 115.98 (d, *J* = 22.5 Hz), 72.21, 712.82, 54.13, 52.98, 49.91, 49.04, 42.31, 42.25, 36.98, 35.81, 31.51, 30.79, 23.79, 22.97, 22.47, 22.14, 21.88, 21.21, 19.22, 18.90, 18.24, 17.37;

HRMS (ES) 467.0995 (MH^+) $C_{18}H_{29}BrFN_2O_4S$ requires 467.1015;

ν_{max} (KBr) 3545 (CHOH), 3298 (SO_2NH), 2953 (C(O)NH), 1337 (CH_2Br).

Preparation of {1*S*-[1*S*-(2-bromo-1(*R*,*S*)-hydroxyethyl)-3-methylbutylcarbamoyl]-2-methylpropyl}carbamic acid benzyl ester (3.33)

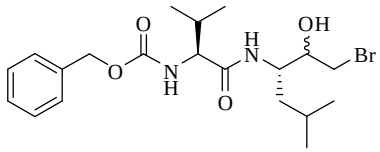

Solid sodium borohydride (0.07 g, 1.84 mmol) was cooled to -78 °C and tetrahydrofuran added dropwise to give a slurry that was stirred vigorously at -78 °C. A cold (5 °C) solution of the α-bromoketone **3.29** (0.41 g, 0.92 mmol) in tetrahydrofuran was added dropwise. The reaction mixture was stirred at -78 °C for 1.5 h after which time the reaction was quenched with 1M aqueous HCl (5 mL) and warmed to rt. The solvent was removed *in vacuo* and the residue sonicated in ethyl acetate. The resulting suspension was diluted with ethyl acetate then sequentially washed with 1M aqueous HCl and brine, dried over $MgSO_4$, filtered and solvent removed to give the crude material. Recrystallisation from ethyl acetate gave the product, a white solid, as a mixture of diastereoisomers (1:1) (0.30 g, 74%).

Spectral data reported for the diastereomeric mixture (1:1).

^{1}H NMR δ(CD_3OD) 7.81 (1H, d, *J* = 7.8 Hz, N**H**), 7.54 (1H, d, *J* = 8.5 Hz, N**H**), 7.37-7.28 (10H, m, Ar**H** (Cbz)), 5.15-5.06 (4H, m, $CC\mathbf{H_2}O$), 4.23-4.18 (1H, m, $C\mathbf{H}CH_2CH(CH_3)_2$), 4.06-4.01 (1H, m, $C\mathbf{H}CH_2CH(CH_3)_2$), 3.94-3.87 (2H, m, CHC**H**OH), 3.78-3.75 (1H, m, $C\mathbf{H}CH(CH_3)_2$), 3.67-3.64 (1H, m, $C\mathbf{H}CH(CH_3)_2$), 3.50 (1H, dd, *J* = 3.9 and 10.5 Hz,

CHC**H**$_2$Br), 3.39-3.25 (3H, m, CHC**H**$_2$Br), 2.09-2.01 (2H, m, CHC**H**$(CH_3)_2$), 1.66-1.53 (4H, m, CHC**H**$_2$CH$(CH_3)_2$), 1.48-1.42 (1H, m, CHCH$_2$C**H**$(CH_3)_2$), 1.36-1.29 (1H, m, CHCH$_2$C**H**$(CH_3)_2$), 0.98-0.85 (24H, m, CHCH(C**H**$_3)_2$ and CHCH$_2$CH(C**H**$_3)_2$);

^{13}C NMR δ(CD_3OD) 173.44, 173.37, 173.22, 173.11, 138.46, 138.42, 129.67, 129.66, 129.13, 129.11, 129.00, 128.97, 74.86, 74.03, 67.29, 67.20, 62.41, 62.38, 37.84, 36.87, 31.60, 31.53, 25.70, 25.66, 24.11, 24.00, 22.88, 22.80, 22.20, 21.99, 20.31, 20.22, 19.18, 19.13, 19.11, 19.05;

HRMS (ES) 443.1559 (MH^+) $C_{20}H_{32}BrN_2O_4$ requires 443.1545;

ν_{max} (KBr) 3302 (CHOH), 2961 (C(O)NH), 2872 (C(O)NH), 1244 (CH_2Br).

Preparation of 2*S*-(4-fluorobenzenesulfonylamino)-3-methyl-*N*-(3-methyl-1*S*-*S*-oxiranylbutyl)butyramide (3.27)

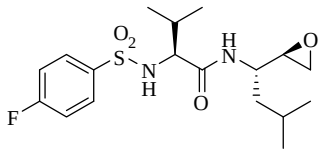

Epoxidation of α-bromomethyl alcohol **3.30** (0.080 g, 0.17 mmol) was achieved in the presence of potassium carbonate (0.044 g, 0.34 mmol) according to **General Procedure Q** to give the product as a colourless oil (0.058 g, 88%)

^{1}H NMR δ(CD_3OD) 7.90-7.87 (2H, m, Ar**H** (Fps)), 7.28-7.24 (2H, m, Ar**H** (Fps)), 4.02-3.99 (1H, m, C**H**$CH_2CH(CH_3)_2$), 3.73 (1H, d, *J* = 7.6 Hz, C**H**$CH(CH_3)_2$), 3.53 (1H, m, CHC**H**OCH_2), 3.35 (1H, dd, *J* = 3.9 and 12.0 Hz, CHCHOC**H**$_2$), 3.18 (1H, dd, *J* = 6.9 and 12.0 Hz, CHCHOC**H**$_2$), 1.98 (1H, m, CHC**H**$(CH_3)_2$), 1.66-1.61 (1H, m, CHCH$_2$C**H**$(CH_3)_2$), 1.22-1.17 (1H, m, CHC**H**$_2$CH$(CH_3)_2$), 1.07-1.02 (1H, m, CHC**H**$_2$CH$(CH_3)_2$), 0.97-0.86 (12H, m, CHCH(C**H**$_3)_2$ and CHCH$_2$CH(C**H**$_3)_2$);

$[\alpha]_D$ = -6.0 (c = 0.1 in CH_3OH);

HRMS (ES) 387.1750 (MH^+) $C_{18}H_{28}FN_2O_4S$ requires 387.1754;

ν_{max} (KBr) 3369 (SO_2NH), 3068 (C(O)NH), 1265 (epox).

Preparation of [2-methyl-1*S*-(3-methyl-1*S*-*S*-oxiranylbutylcarbamoyl)propyl]-carbamic acid benzyl ester (3.34)

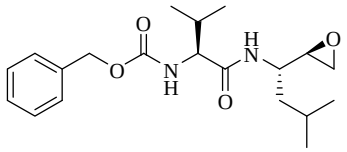

Epoxidation of α-bromomethyl alcohol **3.31** (0.090 g, 0.20 mmol) was achieved in the presence of potassium carbonate (0.056 g, 0.41 mmol) according to **General Procedure Q** to give the product as a white solid (0.036 g, 89%)

mp = 124-126 °C;

^{1}H NMR δ(CD_3OD) 7.36-7.32 (5H, m, Ar**H** (Cbz)), 5.79 (1H, d, *J* = 6.4 Hz, N**H**), 5.32 (1H, d, *J* = 7.2 Hz, N**H**), 5.11 (2H, s, CC**H$_2$**O), 3.94-3.89 (2H, m, C**H**CH$(CH_3)_2$ and C**H**CH_2CH$(CH_3)_2$), 2.84 (1H, bs, CHC**H**CH_2O), 2.72 (2H, bs, CHCHC**H$_2$**O), 1.70-1.58 (1H, m, CHC**H$_2$**CH$(CH_3)_2$), 1.43-1.34 (2H, m, CHC**H$_2$**CH$(CH_3)_2$ and $CHCH_2$C**H**$(CH_3)_2$), 0.96 (3H, dd, *J* = 1.6 and 6.7 Hz, CHCH(C**H$_3$**)$_2$), 0.92-0.91 (6H, m, $CHCH_2$CH(C**H$_3$**)$_2$ and CHCH(C**H$_3$**)$_2$), 0.87 (3H, dd, *J* = 1.7 and 6.4 Hz, $CHCH_2$CH(C**H$_3$**)$_2$);

^{13}C NMR δ(CD_3OD) 174.17, 158.44, 138.27, 129.46, 129.00, 128.82, 67.60, 62.41, 54.88, 49.85, 45.63, 41.33, 31.86, 25.56, 23.80, 23.13, 22.01, 19.71, 18.79;

$[\alpha]_D$ = -39.6 (c = 0.1 in $CHCl_3$);

HRMS (ES) 363.2291 (MH^+) $C_{20}H_{31}N_2O_4$ requires 363.2284;

ν_{max} (KBr) 2961 (C(O)NH), 2872 (C(O)NH), 1244 (epox).

Preparation of 2*S*-(4-fluorobenzenesulfonylamino)-3-methyl-*N*-(3-methyl-1*S*-(*R*,*S*)-oxiranyl-butyl)butyramide (3.35)

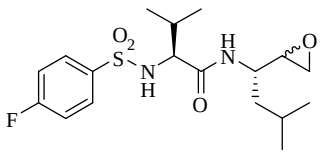

Epoxidation of the diastereomeric α-bromomethyl alcohol **3.32** (0.080 g, 0.17 mmol) was achieved in the presence of potassium carbonate (0.044 g, 0.34 mmol) according to **General Procedure Q** to give the product as a white solid (0.049 g, 74%)

^{1}H NMR δ(CD_3OD) 7.87-7.83 (4H, m, Ar**H** (Fps)), 7.29-7.26 (4H, m, Ar**H** (Fps)), 4.00-3.92 (2H, m, C**H**$CH_2CH(CH_3)_2$), 3.65-3.61 (2H, m, C**H**$CH(CH_3)_2$), 3.55-3.51 (2H, m, CHC**H**OCH_2), 3.33 (1H, dd, *J* = 3.9 and 12.0 Hz, CHCHOC**H$_2$**), 3.30 (1H, dd, *J* = 2.8 and 11.7 Hz, CHCHOC**H$_2$**), 3.13-3.09 (2H, m, CHCHOC**H$_2$**), 1.98-1.92 (2H, m, CHC**H**$(CH_3)_2$), 1.67-1.61 (2H, m, $CHCH_2$C**H**$(CH_3)_2$), 1.22-1.07 (4H, m, CHC**H$_2$**$CH(CH_3)_2$ and CHC**H$_2$**$CH(CH_3)_2$), 0.98-0.81 (24H, m, $CHCH(CH_3)_2$ and $CHCH_2CH(CH_3)_2$);

^{13}C NMR δ(CD_3OD) 172.97, 172.74, 166.34 (d, *J* = 252.3 Hz), 166.28 (d, *J* = 252.2 Hz), 138.83 (d, *J* = 3.2 Hz), 138.38 (d, *J* = 3.2 Hz), 131.23 (d, *J* = 9.5 Hz), 131.16 (d, *J* = 9.4 Hz), 117.11 (d, *J* = 22.8 Hz), 117.08 (d, *J* = 22.8 Hz), 75.03, 74.00, 63.17, 63.13, 51.84, 50.93, 41.65, 39.21, 36.17, 35.53, 33.12, 33.07, 25.56, 25.40, 24.29, 23.40, 22.53, 21.75, 19.99, 19.95, 17.78, 17.69;

HRMS (ES) 387.1756 (MH^+) $C_{18}H_{28}FN_2O_4S$ requires 387.1754;

ν_{max} (KBr) 3354 (SO_2NH), 3064 (C(O)NH), 1258 (epox).

Preparation of [2-methyl-1*S*-(3-methyl-1*S*-(*R*,*S*)-oxiranylbutylcarbamoyl)propyl]-carbamic acid benzyl ester (3.36)

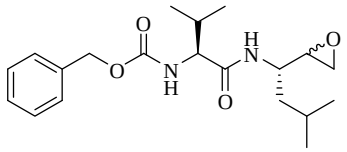

Epoxidation of the diastereomeric α-bromomethyl alcohol **3.33** (0.080 g, 0.18 mmol) was achieved in the presence of potassium carbonate (0.050 g, 0.36 mmol) according to **General Procedure Q** to give the product as a white solid (0.054 g, 83%).

^{1}H NMR δ(CD_3OD) 7.35-7.32 (10H, m, Ar**H** (Cbz)), 5.11-5.07 (4H, m, CC**H$_2$**O), 4.26-4.16 (4H, m, C**H**$CH(CH_3)_2$ and C**H**$CH_2CH(CH_3)_2$), 3.32-3.30 (2H, m, CHC**H**CH_2O), 3.27-3.24 (4H, m, CHCHC**H$_2$**O), 2.13-2.00 (2H, m, CHC**H**$(CH_3)_2$), 1.69-1.26 (6H, m, CHC**H$_2$**$CH(CH_3)_2$ and $CHCH_2$C**H**$(CH_3)_2$), 1.03-0.85 (24H, m, $CHCH_2CH(CH_3)_2$ and $CHCH(CH_3)_2$;

^{13}C NMR δ(CD_3OD) 174.38, 174.36, 168.06, 166.37, 138.26, 138.21, 129.48, 129.47, 129.02, 128.85, 128.83, 87.56, 84.78, 74.52, 70.76, 66.50, 65.49, 64.64, 63.96, 61.23, 59.74, 50.10, 49.92, 41.53, 41.27, 25.66, 24.54, 23.76, 23.10, 22.30, 21.61, 20.00, 19.60, 18.81, 18.44;

HRMS (ES) 363.2272 (MH^+) $C_{20}H_{31}N_2O_4$ requires 363.2284

ν_{max} (KBr) 2953 (C(O)NH), 2870 (C(O)NH), 1254 (epox).

7.4 EXPERIMENTAL WORK AS DESCRIBED IN CHAPTER FOUR

7.4.1 Synthesis of a Macrocyclic Aldehyde

Preparation of 2*S*-[3-(4-allyloxyphenyl)-2*S*-*tert*-butoxycarbonylaminopropionyl-amino]-3-methylbutyric acid methyl ester (4.6)

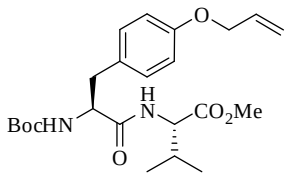

N-Boc-*O*-allyltyrosine **4.5** (5.00g, 16.3 mmol) was reacted with *L*-valine methyl ester using **General Procedure B**. The crude material was purified by flash chromatography on silica (1:4 ethyl acetate and petroleum ether) to yield a white solid (6.08g, 69%).

mp = 74-76 ^{o}C;

^{1}H NMR δ($CDCl_3$) 7.09 (2H, m, Ar**H** (Tyr)), 6.80 (2H, m, Ar**H** (Tyr)), 6.47 (1H, bs, N**H**), 5.97-6.05 (1H, m, C**H**=CH_2), 5.01-5.40 (2H, m, CH=C**H**$_2$), 5.12 (1H, bs, N**H**), 4.47-4.49 (2H, m, OC**H**$_2$CH=CH_2), 4.37-4.46 (1H, m, C**H**CH_2Ph), 4.30-4.34 (1H, m, C**H**$CH(CH_3)_2$), 3.66 (3H, s, CO_2C**H**$_3$), 3.01-3.04 (2H, m, CHC**H$_2$**Ph), 2.04-2.11 (1H, m, CHC**H**$(CH_3)_2$), 1.39 (9H, s, C(C**H**$_3)_3$), 0.85 (3H, d *J* = 6.8 Hz, CHCH(C**H$_3$**$)_2$), 0.82 (3H, d *J* = 6.8 Hz, CHCH(C**H$_3$**$)_2$);

^{13}C NMR δ($CDCl_3$) 174.7, 171.9, 157.5, 133.2, 130.3, 128.6, 117.6, 114.8, 68.7, 57.2, 37.0, 31.0, 28.2, 18.8, 17.6;

$[\alpha]_D$ = -5.0 (c = 0.1 in $CHCl_3$);

HRMS (ES) 435.2501 (MH^+) $C_{23}H_{34}N_2O_6$ requires 435.2495

Microanalysis C, 62.58; H, 7.66; N, 6.58 $C_{23}H_{34}N_2O_6$ requires C, 62.84; H, 7.67; N, 6.66.

Preparation of 2*S*-[3-(4-allyloxyphenyl)-2*S*-*tert*-butoxycarbonylaminopropionyl-amino]-3-methylbutyric acid (4.7)

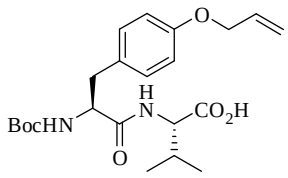

Methyl ester **4.6** (4.90 g, 11.3 mmol) in tetrahydrofuran was hydrolysed according to **General Procedure G**. This gave the product as a colourless glassy solid (4.60 g, 97%).

^{1}H NMR δ($CDCl_3$) 7.11 (2H, m, Ar**H** (Tyr)), 6.83 (2H, m, Ar**H** (Tyr)), 6.64 (1H, d *J* = 8.2 Hz, N**H**), 5.98-6.07 (1H, m, C**H**=CH_2), 5.00-5.39 (2H, m, CH=C**H**$_2$), 5.19 (1H, bs, N**H**), 4.51 (3H, m, C**H**CH_2Ph and OC**H$_2$**CH=CH_2), 4.36-4.40 (1H, m, C**H**$CH(CH_3)_2$), 2.97-3.02 (2H, m, CHC**H$_2$**Ph), 2.16-2.23 (1H, m, CHC**H**$(CH_3)_2$), 1.40 (9H, s, $C(CH_3)_3$), 0.88-0.93 (6H, m, $CHCH(CH_3)_2$);

^{13}C NMR δ($CDCl_3$) 174.31, 172.03, 157.40, 155.73, 133.19, 130.25, 128.57, 117.48, 114.73, 80.29, 68.67, 57.19, 55.70, 37.12, 31.04, 28.16, 18.79, 17.59;

$[\alpha]_D$ = +19.0 (c = 0.1 in $CHCl_3$);

HRMS (ES) 421.2332 (MH^+) $C_{22}H_{32}N_2O_6$ requires 421.2339

ν_{max} (KBr) 3315 (CO_2H), 2968 (C(O)NH), 2905 (C(O)NH), 1500 ($CH=CH_2$).

Preparation of 2*S*-aminopent-4-enoic acid methyl ester (4.8)

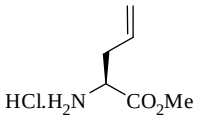

L-Allylglycine (5.00g, 43.4 mmol) was esterified using **General Procedure H** to afford a colourless oil (7.19g, 100%).

^{1}H NMR δ(CD_3OD) 5.78 (1H, m, CH_2C**H**CH_2), 5.25-5.31 (2H, m, CH_2CHC**H$_2$**), 4.16 (1H, dd, *J* = 6.2 and 6.2 Hz, C**H**CO_2CH_3), 3.84 (3H, s, $CHCO_2C$**H$_3$**), 2.69 (2H, m, C**H$_2$**$CHCH_2$);

^{13}C NMR δ(CD_3OD) 169.12, 130.35, 120.34, 52.39, 52.13, 34.42;

LRMS (ES) 130.5 (MH^+) $C_6H_{11}NO_2$ requires 130.1;

$[\alpha]_D$ = +2.0 (c = 1.0 in $CHCl_3$);

HRMS could not be obtained as the mass lies outside the range of the mass spectrometer used.

ν_{max} (KBr) 1638 (CO_2Me), 1618 ($CH=CH_2$).

Preparation of 2*S*-{2*S*-[3-(4-allyloxyphenyl)-2*S*-*tert*-butoxycarbonylaminopropionyl-amino]-3-methylbutyrylamino}pent-4-enoic acid methyl ester (4.9)

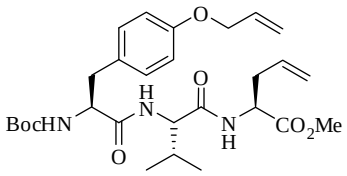

The dipeptidyl acid **4.7** (1.00g, 2.38 mmol) was reacted with alkene **4.8** using **General Procedure B**. The crude material was purified by flash chromatography on silica (1:4 ethyl acetate: pet ether to yield a white solid (1.05g, 83%).

mp = 106-108 ^{o}C;

^{1}H NMR δ($CDCl_3$) 7.09 (2H, m, Ar**H** (Tyr)), 6.82 (2H, m, Ar**H** (Tyr)), 6.61 (1H, d, *J* = 8.4 Hz, N**H**), 6.56 (1H, d, *J* = 6.8 Hz, N**H**), 6.03 (1H, tdd, *J* = 5.3, 10.6 and 17.2 Hz, $OCH_2C\mathbf{H}CH_2$), 5.62-5.71 (1H, m, $CHCH_2C\mathbf{H}CH_2$), 5.10-5.41 (4H, m, $OCH_2CHC\mathbf{H_2}$ and $CHCH_2CHC\mathbf{H_2}$), 5.05 (1H, d, *J* = 5.5 Hz, N**H**), 4.58-4.62 (1H, m, $C\mathbf{H}CH_2CHCH_2$), 4.48-4.50 (2H, m, $OC\mathbf{H_2}CHCH_2$), 4.30-4.33 (1H, m, $C\mathbf{H}CH_2Ph$), 4.25 (1H, dd, *J* = 6.5 and 8.4 Hz, $C\mathbf{H}CH(CH_3)_2$), 3.73 (3H, s, $CO_2C\mathbf{H_3}$), 2.96-3.05 (2H, m, $CHC\mathbf{H_2}Ph$), 2.46-2.59 (2H, m, $CHC\mathbf{H_2}CHCH_2$), 2.07-2.14 (1H, m, $CHC\mathbf{H}(CH_3)_2$), 1.39 (9H, s, $C(C\mathbf{H_3})_3$), 0.90 (3H, d, *J* = 6.8 Hz, $CHCH(C\mathbf{H_3})_2$), 0.86 (3H, d, *J* = 6.8 Hz, $CHCH(C\mathbf{H_3})_2$);

^{13}C NMR δ($CDCl_3$) 171.72, 171.40, 170.45, 157.63, 133.29, 132.22, 130.01, 128.60, 119.30, 117.62, 114.97, 68.74, 58.42, 52.38, 51.78, 36.25, 30.75, 28.22, 19.04;

$[\alpha]_D$ = +5.0 (c = 0.1 in $(CH_3)_2SO$);

HRMS (ES) 532.3010 (MH^+) $C_{28}H_{42}N_3O_7$ requires 532.3023;

ν_{max} (KBr) 2957 (C(O)NH), 2870 (C(O)NH), 1730 (CO_2Me), 1686 ($CH=CH_2$), 1671 ($CH=CH_2$)

Microanalysis C, 63.10; H, 7.76; N, 7.90 $C_{28}H_{42}N_3O_7$ requires C, 63.26; H, 7.77; N, 7.90.

Preparation of (*E*)-13*S*-*tert*-butoxycarbonylamino-10*S*-isopropyl-9,12-dioxo-2-oxa-8,11-diaza-bicyclo[13.2.2]nonadeca-1(18),4,15(19),16-tetraene-7*S*-carboxylic acid methyl ester (4.10)

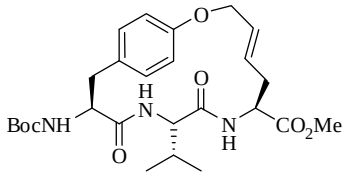

The diene **4.9** (1.80 g, 3.39 mmol, 1.0 equiv) was dissolved in anhydrous 1,1,2-trichloroethane (0.01M) under an atmosphere of argon. To this were added 1M chloro-dicyclohexyl borane in hexanes (0.34 mL, 0.34 mmol, 0.10 equiv) and Grubbs second generation catalyst (0.23 g, 0.34 mmol, 0.10 equiv). The mixture was heated at reflux in the microwave (1200 W) for 20 min. Two further additions of Grubbs second generation catalyst (0.10 equiv) were added and after each the reaction mixture was subjected to a further 20 min heating in the microwave. The mixture was then cooled and concentrated *in vacuo*. The crude material was purified by recrystallisation from methanol (1.11 g, 65%).

mp = 105-107 ^{o}C;

^{1}H NMR δ($CDCl_3$) 7.05 (2H, m, Ar**H** (Tyr)), 6.75 (2H, m, Ar**H** (Tyr)), 5.74-5.75 (2H, m, N**H**), 5.43-5.56 (2H, m, $OCH_2C\mathbf{H}CHCH_2$ and $OCH_2CHC\mathbf{H}CH_2$), 5.32 (1H, d, *J* = 8.7 Hz, N**H**), 4.76 (1H, ddd *J* = 3.4 Hz, *J* = 9.2 and 10.1 Hz, C**H**CO_2CH_3), 4.58-4.64 (2H, m, $OC\mathbf{H_2}CHCHCH_2$), 4.21 (1H, ddd, *J* = 5.2, 8.7 and11.6 Hz, C**H**CH_2Ph), 3.99 (1H, dd, *J* = 4.8 and 7.5 Hz, C**H**$CH(CH_3)_2$), 3.75 (3H, s, $CHCO_2C\mathbf{H_3}$), 3.13 (1H, dd, *J* = 5.2 and 12.5 Hz, $CHC\mathbf{H_2}$Ph), 2.66-2.75 (2H, m, $CHC\mathbf{H_2}$Ph and $OCH_2CHCHC\mathbf{H_2}$), 2.26-2.32 (1H, m, $OCH_2CHCHC\mathbf{H_2}$), 2.07-2.14 (1H, m, $CHC\mathbf{H}(CH_3)_2$), 1.45 (9H, s, $C(C\mathbf{H_3})_3$), 0.81-0.83 (6H, m, $CHCH(C\mathbf{H_3})_2$);

^{13}C δ($(CD_3)_2SO$) 171.70, 170.24, 170.10, 155.41, 154.76, 129.80, 128.50, 128.34, 127.65, 114.72, 77.89, 65.66, 56.73, 55.32, 51.92, 51.85, 36.42, 32.37, 32.19, 28.10, 18.57, 18.04;

$[\alpha]_D$ = -14.0 (c = 0.1 in $(CH_3)_2SO$);

HRMS (ES) 504.2718 (MH^+) $C_{26}H_{37}N_3O_7$ requires 504.2710

Preparation of 13*S*-*tert*-butoxycarbonylamino-10*S*-isopropyl-9,12-dioxo-2-oxa-8,11-diaza-bicyclo[13.2.2]nonadeca-1(18),15(19),16-triene-7*S*-carboxylic acid methyl ester (4.11)

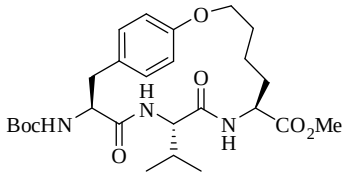

The unsaturated macrocycle **4.10** (1.36 g, 2.70 mmol) was hydrogenated in 50 mL of methanol using **General Procedure T** to afford a white solid (1.36 g, 100%).

mp = 225-228 ^{o}C;

^{1}H NMR δ((CD$_3$)$_2$SO) 7.05 (2H, m, Ar**H** (Tyr)), 6.78 (2H, m, Ar**H** (Tyr)), 6.23 (1H, d, *J* = 7.1 Hz, N**H**), 5.90 (1H, d, *J* = 8.2 Hz, N**H**), 5.29 (1H, d, *J* = 8.6 Hz, N**H**), 4.56 (1H, dt, *J* = 3.9 and 8.2 Hz, C**H**CO$_2$CH$_3$), 4.21-4.30 (2H, m, C**H**CH$_2$Ph, OC**H$_2$**CH$_2$CH$_2$CH$_2$) 4.09-4.13 (1H, m, OC**H$_2$**CH$_2$CH$_2$CH$_2$), 3.84-3.86 (1H, m, C**H**CH(CH$_3$)$_2$), 3.72 (3H, s, CHCO$_2$C**H$_3$**), 3.10 (1H, dd, *J* = 5.4 and 12.2 Hz, CHC**H$_2$**Ph), 2.67 (1H, dd, *J* = 12.2 and 12.2 Hz, CHC**H$_2$**Ph), 1.95-2.02 (1H, m, CHC**H**(CH$_3$)$_2$), 1.86-1.92 (1H, m, OCH$_2$CH$_2$CH$_2$C**H$_2$**), 1.80 (1H, m, OCH$_2$C**H$_2$**CH$_2$CH$_2$), 1.49-1.57 (2H, m, OCH$_2$CH$_2$CH$_2$C**H$_2$** and OCH$_2$C**H$_2$**CH$_2$CH$_2$), 1.44 (9H, s, C(C**H$_3$**)$_3$), 1.25-1.35 (2H, m, OCH$_2$CH$_2$C**H$_2$**CH$_2$), 0.87 (3H, d, *J* = 6.6 Hz, CHCH(C**H$_3$**)$_2$), 0.81 (3H, d, *J* = 6.6 Hz, CHCH(C**H$_3$**)$_2$);

^{13}C NMR δ((CD$_3$)$_2$SO) 172.72, 170.32, 169.85, 156.90, 155.11, 130.05, 128.42, 115.95, 79.64, 66.88, 57.65, 56.84, 52.32, 51.08, 38.43, 32.34, 31.74, 28.20, 21.73, 18.26, 18.17;

$[\alpha]_D$ = -11.0 (c = 0.1 in (CH$_3$)$_2$SO);

HRMS (ES) 506.2871 (MH$^+$) $C_{26}H_{40}N_3O_7$ requires 506.2866;

ν_{max} (KBr) 2967 (C(O)NH), 2887 (C(O)NH), 1754 (CO$_2$Me)

Preparation of 13*S*-benzyloxycarbonyl-10*S*-isopropyl-9,12-dioxo-2-oxa-8,11-diaza-bicyclo[13.2.2]nonadeca-1(18),15(19),16-triene-7*S*-carboxylic acid methyl ester (4.13)

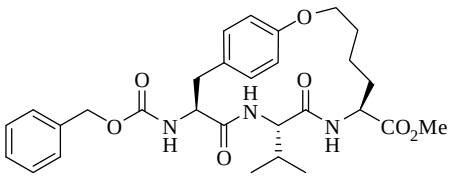

N-Boc protected saturated methyl ester **4.11** (1.00g, 1.97 mmol) was reacted using **General Procedure E** to afford the free amine as the TFA salt **4.12** (0.87 g, 100%) which was reacted immediately in the next reaction.

^{1}H NMR δ((CD$_3$)$_2$SO) 8.51 (2H, bs, N**H$_2$**), 8.16 (1H, d, *J* = 7.2Hz, N**H**), 7.90 (1H, d, *J* = 6.4 Hz, N**H**), 6.98 (2H, d, *J* = 6.8 Hz, Ar**H** (Cbz)), 6.75 (4H, m, Ar**H** (Tyr)), 4.31-4.36 (2H, m, OC**H$_2$**CH$_2$CH$_2$CH$_2$), 4.18-4.25 (1H, m, C**H**CO$_2$CH$_3$), 4.03-4.08 (1H, m, C**H**CH$_2$Ph) 3.84 (1H, dd, *J* = 5.2 and 7.2 Hz, C**H**CH(CH$_3$)$_2$), 3.60 (3H, s, CHCO$_2$C**H$_3$**), 3.08 (1H, dd, *J* = 5.6 and 11.2 Hz, CHC**H$_2$**Ph), 2.60 (1H, dd, *J* = 11.2 and 11.2 Hz, CHC**H$_2$**Ph), 1.96-2.01 (1H, m, CHC**H**(CH$_3$)$_2$), 1.76-1.83 (1H, m, OCH$_2$CH$_2$CH$_2$C**H$_2$**), 1.65-1.74 (1H, m, OCH$_2$C**H$_2$**CH$_2$CH$_2$), 1.48-1.57 (2H, m, OCH$_2$CH$_2$CH$_2$C**H$_2$** and OCH$_2$C**H$_2$**CH$_2$CH$_2$), 1.22-1.36 (2H, m, OCH$_2$CH$_2$C**H$_2$**CH$_2$), 0.84 (3H, d, *J* = 6.4 Hz, CHCH(C**H$_3$**)$_2$), 0.77 (3H, d, *J* = 6.4 Hz, CHCH(C**H$_3$**)$_2$);

LRMS (ES) 406.3 (MH$^+$) $C_{21}H_{31}N_3O_5$ requires 406.2

To the amino acid TFA salt **4.12** (0.87 g, 2.15 mmol, 1.0 equiv) in ice cold ethyl acetate/water (1:1) was added potassium bicarbonate (1.08 g, 10.75 mmol, 5.0 equiv). Benzyl chloroformate (0.34 mL, 2.37 mmol, 1.1 equiv) in ice cold ethyl acetate was added dropwise and a white precipitate immediately formed. The suspension was allowed to return to rt and stirred overnight after which the precipitate was filtered off and washed sequentially with 1M aqueous HCl and water, then dried (0.99 g, 86%). Recrystallisation from ethyl acetate gave the pure product as a white solid.

mp > 250 °C

^{1}H NMR δ((CD$_3$)$_2$SO) 8.11 (1H, d, *J* = 9.2 Hz, N**H**), 7.58 (1H, d, *J* = 6.5 Hz, N**H**), 7.35-7.32 (2H, m, Ar**H** (Cbz)) 7.01 (2H, m, Ar**H** (Tyr)), 6.89, (1H, d, *J* = 8.2 Hz, N**H**), 6.74 (2H, m, Ar**H** (Tyr)), 5.03 (2H, bs, CC**H$_2$**O), 4.38-4.27 (2H, m, OC**H$_2$**CH$_2$CH$_2$CH$_2$), 4.01 (1H, t, *J* = 9.3 Hz, C**H**CO$_2$CH$_3$), 3.80-3.77 (1H, m, C**H**CH$_2$Ph) 3.61-3.55 (4H, m,

C**H**CH$(CH_3)_2$ and $CHCO_2C$**H$_3$**), 2.86 (1H, dd, *J* = 5.6 and 11.2 Hz, CHC**H$_2$**Ph), 2.65-2.60 (1H, m, CHC**H$_2$**Ph), 1.80-1.67 (3H, m, CHC**H**$(CH_3)_2$ and $OCH_2CH_2CH_2C$**H$_2$**), 1.58-1.52 (1H, m, OCH_2C**H$_2$**CH_2CH_2), 1.30-1.20 (4H, m, $OCH_2CH_2CH_2C$**H$_2$** and OCH_2C**H$_2$**CH_2CH_2), 0.89 (1H, m, $OCH_2CH_2CH_2C$**H$_2$**), 0.75 (6H, d, *J* = 6.6 Hz, $CHCH(C$**H$_3$**$)_2$), 0.68-0.60 (1H, m, $OCH_2CH_2CH_2C$**H$_2$**);

^{13}C NMR δ($(CD_3)_2SO$) 172.48, 169.80, 169.77, 155.48, 137.09, 130.15, 128.24, 127.69, 127.62, 115.29, 115.27, 65.97, 65.15, 56.48, 56.20, 51.78, 49.42, 36.74, 32.06, 29.61, 26.17, 21.45, 18.41, 18.05

$[\alpha]_D$ = -6.0 (c = 0.1 in $(CH_3)_2SO$);

HRMS (ES) 540.2723 (MH^+) $C_{29}H_{38}N_3O7$ requires 540.2710;

ν_{max} (KBr) 3035 (C(O)NH), 2960 (C(O)NH), 1738 (CO_2Me), 1688 (OC(O)).

Preparation of (7*S*-hydroxymethyl-10*S*-isopropyl-9,12-dioxo-2-oxa-8,11-diaza-bicyclo[13.2.2]nonadeca-1(18),15(19),16-trien-13*S*-yl)carbamic acid benzyl ester (4.3)

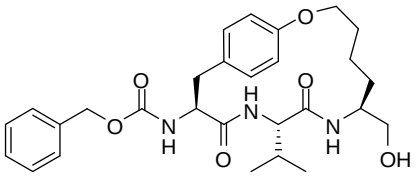

The methyl ester **4.13** (0.90 g, 1.67 mmol) was suspended in tetrahydrofuran and reduced according to **General Procedure K** to give the alcohol **4.3** as a white solid (0.72 g, 84%). Recrystallisation from methanol gave the pure product.

mp >250 °C;

^{1}H NMR δ($(CD_3)_2SO$) 7.57 (1H, d, *J* = 7.0 Hz, N**H**), 7.45 (1H, d *J* = 9.1 Hz, N**H**), 7.35-7.34 (5H, m, Ar**H** (Cbz)), 7.01 (2H, m, Ar**H** (Tyr)), 6.80 (1H, d *J* = 7.9 Hz, N**H**), 6.74 (2H, m, Ar**H** (Tyr)), 5.03 (2H, s, CC**H$_2$**O), 4.62-4.60 (1H, m, CH_2O**H**), 4.35-4.28 (2H, m, C**H**CH_2Ph and OC**H$_2$**$CH_2CH_2CH_2$), 4.04-3.99 (1H, m, OC**H$_2$**$CH_2CH_2CH_2$), 3.76-3.64 (2H, m, C**H**$CH(CH_3)_2$ and C**H**CH_2OH), 3.20-3.14 (1H, m, C**H$_2$**OH), 3.09-3.05 (1H, m, C**H$_2$**OH), 2.85 (1H, dd, *J* = 5.6 and 12.8 Hz, CHC**H$_2$**Ph), 2.65-2.60 (1H, m, CHC**H$_2$**Ph), 1.78-1.68 (2H, m, CHC**H**$(CH_3)_2$) and OCH_2C**H$_2$**CH_2CH_2), 1.51-1.43 (1H, m, $OCH_2CH_2CH_2C$**H$_2$**), 1.32-1.13 (2H, m, OCH_2C**H$_2$**CH_2CH_2 and OCH_2C**H$_2$**CH_2CH_2), 0.86-

0.80 (1H, m, $OCH_2CH_2CH_2C\mathbf{H_2}$), 0.73-0.71 (3H, m, $CHCH(C\mathbf{H_3})_2$), 0.64-0.59 (1H, m, $OCH_2CH_2CH_2C\mathbf{H_2}$);

^{13}C NMR δ($(CD_3)_2SO$) 170.17, 169.62, 156.32, 155.87, 137.30, 130.43, 128.68, 128.43, 128.17, 127.98, 115.76, 66.73, 65.67, 64.56, 57.05, 56.91, 49.44, 37.00, 32.36, 30.11, 27.88, 22.22, 18.92, 18.43;

$[\alpha]_D$ = -8.0 (c = 0.1 in $(CH_3)_2SO$);

HRMS (ES) 512.2763 (MH^+) $C_{28}H_{38}N_3O_6$ requires 512.2761;

ν_{max} (KBr) 3288 (CH_2OH), 2958 (C(O)NH), 2872 (C(O)NH), 1765 (OC(O)).

Preparation of (7*S*-formyl-10*S*-isopropyl-9,12-dioxo-2-oxa-8,11-diazabicyclo[13.2.2]-nonadeca-1(18),15(19),16-trien-13*S*-yl)carbamic acid benzyl ester (4.4)

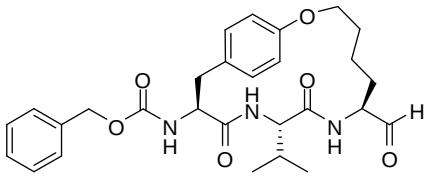

The alcohol **4.3** (0.70 g, 1.37 mmol) was oxidised according to **General Procedure L** to afford the aldehyde as a white solid (0.55 g, 79%).

mp = 193-195 °C;

^{1}H NMR δ($(CD_3)_2SO$) 9.23 (1H, s, C**H**O), 7.56 (1H, d, *J* = 6.7 Hz, N**H**), 7.40 (1H, d *J* = 9.4 Hz, N**H**), 7.33-7.31 (5H, m, Ar**H** (Cbz)), 7.00 (2H, m, Ar**H** (Tyr)), 6.82 (1H, d *J* = 7.7 Hz, N**H**), 6.72 (2H, m, Ar**H** (Tyr)), 5.00 (2H, s, $CC\mathbf{H_2}O$), 4.30-4.26 (2H, m, $C\mathbf{H}CH_2Ph$ and $OC\mathbf{H_2}CH_2CH_2CH_2$), 4.04-3.99 (1H, m, $OC\mathbf{H_2}CH_2CH_2CH_2$), 3.70-3.64 (2H, m, $C\mathbf{H}CH(CH_3)_2$ and C**H**CHO), 2.83 (1H, dd, *J* = 5.4 and 12.4 Hz, $CHC\mathbf{H_2}Ph$), 2.63-2.57 (1H, m, $CHC\mathbf{H_2}Ph$), 1.78-1.68 (2H, m, $CHC\mathbf{H}(CH_3)_2$), and $OCH_2C\mathbf{H_2}CH_2CH_2$), 1.50-1.43 (1H, m, $OCH_2CH_2CH_2C\mathbf{H_2}$), 1.32-1.10 (2H, m, $OCH_2C\mathbf{H_2}CH_2CH_2$ and $OCH_2C\mathbf{H_2}CH_2CH_2$), 0.92-0.90 (1H, m, $OCH_2CH_2CH_2C\mathbf{H_2}$), 0.83-0.81 (3H, m, $CHCH(C\mathbf{H_3})_2$), 0.74-0.69 (1H, m, $OCH_2CH_2CH_2C\mathbf{H_2}$);

^{13}C NMR δ($(CD_3)_2SO$) 201.61, 170.75, 170.56, 156.46, 156.12, 137.84, 130.91, 129.07, 128.97, 128.41, 128.35, 116.09, 66.78, 65.93, 57.41, 57.19, 56.96, 37.53, 32.73, 27.47, 27.18, 22.13, 19.39, 18.80;

$[\alpha]_D$ = -2.2 (c = 0.4 in $(CH_3)_2SO$);

HRMS (ES) 510.2590 (MH^+) $C_{28}H_{36}N_3O_6$ requires 510.2604;

ν_{max} (KBr) 2984 (C(O)NH), 2960 (C(O)NH), 1735 (CHO), 1637 (OC(O)).

7.4.2 Derivatives of the Macrocyclic Aldehyde

Preparation of (7*S*-semicarbazone-10*S*-isopropyl-9,12-dioxo-2-oxa-8,11-diaza-bicyclo[13.2.2]nonadeca-1(18),15(19),16-trien-13*S*-yl)carbamic acid benzyl ester (4.15)

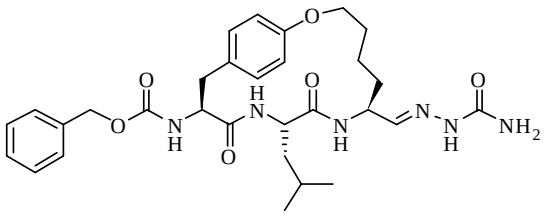

The macrocyclic aldehyde **4.14** (0.20 g, 0.38 mmol) was reacted according to **General Procedure O** to give the crude semicarbazone. Recrystallisation from ethanol gave the pure product as a white solid (0.16 g, 71%).

mp = 226 °C (Dec);

^{1}H NMR δ($(CD_3)_2SO$) 9.33 (1H, s, CNN**H**C(O)NH_2), 8.07 (1H, d, *J* = 7.9 Hz, N**H**), 7.55 (1H, d, *J* = 4.0 Hz, CHC**H**=NNH), 7.52 (1H, d, *J* = 6.1 Hz, N**H**), 7.39-7.35 (5H, m, Ar**H** (Cbz)), 7.17 (1H, d, *J* = 9.4 Hz, N**H**), 7.05-6.98 (2H, m, Ar**H** (Tyr)), 6.78-6.74 (2H, m, Ar**H** (Tyr)), 5.06-5.02 (2H, m, CC**H$_2$**O), 4.36-4.26 (2H, m, C**H**CH_2Ph and OC**H$_2$**$CH_2CH_2CH_2$), 4.09-4.00 (1H, m, OC**H$_2$**$CH_2CH_2CH_2$), 3.66-3.57 (1H, m, C**H**$CH_2CH(CH_3)_2$), 3.18-3.13 (1H, m, C**H**CH=NNH), 2.88-2.84 (1H, m, CHC**H$_2$**Ph), 2.66-2.58 (1H, m, CHC**H$_2$**Ph), 1.78-1.67 (1H, m, OCH_2C**H$_2$**CH_2CH_2), 1.53-1.45 (1H, m, $OCH_2CH_2CH_2$C**H$_2$**), 1.35-1.13 (7H, m, CHC**H$_2$**$CH(CH_3)_2$ and $CHCH_2$C**H**$(CH_3)_2$ and OCH_2C**H$_2$**CH_2CH_2 and $OCH_2CH_2CH_2$C**H$_2$**), 1.05-1.00 (1H, m, OCH_2CH_2C**H$_2$**CH_2), 0.84-0.69 (7H, m, $CHCH_2CH$(C**H$_3$**)$_2$ and OCH_2CH_2C**H$_2$**CH_2);

^{13}C NMR δ($(CD_3)_2SO$) 200.99, 171.30, 169.52, 155.80, 155.30, 137.12, 130.11, 128.23, 127.67, 127.59, 115.46, 104.25, 66.05, 65.14, 56.50, 55.99, 50.58, 43.29, 37.03, 26.89, 26.39, 23.83, 22.78, 21.84, 21.41, 18.50;

$[\alpha]_D$ = -3.0 (c = 1.3 in $(CH_3)_2SO$);

HRMS (ES) 581.3086 (MH^+) $C_{30}H_{41}N_6O_6$ requires 581.3088;

ν_{max} (KBr) 2952 (C(O)NH), 2880 (C(O)NH), 2254 (C=NNH), 1654 (C(O)NH_2).

Preparation of [7-(*R*,*S*)-(cyanohydroxymethyl)-10*S*-isobutyl-9,12-dioxo-2-oxa-8,11-diaza-bicyclo[13.2.2]nonadeca-1(18),15(19),16-trien-13*S*-yl]carbamic acid benzyl ester (4.16)

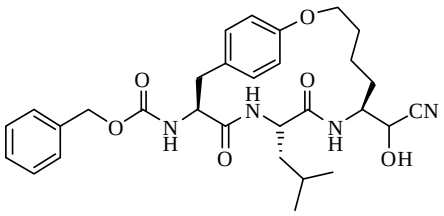

The macrocyclic aldehyde **4.14** (0.50 g, 0.96 mmol) was reacted according to **General Procedure I** to afford the crude material. Recrystallisation from methanol gave the pure cyanohydrin as a white solid (0.43 g, 81%).

NMR data reported for the diastereomeric mixture (1:1)

^{1}H NMR δ($(CD_3)_2SO$) 7.99 (1H, d, *J* = 8.7 Hz, N**H**), 7.90 (1H, d, *J* = 9.5 Hz, N**H**), 7.52 (1H, d, *J* = 7.4 Hz, N**H**), 7.35 (10H, s, Ar**H** (Cbz)), 7.31 (1H, d, *J* = 5.5 Hz, N**H**), 7.07 (1H, d, *J* = 8.3 Hz, N**H**), 7.03-6.99 (4H, m, Ar**H** (Tyr)), 6.96 (1H, d, *J* = 8.1 Hz, N**H**), 6.76 (4H, d, *J* = 7.8 Hz, Ar**H** (*m*tyr), 6.61 (1H, d, *J* = 6.9 Hz CHC**H**OH), 6.55 (1H, d, *J* = 5.8 Hz CHC**H**OH), 5.08-4.99 (4H, m, CC$\mathbf{H_2}$O), 4.37-4.29 (4H, m, C**H**CH_2Ph and OC$\mathbf{H_2}CH_2CH_2CH_2$), 4.13-4.10 (1H, m, C**H**$CH_2CH(CH_3)_2$), 4.08-4.01 (3H, m, C**H**$CH_2CH(CH_3)_2$ and OC$\mathbf{H_2}CH_2CH_2CH_2$), 3.98-3.94 (2H, m, OC$\mathbf{H_2}CH_2CH_2CH_2$), 3.89-3.85 (2H, m, C**H**CHOH), 2.85 (2H, dd, *J* = 5.2 and 13.1 Hz, CHC$\mathbf{H_2}$Ph), 2.64-2.58 (2H, m, CHC$\mathbf{H_2}$Ph), 1.76-1.67 (2H, m, $OCH_2C\mathbf{H_2}CH_2CH_2$), 1.61-1.45 (4H, m, CHC$\mathbf{H_2}CH(CH_3)_2$ and $OCH_2CH_2CH_2C\mathbf{H_2}$), 1.37-1.12 (10H, m, CHC$\mathbf{H_2}CH(CH_3)_2$ and $CHCH_2C\mathbf{H}(CH_3)_2$ and $OCH_2C\mathbf{H_2}CH_2CH_2$ and $OCH_2CH_2C\mathbf{H_2}CH_2$ $OCH_2CH_2CH_2C\mathbf{H_2}$), 0.84-0.75 (14H, m, $CHCH_2CH(C\mathbf{H_3})_2$ and $OCH_2CH_2C\mathbf{H_2}CH_2$);

^{13}C NMR δ($(CD_3)_2SO$) 171.19, 170.91, 169.41, 156.13, 155.76, 155.25, 137.10, 130.03, 128.21, 127.65, 127.58, 119.86, 119.33, 115.39, 115.34, 115.30, 66.18, 66.14, 65.11, 65.06, 63.40, 62.85, 56.04, 55.93, 50.54, 50.50, 49.95, 49.74, 43.46, 43.43, 43.34, 43.28, 37.06, 30.02, 29.17, 28.13, 27.52, 27.18, 23.88, 23.63, 22.91, 22.77, 22.60, 21.68, 21.53;

HRMS (ES) 551.2876 (MH^+) $C_{30}H_{39}N_4O_6$ requires 551.2870;

ν_{max} (KBr) 3319 (CH(OH)), 3064 (C(O)NH), 2922 (C(O)NH), 1882 (CH(OH)CN).

Preparation of (7*S*-azidomethyl-10*S*-isobutyl-9,12-dixoxo-2-oxa-8,11-diazabicyclo-[13.2.2]nonadeca-1(18),15(19),16-trien-13*S*-yl)carbamic acid benzyl ester (4.19)

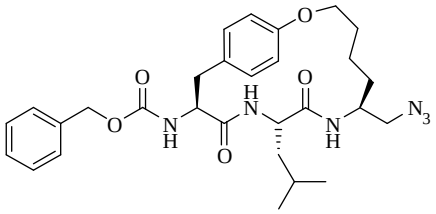

To the macrocyclic alcohol **4.20** (0.19 g, 0.36 mmol, 1.0 equiv) in dichloromethane was added triethylamine (120 µL, 0.90 mmol, 2.5 equiv) and mesyl chloride (16 µL, 0.36 mmol, 1.0 equiv). The reaction mixture was stirred at rt overnight, then the solvent removed *in vacuo*. The residue was dissolved in *N,N*-dimethylformamide and sodium azide (0.02 g, 0.36 mmol, 1.0 equiv) added and the reaction mixture stirred at rt for 4 h after which it was diluted with ethyl acetate. The organic phase was washed with brine, dried over $MgSO_4$ and solvent removed under reduced pressure to give the crude material. Recrystallisation from ethyl acetate/petroleum ether afforded the product as a white solid (0.12 g, 61%)

mp > 250 °C

^{1}H NMR δ((CD3)2SO) 7.55 (1H, d, *J* = 9.1 Hz, N**H**), 7.52 (1H, d, *J* = 7.1 Hz, N**H**), 7.38-7.35 (5H, m, Ar**H** (Cbz)), 7.01 (2H, m, Ar**H** (Tyr)), 6.93 (1H, d, *J* = 7.7 Hz, NH), 6.74 (2H, m, Ar**H** (Tyr)), 5.07 (2H, d, *J* = 12.6 Hz CC**H**$_2$O), 4.99 (2H, d, *J* = 12.6 Hz CC**H**$_2$O), 4.59-4.57 (1H, m, C**H**CH$_2$Ph), 4.34-4.29 (2H, m, OC**H$_2$**CH$_2$CH$_2$CH$_2$ and C**H**CH$_2$N$_3$), 4.06-4.01 (2H, m, OC**H$_2$**CH$_2$CH$_2$CH$_2$ and C**H**CH$_2$CH(CH$_3$)$_2$), 3.18-3.14 (1H, m, CHC**H$_2$**Ph), 3.08-3.03 (1H, m, CHC**H$_2$**Ph), 2.86 (1H, dd, *J* = 5.6 and 13.1 Hz, CHC**H$_2$**N$_3$), 2.62-2.60 (1H, m, CHC**H$_2$**N$_3$), 1.77-1.68 (2H, m, CHCH$_2$C**H**(CH$_3$)$_2$), 1.52-1.44 (2H, m, OCH$_2$C**H$_2$**CH$_2$CH$_2$), 1.33-1.14 (4H, m, OCH$_2$CH$_2$C**H$_2$**CH$_2$ and CHC**H$_2$**CH(CH$_3$)$_2$), 0.87-0.82 (1H, m, OCH$_2$CH$_2$CH$_2$C**H$_2$**), 0.80-0.77 (6H, m, CHCH$_2$CH(C**H$_3$**)$_2$), 0.64-0.59 (1H, m, OCH$_2$CH$_2$CH$_2$C**H$_2$**);

^{13}C NMR δ((CD$_3$)$_2$SO) 170.92, 169.90, 156.54, 155.80, 137.46, 130.45, 128.72, 128.60, 128.03, 115.03, 66.77, 65.65, 64.47, 56.62, 51.13, 49.60, 43.63, 37.38, 30.26, 28.28, 24.24, 23.27, 23.12, 22.35

$[\alpha]_D$ = -3.0 (c = 0.1 in $(CH_3)_2SO$);

ν_{max} (KBr) 2955 (C(O)NH), 2864 (C(O)NH), 2783 (C(O)NH), 2406 (CH_2N_3), 1701 (OC(O)).

7.5 REFERENCES FOR CHAPTER SEVEN

(1) Parikh, J. R.; Doering, W. v. E. *Journal of the American Chemical Society* **1967**, *89*, 5505-5507.

(2) Harvey, A. J., University of Canterbury, 2000.

(3) Anelli, P. L.; Biffi, C.; Montanari, F. *Journal of Organic Chemistry* **1987**, *52*, 2559-2560.

(4) Inoue, J.; Nakamura, M.; Cui, Y.-S.; Sakai, Y.; Sakai, O.; Hill, J. R.; Wang, K. K. W.; Yuen, P.-W. *Journal of Medicinal Chemistry* **2003**, *46*, 868-871.

(5) Nakamura, M.; Yamaguchi, M.; Sakai, O.; Inoue, J. *Bioorganic & Medicinal Chemistry* **2003**, *11*, 1371-1379.

(6) Tao, M.; Bihovsky, R.; Wells, G. J.; Mallamo, J. P. *Journal of Medicinal Chemistry* **1998**, *41*, 3912-3916.

(7) Nakamura, M.; Inoue, J. *Bioorganic & Medicinal Chemistry Letters* **2002**, *12*, 1603-1606.

(8) Payne, R. J.; Brown, K. M.; Coxon, J. M.; Morton, J. D.; Lee, H. Y.-Y.; Abell, A. d. *Australian Journal of Chemistry* **2004**, *57*, 877-884.

(9) Choi, Y.-S.; Inoue, A.; Nakamura, M.; (Senju Pharmaceutical Co., Ltd., Japan). Application: JPJP, 2002, p 9 pp.

(10) Hamze, A.; Hernandez, J.-F.; Fulcrand, P.; Martinez, J. *Journal of Organic Chemistry* **2003**, *68*, 7316-7321.

(11) Bodanszky, A.; Bodanszky, M.; Chandramouli, N.; Kwei, J. Z.; Martinez, J.; Tolle, J. C. *Journal of Organic Chemistry* **1980**, *45*, 72-76.

(12) Damkaci, F.; DeShong, P. *Journal of the American Chemical Society* **2003**, *125*, 4408-4409.

(13) Brown, H. C.; Subba Rao, B. C. *Journal of Organic Chemistry* **1958**, *80*, 5377-5380.

APPENDIX

A1 Raw Assay Data and IC_{50} Calculation Example

The data in **Table A1** is that collected for one assay run of SJA6017. Rows 1-3 correspond to the calcium blank; 4-6 EDTA blank; 7-12 m-calpain; 13-15 SJA at 50 µM; 16-19 SJA at 10 µM; 20-22 SJA at 4 µM; 23-25 SJA at 2 µM; 26-28 SJA at 0.4 µM; 29-31 SJA at 0.2 µM; 32-34 SJA at 0.1 µM; 35-37 SJA at 0.05 µM. The columns labelled t = 1 to t = 10 show the amount of fluorescence (in fluorescence units) recorded at 1 min time intervals for a total of 10 min. The column labelled t10-t1 shows the change in fluorescence that occurs over the time of the assay. The numbers in the column labelled Adjusted are the values obtained by using **Eqn A1** in the case of the inhibitor samples or **Eqn A2** in the case of the uninhibited enzyme and represent the baseline corrected fluorescence.

	t = 1	t = 3	t = 4	t = 5	t = 6	t = 7	t = 8	t = 9	t = 10	*t*10-*t*1	Averages	Adjusted	% inhib
Ca blank	1326	1115	964	897	847	855	854	860	845	-481			
	1274	1040	939	927	874	894	889	892	883	-391			
	806	771	708	684	638	648	653	633	632	-174			
EDTA blank	689	675	666	659	645	645	625	631	628	-61			
	715	697	684	675	658	659	647	641	652	-63			
	682	672	664	641	636	633	623	620	619	-63	**-205.5**		
m-calpain	1009	1166	1289	1400	1458	1565	1650	1734	1796	787			
	967	1138	1260	1355	1421	1505	1587	1669	1746	779			
	952	1108	1246	1344	1438	1513	1627	1681	1747	795			
	946	1059	1184	1298	1367	1467	1539	1597	1684	738			
	926	1099	1214	1323	1381	1479	1581	1649	1720	794			
	909	1094	1212	1332	1409	1508	1575	1655	1721	812	784.16	**989.66**	
SJA 50.0 µM	461	456	451	439	425	423	422	427	413	-48			

	475	465	454	437	429	429	428	437	423	-52			
	463	458	454	442	425	423	423	429	421	-42	-47.33	158.16	84
SJA 10.0 µM	514	510	496	497	483	484	484	483	483	-31			
	485	498	487	483	458	471	473	469	465	-20			
	490	495	478	482	470	467	460	471	470	-20	-23.66	181.83	82
SJA 2.00 µM	571	575	577	573	550	559	555	552	568	-3			
	569	579	567	564	559	554	558	553	547	-22			
	577	586	569	575	562	558	563	567	560	-17	-14.00	191.50	81
SJA 0.40 µM	720	722	731	720	709	712	717	721	724	4			
	764	764	775	776	749	757	774	773	773	9			
	782	791	803	797	778	787	792	811	818	36	16.33	221.83	78
SJA 0.20 µM	827	869	895	907	899	911	931	933	944	117			
	810	873	917	928	924	924	935	949	950	140			
	808	860	886	897	900	898	899	914	934	126	127.66	333.16	66
SJA 0.10 µM	852	942	1007	1040	1048	1064	1084	1094	1106	254			
	843	930	998	1025	1019	1044	1062	1084	1108	265			
	835	955	1015	1030	1044	1072	1094	1111	1114	279	266.00	471.50	52
SJA 0.05 µM	843	963	1036	1065	1088	1129	1160	1204	1231	388			
	837	950	1032	1092	1117	1167	1198	1230	1243	406			
	865	989	1086	1127	1151	1180	1226	1262	1280	415	403.00	608.50	39

Table A1 Raw assay data and calculations

The equations **A1-A3** are used for determining the % inhibition, where FU represents the change in fluorescence units over 10 min:

$FU_{avg\ inhibitor} = FU_{avg\ sample} - FU_{avg\ blanks}$ **Eqn A**

$FU_{uninhibited} = FU_{enzyme} - FU_{avg\ blanks}$ **Eqn A2**

Where in this example the $FU_{avg\ blanks}$ corresponds to the calculated value of -205.5 and FU_{enzyme} to the calculated value 784.16

$$\% \text{ Inhibition} = \{(FU_{uninhibited} - FU_{inhibited})/FU_{uninhibited}\} \times 100 \qquad \textbf{Eqn A3}$$

Where in this example the $FU_{uninhibited}$ is the calculated value of 989.66 and $FU_{inhibited}$ corresponds to the values calculated in the Adjusted column for each of the inhibitor samples assayed.

The % inhibition values for the various dilutions of the inhibitor are graphed as the log of the concentration versus % inhibition as shown in **Table A2**. IC_{50} values are calculated from the linear part of the graph using the equation generated from the trend line (y = 50, solving for x). The uncertainty of the IC_{50} values have been approximated to be within 10% error.

conc (µM)	Log(conc)	% inhib
50	1.69897	84
10	1	82
2	0.30103	81
0.4	-0.39794	78
0.2	-0.69897	66
0.1	-1	52
0.05	-1.30103	39

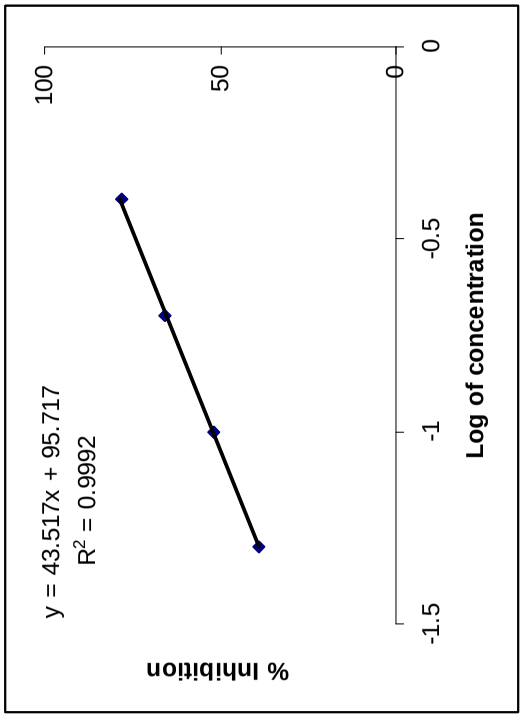

Table A2 Calculation of IC_{50} value

A2 Percentage Inhibition at 50 µM

The **Table A.2** below outlines all compounds assayed using the assay protocols in **Chapter Five**. Values given are the % inhibition for each compound at a concentration of 50 µM. This was used as a screening process to determine which compounds would be assayed at lower concentrations (down to a concentration of 50 nM). Any compounds exhibiting a % inhibition of the enzyme greater than 50% at 50 µM underwent this process and an IC_{50} value calculated in the manner illustrated in **A1**.

	Compound	% Inhibition at 50 µM					
		m-calpain	µ-calpain	cathepsin B	papain	pepsin	α-chymo-trypsin
2.24	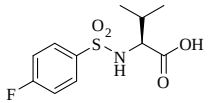	16	30	15	24	0	0
2.25	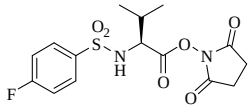	52	50	100	15	0	0
2.6	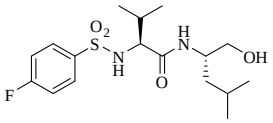	46	51	87	28	0	9
2.3	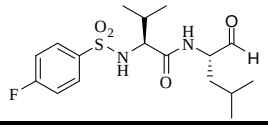	100	100	100	100	0	0

	Compound	% Inhibition at 50 μM					
		m-calpain	μ-calpain	cathepsin B	papain	pepsin	α-chymo-trypsin
2.26	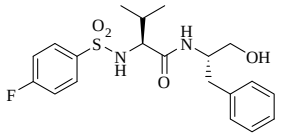	91	84	89	91	30	0
2.27	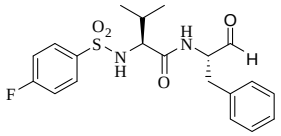	100	99	98	97	20	0
2.29	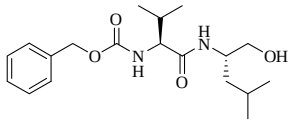	28	54	24	70	5	0
2.19	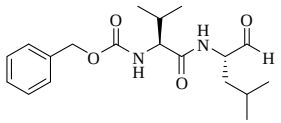	100	100	100	84	11	0
2.30	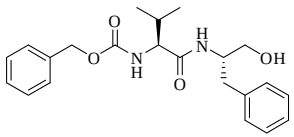	93	71	97	48	7	0
2.2	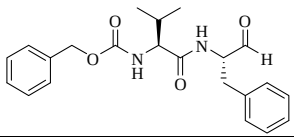	100	96	98	67	60	6

	Compound	% Inhibition at 50 μM					
		m-calpain	μ-calpain	cathepsin B	papain	pepsin	α-chymo-trypsin
2.34	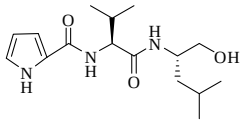	10	19	97	18	3	17
2.21	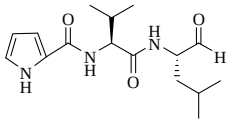	97	96	100	96	5	9
2.35	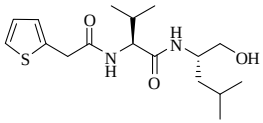	18	4	75	22	14	5
2.22	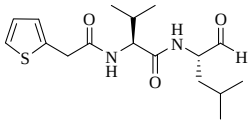	97	95	00	93	0	12
2.37	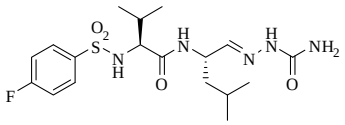	87	92	96	68	25	15
2.38	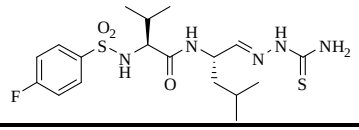	95	90	100	98	27	0

	Compound	% Inhibition at 50 μM m-calpain	μ-calpain	cathepsin B	papain	pepsin	α-chymo-trypsin
2.39	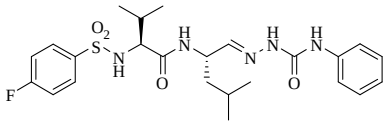	94	92	100	86	36	0
2.40	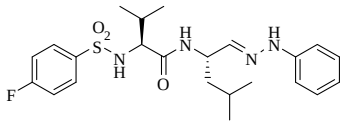	94	85	100	98	38	0
2.44	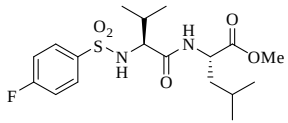	13	11	93	0	0	0
2.7	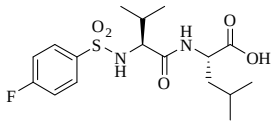	13	20	81	45	9	0
2.48	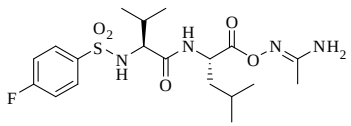	79	49	43	47	0	12
2.41	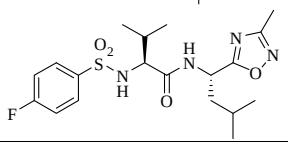	25	32	86	64	0	7

	Compound	% Inhibition at 50 μM					
		m-calpain	μ-calpain	cathepsin B	papain	pepsin	α-chymo-trypsin
2.45	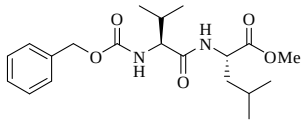	4	2	78	0	37	12
2.46	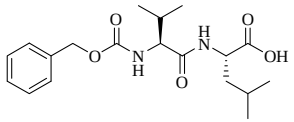	0	3	100	0	42	8
2.49	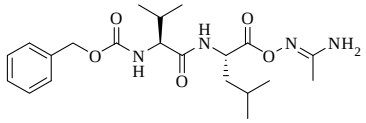	24	27	96	49	27	0
2.50	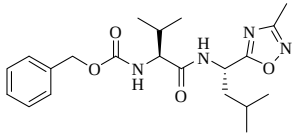	16	5	91	4	27	11
2.51	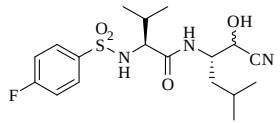	97	100	100	94	4	0
2.52	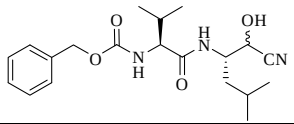	89	95	98	61	63	10

	Compound	% Inhibition at 50 μM					
		m-calpain	μ-calpain	cathepsin B	papain	pepsin	α-chymo-trypsin
2.53	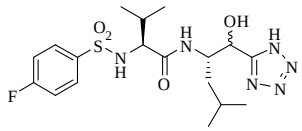	56	14	99	50	48	0
2.43	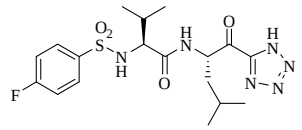	48	0	44	81	48	5
2.54	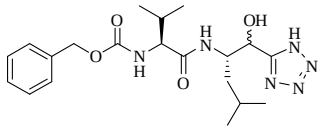	51	34	93	71	10	0
2.55	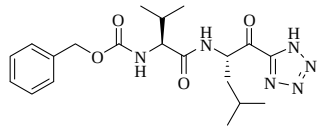	44	0	45	77	78	23
2.56	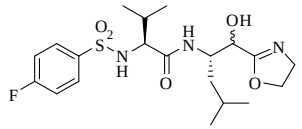	58	43	67	69	26	0
2.42	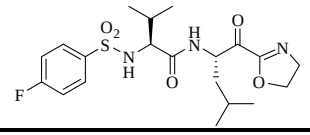	96	89	100	91	32	0

	Compound	% Inhibition at 50 μM					
		m-calpain	μ-calpain	cathepsin B	papain	pepsin	α-chymo-trypsin
2.57	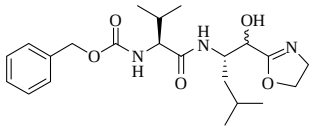	62	27	57	64	57	0
2.58	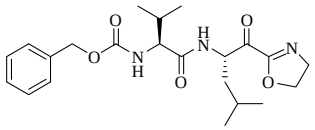	68	30	61	56	45	13
2.60	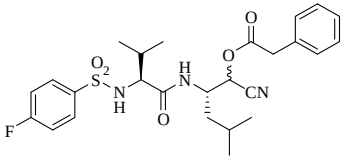	79	77	100	43	36	41
2.61	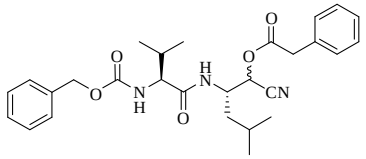	88	53	97	11	69	34
2.62	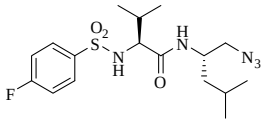	19	15	100	69	18	18
3.14	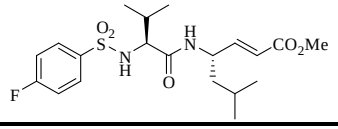	9	3	67	78	21	0

	Compound	% Inhibition at 50 μM m-calpain	μ-calpain	cathepsin B	papain	pepsin	α-chymo-trypsin
3.15	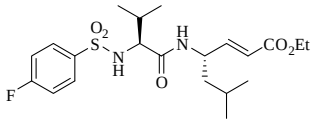	9	0	95	58	14	0
3.16	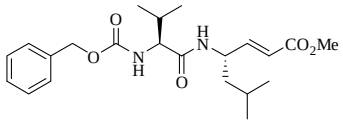	90	81	100	85	19	0
3.17	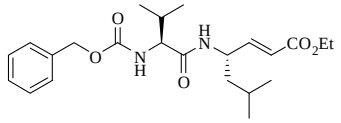	17	11	90	36	16	0
3.18	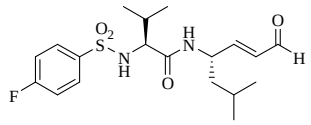	89	93	95	76	41	14
3.20	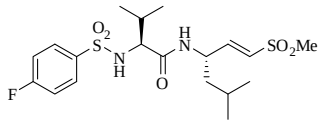	71	77	100	64	12	6
3.21	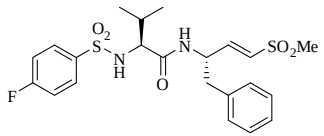	11	16	100	72	12	21

	Compound	% Inhibition at 50 μM m-calpain	μ-calpain	cathepsin B	papain	pepsin	α-chymo-trypsin
3.22	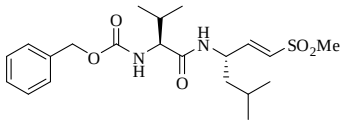	21	18	69	26	24	0
3.23	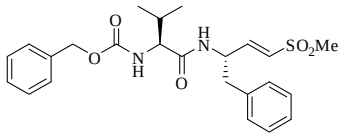	2	1	79	33	11	27
3.25	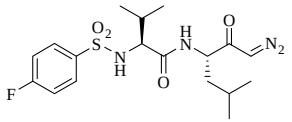	36	44	68	59	12	0
3.26	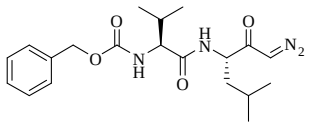	84	65	87	54	11	0
3.28	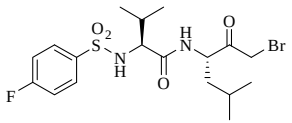	53	64	100	73	18	0
3.30	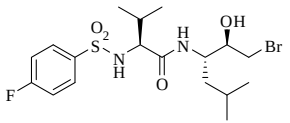	66	72	100	100	22	34

	Compound	% Inhibition at 50 μM					
		m-calpain	μ-calpain	cathepsin B	papain	pepsin	α-chymo-trypsin
3.33	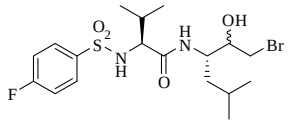	68	72	100	73	28	0
3.29	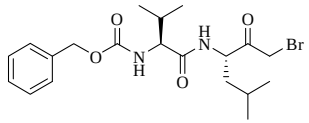	70	61	100	77	15	6
3.32	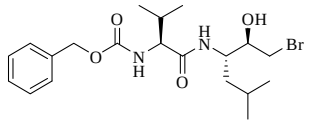	22	38	64	38	9	0
3.34	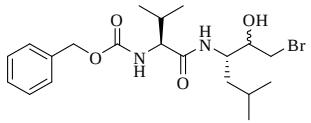	48	60	100	77	38	0
3.27	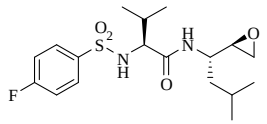	10	2	92	54	23	12
3.34	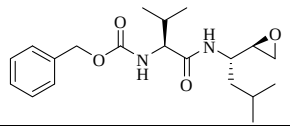	13	18	78	12	37	0

	Compound	% Inhibition at 50 μM					
		m-calpain	μ-calpain	cathepsin B	papain	pepsin	α-chymo-trypsin
3.35	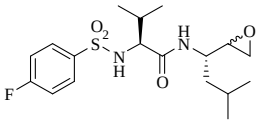	77	9	81	20	35	9
3.36	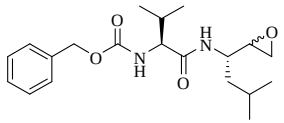	17	6	91	0	49	1
4.13	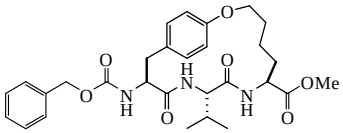	16	0	67	25	27	12
4.3	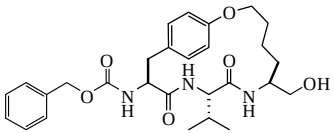	90	85	71	53	12	0
4.4	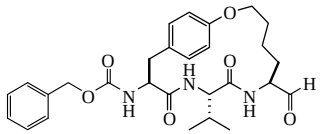	92	95	100	74	90	18
4.15	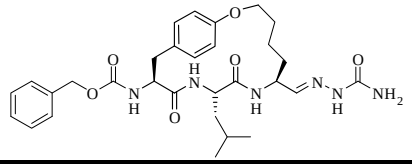	92	95	100	93	45	0

Compound		% Inhibition at 50 µM					
		m-calpain	µ-calpain	cathepsin B	papain	pepsin	α-chymo-trypsin
4.16	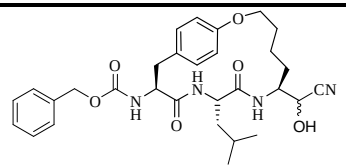	87	60	100	87	52	0
4.19	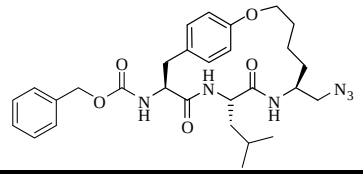	51	0	25	22	42	5

Table A.2 Percentage Inhibitions for synthesised compounds at a concentration of 50 µM